2011 Functional and Structural Nanomaterials: Fabrication, Properties, Applications and Implications: Fabrication of Nanomaterials I

Sponsored by: The Minerals, Metals and Materials Society, TMS Electronic, Magnetic, and Photonic Materials Division, TMS: Nanomaterials Committee

Program Organizers: Jiyoung Kim, Univ of Texas; David Stollberg, Georgia Tech Research Institute; Seong Jin Koh, University of Texas at Arlington; Nitin Chopra, The University of Alabama; Suveen Mathaudhu, U.S. Army Research Office

| Tuesday AM | Room: 8 |
|---------------|-------------------------------|
| March 1, 2011 | Location: San Diego Conv. Ctr |

Session Chairs: David Stollberg, Georgia Tech Research Institute; Greg Thompson, University of Alabama

8:30 AM Introductory Comments

8:35 AM Invited

Atomic Layer Deposition for the Functionalization of Nanoporous Materials: *Jeffrey Elam*¹; ¹Argonne National Laboratory

Atomic layer deposition (ALD) is a thin film growth technique that uses alternating, self-limiting chemical reactions to deposit materials in an atomic layer-by-layer fashion. Although this process is already used commercially for microelectronics manufacturing, ALD promises to have a much broader impact extending far beyond microelectronics. In particular, the capability to infiltrate and coat nanoporous substrates coupled with a broad palate of available materials make ALD a versatile technique for synthesizing nanostructured materials. At Argonne we are pursuing a variety of new applications for ALD including photovoltaics, catalysis, and energy storage. A central theme in these efforts is that we use ALD to apply precise, conformal coatings onto nanostructured scaffolds to impart the desired optical, electrical, or chemical properties to advance these technologies.

9:05 AM Invited

One Dimensional Nanomaterials Synthesis Using Atomic Layer Deposition: *Hyungjun Kim*¹; ¹Yonsei University

Atomic layer deposition (ALD) has been considered as a promising thin film deposition technique for nanoscale semiconductor device fabrication. Recently, however, the exclusive benefits of ALD make it viable tool for nanotechnology. In this presentation, I will present several examples on the one dimensional nanomaterials synthesis using ALD. Due to its excellent conformality, ALD is an ideal technique to produce nanomaterials with combination of nanopatterning techniques. Utilizing highly conformal Ru and ZnO ALD with nanotemplates, 1 D nanomaterials were fabricated. Moreover, by adding SiH4 to the NH3 plasma reactant during Co plasmaenhanced ALD process, Co nanorods array was formed on Si substrates without using nanotemplates. Also, by applying highly conformal ALD processes for transition metals followed by annealing, silicide nanowires were synthesized. The physical and structural properties of these nanomaterials were investigated by various analysis techniques.

9:35 AM

Recent Progress on Synthesis and Characterization of Boron-based One-Dimensional Nanostructures: *Terry Xu*¹; XiaoXia Wu¹; Zhe Guan¹; Youfei Jiang¹; ¹UNC Charlotte

Boron-based (i.e., boron and metal boride) one-dimensional (1D) nanostructures have recently attracted much attention due to their predicted superior electrical and mechanical properties. Combining with other properties such as low density and high chemical stability, boron-based 1D nanostructures are appealing candidates for applications such as thermoelectric energy conversion, nanocomposites and nanoelectronics. In this presentation, our recent progress on synthesis and characterization of boron-based nanomaterials, such as α -tetragonal boron, MB₆ (M=Ca, Sr and Ba), and B₄C-type 1D nanostructures will be reviewed. Special discussion

will be on (1) the need of carbon to achieve high volume fabrication of a-tetragonal boron nanostructures, (2) Young's modulus measurement of MB_6 1D nanostructures and α -tetragonal boron nanostructures, and (3) thermal stability of α -tetragonal boron nanostructures. The thermoelectric property of these boron-based nanostructures will also be briefly discussed.

9:50 AM

Superhydrophobicity of Boron Nitride Nanotubes Structures: Chee Huei Lee¹; *Jaroslaw Drelich*¹; Yoke Khin Yap¹; ¹Michigan Technological University

Boron nitride is a chemically inert, resistive to oxidation up to 900\176C, and transparent to visible-UV light, potentially attractive insulating material for applications under rigorous chemical and thermal conditions. Recently, we also demonstrated (Langmuir 25(9), 2009, 4853-4860) that boron nitride nanotubes can be structured into a superhydrophobic coating. Dense structures of partially vertically aligned boron nitride nanotubes demonstrate excellent water repellency, with advancing and receding contact angles exceeding 150 and 140 degrees, respectively. Boron nitride nanotubes demonstrate superhydrophobicity in both air environment and oil phase. Our results also show that the pH value of water does not affect wetting characteristics of boron nitride nanotubes. On a contrary, lowering the surface tension of liquid by adding ethanol to water reduces the receding contact angle to nearly zero value.

10:05 AM Break

10:20 AM Invited

Solution-Synthesized ZnO Nanomaterials for Hybrid Solar Cells: Julia Hsu¹; ¹University of Texas at Dallas

There has been great interest in hybrid organic:inorganic solar cells due to their potential for large-scale, cost-effective solar cells. These devices commonly use zinc oxide (ZnO) as the electron acceptor and a conjugated polymer, e.g. poly(3-hexylthiophene), as the electron donor. ZnO nanomaterials are readily synthesized using solution methods. In this talk, I will review using various ZnO nanomaterials for hybrid solar cells. For example, by changing the pyrolysis temperature in the sol gel process, we are able to reduce the size of ZnO crystallites. Consequently, the band gap of the ZnO acceptor is increased due to greater quantum confinement, leading to a larger donor-acceptor energy level offset. We find that a direct correlation between the increase in ZnO Eg and device open-circuit voltage. Nanomaterials enables larger donor-acceptor interfacial area. I will also discuss the gain in device performance by using ZnO nanomaterials in the active layer.

10:50 AM

Unipolar Assembly of ZnO Rods: Polarity Driven Collective Luminescence: *Ujjal Gautam*¹; Masataka Imura¹; Xiaosheng Fang¹; Yoshio Bando¹; Dmitri Golberg¹; ¹National Institute for Materials Science

Crystal assemblies are omnipresent and are useful for many devices. Nature too has shown phenomenal control over biomineralization processes to produce exquisite looking crystal assemblies. We have discovered a new phenomenon associated with concentric assemblies of ZnO rods. Usually, a ZnO rod always has an intrinsically positive and a negative polar end induced by the non-centrosymmetric arrangement of Zn and O atoms. We found two distinct types of assemblies wherein all the rods in a single assembly emanate out of a central core maintaining a single polar direction. Due to growth along the two polar surfaces with different atomic arrangements, these assemblies are distinct in their intrinsic properties and exhibit strong UV luminescence in the exterior of Zn-polar assemblies, unlike the O-polar assemblies. While novel applications can be envisioned, these observations suggest that hierarchical organization with respect to internal asymmetry such as polarity might be widespread in natural crystal assemblies.

11:05 AM

Hierarchical Graphene Nanomaterials and Applications: *Cengiz Ozkan*¹; ¹University of California

I will first describe the patterning of DNA molecules and block copolymers on CVD grown large-area graphene layers to modulate their



electronic properties. DNA molecules are found to act as negative potential gating agents that increase the hole density in single layer graphene. Highly sensitive and cost-effective field effect transistor biosensors are fabricated based on large area graphene layers. Next, I will describe new classes of CVD grown hierarchical graphene nanomaterials in the form of three dimensional architectures called pillared graphene nanostructures (PGN), which are combinations of graphene floors and carbon nanotube pillars. The dependence of the morphology of large-area PGN on the process conditions was investigated by Raman spectroscopy, SEM, TEM, and HRTEM techniques. The successful transfer of the large area PGN onto arbitrary substrates while keeping the 3D architecture intact is demonstrated. Hierarchical graphene nanomaterials are envisioned for future applications in fuel cells, ultracapacitors and hydrogen storage.

11:20 AM Invited

Atomic Layer Deposition of Al2O3 and ZnO at Atmospheric Pressure in a Flow Tube Reactor: *Gregory Parsons*¹; Jesse S. Jur¹; ¹North Carolina State University

Atomic layer deposition typically proceeds at ~1 Torr because the pressure is high enough to minimize precursor/reactant gas mixing, and the pressure is sufficiently low so that precursors with moderate vapor pressure can be delivered directly into the growth zone. Recently, to investigate capabilities of continuous ALD processes at under atmospheric pressure, our group developed a unique flow tube ALD reactor that operates at pressures between ~1 and 760 Torr. We have characterized ZnO and Al2O3 film growth versus pressure, and used it on several soft material substrates, including polypropylene, nylon-6 and cellulose cotton. We find that ALD growth can be readily achieved for ZnO, whereas some excess growth is observed consistent with ALD+CVD for Al2O3 growth under similar conditions. We will discuss likely mechanisms for these differences, and present possible new applications of ALD performed at atmospheric pressure.

11:50 AM

Boron Carbide-Nanowires/Carbon-Microfiber Hybrid Structures and Composites from Cotton T-shirts: Xinyong Tao¹; Lixin Dong²; Xinnan Wang¹; Wenkui Zhang³; Bradley Nelson²; *Xiaodong Li*¹; ¹University of South Carolina; ²ETH Zurich; ³Zhejiang University of Technology

Boron carbide-nanowire/carbon-microfiber hybrid structures have been fabricated using a cotton T-shirt as both the template and carbon source. The boron carbide nanowires exhibit a high elastic modulus of 428.1 GPa and elastic recovery after multiple high-strain bending cycles without brittle failure or obvious residual deformation for the strain up to 45%. The boron carbide-nanowire/carbon-microfiber hybrid structures can block 99.8% UV irradiation and achieve a superior reinforcing effect in their epoxy composites. The boron carbide-nanowire formation mechanisms and corresponding synthesis techniques presented here can be extended to other carbide nanowires such as SiC, TiC, MoC, and WC by introducing suitable carbide-sources and catalysts.

12:05 PM Concluding Comments

2nd International Symposium on High-Temperature Metallurgical Processing: Refractories, Slag and Recycling

Sponsored by: The Minerals, Metals and Materials Society, TMS Extraction and Processing Division, TMS: Pyrometallurgy Committee, TMS: Energy Committee *Program Organizers:* Jiann-Yang Hwang, Michigan Technological University; Jerome Downey, Montana Tech; Jaroslaw Drelich, Michigan Technological University; Tao Jiang, Central South University; Mark Cooksey, CSIRO

| Tuesday AM | Room: 18 |
|---------------|-------------------------------|
| March 1, 2011 | Location: San Diego Conv. Ctr |

Session Chairs: Patrick Masset, TU Bergakademie Freiberg; Gabriella Tranell, Norwegian University of Science and Technology

8:30 AM

Study on Preparation of High-Quality Synthetic Rutile from Titanium Slag by Activation Roasting Followed by Acid Leaching: Yufeng Guo¹; Shuishi Liu¹; *Tao Jiang*¹; Guanzhou Qiu¹; ¹Central South University

The preparation of high-quality synthetic ruitle from electric furnace titanium slag was systematically investigated by activation roasting followed by acid leaching method. The results showed that impurities such as Ca and Mg in titanium slag can be effectively removed by roasting with phosphoric acid followed by acid leaching and TiO2 grade of the product was markedly improved. High-quality synthetic rutile containing 88.54% TiO2, 0.42% (CaO+MgO) was obtained under the conditions that roasted with 7.5%(wt) H3PO4 at 1000 \176C for 2h, two-stage leached in sulfuric acid of boiling for 2h. Mechanism studies showed that anosovite solid solution and silicate minerals were reacted with phosphoric acid in the roasting process, as a result, titanium components in titanium slag turned into rutile TiO2, impurities turned into acid-soluble phosphate and quartz, therefore, the structures of anosovite solid solution and silicate minerals were destroyed, which is favorable for impurities' removing.

8:50 AM

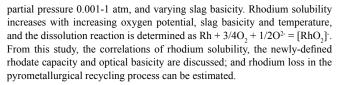
Calculation of Phase Equilibria Relations in CaO-SiO2-FeOx-MgO System: Cuihuan Huang¹; ¹Northeastern University

SiO2, CaO, Al2O3, Fe2O3, Na2O and MgO account for more than 90% by weight of the bottom ash slag from municipal solid waste incineration. These compositions have direct effect on the harmless disposal and efficient utilization of bottom ash alsg. The phase transformation and phase relations of sub-systems in CaO-SiO2-FeOx-MgO system was considered to be important to provide essential data for the thermodynamic properties of the CaO-Al2O3-SiO2-FeOx-MgO-Na2O system.Based on FactSage software, a set of optimized parameters for the thermodynamic properties of CaO-SiO2-FeOx-MgO system was obtained, and the phase equilibria relations were calculated for different temperatures and oxygen partial pressures. Spinel solid solution emerged with the increase of partial pressure of oxygen, which changed the phase relations in FeOx-rich area, and the liquid phase region moved to the poor-FeOx area in MgO-SiO2-FeOx system. At 1873K and 10-8atm oxygen partial pressure, MgO solid phase can be found in CaO-SiO2-FeOx-MgO system.

9:10 AM

Dissolution Behavior of Rhodium into Molten Slag: Chompunoot Wiraseranee¹; Toru Okabe¹; Kazuki Morita¹; ¹The University of Tokyo

Due to very limited resources, recycling of rhodium becomes essential so that rhodium can be sustainably used. By the pyrometallurgical recycling process, rhodium can be separated from various impurities. However, the rhodium dissolution behavior in the process is not yet clarified; thus rhodium loss into slag cannot be estimated. Aiming at the development of more effective recycling processes, rhodium dissolution behavior into molten slag was investigated. Using a pure rhodium crucible and Na₂O-SiO₂ slag system, equilibration experiments carried out for 18 h at 1423-1573 K, under oxygen



9:30 AM

"One Step" Technology to Separate Copper, Zinc, Lead from Iron in Metallurgical Slag and Pyrite Cinder: Part 2- Pilot Test: *De-qing Zhul*; Dong Chen¹; Jian Pan¹; Yu Cui¹; Tie-jun Chun¹; ¹Central South University

A study of processing pyrite cinder and metallurgical slag using "one step" technology in strand grate - rotary kiln is presented, which aims to efficiently recover valuable metals of iron, lead, zinc and copper. The effect of chlorination roasting parameters including roasting time and temperature on the nonferrous metal removal rate was investigated. It is shown that copper and zinc are low removed and lead is removed more easily. Then the preheated pellets were reduced in rotary kiln, which indicates zinc and lead can be removed easily and high iron grade and good metallurgical performance prereduced pellets can be obtained. Furthermore, the chlorination and reduction mechanisms of copper, lead and zinc are discussed. It is revealed that the phases of copper, lead and zinc in slag are complex and ferrite and silicate of metals are hardly removed.

9:50 AM

Effect of Oxygen to Alumina Ratio on the Viscosity of Aluminosilicate and Aluminate Systems: *Jifang Xu*¹; Jieyu Zhang¹; Chang Jie¹; Fei Ruan¹; Kuochih Chou¹; ¹Shanghai Key Laboratory of Modern Metallurgy and Material Processing, Shanghai University

Viscosity is an important physical parameter of slag in metallurgical process. Most of studies of aluminosilicate and aluminate systems assume that aluminum occurs in tetrahedral coordination. In this case the O/Al value was utilized to describe the slag structure in terms of the network character of aluminosilicate and aluminate systems. Data of composition and viscosity were come from the literatures, and the trends have been analyzed according to the O/Al value and temperature. It is shown that the O/Al value can be used to explain the trends in more than ten systems successfully, containing more than 200 data points. In aluminosilicate system, the trend that viscosity value changed with the O/Al value implied that alumina works as network modifier such as basic oxides or works as network former. In aluminate system, irrespective of the system and temperature, viscosity would decrease steadily when O/Al value increasing.

10:10 AM Break

10:20 AM

Blast Furnace Burdens Preparation from Blast Furnace Burdens Preparation from Metallurgical Dusts and Sludges with Composite Binder: Kecheng Zhang¹; *Yuanbo Zhang*¹; Tao Jiang¹; Guanghui Li¹; Zhucheng Huang¹; ¹Central South University

With rapid development of Iron and Steel industry, plenty of metallurgical dusts & sludges are generated, which have not been effectively utilized because of their poor hydrophilicity and bad ballability. Agglomeration and roasting of metallurgical dusts & sludges with a new-type composite binder are studied in this paper. The results indicate that the dosage of the new binders can be decreased to 2.5% from 3.5% when using the wet-grinding process. Under the optimal conditions of briquetting pressure 2070 N/cm2, briquetting moisture content 13%, roasting temperature 1000° and roasting time 40 min, the qualities of the green, dry and roasted briquettes meet the requirements of the industry production. The finished products have the compression strength of more than 2000 N/cm2, which can be used as high-quality burdens for blast furnaces.

10:40 AM

Determination of FeO Containing Liquid Slag Surface Tensions Using the Sessile Drop Method: *Clemens Schmetterer*¹; Patrick Masset¹; ¹TU Bergakademie Freiberg

Surface and interfacial tensions are important properties of slags for the virtualization of the blast furnace process, since they influence the interactions between the components in the blast furnace, e.g. at the slag – Fe interface. In this work the dependence of the surface tension of Al2O3 – CaO – SiO2 mixtures with varying FexO content and oxygen partial pressure was determined at different temperatures using the sessile drop technique with boron nitride (BN) as a substrate material under partial oxidation conditions. In addition, structural investigations using powder X-ray diffraction and Mössbauer spectroscopy (Fe3+/Fe2+ ratio) on quenched specimens were performed as a start in developing a model combining the slag structure, the surface tension and its thermodynamic properties. The obtained experimental data will be discussed with respect to the slag structure and will be compared to results reported in the literature and obtained from modelling.

11:00 AM

Preparation of Partially Stabilized Zirconia and Interface Structure Analysis: *Dong Bo Li*¹; Sheng Hui Guo¹; Li Jun Liu¹; Jin Hui Peng¹; Li Bo Zhang¹; Cheng Dong He¹; ¹Kunming University of Science & Technology

In present study, partially stabilized zirconia(PSZ) was prepared from CaO doped fused zirconia heated by Microwave furnace at the temperature of 1450° and holding time of 120 min. The characterization of XRD results show that untreated fused zirconia mainly consists of crystalline compounds of cubic ZrO2 phase; while the roasted one mainly composed of crystalline compounds of cubic ZrO2 phase and monoclinic ZrO2 phase. It is shown through the optimization of structures of two phases that structure of cubic ZrO2 and monoclinic ZrO2 reject, revealing its difficulty of forming coinciding interface and linkage of two phases being of Ca atom.

11:20 AM

Characteristic of Mineralization of Specularite Iron Ores during Composite Agglomeration Processing: Helei Zhang¹; Heng Yu¹; *Guanghui Li*¹; Yuanbo Zhang¹; Qian Li¹; Tao Jiang¹; ¹Central South University

Large reserves of specularite iron ores had been found all over the world, which is characterized as high total iron grade, low gangues content, as well as low commercial price. However, it has not been widely used in sinter or pellet production due to its inferior sintering and roasting characters. It has shown that the proportion of specularite ores reaches as high as 40%~50% and achieves good results by using Composite Agglomeration Process (CAP), an innovative agglomeration process invented by Central South University. But the mineralization of specularite is still unknown during composite agglomeration processing. In this paper, the induration characteristics of specularite ore is studied by simulating CAP in laboratory, as well as phase and microstructure analysis of CAP product. The results show that specularite pellet is mainly indurated through recrystallization of Fe2O3, calcium ferrite within high basicity sinters matrix interweaves with the recrystallized Fe2O3 on the surface of the pellet, which forms an integral microstructure, and ensures high strength of CAP product for ironmaking.

11:40 AM

Enrichment Behavior of Phosphorous in CaO-SiO2-FetO-P2O5 Based Slag: *Yingying Shen*¹; ¹Northeastern University

As a by-product of steelmaking, not only environmental pollution can be removed, but also huge economical benefits can be created if reutilization of steel slag can be developed deeply. In order to enhance the reuse of convert slag to the metallurgical flowsheet, it's need to promote the enrichment of phosphorous to phosphorous-containing phase and separate the phosphorouscontaining phase from steel slag to avoid the deterioration of refining process caused by the accumulation of phosphorous. In this paper, the enrichment behavior of phosphorous to CaO-SiO2 particle in CaO-SiO2-FetO-P2O5 based slag was studied and the phosphorous contents in the molten bulk slag, as well as the interior and surface of 2CaO•SiO2 particle for different temperatures were also investigated. The enrichment process of phosphorous in CaO-SiO2-FetO-P2O5 based slag can be considered to be mix-controlled



by the two steps of diffusion in molten bulk slag and internal diffusion through 2CaO•SiO2-3CaO•P2O5 solid solution reactant layer.

Advances in Science-Based Processing of Superalloys for Cost and Sustainment: Residual Stress and NDE Technologies for Components

Sponsored by: The Minerals, Metals and Materials Society, TMS Materials Processing and Manufacturing Division, TMS Structural Materials Division, TMS/ASM: Computational Materials Science and Engineering Committee, TMS: High Temperature Alloys Committee, TMS: Advanced Characterization, Testing, and Simulation Committee

Program Organizers: Donna Ballard, US Air Force; David Furrer, Pratt & Whitney; Paul Jablonski, US Department of Energy; Christopher Woodward, Air Force Research Laboratory; Jeff Simmons, AFRL; Mark Blodgett, Wright-Patterson AFB

| Tuesday AM | Room: 33B |
|---------------|-------------------------------|
| March 1, 2011 | Location: San Diego Conv. Ctr |

Session Chairs: Mark Blodgett, Wright-Patterson AFB; Reji John, Air Force Research Laboratory

8:30 AM Introductory Comments

8:35 AM Invited

Predicting and Managing Bulk Residual Stresses within Superalloys: Ronald Wallis¹; ¹Wyman Gordon Forgings

The residual stresses developed in superalloy forgings during heat treatment result in a number of potential problems during subsequent manufacturing. They may lead to distortion of the forging which results in extra material being needed to ensure a part may be manufactured from it. The residual stress pattern may also lead to issues in machining the final component from the forging (the part moving during machining as the stresses attain a new equilibrium). A brief history of the numerical calculation of residual stresses during heat treatment (data needed and validation) is presented together with some examples of typical results obtained. The paper also gives examples where modifications to the manufacturing process have resulting in alleviating the problems. Finally the paper discusses more recent developments where models together with more versatile production equipment has been adopted to control the magnitude and distribution of residual stresses developed in a forging.

9:05 AM Invited

Microstructural Effects on Electrical Resistivity in Comparison to Residual Stresses and the Implications for Eddy Current Methods in Measuring Residual Stress in IN718: *Triplicane Parthasarathy*¹; Pavel Mogilevsky¹; Sonya Boone¹; Satish Rao¹; Peter Nagy²; Mark Blodgett³; ¹UES, Inc.; ²Univ. of Cincinnati; ³Air Force Research Laboratory

As part of a sustainment program, the ability to measure residual stresses on the surface of turbine disks using eddy current methods has been of great interest. In IN718, a widely used disk alloy, initial results have shown that complex metallurgical phenomena interfere with this approach yielding an anomaly in eddy current measurements. The objective of this work was to determine the various possible metallurgical factors that might affect electrical resistivity and to identify the one that is responsible for the anomaly. A systematic investigation was carried out to evaluate and model the effects of chemistry, heat treatment, plastic deformation and recovery after cold work during annealing on the electrical resistivity of an IN718 alloy. The results were analyzed using semi-empirical models. The experimental results were fit to analytical models for use in calibrating eddy current methods for measuring residual stress in shot-peened or LPB treated engine parts.

9:35 AM Invited

Modeling and Simulation of Residual Stresses Resulting from Superalloy Processing: *Wei-Tsu Wu¹*; Ravi Shankar¹; Alex Bandar¹; Byung-Kwan Chun¹; ¹Scientific Forming Technologies Corp

To meet the demands of increasing thrust and higher operating temperatures, sophisticated nickel based superalloy turbine disks are processed with spatially varying properties. Dual Microstructure Heat Treatment (DMHT) induces fine grained, high strength, fatigue resistant microstructure at the bore, while creating coarser grained, creep resistant microstructure at the rim. Accurate modeling of disks under thermal-mechanical loading require appropriate initial conditions, including variation of microstructure and properties resulting from forging, heat treatment, and machining. Current approach is to couple the multi-physics phenomena: heat transfer, non-linear deformation, and micro-structure evolution. The mechanical properties, such as flow stress, Young's modulus, creep property, etc evolve due to changes in microstructure during the thermo-mechanical processes. The microstructure evolution is impacted by changes in temperature and deformation history, and precipitation kinetics. To demonstrate the methodology, a dual microstructure heat treatment process (DMHT), followed by machining (material removal), and spinning process were simulated and presented.

10:05 AM Break

10:20 AM Invited

Probabilistic Fatigue Life-Prediction of Turbine Engine Materials: *Reji John*¹; Sushant Jha²; Michael Caton¹; James Larsen¹; Patrick Golden¹; ¹Air Force Research Laboratory; ²Universal Technology Corporation

Physics-based probabilistic methods are essential in appreciably reducing the uncertainty in fatigue life prediction. Towards this objective, the role of competing mechanisms in producing dual-fatigue variability behavior in turbine engine materials is discussed. The competing modes could be related to randomly occurring microstructural configurations, differing in the degree of heterogeneous deformation accumulation in fatigue. The fatigue variability is described as a sequence of mechanisms, probabilistically originating from these configurations, in the order of decreasing heterogeneity level. These mechanisms separated into two primary contributions to the lifetime probability density: (i) the mean-lifetime response and (ii) the crack-growthcontrolled, life-limiting behavior. A model incorporating this dual behavior was developed and provided reasonable predictions of the influence of material and extrinsic variables on the lifetime density and the probabilistic lifetime-limit.

10:50 AM Invited

Advancements in NDE Technologies to Support Superalloy Component Lifing: R. Thompson¹; *Norio Nakagawa*; Lisa Brasche¹; ¹Iowa State University

NDE has a well established role in managing the lives of superalloy components such as the rotating disks in aircraft engines. Historically, this has been based on the detection of flaws, a capability that is quantified by the Probability of Detection. NDE techniques often employed for this purpose and the lifting strategies employed by the U.S. Air Force and Federal Aviation Agency, based on this strategy will be briefly reviewed. Attention will then turn to emerging NDE techniques that are intended to detect more subtle microstructural features that also influence component lifting, such as grain structure, dislocation density, inclusions, texture and residual stress. The current status of such techniques will be discussed. Finally, potential Bayesian strategies for integrating this information with the predictions of failure models to make lifetime predictions will be outlined.

11:20 AM

Nondestructive Evaluation of Microstructure in Super Alloy Disk Material: James Blackshire¹; Enrique Medina¹; Jeong Na²; ¹Air Force Research Laboratory; ²University of Dayton Research Institute

Nickel-based super alloy materials with dual-microstructure characteristics are being engineered to increase both fatigue and creep resistance properties in turbine engine disks. Nondestructive evaluation methods are needed to assess grain structure and size distributions, and for estimating material property changes due to thermal and mechanical loads. Ultrasonic measurements represent one of the most promising candidates for characterization, where sound velocity, attenuation, and backscatter are known to be sensitive to microstructure in polycrystalline materials. The feasibility of three ultrasonic measurement approaches is investigated for grain size estimation in dualmicrostructure materials including contact ultrasound, scanning immersion ultrasound, and scanning laser vibrometry detection of ultrasound energy. Finite element models are also used to study the ultrasonic forward problem, where the characteristic response of ultrasonic waves propagating through coarse and fine grain microstructures is investigated. Results indicate that qualitative measurements of coarse grain, transition, and fine grain regions are possible in realistic geometry samples.

11:40 AM

Application of Model-Based Inversion to Materials Characterization: *Harold Sabbagh*¹; R. Murphy¹; Elias Sabbagh¹; John Aldrin²; ¹Victor Technologies, LLC; ²Computational Tools

Model-based inversion (MBI) is of increasing importance in eddycurrent nondestructive evaluation (NDE). We apply MBI to two important problems: characterizing ferritic stainless steels and characterizing thermal barrier coatings. Ferritic stainless steels are being increasingly used in heat-exchanger tubes because of the increased resistance to chloride stress corrosion and intergranular attack. This presents interesting modeling opportunities for the eddy-current NDE of these tubes because their magnetic permeability is quite large, being of the order of 950 for low stress, decreasing to 500 for a state of shear stress. We will present examples of direct and inverse problems involving such tubes, using the proprietary code VIC-3D(c). The application of NDE to high-temperature coatings is one of the important factors in achieving a high level of structural integrity in advanced gas turbines. We will demonstrate that sophisticated eddy-current inverse techniques can be utilized to measure the thickness and remaining life of high-temperature coatings.

12:00 PM

Conductivity Profile Determination via Model-Based Inversion of Swept Frequency Eddy Current Data and Its Use for Near-Surface Material Characterization: Norio Nakagawa¹; *Chester Lo*¹; Anatoli Frishman¹; ¹Iowa State University

This paper reports on a nondestructive residual stress characterization methodology for superalloy components having residual stresses ranging in depth between tens of micrometers and an order of a millimeter. Using high frequency eddy current (EC) instrumentations, we measure the near-surface conductivity deviation profiles and relate them to the residual stress profiles via the piezoresistivity. We have been examining precipitation hardened superalloys such as Inconel 718, while recently adding other types of superalloys in the scope of applications. When inverting swept frequency impedance data into conductivity deviation profiles, we utilize the lift-off normalized vertical component signals for direct comparison with model predictions without being adversely affected by instrumentation and lift-off noise. The critical step is to convert conductivity profiles into residual stress profiles, where the apparent piezoresistivity is strongly affected by the specific material conditions. We will present recent findings regarding precipitation hardening and other material effects on residual stress characterization.

Alumina and Bauxite: Bayer Process I

Sponsored by: The Minerals, Metals and Materials Society, TMS Light Metals Division, TMS: Aluminum Committee, TMS: Aluminum Processing Committee

Program Örganizers: James Metson, University of Auckland; Carlos Suarez, Hatch Associates Consultants Inc

| Tuesday AM | Room: 17A |
|---------------|-------------------------------|
| March 1, 2011 | Location: San Diego Conv. Ctr |

Session Chair: To Be Announced

8:30 AM

Application of Operation Integrity Management to the Alumina Industry: *Carlos Suarez*¹; Daniel Welshons¹; John McNerney²; Jim Webb²; ¹Hatch Associates Consultants Inc; ²Warren-Fortought Inc

In today's economic environment the Safety of our industry assets – People, Equipment and Processes – have become even more demanding. This paper attempts to provide means to apply Operation Integrity Management System (OIMS) to the Alumina Industry. It discusses what OIM is about, its implementation parameters such as cost and time, as well as an effective way to integrate such a system into refineries day to day operations. A series of Key Process Performance Indicators (KPPIs) are presented as well as an Electronic Knowledge Support System (EKSS) Mockingbird ® as a tool to support the implementation of OIM.

8:55 AM

Influence of Solid Concentration, Particle Size Distribution, pH and Temperature on Yield Stress of Bauxite Pulp: *Carla Barbato*¹; Márcio Nele²; Silvia França³; ¹EQ/UFRJ/CETEM; ²EQ/UFRJ; ³CETEM

In Northern Brazil, bauxite pulp is transported through pipelines to the plant where alumina is produced. In slurry transportation through pipelines, knowing the yield stress value is essential for pumps and pipeline design. Yield stress is the minimum shear stress and corresponds to the first evidence of flow. This rheological property is influenced by some factors, such as: particle form, temperature, particle size distribution and interaction among the particles. Within the context above, the objective of this work is to verify the influence of solid concentration, particle size distribution, temperature and pH on the yield stress of bauxite pulp. It was verified that the yield stress of bauxite slurry increases as solid concentration goes up, decreases with particle size, temperature and pH.

9:20 AM

A New Method of Organics Removal in Bayer Process: *Bai Yingwei*¹; Gao Zhenwen¹; Shen Mingliang¹; Yi Xiaobing¹; ¹CHALIECO

This article introduces briefly main organics sources at Bayer process alumina production and the harms due to accumulation during process flow, specifies the organics removal methods applied generally in world alumina refineries, and explains briefly advantages & disadvantages of each method. The article stresses the new super-concentrated organics removal method developed successfully by CHALIECO GAMI with Guizhou University together, which not only has good organics removal effect (total removal rate of 57~67%), but also removes the carbonates in the process flow.

9:45 AM

Alunorte Expansion 3 – The New Lines Added to Reach 6.3 Million Tons per Year: *Daryush Khoshneviss*¹; Luiz Corrêa²; Joaquim Ribeiro Alves Filho¹; Hans Marius Berntsen³; Ricardo Carvalho²; Daryush Albuquerque Khoshneviss¹; ¹Alumina do Norte do Brasil S.A.; ²Vale S.A.; ³Hydro Aluminium AS

Alunorte started operation in 1995 with a design production capacity of 1.1 Mtpy. Since then the plant was expanded three times and consists today of seven production lines with a total production capacity of 6.3 Mtpy. Expansion 3 was commissioned in 2008 and consists of process lines 6 and 7. Their nominal production capacity was reached after a short startup phase. In Expansion 3 a number of new technology developments were



implemented. The impact of the process modifications applied in lines 6 and 7 compared to the previous lines are discussed with regard to effects on production volume, productivity, alumina quality and availability. However, a number of challenges are associated with the operation of a plant of the size of Alunorte which has grown very fast: the management of seven process lines, the operation of the plant with a very young organization and strong demand for training.

10:10 AM Break

10:20 AM

One Green Field Megaton Grade Large Alumina Refinery with Successful Engineering and Operation Experience: *Luo Xianqing*¹; Yang Xiaoping¹; Yi Xiaobing¹; ¹CHALIECO

Phase I alumina project (1.6million tons/a metallurgical grade alumina) of Guangxi Huayin Aluminum Corporation Limited is one green field construction project with largest disposable investment in China alumina industry, and its diaspore bauxite is difficult to be ground and dissolved with high aluminum and low silicon content. Now two year's operation practice shows that the comprehensive energy consumption per ton alumina production is only 10.51GJ. This article introduces the process scheme and technical measures adopted in the engineering and operation stage for the features of this project.

10:45 AM

Advanced Process Control in the Evaporation Unit: *C. Satish Kumar*¹; Uttam Giri¹; Rosalin Pradhan¹; Tonmoy Banerjee¹; Ramu Saha¹; Pratichi Pattnaik¹; ¹Vedanta Aluminium limited

Energy consumption is a significant constituent of production cost in an Alumina refinery. Indian refineries are striving to reach global benchmarks and have made conscious efforts to minimize energy consumption. Evaporation plays a significant role in conserving energy and is responsible for 30% of the thermal energy consumption. In the Evaporation unit, due to a large number of interacting processes, frequent disturbances and the presence of single line equipment, it is necessary to maximize the utilization of assets to ensure the production volumes at targeted efficiencies. The need for reduction in process variability resulting in optimizing operations, challenged by plant constraints, was derived by adopting Advanced Process Control (APC) application in the Evaporation unit. APC incorporates a matrix of modeled dynamic process responses with an optimizer to maintain the unit at the most profitable vertex of the allowable operating envelope. This paper will discuss the area selection criteria, activities carried out during the project tenure and post benefit analysis.

11:10 AM

Reduction in Metallic Impurities by Improvement in Process Control: Ruth Headlam-Shaw¹; ¹Alcoa Minerals of Jamaica

Alcoa's Clarendon Alumina Works recorded a significant improvement in the control of and reduction of impurities in its smelter grade alumina (SGA). This marked improvement came about as a result of a change in green liquor filter technology from gravity sand filtration to short cycle pressure filtration and improvement in process management systems. This paper discusses the impact the change had on Iron,Chromium, Titanium, Phosphorous and Calcia in alumina product.

Aluminum Alloys: Fabrication, Characterization and Applications: Solidification

Sponsored by: The Minerals, Metals and Materials Society, TMS Light Metals Division, TMS: Aluminum Processing Committee *Program Organizers:* Subodh Das, Phinix LLC; Zhengdong Long, Kaiser Aluminum; Tongguang Zhai, University of Kentucky

| Tuesday AM | Room: 14A |
|---------------|-------------------------------|
| March 1, 2011 | Location: San Diego Conv. Ctr |

Session Chair: Hiromi Nagaumi, Suzhou Research Institute for Nonferrous Metals

8:30 AM

Simulation of the Deformation of a Flexible Combo Bag in a DC Aluminium Casting: *Abdellah Kharicha*¹; ¹University of Leoben

In the latest years combo bags were introduced in the DC aluminium casting to give better production results. In order to understand why this is the case, hydrodynamic simulations are performed. The movement of the Combo bag surface is modelled though the introduction of particles markers. The particles are allowed to move according to a dynamic law using an assumed flow-bag drag interaction. An additional artificial elastic force is introduced between neighbour particles in order to keep the total bag surface constant. The specificity of the present liquid/bag drag is not only its dependence on the relative movements, but also on the relative liquid velocity/bag surface angle. This kind of fluid/structure approach allows a full coupling between the liquid flow hydrodynamic and the bag shape movement. The results will focus on the quantification of the impact of the bag on the global heat transfer and solidification pool shape.

8:50 AM

Solidification Analysis of Al-Si Alloys Modified with Addition of Cu Using In-Situ Neutron Diffraction: *Dimitry Sediako*¹; Wojciech Kasprzak²; Ian Swainson³; Ovidiu Garlea⁴; ¹National Research Council Canada ; ²CANMET-MTL, Natural Resources Canada; ³National Research Council Canada; ⁴Oak Ridge National Lab

The potential of application of in-situ neutron diffraction for studies of solidification of Al alloys were earlier reported by the authors for the binary hypereutectic A-Si system. This illustrated the potential of neutron diffraction for high resolution melt analysis at near-liquidus temperatures required for advanced studies of grain refining, eutectic modification, etc. The solid and liquid volume fractions were determined based on the change of intensity of neutron diffraction peaks over the solidification interval. The path of non-equilibrium solidification for the alloy modified with addition of copper and magnesium is very complex. Phase diagrams and FactSage-based computations give only approximate kinetics of solid phase(s) evolution during cooling and solidification. On the other hand, in-situ neutron diffraction, coupled with the results of thermal analysis, provided non-biased experimental data on phase evolution; for example, on formation of FCC Al-Cu-Si, diamond silicon, and Al-Cu theta phase during solidification of hypereutectic Al-Si-Cu alloy.

9:10 AM

Development of Novel Grain Refiner for Al-Si Alloys: *Magdalena Nowak*¹; Hari Babu Nadendla¹; ¹BCAST

A novel effective grain refiner for aluminium alloys has been developed. The composition of the grain refiner has been optimised to produce a fine grain structure for Al-Si alloys. Effectiveness of grain size under various cooling conditions has also been investigated to simulate various practical casting conditions. For comparative purposes, a wide range of Al alloys have been produced with the addition of commercially available Al-STi-B master alloys. The results show that the addition of novel grain refiner reduces the grain size significantly when compared to that of the commonly used Al-STi-B grain refiner addition. As a result of fine grains, the porosity in the

9:30 AM

Application of Neutron Diffraction in Analysis of Residual Stress Profile in the Cylinder Web Region of As-Cast V6 Aluminum Engine Block with Cast-In Iron Liners: *Dimitry Sediako*¹; Ravi Ravindran²; Camden Hubbard³; Francesco D'Elia²; Anthony Lombardi²; Alan Machin²; Robert Mackay⁴; ¹National Research Council Canada ; ²Ryerson University; ³Oak Ridge National Laboratory; ⁴Nemak of Canada

Nowadays aluminum alloys are widely used for production of gasoline engine blocks. In this study 319 aluminum is sand cast around Fe-liner cylinder inserts, then undergoes the T7 heat treatment process. One of the critical factors determining the quality of the final product is the type, level, and profile of residual stresses along the Fe liners (or extent of liner distortion) that are always present in a cast component. In this study neutron diffraction was used to characterize residual stresses along the Al and the liners in the web region of the cast engine block. The strains were measured both in aluminum and iron in hoop, radial, and axial orientations and stresses were determined using generalized Hook's law. The study gives invaluable insight on anticipated service properties of the engine block and demonstrates that neutron strain mapping is an efficient tool for optimization of manufacturing technologies.

9:50 AM

Surface Modification of Aluminum Alloys by Electrolytic Plasma Processing: *Mark Liu*¹; Xijin Li; Ben Li Luan¹; ¹National Resaerch Council Canada

Aluminum alloys are widely used as lightweight materials in the transportation industry. For applications in aggressive wear and corrosive environments, proper surface treatment and protection of aluminum alloys are required. Electrolytic plasma processing is a relatively new surface coating technology that offers an environmentally friendly and cost effective solution for the surface protection of lightweight materials. In this presentation, the effect of electrolyte chemistry and various processing parameters on the microstructure, phase constituents, and the properties of the surface coating of aluminum alloys is discussed.

10:10 AM Break

10:25 AM

Solidification Characteristics of Aluminium Alloys under Electron Beam Fabrication Conditions: *Ma Qian*¹; Dacian Tomus²; ¹The University of Queensland; ²Monash University

Wire-based electron beam direct manufacturing (EBDM) is a novel layer additive near-net shape metal fabrication technique. The process can be advantageous for aluminium alloys if new compositions can be created that leverage the near rapid solidification conditions inherent to the process. As most structural aluminium alloys utilize some form of precipitation strengthening, to capitalise on the EBDM attributes, it is important to understand the as-solidified microstructural characteristics under electron beam fabrication conditions. This paper describes the results of an investigation of the microstructures of electron beam processed AA 2219 and AA 6061 alloys and binary Al-Sc and Al-Ti alloys. Electron beam processing led to unique microstructural features in each alloy. The experimental observations are compared with Thermo-Calc predictions for metastable solidification. It will be demonstrated that electron beam processing offers promising alloy design opportunities for advanced aluminium alloy development.

10:45 AM

Formation of Intermetallic Compound Layer between A356 Al Alloy and Cast Iron in Isothermal Condition.: *Kwang Suk Son*¹; Sungmin Kang¹; Jinsu Kim¹; Donggyu Kim¹; ¹Dong-A university

A356 alloy and cast iron have many advantages for industrial purpose despite of insufficient properties. Bonding of dissimilar materials which would compensate their weaknesses, could increase its applicability to the industrial usages. But some problems have been remained in bonding these alloys by casting due to the role of graphite and the complexity of intermetallic compound layer of Al-Fe-Si system. This work, the interactions between liquid A356 alloy and cast iron, and the structural investigation of compound layer were performed with the variables of contact temperature and time by hot dip aluminizing. Microstructure of interlayer was investigated by TEM, FESEM and EDS. Intermetallic compound layer showed two growth steps, during and after dipping. Poly crystalline compound layer consisting of t1(Al0.42Fe0.39Si0.15) and \Box (FeAl2) was formed during dipping and columnar ternary phase of \Box (FeAl3) and t5(Al0.72Fe0.18Si0.10) was formed after dipping. In addition, the growth mechanisms of compound layer was also discussed.

11:05 AM

Effects of Al–8B Grain Refiner on the Structure, Hardness and Tensile Properties of a New Developed Super High-Strength Aluminum Alloy: Mohammad Alipour¹; Masuod Emamy¹; *Jafar Rassizadehghani*¹; Mostafa Karamouz¹; Mortaza Azarbarmas¹; ¹University of Tehran

In this study the effect of Al–8B grain refiner on the structural characteristics, hardness and tensile properties of Al–12Zn–3Mg–2.5Cu aluminum alloy was investigated. The results show that by adding 3.75 wt.% Al–8B grain refiner in the cast alloy, the grains can be refined to a fine degree. T6 heat treatment was applied for all specimens before tensile testing. In heat treated condition, the average tensile strength of 500 MPa was found to be increased to 590 MPa for sample refined with 3.75 wt.% Al–8B (0.3 wt.% B). SEM fractography of the fractured faces of several castings showed an overall macroscopically brittle appearance at low magnifications. At higher magnifications, unrefined specimens showed cracking along the grains, whereas B-refined specimens showed cracks in individual intermetallic compounds.

Aluminum Reduction Technology: Environment-Emissions/ Anode Effect II

Sponsored by: The Minerals, Metals and Materials Society, TMS Light Metals Division, TMS: Aluminum Committee, TMS: Aluminum Processing Committee

Program Organizers: Mohd Mahmood, Aluminium Bahrain; Abdulla Ahmed, Aluminium Bahrain (Alba); Charles Mark Read, Bechtel Corporation; Stephen Lindsay, Alcoa, Inc.

| Tuesday AM | Room: 17B |
|---------------|-------------------------------|
| March 1, 2011 | Location: San Diego Conv. Ctr |

Session Chair: Marco Stam, Aluminium Delfzijl

8:30 AM

On Continuous PFC Unrelated to Anode Effects: *Xiping Chen*¹; Wangxing Li¹; Jerry Marks²; ¹Zhengzhou Research Institute of Chalco; ²J Marks & Associates

It was investigated what result in continuous PFC emission unrelated to anode effects in two smelters. Anode current distribution was measured in QY smelter, no obvious correlation was observed between non-homogenous anode current and continuous PFC emission. Bath temperature and alumina concentration were synchronously measured during PFC monitoring in LX smelter, no continuous PFC emit when cells are operated at stable bath temperature and alumina concentration. But no clear relationship among them was concluded and further survey need to be made in other smelters. The effect of feeding mechanism was also investigated. Metal tapping and anode exchange can disturb cells' balance, which result in cell voltage rising, then may cause continuous PFC emission. It is found out that continuous PFC emission only occurs in some particular cells and is different from cell to cell even with the same line current. It is only a small portion in total PFC emission.



8:50 AM

Reduction of Anode Effect Duration in 400kA Prebake Cells: *Wei Zhang*¹; David Wong¹; Michel Gilbert¹; Yashuang Gao¹; Mark Dorreen¹; Mark Taylor¹; Alton Tabereaux²; Melinda Soffer²; Xiaopu Sun²; Changping Hu³; Xuemin Liang⁴; Haitang Qin⁴; Jihong Mao⁵; Xuehui Lin⁵; ¹Light Metals Research Centre; ²Institute for Governance and Sustainable Development; ³China Nonferrous Metals Industry Association; ⁴Henan Zhongfu Industrial Co. Ltd.; ⁵Northeastern University

In order to improve energy efficiency and reduce green house gas emissions, the aluminum smelting industry has been continuously working on reducing both anode effect frequency (AEF) and duration (AED). However, there is still a long way to go to achieve zero anode effect (AE) on very high amperage, low specific power consumption cells due to the added complexity of the process. A new program to quickly terminate AEs has been developed by Light Metals Research Centre, the University of Auckland, in conjunction with the efforts of the Asia Pacific Partnership on Clean Development and Climate (APP) to facilitate investment in clean technologies and to accelerate the sharing of energy efficient best practices. A pilot project was initiated to test an automatic Anode Effect Termination (AET) program on 400kA cells in Zhongfu, China. This paper demonstrates the success of the new anode effect termination (AET) program in killing AEs on this cell technology without conflicting with normal cell operations. The resulting decrease in average anode effect duration (AED) is demonstrated.

9:10 AM

Sustainable Anode Effect Based Perfluorocarbon Emission Reduction: *Neal Dando*¹; Lise Sylvain¹; Janice Fleckenstein¹; Ciro Kato¹; Vince Van Son¹; Laura Coleman¹; ¹Alcoa

Alcoa has been performing plant-specific perfluorocarbon (PFC) emission testing at operating smelters for over 15 years and has the largest Tier 3 data base in the aluminum industry. From 2005-2009, Alcoa smelters have reduced anode effect (AE) based PFC emissions by over 0.48 T CO2e/T Al produced, resulting in an absolute annual reduction of 2.3 million tonne CO2e over this same time period. These PFC reductions were the result of 1) continuous local optimization at operating locations 2) focused monthly reporting on anode effect performance, 3) internal workshops regarding shared AE reduction efforts and 4) technology improvements. This paper will discuss examples of key enablers employed for sustaining AE-based PFC reductions of 15.9 million tonnes over the period 1990 to 2009.

9:30 AM

The Initiation, Propagation and Termination of Anode Effects in Hall-Heroult Cells: *Gary Tarcy*¹; Alton Tabereaux²; ¹Alcoa; ²Consultant

Anode effects in Hall-Herout cells have been the subject of multiple investigations and studies. The current state of the knowledge is fairly well advanced and there is very little discrepancy or controversy with respect to many of the phenomena associated with anode effects. Included in this is the belief they are: 1) AE are the predominate emitter of PFC into the atmosphere 2) AE are triggered by low alumina concentrations near the anode surface 3) Short circuiting of at least part of the anode cathode inter electrode gap is required to terminate an anode effect. This paper will cover some of less discussed aspects of anode effect including the 1) the initiation at a single random anode in the circuit. 2) The propogation to multiple anodes until the whole circuit is on anode effect 3) The reason it is necessary to short circuit the anodes to terminate anode effect.

9:50 AM

Towards Eliminating Anode Effects: *Ali Al Zarouni*¹; Barry Welch²; Maryam Al-Jallaf¹; Arvind Kumar¹; ¹DUBAL; ²Welbank Consulting Ltd

It has been established that the atmosphere contains appreciable amount of per fluorocarbon (PFC) gases. These are powerful greenhouse gases and with extremely long lifetime. Although these gases are being used in the semiconductor industry, it has been established that aluminium smelters are the main source. Emissions of PFC Gases from the aluminium industry have therefore become an environmental issue. The PFCs are emitted from an aluminium reduction cell when it is on an 'anode effect'. The exact nature of the onset of an anode effect is still shrouded in mystery. However, an astounding reduction in number of anode effects has been achieved by understanding, attributing and implementing a strict process control regime to eliminate assignable causes. Dubal's progress in reducing anode effect frequency to less than 0.05 AE/pot-day in a sustained manner in poline 5B has been discussed and presented.

10:10 AM Break

10:20 AM

Monitoring Air Fluoride (F-) Concentration around ALUAR Smelter in Puerto Madryn (Chubut Province, Argentina): *Jorge Zavatti*¹; Claudio Lopez Moreno¹; Juliana Lifschitz¹; Gabriela Quiroga¹; ¹ALUAR Aluminio Argentino SAIC

The emissions of F- is a significant environmental aspects of aluminum industry. Therefore the government have established regulations aimed at controlling the environmental performance of smelters through monitoring of F- emissions. Chubut Province (Argentina), sets emission limits, 1 kg F-/ ton Al and following recommendations by the World Health Organization, they set a guideline for inmission at 16.0 μ g F-/m³. In this paper we present: i)the monitoring network that ALUAR deployed in Puerto Madryn, 14 air sampling stations; ii)sampling procedures and analysis adopted; iii)the results of air fluoride concentration from July 2009 to June 2010; iv)the validation of these results by three scientific institutes of Argentina. The results show that in Puerto Madryn (100000 inhabitants; 2 km from ALUAR's Plant), the median concentration in air was 1.61 μ g F-/m³ (N = 471 – p95 = 5.32). These values met the inmission guideline level determined by the supervisory authority.

10:40 AM

Correlation between Moisture and HF Formation in the Aluminium Process: *Camilla Sommerseth*¹; Karen Osen²; Thor Aarhaug²; Egil Skybakmoen²; Asbjoern Solheim²; Christian Rosenkilde¹; Arne Ratvik¹; ¹Norwegian University of Science and Technology, NTNU; ²SINTEF

Hydrogen fluoride (HF) emission to the working atmosphere is still a problem in the aluminium industry. Moisture in secondary alumina fed to the cell and humidity in the ambient air reacts with fluorides in the bath and fluoride vapours to form hydrogen fluoride. The relation between the various sources of water and the resulting HF emission is still not well understood. In this work, industrial measurements have been done to determine where HF escapes from the bath. The quantities of HF and moisture at the specific sites have also been determined. Measurements were done in the duct during normal operation as well as during anode change, above the feeder hole and above an open hole in the crust. A strong correlation between feed cycle and HF levels was measured. Increased HF emissions were also recorded during anode change.

11:00 AM

Particulate Emissions from Electrolysis Cells: *Heiko Gaertner*¹; Arne Ratvik¹; Thor Aarhaug²; ¹NTNU; ²SINTEF

In the dry cleaning of the exhaust gas from the aluminium cells impurities are accumulated in the finer fractions of secondary alumina from the dry scrubbers. The present work describes new methods for the determination of dust composition, aiming at increasing the understanding of the effect of cell operation on the amount and the composition of dust in the fume. New and advanced analysis methods are used to characterize a broad specter of emissions. An Electrical Low Pressure Impactor is used to sample and analyze the dust from the cells. The equipment enables real-time particle size distribution analysis of 12 particle classes in the range 30 nm - 10 µm. The size classified samples are analyzed by means of SEM/EDS and XRD to determine the characteristic chemical composition of the different fractions. Understanding the evolution, evaporation, and condensation of particulates in the cell emissions under different operational conditions may facilitate new standards for environmental friendly and energy efficient high amperage electrolysis cells.

11:20 AM

Investigation of Solutions to Reduce Fluoride Emissions from Anode Butts and Crust Cover Material: *Guillaume Girault*¹; Maxime Faure¹; Jean-Marc Bertolo¹; Stéphanie Massambi¹; Georges Bertran¹; ¹Rio Tinto Alcan

For many aluminium smelters, reducing fluoride emissions is often a condition to increase production. Since they contribute up to 40% of the overall roof vent emissions, anode change operations are often targeted for improvements and specifically the emissions from the anode butts and crust cover. The Rio Tinto Alcan Research Centre, LRF, has been conducting an R&D programme over the past few years aimed at improving the understanding of the physical phenomena involved and ultimately minimising this specific contribution. On this basis, different conceptual solutions have been developed and their relative performance evaluated. These tests, associated with past experience of enclosed butt boxes and crust bins, concluded that any container receiving a hot butt and bath crust would require almost complete sealing to be effective. The next stage in this programme is engineering design with the aim of developing smelter technology with the lowest environmental footprint.

11:40 AM

PFC Survey in Some Smelters of China: Wangxing Li¹; *Xiping Chen*¹; ¹Zhengzhou Research Institute of Chalco

PFC survey was performed by CHALCO. Results of the first PFC survey from seven different Chinese potlines are discussed in this paper. This survey included normally-operated, newly-started, power-limitation and controlmode changing potlines. The measurement equipment used in the survey is MG2030 FTIR which comes from MKS Instruments. Gas sampling was directly pumped out of main exhaust duct before stack and transmitted into FTIR by Teflon tube. Fugitive PFC emission was not measured. The calculation of PFC amount was based on IPCC Tier 3a method. Total PFC emission was calculated from duct PFC emission divided by collection efficiency. Newly-started, control-mode changing and power-limitation potlines emitted much more PFC than normally-operated ones. PFC emission from power-limitation potline was the highest among seven. Three of seven potlines have PFC emission close to IAI 2010 target. Two potlines have similar PFC emission to Australia 2006 average level. The lowest PFC emission is 0.21 tCO2-e/t-Al.

Approaches for Investigating Phase Transformations at the Atomic Scale: Transformations in Fe, Ni and AI Based Systems II

Sponsored by: The Minerals, Metals and Materials Society, ASM International, TMS Materials Processing and Manufacturing Division, TMS/ASM: Computational Materials Science and Engineering Committee, TMS/ASM: Phase Transformations Committee *Program Organizers:* Neal Evans, Oak Ridge National Laboratory; Francisca Caballero, Spanish National Research Center for Metallurgy (CENIM-CSIC); Chris Wolverton, Northwestern University; David Seidman, Northwestern University; Rajarshi Banerjee, University of North Texas

| Tuesday AM | Room: 32B |
|---------------|-------------------------------|
| March 1, 2011 | Location: San Diego Conv. Ctr |

Session Chairs: Rajarshi Banerjee, University of North Texas; Hamish Fraser, Ohio State University

8:30 AM Invited

Nuclear Reactor Materials at the Atomic Scale: Emmanuelle Marquis¹; Ceri Williams²; Nadine Baluc³; Samuel Humphry-Baker²; ¹University of Michigan; ²University of Oxford; ³Paul Scherrer Institute

The development of next-generation fission and fusion reactors requires new and improved materials, which will withstand extreme combinations of temperature, stress and irradiation. In order to develop these materials, fundamental understanding is required of the atomic-scale behaviour of candidate alloys subjected to extreme treatment. We report progress in the combined use of 3-D atom probe analysis and transmission electron microscopy to study the atomic processes occurring in Fe-Cr,oxide-dispersion-strengthened steels and W alloys after thermal and heavy ion irradiation treatments. In each case, the materials exhibit highly complex patterns of behaviour on the nanometre scale, including solute clustering, segregation to dislocations, grain boundaries and interphase interfaces, and the formation of second phase particles. These phenomena have been quantitatively investigated. Similarities and differences in the behaviour of the different materials will be described, and implications for the optimisation of future reactor materials design will be discussed.

8:55 AM Invited

A Multiple Technique Approach for Understanding Phase Separation in Nanostructured Ferritic Steels: *Michael Miller*¹; C.L. Fu¹; C.M. Parish¹; X.-L. Wang¹; ¹Oak Ridge National Laboratory

Nanostructured ferritic steels are under consideration for use in future generations of advanced nuclear systems due to their stability against high temperature creep and, more importantly, their remarkable tolerance to high dose neutron and ion irradiation. A synergistic combination of first principle calculations with atom probe tomography, transmission electron microscopy, and neutron scattering experiments have been used to understand the phase separation and diffusion processes that occur in these mechanically alloyed, nanostructured ferritic steels. From this multiple characterizations approach, the microstructural features responsible for these remarkable properties, including high number densities of nanoclusters and solute segregation to the grain boundaries, have been identified. This research was sponsored by the U.S. Department of Energy, Materials Sciences and Engineering Division. Research at the Oak Ridge National Laboratory SHARE User Facility is sponsored by the Scientific User Facilities Division, Office of Basic Energy Sciences, U.S. Department of Energy.

9:20 AM Invited

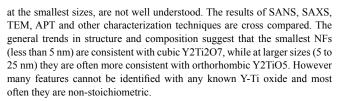
Atomic Scale Investigation of Y-Ti-O Nanoclusters in Nanostructured Ferritic Alloys: *Brian Wirth*¹; Hyon-Jee Lee²; Lauren Marus²; G. Robert Odette³; ¹University of Tennessee; ²University of California, Berkeley; ³University of California, Santa Barbara

Nanostructured ferritic alloys (NFAs) are characterized by very high tensile and creep strength, and resistance to neutron irradiation. These properties result from a very high number density dispersion of nm-scale Y-Ti-O rich features (NFs) that precipitate homogeneously at high consolidation temperatures from mechanically alloyed Fe-Cr-Ti-Y2O3 powders. The NFs have been studied by small angle neutron scattering, atom probe tomography, transmission electron microscopy, positron annihilation spectroscopy, and x-ray absorption spectroscopy. NFs form rapidly at number densities, sizes and characters (compositions and structures) that are dictated by the processing temperature and alloy composition. However, the precise natures of various NFs are not well understood, and appear to range from coherent solute enriched GP-type zones to near stoichometric complex oxides, such as Y2TiO5 and Y2Ti2O7. In this presentation, atomic scale modeling results, developed from ab-initio electronic structure calculations, are presented that provide insight into the structure and composition of the NFs.

9:45 AM

Characterization of Nanofeatures and Oxides in Nanostructured Ferritic Alloys – Cross Comparison SANS, SAXS, TEM, APT and Other Techniques: *G. Robert Odette*¹; Nicholas Cunningham¹; Takuya Yamamoto¹; Yuan Wu¹; Auriane Etienne¹; Erich Stergar¹; ¹UC Santa Barbara

Nano-structured ferritic alloys (NFAs) have high tensile and creep strength permitting service up to 800°C and manifest remarkable resistance to radiation damage. These outstanding properties derive from an ultrahigh density of Ti-Y-O enriched nano-features (NFs) that provide dispersion strengthening, help stabilize dislocation and fine grain structures, reduce excess concentrations of displacement defects by enhancing vacancy-selfinterstitial recombination and trap helium in fine, and relatively harmless, bubbles. However, the compositions and structures of the NFs, especially



10:00 AM

Effect of Elastic Strain on Phase Separation in Fe-20% Cr-6% Al-0.5% Ti ODS Alloy: *Carlos Capdevila-Montes*¹; Mike Miller²; Isaac Toda¹; Jesus Chao¹; ¹CENIM-CSIC; ²ORNL

The effect of elastic deformation on temporal evolution of the microstructure resulting from phase separation of an Fe-20% Cr-6% Al-0.5% Ti oxide dispersion strengthened (ODS) alloy at a temperature of 708 K has been analyzed by atom probe tomography (APT). Microstructures with high (as-cold rolled material) and low (coarse grained recrystallized material) dislocation densities have been tested at both 0.8 and 1 times the yield strength of this material during aging at 708 K. Microstructural analysis by APT revealed simultaneous phase separation kinetics into Fe-rich a, Cr-rich a' and Fe-Ti-Al phases. The roles of Al and Ti during the decomposition process have been investigated. Proximity histogram analysis revealed significant partitioning of Al and Ti, which is consistent with theoretical calculations. Research at the Oak Ridge National Laboratory SHaRE User Facility was sponsored by the Scientific User Facilities Division, Office of Basic Energy Sciences, U.S. Department of Energy.

10:15 AM Break

10:30 AM Invited

Nano-Structural Characterizations Using Advanced Methods - A Case Study of Nanosized Cu Precipitates in C Containing Fe-1.2 Wt% Cu Alloys: *Rajashekhara Shabadi*¹; Roland Taillard¹; ¹University of Science and Technology of Lille, France

This study deals with the sole effect of C on Cu precipitation in Fe-1.2 wt% Cu steels. Four C contents up to 750 ppm were studied. Addition of carbon substantially increases both the kinetics and magnitude of precipitation strengthening up to longer aging times. Advanced methods of characterization such as Small Angle X-ray Scattering (SAXS) and Tomographic Atom Probe (TAP) were adopted to precisely determine the composition, size, density and volume fraction of the nanometer sized precipitates after different aging periods. It was observed that C was not co-precipitated with Cu, but C agglomerations were present close to the precipitates. The accelerating effect on the Cu precipitation is discussed with regards to both the driving force of nucleation and the kinetics of Cu diffusion. Combining results of SAXS, TAP and TEM gave complementary results in following Cu precipitation sequence in the presence of the third alloying element.

10:55 AM

Anharmonic Phonon Behavior in α -Fe at Temperatures near the Structural Phase Transition: *Lisa Mauger*¹; Matthew Lucas²; Jorge Munoz¹; Brent Fultz¹; ¹California Institute of Technology; ²Air Force Research Laboratory

The phonon density of states (DOS) of bcc Fe was measured from room temperature up through the 1185K fcc phase transition using Nuclear Resonant Inelastic X-ray Scattering of ⁵⁷Fe. At higher temperatures all phonons shift to lower energies (soften) with thermal expansion. Above the 1043K Curie temperature, low energy transverse modes soften more rapidly, suggesting strongly anharmonic behavior before the α -Fe to γ -Fe structural transition. Interatomic force constants for the bcc phase were obtained by iteratively fitting a Born von-Karman model to the experimental phonon spectra using a global optimizer. Trends in these force constants are used to interpret the thermal softening of the different phonon modes. The unusually large phonon anharmonicity of the transverse modes at elevated temperatures is assessed with the temperature dependences of the first and second-neighbor interatomic force constants.

11:10 AM

140th Annual Meeting & Exhibition

Atomic Scale Investigation of Gamma Prime Precipitation in Nickel Base Alloys Coupling Aberration-Corrected STEM with Atom Probe Tomography: Antariksh Singh¹; Gopal Viswanathan²; Soumya Nag¹; Junyeon Hwang¹; Jaimie Tiley²; Hamish Fraser³; *Rajarshi Banerjee*¹; ¹University of North Texas; ²Air Force Research Laboratory; ³The Ohio State University

The compositional and microstructural evolution of gamma prime precipitates during continuous cooling at different rates, followed by isothermal aging, of a commercial nickel base superalloy, Rene 88DT, have been characterized by coupling multiple atomic scale characterization techniques. The primary focus was on investigating the mechanisms governing gamma prime precipitation as a function of cooling rate. Classical nucleation and growth is the dominant mechanism of precipitation in case of slower cooling rates, especially at lower undercoolings. In contrast, at faster cooling (quench) rates, the gamma prime precipitation appears to take place via a spinodal clustering (phase separation or compositional partitioning) within the disordered gamma matrix followed by chemical ordering. Direct experimental atomic scale evidence for such a mechanism will be presented based on results of aberration-corrected HAADF-STEM at atomic resolution and atom probe tomography.

11:25 AM Invited

Exploring Initial Stages of Precipitate Formation in Aluminum Alloys through Kinetic Lattice Monte Carlo Simulations: *Marcel Sluiter*¹; ¹TU Delft

The very first stages of clustering that precede precipitation are still poorly understood. However, those stages can be important for the ultimate mechanical properties as empirical treatments such as spike pre aging prior to natural aging during storage in industrial alloys have shown. In order to augment atom probe experiments and to illuminate the role of vacancy-solute interactions, kinetic lattice Monte Carlo simulations have been employed for multicomponent Al alloys with realistic compositions, such as those based on Al-Mg-Cu and Al-Mg-Li. It is shown that these simulations, at least during the initial stages, can yield cluster distributions as function of time that resemble those from atom probe experiments provided that the solutevacancy binding and vacancy dynamics are properly accounted for.

11:50 AM

Primary Crystallization Behavior Change Induced by Minor Element Substitution: *Feng Yi*¹; Seth Imhoff¹; John Perepezko¹; Paul Voyles¹; ¹UW-Madison

Structural characterization by fluctuation electron microscopy (FEM), a technique sensitive to nanoscale order in glasses, combined with conventional techniques including BFTEM, XRD, and DSC, and computer simulations was applied to understand the primary crystallization reaction in Al-based metallic glasses. FEM shows that the glass contains nanoscale, Al-like medium range order (MRO) regions; other kinetics data demonstrate that these regions act as nucleation sites. Comparison of the FEM results to computer simulations indicates that the MRO size *d* and number density \961 are (1.92\177 0.34) nm and (1.81\177 1.67)\215 10²⁵/m³ in Al₈₈Y₇Fe₅. Substitution of 1 at.% Cu for Y decreases the crystallization onset, T_x by 50 \176C with a doubling of \961 while substitution 1 at.% Cu for Al increases T_x by 10 \176C, and reduces \961 by 30%. All the observations are consistent with a classical nucleation theory model including transient kinetics.

Biological Materials Science: Surface Engineering and Biological Interactions

Sponsored by: The Minerals, Metals and Materials Society, TMS Electronic, Magnetic, and Photonic Materials Division, TMS Structural Materials Division, TMS: Biomaterials Committee *Program Organizers:* Jamie Kruzic, Oregon State University; Nima Rahbar, University of Massachusetts, Dartmouth; Po-Yu Chen, University of California, San Diego; Candan Tamerler, University of Washington

| Tuesday AM | Room: 15A |
|---------------|-------------------------------|
| March 1, 2011 | Location: San Diego Conv. Ctr |

Session Chairs: Candan Tamerler, University of Washington; Po-Yu Chen, University of California, San Diego

8:30 AM Introductory Comments

8:35 AM Keynote

Role of Substrate Material Properties in Modulating Cell Fate and Function: *Shu Chien*¹; ¹University of California, San Diego

Variations in physicochemical properties of the substrate can modulate the fate (proliferation and differentiation) of pluripotent stem cells (hPSCs) and the structure and function of adult cells such as vascular endothelial cells (ECs). Using a high-throughput screening approach, we have identified synthetic polymers that can be used as matrix macromolecules to support attachment, proliferation and self-renewal of several types of human hPSCs. Such findings can help to accelerate the translational applications of hPSCs in regenerative medicine. Variations in substrate rigidity under the extracellular matrix (ECM) can also regulate the proliferation and differentiation of hPSCs, with modulations of their mechanical properties. Culture of ECs on ECM seeded on substrates with different rigidity leads to alterations of their intracellular rheology and functional behavior, including signal transduction and gene expression. The material properties of the substrate can exert significant effects on the rheology of cells to modulate cell structure and function.

9:15 AM Invited

Strategies to Promote Mammalian Cell Functions Pertinent to Tissue Formation at the Tissue-Implant Interface: A Materials Perspective: *Rena Bizios*¹; ¹UTSA

Cellular and molecular events at tissue/implant interfaces dictate the fate of implants and, thus, have crucial clinical implications. The need (1) for biomaterials with properties similar to those of physiological tissues (characterized by surface grain sizes in the nanometer range) and (2) for identification/characterization of the optimal conditions, which maximize specific cell functions responsible for neotissue formation surrounding implants in the human body, has motivated investigation of chemical and topographical modifications of existing materials as well as design of nanostructured material formulations and of protein-engineered biomaterials. Biomaterials, which reliably and predictably promote specific interactions of biomolecules leading to targeted modulation of select mammalian cells and/or control of subsequent cell functions pertinent to new tissue formation and regeneration, have the potential of novel biotechnology-related and tissue-engineering-related applications as well as of major clinical impact. This presentation will highlight bio-inspired biomaterials-related accomplishments, current challenges and novel developments of great promise.

9:45 AM

Protein Adsorption on Bioceramic Nanoparticles and Monoliths: *Kenneth Stanton*¹; Éilis McGrath¹; John Gibbons²; Iseult Lynch¹; Kenneth Dawson¹; ¹University College Dublin; ²Royal College of Surgeons in Ireland

When a biomaterial is placed in-vivo, proteins will immediately adsorb to the surface and mediate the response of other biological entities such as cells. Over a short amount of time, a specific group of proteins will form a quasi-equilibrium layer which has become known as the hard-corona while other less-tightly bound proteins comprise the soft corona. The nature of the corona will depend not only on the surface-charge distribution on the material but also on the way the material presents to the medium: i.e. as an effective monolithic surface or as a nano-particle and also on the specific proteins present and finally the nature of the suspension medium. Here, we present the results of protein adsorption experiments using human blood plasma and a range of bio-ceramic materials including hydroxyapatite, alumina and zirconia. Hard coronas are characterized using 1-D SDS-PAGE and the results from nano-particles are compared with those of monoliths.

10:05 AM

Utilization of Diatoms to Collect Metallic Ions: Itaru Jimbo¹; *Takahiro Sekiguchi*¹; HIroaki Onizawa¹; ¹Tokai University

Microalgae have a capability to collect metallic ions from the aqueous solutions for their negatively charged surface. A number of works have already been published where heavy metals could be collected and contaminated water system was cleaned by biological measures. In the present study, diatoms are utilized to collect metallic ions such as silver and lead ions from the aqueous solution. Collecting processes are adsorption of ions on the diatoms surfaces and taking the ions inside the diatoms bodies through the cell membrane. Analyses were accomplished with the observation of the dried specimen with SEM and EPMA. Experimental results revealed that these processes depended both on illumination and temperature. These processes seem to be closely related to photosynthesis. Discussion will also include seasonal variations in the yields of the metals by the diatoms.

10:25 AM Break

10:35 AM Invited

Aligned TiO2 Nanotubes for Strong Osseo-Integration in Orthopaedic Implants: Sungho Jin¹; ¹UC San Diego

For improvement of the structural connection between living bone and implant, vertically aligned TiO2 nanotubes with different dimensions were introduced on Ti implant surface by anodization and used for in vitro and in vivo studies. The presence of surface nanotube structure on titanium orthopaedic implants significantly enhances the kinetics of bone formation and interfacial bond strength as demonstrated by in vitro and in vivo experiments with rabbit and mice. It is also shown that the nanotube geometry has a profound effect on osteoblast and mesenchymal stem cell behavior, with the cell stretching and elongation becoming quite pronounced at a particular nanotube diameter regime, affecting the osseo-integration and bone bonding[1-2]. [1] Karla Brammer, et al, Acta Biomaterialia 5(8), 3215-3223 (2009). [2] Lars M. Bjursten, et al, J. Biomed. Mater. Res. 92A, 1218-24 (2010).

11:05 AM

Surface Free Energy Modification of Titania for Bioactive Surfaces: Kyle Krzywosinski¹; *Molly Gentleman*¹; ¹Texas A&M University

Titanium implants have gained popular use in orthopedic implants, specifically hip implantation. As a result, effort is being made to increase the osseointegration between these load bearing artificial implants and native bone. In previous studies the observed wettability of a surfaces has been shown to be a good indicator of the quality and rate of osseointegration. In this study, the surface energy properties of titanium dioxide, the native oxide on titanium metal implants, is modified by to identify the relationship between surface energy and subsequent osseointegration. It has been demonstrated that thermal exposure increases the wettability of single crystal titania wafers by increasing both the acid and base components of surface energy to oxidation and reduction of the titania surface. These surfaces were then examined for cell adhesion to elucidate this relationship.



11:25 AM

Cellular Response of Grain Boundary Grooved Nanograined/Ultrafinegrained Structures: *Pavan Challa*¹; Devesh Misra¹; ¹University of Louisiana at Lafayette

We describe here the significance of grain boundary grooved nanograined/ ultrafine-grained (NG/UFG) metallic substrates in comparison to planar (non-grooved) NG/UFG substrate in terms of improved surface and biological properties. In this regard, grooving of nano/ultrafine-grains by electrochemical etching is a potential approach to increase the biomechanical interlocking which results in improved cellular response. The differences in the cellular response of planar and grain boundary grooved NG/UFG surface are attributed to favorable surface topography that accelerates the cellular activity. Experiments on the effect of grain boundary grooved NG/UFG substrate indicated that cell attachment, proliferation, viability, morphology, and spread are favorably modulated and significantly different from planar (non-grooved) NG/UFG substrate.

11:45 AM

Enhanced Bone Cell Response on Zirconium Oxide Nanotube Surface: *Christine Frandsen*¹; Karla Brammer¹; Kunbae Noh¹; Sungho Jin¹; ¹University of California, San Diego

The present work investigates the bio-feasibility of a unique verticallyaligned, laterally-spaced nanotube nanostructure made of ZrO_2 fabricated by anodization. The growth, morphology, and functionality of osteoblasts cultured on ZrO_2 nanotubes have been examined. The initial cell response of adhesion and spreading was considerably improved on the nanotube surface as compared to a Zr surface without nanostructure. The morphology of adhered cells on the nanotube surface elicited a highly organized cytoskeleton with crisscross pattern actin, which was lacking on the flat Zr. Increased alkaline phosphatase levels, indicative of increased bone forming ability, and the formation of concentrated calcified extracellular matrix implied improved osteoblast functionality and mineralization on the nanotube substrate. This in vitro study shows that ZrO_2 nanotubes are highly promising as a biomedical implant surface because of their large surface area and unique nanoscale geometry which enhanced the osteoblast response and apparent role in providing a platform for bone growth.

12:05 PM

Quantification of Osteoblast Adhesion Strength on Hydroxyapatite-Carbon Nanotube Coated Bioimplant Surface: Debrupa Lahiri¹; Ana Paula Benaduce¹; Lidia Kos¹; Arvind Agarwal¹; ¹Florida International University

Adhesion of cells on orthopedic implant surface is important for integration of the implant with the bone. This study proposes the nanoscratch technique as an effective method to quantify the shear strength required to detach a single cell, from the underlying substrate. The method has been evaluated for osteoblast cells grown on plastic slides as well as hydroxyapatite (HA) coatings on Ti-6Al-4V alloy, with and without carbon nanotube (CNT) reinforcement. The cells were grown on the plastic slides and HA coatings for 1, 3 and 5 days. The measurement shows no change in the adhesion strength of osteoblast on plastic slides, with increasing culture-time. On the contrary, the adhesion strength of osteoblast increases with culture time for both HA and HA-CNT coated surfaces. Interaction of osteoblast cells with HA is responsible for such behavior. Addition of CNT to HA further increases the adhesion strength of osteoblast to the coating surface.

Bulk Metallic Glasses VIII: Structures and Mechanical Properties I

Sponsored by: The Minerals, Metals and Materials Society, TMS Structural Materials Division, TMS/ASM: Mechanical Behavior of Materials Committee

Program Organizers: Gongyao Wang, University of Tennessee; Peter Liaw, Univ of Tennessee; Hahn Choo, Univ of Tennessee; Yanfei Gao, Univ of Tennessee

| Tuesday AM | Room: 6D |
|---------------|-------------------------------|
| March 1, 2011 | Location: San Diego Conv. Ctr |

Session Chairs: Takeshi Egami, University of Tennessee; John Lewandowski, Case Western Reserve Univ

8:30 AM Keynote

Mechanical Properties of Metallic Glasses: An Atomistic View: Takeshi Egami¹; ¹University of Tennessee

Many mysteries surround the mechanical properties of metallic glasses, and make it a fascinating subject of study. For instance people assume that deformation occurs because of some defects, such as free-volume or shear transformation zones, but nobody seems to have seen them in action. I propose a rather different view, that the "potential" defects are abundant, as much as a quarter in volume fraction. But fluctuations, thermal or otherwise, statistically activate only a few of them, making precise prediction difficult. Defects are defined by topological instability of the nearest neighbor shell, and can be detected by simulation of the structure, static or dynamic under stress, or by diffraction measurements carried out with applied stress. In this view mechanical failure is the stress-induced glass transition, that can occur without heating nor volume dilation. This work was supported by the Department of Energy, Basic Science Program.

9:00 AM

Structural Changes in BMG after Mechanical Fatigue and Pre-Loading: *Wei Guo*¹; Wojciech Dmowski¹; Andrew Chuang¹; Gongyao Wang¹; Yoshihiko Yokoyama²; Yang Ren³; Peter Liaw¹; Akihisa Inoue²; Takeshi Egami¹; ¹University of Tennessee; ²Tohoku University; ³Advanced Photon Source

We studied changes in the atomic structure of bulk metallic glasses after a mechanical fatigue and elastic pre-loading below the yield stress. The Zrbased BMGs were fatigued for 10⁶ cycles with mechanical load amplitude corresponding to 10, 50 and 70% of the elastic limit and 10⁵ cycles at 80%. The mechanical preloading was done for 24 hrs at 1.5 GPa. The x-ray diffraction was carried out at APS using high energy x-rays and the structure function and PDF were determined. Measurements were performed at room temperature and at 5 K. In addition to statistical errors several sample cross-sections and spots were examined to assess systematic errors. Both room and low temperature data indicated small changes in the fatigued samples that were consistent with structural disordering. However, at the largest load amplitude we also observed that small volume of the sample was crystallized. Supported by the NSF-DMR-0906744 and U.S. DOE DE-AC05-00OR-22725

9:10 AM Invited

X-Ray Strain Measurements in Metallic Glasses: *Todd Hufnagel*¹; ¹Johns Hopkins University

Several groups have recently used x-ray or neutron scattering to examine the structural effects of nominally elastic loading of metallic glasses. Most of the published data report x-ray elastic moduli that are uniformly larger (by some 5-20%) than the moduli determined by ultrasonic measurements. Furthermore, when strain is measured from shifts in the peak of the pair correlation function g(r), a length-scale dependence of strain is observed, with the strain at small atomic separations being smaller than the macroscopic strain, increasing to asymptotically approach the macroscopic strain at large distances. In this talk, we review these results in light of several possible physical mechanisms, including local anelastic deformations and the proposed presence of elastic heterogeneities in metallic glasses. We also discuss the application of scattering techniques to problems of interest, including x-ray measurements of the strain distribution around crack tips in metallic glasses under load.

9:30 AM Invited

Insights on Thermomechanical Deformation in Bulk Metallic Glasses from In-Situ X-Ray and Neutron Scattering Experiments: Alexandru Stoica¹; Dong Ma¹; John Daniels²; Ken Littrell¹; *Xun-Li Wang*¹; ¹Oak Ridge National Laboratory; ²European Synchrotron Radiation Facility

We have used in-situ neutron diffraction and synchrotron x-ray scattering to investigate the compressive deformation in several bulk metallic glass materials at temperatures below the glass transition temperatures. In situ, time resolved data revealed the structure evolution from atomic to nanometer length scales resulting from the thermomechanical deformation. In the case of a Ca-based metallic glass, after yielding the sample exhibits a transient softening stage that characterizes the homogeneous flow due to the local atomic structure rearrangement, followed by a hardening stage that originates from nano-scale crystallization. Our study provides insights for understanding homogeneous and inhomogeneous flows in metallic glasses from structure changes at multiple length scales.

9:50 AM Invited

Atomic Structure and Dynamics of BMG during Mechanical Deformation: *Wojciech Dmowski*¹; Andrew Chuang¹; Wei Guo¹; Konstantin Lokshin¹; Yoshihiko Yokoyama²; Tatsuya Iwashita¹; Yang Ren³; Matt Stone⁴; Peter Liaw¹; Akihisa Inoue²; Takeshi Egami⁵; ¹University of Tennessee; ²Tohoku University; ³Advanced Photon Source; ⁴SNS; ⁵ORNL

We studied changes in the atomic structure and dynamics of metallic glasses during mechanical deformation below the yield stress. The x-ray diffraction was carried in-situ in tensile and compressive loading with applied stress up to 1.75 GPa. The inelastic neutron scattering was performed during compression up to 1.5 GPa. We obtained anisotropic components of the x-ray S(Q) and PDF in the nominal elastic mechanical regime as function of the applied load at room temperature and after the high temperature creep. Analysis of the anisotropic PDF showed that "elastic" deformation is not affine. However, the anisotropic PDF could be divided into elastic (affine) and anelastic components. Analysis showed that for any applied stress level about 24% of the apparent strain was anelastic. The inelastic neutron data show anisotropic component. We also observed changes in the inelastic part of the neutron scattering with the applied stress.Supported by the U.S. DOE, DE-AC05-00OR-22725.

10:10 AM Break

10:20 AM Invited

Fracture Toughness of Bulk Metallic Glasses: *John Lewandowski*¹; ¹Case Western Reserve Univ

The effects of changes in chemistry and stress state on the fracture toughness has been determined for a number of different metallic glass systems. Both notched and fatigue precracked samples have been tested in order to determine the effects of changes in notch severity on the fracture energy/toughness of a number of systems. In addition, the effects of different loading rates and test temperatures on the fracture energy of a Zr-based bulk metallic glass have been determined. The results will be reviewed in the light of previous and ongoing work documenting the effects of such changes on damage tolerance of bulk metallic glass systems.

10:40 AM

Using Artificial Microstructures to Understand Microstructure Property Relationship in Metallic Glasses: *Baran Sarac*¹; Golden Kumar¹; Jan Schroers¹; ¹Yale University

Materials science seeks to correlate microstructure with (mechanical) properties. Various approaches have been employed to understand this correlation including conventional direct approaches where the microstructure is varied through processing parameters and composition and the effects on the mechanical properties determined. Technologically relevant materials have reached a level of complexity that conventional metallurgical strategies

as well as above mentioned model and simulation strategies are at their limit. Therefore, we propose a novel approach to study microstructure-property relationship; artificial microstructures, which allow us to individually and independently vary parameters and thereby determine their individual effects on mechanical properties. The artificial microstructure will be fabricated using our recently developed miniature fabrication method. Examples of this novel approach are toughening mechanism in metallic glasses, size effects, and the transition from plastic deformation to elastic buckling in metallic glass heterostructures.

10:50 AM Invited

Incipient Plasticity in Bulk Metallic Glasses at Elevated Temperatures and under Cyclic Loading: *Oliver Franke*¹; Cristopher Schuh¹; ¹MIT

Nanoindentation is used to study the initial yielding of bulk metallic glasses (BMG). The distribution of the pop-in events in the load displacement curves gives insight into the factors that control deformation. BMGs exhibit a high sensitivity to structural inhomogeneities which is studied at different rates, temperatures and different preconditions. One particular preconditioning of the BMGs is to cyclically load the sample in the elastic regime. At room temperature the passing of a critical threshold load causes significant hardening, while below the threshold several thousand cycles do not have any measurable effect. At elevated temperatures the emergence of thermal relaxation affects the ability of the glass to cyclically harden.

11:10 AM Invited

Inhomogeneous Deformation and Kinetics of Shear Banding in Metallic Glasses: *Robert Maass*¹; David Klaumünzer¹; Jörg Löffler¹; ¹Swiss Federal Institute of Technology (ETHZ)

Inhomogeneous flow in bulk metallic glasses is still an elusive topic with respect to the underlying deformation mechanisms which govern localized shear band operations. In this study we investigate the inhomogeneous flow both in the serrated and non-serrated regimes. In particular, we evaluate the characteristic times and velocities of the deformation kinetics during shear banding. Using temperature-dependent measurements we are able to show that the shear band propagation of an individual flow serration is a thermally activated process and not a catastrophic event. Electron microscopy investigations before and after an individual serration reveal that shear banding is not a nucleation-controlled mechanism, but rather that there is a one-to-one correspondence between flow serration and shear-offset formation. We also assess the behaviour of a single shear band operating at sub-ambient temperatures. These results indicate that stable flow at low temperatures is not an intrinsic property of cryogenic temperature plasticity.

11:30 AM Invited

Elastic, Plastic and Fracture Response of Bulk Metallic Glass Matrix Composites: Upadrasta Ramamurty¹; R. L. Narayan¹; P.S. Singh¹; K. Boopathy¹; Indrani Sen¹; D. C. Hofmann²; ¹Indian Institute of Science; ²California Institute of Technology

Bulk metallic glasses (BMGs) exhibit extraordinary strengths but suffer from low ductility and fatigue resistance. A possible way to alleviate these problems is through the composite route. In the recent past, it has been shown that BMG matrix composites with tailored microstructures of crystalline dendrite phase in the amorphous matrix yield a combination of higher ductility, strength and toughness. The role of the constituent phases on the elastic, plastic and fatigue crack growth behaviors of several BMG matrix composites are investigated in this work. For this purpose, a variety of experimental tools such as nanoindentation, in-situ testing are employed. Further, the influences of temperature and strain rate are explored. The results of these experiments will be presented and the micromechanisms of deformation and fracture in BMG composites will be discussed.

11:50 AM

Mechanical Inhomogeneity in As-Cast Bulk Metallic Glass: John Plummer¹; Russell Goodall¹; Ignacio Figueroa²; Iain Todd¹; ¹University of Sheffield; ²Universidad Nacional Autonoma de Mexico

A surface softening effect induced during copper-mould casting of bulk metallic glass is investigated as a function of rod diameter and kinetic glass



fragility index by nanoindentation. A reduction in hardness and reduced modulus at the rod surface is found to not be present in all rods and is favoured in small diameter castings and in fragile systems. Enhanced propensity for shear transformation zone nucleation in the low moduli surface is explained in terms of reduced atomic connectivity, arising from a reduction in local coordination number and a lowering of the shear modulus. Finally, the structure and mechanical diversity that is possible in a single as-cast bulk metallic glass rod is explored through a relative quantification of shear modulus and plastic zone size.

12:00 PM Invited

Effect of Structure of β Phase on the Mechanical Properties of Ti-Based Bulk Metallic Glass Composites: Chang Wook Bang¹; Ka Ram Lim¹; Jin Man Park¹; Won Tae Kim¹; *Do Hyang Kim*¹; ¹Yonsei University

Ductile-phase-reinforced BMG composites show enhanced global plasticity and more graceful failure since soft crystalline inclusions stabilize the glass against the catastrophic failure associated with unlimited extension of a shear band. In the present study, role of ductile dendritic phase in optimizing the mechanical properties of Ti-rich Ti-Zr-Be-Cu-Ni-Nb BMG composites has been investigated from major two aspects: 1) quasi-stable equilibrium condition for beta phase and glass matrix and 2) effect of structure of beta phase on the mechanical properties of composites. As a result, combination of strength and plasticity is optimized by tailoring relative volume fraction of beta phase and glass matrix. The effect of martensitic transformation in beta phase during cooling and deformation has been investigated. Depending on the composition of beta phase, martensitic transformation occurs in the beta phase affecting the mechanical properties and deformation behavior of the bulk metallic glass matrix composites.

12:20 PM Invited

In-Situ TEM/STEM Investigations on Crack Propagation with Plasticity in Zr-Based Metallic Glass: Jingwei Deng¹; *Manling Sui*²; ¹Shenyang National Laboratory for Materials Science, Institute of Metal Research, Chinese Academy of Sciences; ²Beijing University of Technology

By in situ tensile test in a transmission electron microscope (TEM), the crack propagation with plasticity was observed in Zr-based metallic glass without nanocrystals formation. Different from that the dislocations generated at the crack tip and propagated along crystallographic planes in the crystalline materials, the plastic flow zone in front of crack presented in a zigzag trace in the monolithic metallic glass. Shear events were observed dynamically in the plastic flow zone by using a scanning imaging mode in TEM, i.e. STEM. It was found that the shear events were sensitive to the local sample thickness. The zigzag propagation of the crack is associated with every shear event in front of the crack. This work was supported by the Cheung Kong Scholars Programme of China and the Natural Sciences Foundation of China

12:40 PM

In-Situ Studies of Micromechanical Behavior of Porous W/Zr-Based Amorphous Alloy Composite: Yunfei Xue¹; ¹Beijing Institute of Technology

The in-situ high energy X-ray diffraction (HEXRD) was employed to investigate the micromechanical behavior of the porous W/Zr-based amorphous alloy composite during compressive deformation. The lattice strain was measured by HEXRD along the loading direction for different {h k l} planes of W phase in the yielding stage. When the stress is less than 1250 MPa, the lattice strains responds linearly to the applied stress, indicating that only elastic deformation occurs during this stage in W phase. With the increment of stress, the lattice strains exhibit greater deformation, suggesting that the W phase still subjected to a great stress at this stage of deformation and it is an evidence of work-hardening for the W phase. The non-linearity was mainly due to the redistribution caused by interactions of grain-to-grain within W phase and phase-to-phase between the amorphous matrix and W phase.

Cast Shop for Aluminum Production: Direct Chill Casting

Sponsored by: The Minerals, Metals and Materials Society, TMS Light Metals Division, TMS: Aluminum Committee, TMS: Aluminum Processing Committee

Program Örganizers: Geoffrey Brooks, Swinburne University of Technology; John Grandfield, Grandfield Technology Pty Ltd

| Tuesday AM | Room: 16A |
|---------------|-------------------------------|
| March 1, 2011 | Location: San Diego Conv. Ctr |

Session Chairs: Dmitry Eskin, Delft University of Technology; Arild Hakonsen, Hydro Aluminium

8:30 AM Introductory Comments

8:35 AM

Cold Cracking during Direct-Chill Casting: *Dmitry Eskin*¹; Mehdi Lalpoor¹; Laurens Katgerman²; ¹Materials innovation institute; ²Delft University of Technology

Cold cracking phenomenon is the least studied, yet very important defect occurring during direct-chill casting. The spontaneous nature of this defect makes its systematic study almost impossible, and the computer simulation of the thermo-mechanical behavior of the ingot during its cooling after the end of solidification requires constitutive parameters of high-strength aluminum alloys in the as-cast condition, which are not readily available. In this paper we describe constitutive behavior of high-strength 7XXX-series alloys in the as-cast condition based on experimentally measured tensile properties at different strain rates and temperatures, fracture and impact toughness at different temperatures, and thermal contraction. In addition fracture and structure of specimens and real cold-cracked billets are examined. As a result a fracture-mechanics-based criterion of cold cracking is suggested based on the critical crack length, and is validated upon pilot-scale billet casting.

9:00 AM

Surface Defect Structures On Direct Chill Cast 6xxx Aluminum Billets: Mikael Erdegren¹; *Torbjörn Carlberg*¹; ¹Mid Sweden University

The surface zone in air-slip DC cast aluminum ingots of the alloys 6063, 6005 and 6082 have been analysed by metallographic methods and by chemical analysis. Inverse segregation to the surface was quantitatively analysed. The concentration profiles were coupled to the appearance of the defects and to microstructures from corresponding areas. Surface defects, of the type vertical drags (VD), were investigated and compared to defect free surfaces for the different alloys. It was shown, that for the 6005 VD defects, there was no change, neither for the segregation zone depth nor for the intermetallic phase particles, compared to undamaged surface areas. In the defect zones the grains started to come apart thus creating an increase in porosity. For the 6063 samples the defect zones had different particles compared to the general surface. The segregation in a defect free surface area contained mostly β-particles while at the defects a-particles dominated.

9:25 AM

Effect of Cooling Water Quality on the Dendrite Arm Spacing of DC Cast Billets: Satya Mohapatra¹; Suvendra Nanda¹; Anindya Palchowdhury¹; ¹National Aluminium Company

For a given alloy chemistry and casting technology, the quality of a billet produced through DC casting route is largely defined by the DAS (Dendrite arm spacing). DAS in turn is determined by the cooling rate and local solidification time. The cooling rate is influenced by the quality and quantity of water besides casting speed and melt temperature. This paper focuses on the relationship between the quality of cooling water and the resultant DAS during production of billets during DC casting process. An empirical relation is derived to indicate the influence of cooling water characteristics on the DAS, based on a mathematical model supplemented by experimental investigations. The model has been validated in plant scale trials.

9:50 AM

Mould Wall Heat Flow Mechanism in a DC Casting Mould: Arvind Prasad¹; Ian Bainbridge¹; ¹University of Queensland

Experiments have been performed to study the effect of the mode of heat transfer on the heat flow in the wall of a DC casting mould. Billet casting uses graphite as inner lining material within the mould-wall. Graphite being a black-body, provides a possible pathway for radiation to play a role in the mould-wall heat transfer. As such, experiments were performed with a graphite probe on the experimental apparatus presented at TMS 2010. An overview of these results will be presented together with the implications of the results for the DC casting process.

10:15 AM Break

10:25 AM

Productivity Improvements at Direct Chill Casting Unit at Aluminium Bahrain (ALBA): Abdulla Ahmed¹; *Sukanta Chateeriji*¹; A Rasool Maki¹; ¹Aluminium Bahrain (Alba)

ALBA has been producing Rolling Ingots utilizing two DC casting units via., DC1 and DC6. Out of total annual production of 140,000 MT of Rolling Ingot, DC6 production was 100,000 MT (1XXX, 3XXX and 8XXX series alloys) while DC1 production was 40,000 MT of 5XXX series alloy. Due to higher cost of production and low productivity at DC1 ALBA management decided to close down DC1 as a part of restructuring exercise and maximizing production at DC6 to meet customers demand. An extensive study was carried out towards improving productivity. Four levers of improvement which has the maximum impact were identified e.g., furnace preparation practices, preparatory activities between casts, increasing casting speed etc. Various action plans were drawn up and were implemented. These actions were closely monitored by DC operators themselves by using trend charts. As a result a 30% improvement in productivity was achieved at DC6 on a consistent basis

10:50 AM

The Coupling of Macrosegregation With Grain Nucleation, Growth and Motion in DC Cast Aluminum Alloy Ingots: *Miha Založnik*¹; Arvind Kumar¹; Hervé Combeau¹; Marie Bedel²; Philippe Jarry²; Emmanuel Waz²; ¹Institut Jean Lamour; ²Alcan CRV

The phenomena responsible for the formation of macrosegregations and grain structures during solidification are closely intertwined. We present a model study of a DC cast extrusion ingot. The modeling of these phenomena in DC casting is a challenging problem due to the size of the products, the variety of the phenomena to be accounted for, and the nonlinearities involved. We used a two-phase multiscale model that describes nucleation on inoculant particles and grain growth, coupled with macroscopic transport: fluid flow driven by natural convection and shrinkage, transport of free equiaxed grains, heat transfer, solute transport. The roles of shrinkage, natural convection and grain motion on the sump shape and macrosegregation are analyzed. The formation and evolution of inoculated grains are discussed. We show that it is important to account for all these phenomena and the coupling of segregation and structure formation to be able to explain macrosegregation patterns observed experimentally.

11:15 AM

Investment Casting of Surfaces with Microholes and Their Possible Applications: *Todor Ivanov*¹; Andreas Buehrig-Polaczek¹; Uwe Vroomen¹; Claudia Hartmann²; Arnold Gillner²; Kirsten Bobzin¹; Jens Holtkamp²; Nazlim Bagcivan¹; Sebastian Theiss¹; ¹RWTH Aachen University; ²Fraunhofer-Institute for Laser Technology

The common way to realize microstructured features on metallic surfaces is to generate the designated pattern on each single part by means of laser ablation, electro discharge machining or micromilling. The disadvantage of these process chains is the limited productivity due to the additional processing of each part. The approach to overcome this bottle neck is to replicate microstructured surfaces together with the parts. Therefore an investment casting process to produce functional 3D-surfaces with geometrical features in micrometer range on near-net-shape-cast parts is investigated. The main research objective deals with the investigation of the single process steps of the investment casting process with regard to the molding accuracy. To demonstrate the potential of microcasted surfaces, current results of the casting of a microstructured hydrophobic surface are shown.

11:40 AM

Using SEM and EDX for a Simple Differentiation of α - and β -AlFeSi-Phases in Wrought Aluminum Billets: *Marcel Rosefort*¹; Christiane Matthies¹; Hinrich Buck¹; Hubert Koch¹; ¹TRIMET ALUMINIUM AG

Aluminum 6xxx extrusions have considerable potential to make cars lighter. Thus there is a growing demand for high quality aluminum billets. Additionally there is a requirement to improve the aluminum properties. An important issue to fulfill these increasing requirements is the optimization of the microstructure. While utilizing 6xxx-alloys the formation and optimization of the AlFeSi-phase is important. The determination of α - and β -AlFeSi-phases is a challenge, because β -AlFeSi-phases affect the mechanical properties negatively. A determination in wrought alloys via microscopy is often complicated and leads to questionable results due to the low amount of the phases. TRIMET has investigated one possibility of determining α - and β -AlFeSi-phases with the help of scanning electron microscope and energy dispersive X-ray. The paper describes the first tests, the phase simulations and the casting experiments. Finally it presents the tests of such phase determinations in the production of 6xxx-alloys like the new TRIMAL 52.

Characterization of Minerals, Metals and Materials: Characterization of Steel and Cast Iron

Sponsored by: The Minerals, Metals and Materials Society, TMS Extraction and Processing Division, TMS/ASM: Composite Materials Committee, TMS: Materials Characterization Committee *Program Organizer:* Sergio Monteiro, State University of the Northern Rio de Janeiro - UENF

| Tuesday AM | Room: 14B |
|---------------|-------------------------------|
| March 1, 2011 | Location: San Diego Conv. Ctr |

Session Chairs: Mingdong Cai, Exova; John Bridge, Maine Maritime Academy

8:30 AM

Effect of Initial Structure on Grain Refinement of Medium Carbon Steel Processed by ECAP: *Jozef Zrnik*¹; Sergey Dobatkin²; George Raab³; Martin Fujda⁴; Libor Kraus⁵; ¹Comtes FHT, Inc.; ²Russian Academy of Science; ³Ufa State University; ⁴Technical University of Kosice; ⁵COMTES FHT Inc.

The work deals with grain refinement of medium carbon steel having different initial microstructure modified by thermal and/or thermomechanical treatment.In case of TM treated steel preliminary structure refinement was achieved due to multistep open die forging. Fine recrystallized ferrite structure and with nest-like pearlite colonies was obtained. The further grain refinement of steel samples was accomplished during warm Equal Channel Angular Pressing (ECAP) at 400°C. Employment of this processing route resulted in extensive deformation of ferrite grains where mixture of subgrains and ultrafine grain was found regardless the preliminary treatment of steel. The dynamic polygonization and recrystallization became active to form mixture of polygonized subgrains and submicrocrystalline grains. The straining and moderate ECAP temperature caused the partial cementite lamellae fragmentation and spheroidization. The tensile behaviour was characterized by strength increase for both structural steel states. The work hardening behaviour was modified in steel where preliminary TM treatment was introduced.



8:45 AM

Effect of Test Temperature and Prior Straining on the Deformation Mode of Austenitic Stainless Steel during Tensile Testing: Supratik Roychowdhury¹; Suman Neogy¹; Mayank Gupta²; Vivekanand Kain¹; Dinesh Srivastava¹; G.K. Dey¹; R.C. Prasad³; *Raghvendra Tewari*⁴; ¹Bhabha Atomic Research Centre; ²PEC; ³IIT, Bombay; ⁴Bhabha Atomic Resrach Centre

Austenitic stainless steels are an important material of construction for Boiling Water Reactors (BWR). These stainless steels are amenable to strengthening by strain hardening. Various deformation modes at different test temperatures and strain become active. In the present investigation type 304LN stainless steel was used in the annealed and strain hardened condition. Thin foils were prepared from gauge section for TEM investigation after tensile testing at room temperature and at 288°C. TEM investigation reveals that twinning is the major mode of deformation for the tests carried out at room temperature while dislocation cross slip is the major mode of deformation at higher temperature. Stacking faults were also observed to a limited extent. The extent of twinning was much higher for the tests carried out using the rolled material. The formation of martensite in the stainless steel due to straining was investigated by the analysis of selected area diffraction patterns.

9:00 AM

Susceptibility of Low and High Manganese X70 Pipeline Steel to Hydrogen Embrittlement: Daniel Hejazi¹; Ayesha Haq¹; Nima Yazdipour¹; Druce Dunne¹; Andrzej Calka¹; Frank Barbaro²; *Elena Pereloma*¹; ¹University of Wollongong; ²BlueScope Steel

Hydrogen, even in very low concentrations, can diffuse to regions of high stress concentration resulting in a degradation of mechanical properties. The transport of hydrogen depends on the interaction between hydrogen atoms and the traps which, in turn, is related to microstructure. The influence of composition and microstructure on hydrogen embrittlement susceptibility was investigated by selecting pipeline steels with different Mn and S contents and in different conditions – normalized transfer bar, as-received strip and heat affected zone (HAZ). HAZ simulations were conducted using Gleeble thermo-mechanical machine to simulate a thermal cycle typical of in-service repairs. Notched and fatigue pre-cracked samples were subjected to electrochemical hydrogen charging using a solution of H2SO4 and NaAsO2 to achieve 2 and 4 ppm hydrogen content. Three point bend tests were conducted on as-received and hydrogen-charged samples. The results obtained are discussed in relation to the microstructure and fractography of the samples

9:15 AM

Evaluation of Aging Embrittlement of Austenitic Stainless Steels JN1, JJ1 and JK2 by Cryogenic Small-Punch Testing: Maribel Saucedo-Muñoz¹; *Victor Lopez-Hirata*¹; Shin-ichi Komazaki²; Toshiyuki Hashida³; ¹Instituto Politecnico Nacional (ESIQIE); ²Muroran Institute of Technology; ³Tohoku University

Small-punch tests were conducted at 4, and 77 K on three types of austenitic stainless steels JN1, JJ1 and JK2, which were solution treated, and then aged at 923-1073 K for 5 hours. Small-punch test energy was employed for the evaluation of the aging-induced embrittlement behavior in these materials. Fracture surface of small punch test specimen for the solution treated steels exhibited a ductile fracture, showing the highest SP test energy values. The presence of intergranular brittle fracture was observed in aged specimens. Small-punch test energy decreased significantly as the aging process progressed. The highest and lowest decrease in small-punch test energy with aging temperature occurred in JN1 and JK2 steels, respectively. The decrease in small-punch test energy showed to examine appropriately the aging-induced embrittlement in these materials. The difference in aging-induced embrittlement behavior for these steels was explained based on the volume fraction of intergranular precipitates in aged samples.

9:30 AM

Investigations on the Cyclic Crack Growth Behaviour of Spring Steel Wire Reinforced EN AW-6082: *Matthias Merzkirch*¹; Kay Weidenmann¹; Volker Schulze¹; ¹Karlsruhe Institute of Technology

Unidirectional reinforced light weight materials such as the aluminium alloy EN AW-6082 are adequate partners for the future use in transportation means like automobiles and airplanes. Due to the occurring cyclic loads knowledge about the crack growth behaviour of these composites is needed. The investigations at a load ratio of R=0.18 show that the crack growth rate of the aluminium matrix is reduced if it is reinforced by spring steel wire with a reinforcing ratio of only about 1 Vol.-%. Further analyses with the help of a self designed capacitive travel measuring gauge show that the reinforcing element causes an increase of the stiffness resulting in a smaller crack opening in comparison to the pure matrix material. Additionally, the acoustic emission analysis allows to detect crack growth within the matrix material, crack propagation along the interface wire/matrix and crack closure. The qualitative results are verified by metallographic and SEM investigations.

9:45 AM Invited

Effect of Cr Content on Corrosion Resistance of Fe-Based Alloys under SCW Condition: *Jian Li*¹; Wenyue Zheng¹; William Cook²; ¹CANMET-MTL; ²University of New Brunswick

Resistance to high temperature corrosion is one of the key challenges in future nuclear reactor material development. Iron based materials with low Cr content shows superior high temperature mechanical properties. However, due to relative low Cr content, their corrosion resistances under SCW conditions are generally poor. High-Cr alloys although show much improved corrosion resistance, often suffer from embitterment due to the pre-cipitation of sigma phase in the microstructure. In this study, corrosion resistance high Cr alloy (25%Cr) showed much better corrosion resistance compared to that of low Cr alloy (14%Cr). The high-Cr alloy was subsequently used as coating material for commercial P91 alloy.

10:15 AM Break

10:30 AM

Variations of Elastic Modulus of Automotive Steels after Yielding: Paolo Matteis¹; Giorgio Scavino¹; Donato Firrao¹; ¹Politecnico di Torino

Numerical simulations of both production processes (e.g.: sheet cold forming) and service behavior (e.g.: low-speed car impact), used in the automotive industry to minimize the tests number and shorten the car design and industrialization, can be significantly affected by the variation of the steel elastic modulus due to plastic deformation. However, this phenomenon is not usually modeled, also for lack of specific data. Hence, five steel grades, belonging to different categories, were examined before and after several successive 4% true strain steps, and up to the uniform elongation. After each deformation step, the specimen was unloaded, the cross-section was re-measured, and the modulus was evaluated from a series of loading and unloading ramps in the elastic range. In most cases, the elastic modulus decreases approximately from 205 GPa in the as-received condition to 165 GPa after deformation, with most of this drop often occurring in the first deformation step alone.

10:45 AM

The Development of a High Strength Microalloy Steel TiC Deposited by Reactive Magnetron Sputtering: *Narayanna Ferreira*¹; Edalmy Almeida¹; Marcio Mendes¹; Clodomiro Alves Júnior¹; ¹UFRN

High strength low alloy steels (HSLA) are generally composed of micro-alloying elements Nb, V and Ti. Commonly are microalloyed with niobium and vanadium, however, the development of steels microalloyed with Ti have been objects of constant research. The mechanical properties of microalloyed steels result from the interaction between different hardening mechanisms involving dislocations, solid solution, ferritic grain refinement and precipitation of carbonitrides. The aim of this study was developed from a titanium microalloyed steel using the technique of enrichment by precipitation of TiC powder of iron deposition by reactive magnetron sputtering using different proportions of the mixture CH4, H2, Ar. This

work was realized on the microstructural characterization by SEM / EDX, XRD, XRF and microhardness. The results showed that the precipitation of titanium carbide by magnetron sputtering is viable and confirmed by the characterization techniques performed in this study.

11:00 AM

Microstructure and Properties of New Wear Resistant Steel with High Strength and High Toughness: *Li Hongbin*¹; ¹Baosteel

A multi-element wear-resistant low-alloy steel with high strength and high toughness was developed. Microstructure, hardness, tensile properties and impact properties were carried out in order to establish a correlation amongst the parameters and to optimize the microstructural features and mechanical properties for superior wear performance. The results show that the optimal microstructure and mechanical properties were got when quenching at 880 and tempering at 180°. Fine martensite can be obtained, and the hardness is above 550HB, the tensile strength is above 1700MPa, the yield strength is above 1350MPa, the elongation is above 10%, and the impact energy is about 50J. The results obtained have been supplemented through the characteristics of the worn surfaces, subsurface regions, debris and fractured surfaces. These analyses also helped to understand the operative mechanisms of material removal and failure.

11:15 AM

Evaluation of Growth Rates of Austenitic Transformation Products in Fe-C-Cr Alloys Using Laser Scanning Confocal Microscopy: *Peter Kolmskog*¹; Peter Hedström¹; Annika Borgenstam¹; ¹Royal Institute of Technology, KTH

An evaluation of the growth rates of the transformation products from austenite in three Fe-C-Cr alloys (Fe-1C-1Cr, Fe-1C-4Cr and Fe-0.15C-4Cr) during isothermal heat treatment has been performed in-situ using Laser Scanning Confocal Microscopy (LSCM) equipped with a hot-stage. The LSCM technique enables the clear observation of phase transformation that gives a surface relief e.g. Widmanstätten cementite and ferrite, bainite and inverse bainite. Specimens have been isothermally heat treated at temperatures from 275 to 700°C and the growth rate of the different austenitic transformation products has been evaluated. The microstructures of the transformed specimens have been analyzed using LOM and SEM in order to verify the obtained results.

11:30 AM

Internal Friction and Three Dimensional Atom Probe Analysis of Bake Hardening Phenomenon in Ultra-Low Carbon Bake Hardening Steel: *Hua Wang*¹; Wen Shi¹; Lin Li¹; ¹Shanghai University

Two samples of Ultra-Low Carbon Bake Hardening (ULC-BH) steel with different compositions were prepared by annealing and water quenching. These samples were pre-deformed with various levels from 2% to 10%, and further baked at 170°C for 20min. The distribution of solute C in the processed samples was characterized by 3DAP, and the BH values of the samples with different pre-deformation were also determined. In addition, the relationship between the distribution of solute C in BH steels and the BH values was analyzed.

11:45 AM

A New Understanding on the Initiation of Pitting Corrosion of Austenitic Stainless Steels in Salt Water: *Xiu-Liang Ma*¹; ¹Institute of Metal Research, Chinese Academy of Sciences

The pitting corrosion of stainless steels is generally believed to result from the local dissolution in MnS inclusions which are more or less ubiquitous in stainless steels. Nevertheless, the microstructure information on the local site where MnS dissolution preferentially occurs is lacking, which makes pitting corrosion remain the big headache for numerous engineering materials. We have applied in-situ ex-environment transmission electron microscopy and have identified the initial site, at an atomic scale, of MnS dissolution. We find that fine nano-octahedral precipitates of spinel MnCr2O4 are dispersedly distributed in the MnS inclusions. In-situ TEM studies indicate that the MnS initially dissolves at the MnCr2O4/MnS interface in the presence of salt water. First-principles calculations indicate that the MnCr2O4 nanooctahedron with metal terminations is more reactive in catalyzing the MnS dissolution than O-terminated ones. This work sets up a new basis for understanding the initiation of pitting corrosion.

Chloride 2011: Practice and Theory of Chloride-Based Metallurgy: Molten Salts, Magnesium and Aluminum

Sponsored by: The Minerals, Metals and Materials Society, Canadian Institute of Metals, TMS Extraction and Processing Division, TMS: Magnesium Committee, TMS: Energy Committee *Program Organizers:* Dirk Verhulst, Consultant, Extractive Metallurgy; V.I. (Lucky) Lakshmanan, Process Research Ortech, Inc.

| Tuesday AM | Room: 19 |
|---------------|-------------------------------|
| March 1, 2011 | Location: San Diego Conv. Ctr |

Session Chairs: Neale Neelameggham, US Magnesium LLC; Vladimiros Papangelakis, University of Toronto

8:30 AM

Evaluation of 2.25Cr-1Mo Alloy for Containment of LiCl/KCl Eutectic during the Treatment of Used Nuclear Fuel: *Brian Westphal*¹; S. Li¹; G. Fredrickson¹; D. Vaden¹; T. Johnson¹; J. Wass¹; ¹Idaho National Laboratory

Recovery of uranium from the Mk-IV and Mk-V electrorefiner vessels containing a LiCl/KCl eutectic salt has been on-going during the pyrometallurgical processing of used nuclear fuel for 14 and 12 years, respectively. Although austenitic stainless steels are typically utilized for LiCl/KCl salt systems, the presence of cadmium in the Mk-IV electrorefiner dictates an alternate material. A 2.25Cr-1Mo alloy (ASME SA-387) was chosen due to the absence of nickel in the alloy which has a considerable solubility in cadmium. Using the transition metal impurities (iron, chromium, nickel, molybdenum, and manganese) in the electrorefined uranium products, an algorithm was developed to derive values for the contribution of the transition metals from the various input sources. Weight loss and corrosion rate data for the Mk-V electrorefiner vessel were then generated based on the transition metal impurities in the uranium products. To date, the corrosion rate of the 2.25Cr-1Mo alloy in LiCl/KCl eutectic is "outstanding" assuming uniform (i.e. non-localized) conditions.

8:50 AM

Numerical and Experimental Study of Fluid Flow during Electrolytic Process for Magnesium Production: *Hyun Na Bae*¹; Myung Duk Seo¹; Seon Hyo Kim¹; Go-Gi Lee²; Jae Young Jung²; ¹POSTECH; ²RIST

Bubbles form at the anode during the electrowinning of magnesium and cause hydrodynamic acceleration and electrical field disturbance. A threedimensional computational model was developed to investigate the effect of the geometry of the electrochemical chamber and the size distribution of bubbles on the fluid flow in the cell of a pilot plant. The results were validated by measurements of the surface characteristics of molten salt and of the formed bubbles. Fluid flow at the surface was recorded with a high speed camera, and the distribution of bubble size was determined by inspecting the video images frame by frame. The measured size distribution of the bubbles was entered into the computer simulation for multi-phase flow. A sloped roof was installed above the electrodes and enhanced the flow of the molten salt, resulting in higher current efficiency, lower energy consumption, and higher quality of magnesium metal.

9:10 AM

Magnesium Removal from Secondary Aluminum Melts in Reverberatory and Rotary Furnaces: *Eulogio Velasco*¹; Marcos Cardoso²; Jose Nino²; ¹Texas State University; ²NEMAK

Recycling of aluminum scrap for production of secondary alloys used for automotive applications is increasing continuously. Aluminum can be recycled with large energy and emission savings with minimal loss in material properties. Automotive alloys require a strict control to remove



alloy impurities, inclusions and excess of magnesium. The aim of this work is to study the magnesium removal from recycled aluminum by chlorine injection in a reverberatory furnace, and removal by an oxidation process at high temperature in an industrial rotary furnace. The magnesium removal by gas injection is carried out by the reaction between chlorine and magnesium, with its efficiency associated to kinetic factors. In the rotary rapid oxidation of aluminum and magnesium elements at high temperature is characterized by the formation of surface films composed of magnesium oxide. Additionally this work reviews the benefits of an efficient demagging process.

9:30 AM

Rapid Removal of Chlorine in Molten Salt Electrolysis of Magnesium Chloride: *Gökhan Demirci*¹; Ishak Karakaya²; ¹Aselsan Inc.; ²Middle East Technical University

Energy consumption in electrolytic magnesium cells is well above the theoretical values. However, the mechanism of the back reaction, the main cause of the current losses, has not been fully understood yet. Magnesium dissolution into the melt is generally regarded as the limiting step for the back reaction. Accordingly, present cell designs are made with priority given to fast magnesium removal from the cell. However, experimental data and modeling results in this study indicate that the limiting step for the back reaction between magnesium and chlorine is the chlorine dissolution into the electrolyte when physical contact between electrolysis products was eliminated. Effects of chlorine bubbles on the current efficiency and the cell potential were investigated. Results show that the extent of back reaction is proportional to the chlorine surface area in contact with the electrolyte per unit time, and the cell potential increases with the amount of chlorine bubbles inside the electrolyte.

9:50 AM

Preparation of Al-Ca Alloys by Molten Salt Electrolysis Method: *Sh Yang*¹; Fengli Yang¹; Mingzhou Li¹; Xianwei Hu²; Zhaowen Wang²; Zhongning Shi²; Bingliang Gao²; ¹Jiangxi University of Science and Technology; ²School of Materials and Metallurgy117#, Northeastern University

Aluminum-calcium alloys were prepared by molten salt electrolysis method. 15w%KCl-80w%CaCl2-5w%MgF2 was taken as electrolysis. Content of calcium in alloys was to be higher than 13w%, and tests were carried out with 0.80-1.20A•cm-2 of cathode current density at 680-720°. The highest current efficiency was 80%. Aluminum-calcium alloys with different calcium contents could be prepared directly from the cell by molten salt electrolysis method. Compared with traditional method, the method not only could reduce the loss of calcium in the alloy manufacture process, but to reduce Greenhouse Gases and energy consumption. Moreover, component of alloys prepared by molten salt electrolysis method was even, and production could be carried out continuously.

10:10 AM Break

10:25 AM

The Dissolution Behavior of TiCxO1-x Solid Solutions in Chloride Melt: Xiaohui Ning¹; Chao Du¹; Qiuyu Wang¹; Shuqiang Jiao¹; *Hongmin Zhu*¹; ¹University of Science and Technology Beijing

TiCxO1-x solid solutions were synthesized by sintering a mixture of titanium carbide and titanium monoxide at 1600 °C. The corresponding structures and morphologies of the TiCxO1-x solid solutions were characterized by XRD and SEM. A series of tests has been performed on the electrochemical dissolution behavior of TiCxO1-x solid solutions in NaCl-KCl molten salt. The influences of synthesis time and electrochemical parameters on the anodic dissolution behavior were also investigated in detail. The results showed that TiCxO1-x solid solutions can dissolve as Ti2+ into alkali chloride melt. The tail gas on the anode was monitored by a mass spectrometer. And it was found the synthesis time significantly affects the components of the anodic gas. Titanium ion species dissolved from TiCxO1-x solid solutions changes between Ti2+ and Ti3+ depending on the applied potential.

10:45 AM

Study on Mechanism of Alumina Carbothermic Reduction-Chlorination Process in Vacuum: *Fulong Zhu*¹; Bin Yang¹; Qingchun Yu¹; Baoqiang Xu¹; Yongnian Dai¹; ¹National Engineering Laboratory for Vacuum Metallurgy

In this paper, the mechanism of the carbothermic reduction-chlorination process to extract aluminum from alumina in vacuum was investigated. Content of CO in gas, phases of the reduction slag, surface morphology of the reduction slag and the product aluminum were measured by means of gas chromatography (GC), XRD, and SEM. The experimental results indicated that content of CO in gas decreased, but Al4C3 increased with reduction time increasing at 1773K during carbothermic reduction process of alumina. AlCl(g) and C were produced by the reaction between Al4C3 and AlCl3(g) at 1773K, then aluminum beads were generated after decomposition of AlCl(g). It implied that mechanism of alumina carbothermic reduction-chlorination process in vacuum should match with the following three steps: the carbothermic reduction process of Al4C3 by AlCl3(g) to produce Al4C1(g), and the decomposition process of Al2Cl3 to produce Al4C1(g).

11:05 AM

Investigation on the Corrosion Resistance of Several Steel Materials to LiCl-KCl Melt: *Bing Li*¹; ¹East China University of Science and Technology

In this paper the corrosion resistances of three steel materials including 304, 306, Q235A steels to the LiCl-KCl melt were investigated. The electrochemical impedance spectroscopies, Tafel curves and polarization curves of the three steel materials in the LiCl-KCl melt were measured and some dynamic parameters such as corrosion current, corrosion potential, exchange current density, transfer coefficient and electron transfer resistance were obtained. And then the corrosion resistances of the three steel materials were tested by immersing into the LiCl-KCl melt at 600° for 50h and then their surface morphology and composition were characterized by SEM and EDS, and their weight changes before and after immersion into the melt were compared. At the same time, electrolysis experiments were carried out in LiCl-KCl melt at about 450° by selecting the three steel materials as cathodes, respectively, and the corrosion of metal Li produced in-situ on them were analyzed.

11:25 AM

Electrochemical Removal of Impurity Mg from LiCl-KCl Containing MgCl2 Melt: *Bing Li*¹; Miao Shen¹; Jingwei Lou¹; ¹East China University of Science and Technology

As a main impurity in primary lithium metal, magnesium is difficult to remove because of the very close relative volatility of the two metals. Electrochemical refining provides a possibility to completely remove Mg in the LiCl-KCl melt prior to Li reduction. MgCl2 reduction processes in LiCl-KCl- MgCl2 melt were investigated by cyclic voltametry (CV)and square wave voltametry (SWV). The results showed that MgCl2 is reduced in one step with two-electron transfer. The reduction potential was well defined. By constant potential electrolysis at the Mg reduction potential, Mg was reduced on a solid cathode (mild steel) and a liquid cathode (Zinc and Lead). Cyclic voltametry (CV) and square wave voltametry (SWV) were also employed to compare the removal effect after several hours of electrolysis. The dissolution kinetics of the deposited Mg in the above melt was investigated, and the relations between the activity and the dissolution kinetics of deposited Mg were discussed.

11:45 AM

Direct Synthesis of Niobium Aluminides Powders by Sodiothermic Reduction in Molten Salts: Na Wang¹; Chao Du¹; Shuqiang Jiao¹; Kai Huang¹; *Hongmin Zhu*¹; ¹University of Science and Technology Beijing

Niobium aluminides were directly synthesized by a sodiothermic reduction process of NbCl5 - AlCl3 which was dispersed into LiCl - KCl - NaCl -CaCl2 melts. The melt supplied a homogenous reaction medium which was substantially beneficial to the co-reduction of Nb and Al to form niobium aluminides in situ. The reduction was performed at 500° for 4 hours. The products were analyzed by X-ray diffraction (XRD) and scanning electron

Computational Thermodynamics and Kinetics: Brent Fultz Honorary Session II

Sponsored by: The Minerals, Metals and Materials Society, ASM International, TMS Electronic, Magnetic, and Photonic Materials Division, TMS Materials Processing and Manufacturing Division, TMS: Alloy Phases Committee, TMS: Chemistry and Physics of Materials Committee, TMS/ASM: Computational Materials Science and Engineering Committee, ASM: Alloy Phase Diagrams Committee *Program Organizers:* Raymundo Arroyave, Texas A & M University; James Morris, Oak Ridge National Laboratory; Mikko Haataja, Princeton University; Jeff Hoyt, McMaster University; Vidvuds Ozolins, University of California, Los Angeles; Xun-Li Wang, Oak Ridge National Laboratory

| Tuesday AM | Room: 9 |
|---------------|-------------------------------|
| March 1, 2011 | Location: San Diego Conv. Ctr |

Session Chairs: Matthew Lucas, Air Force Research Laboratory; Lee Roberson, Oak Ridge National Laboratory

8:30 AM Invited

Iron Alloys through the Lens of Nuclear Resonant Spectroscopy: *Wolfgang Sturhahn*¹; ¹Jet Propulsion Laboratory

In recent years, nuclear resonant scattering techniques that utilize synchrotron radiation have provided new opportunities for the study of vibrational and magnetic properties of condensed matter under extreme conditions. In particular, the determination of the vibrational density of states with nuclear resonant inelastic x-ray scattering (NRIXS) and the study of valencies and magnetic properties with synchrotron Mössbauer spectroscopy (SMS) provided unique results. In this presentation, the work of Prof. Brent Fultz on the vibrational and magnetic properties of iron and its alloys using these novel nuclear resonant scattering techniques will be highlighted. In particular, we will discuss the effects of particle size and high pressure in iron metal as well as chemical disorder in various iron alloys on atomic vibrations and magnetic properties. This work is supported by grants from the National Aeronautics and Space Administration (NASA).

9:00 AM Invited

Mixing Properties in Oxide Solid Solutions Relevant to Nuclear Fuels: Ben Hanken¹; *Mark Asta*²; Chris Stanek³; Fei Zhou⁴; Vidvuds Ozolins⁴; Niels Gronbech-Jensen¹; ¹University of California, Davis; ²University of California, Berkeley; ³Los Alamos National Laboratory; ⁴University of California, Los Angeles

Among Professor Fultz's many accomplishments are his important contributions to the field of alloy theory. His experimental measurements of vibrational entropy inspired an extensive body of theoretical work aimed at incorporating non-configurational contributions to the entropy of mixing and ordering in first-principles calculations of alloy phase diagrams. In this talk we discuss non-configurational contributions to the mixing thermodynamic properties of oxide solid solutions, originating from electronic degrees of freedom. The work focuses on urania-ceria solid solutions, a surrogate system for mixed-oxide nuclear fuels. First-principles calculations, combined with classical interatomic-potential modeling are used to investigate contributions to mixing thermodynamic properties associated with electronic disorder arising from charge transfer between uranium and cerium ions. The results are discussed in light of conflicting experimental measurements in the literature. Overall, our results suggest that charge disorder likely plays an important role in governing the thermochemical and phase stability properties in this system.

9:30 AM Invited

Time-Resolved Measurements of Transient Behaviors by Asynchronous In-Situ Neutron Diffraction at the Spallation Neutron Source: *Ke An*¹; Alexandru Stoica¹; Harley Skorpenske¹; Abhijit Pramanick¹; Rick Riedel¹; Steve Miller¹; Hahn Choo²; Jabob Jones³; James Kohl¹; Xun-Li Wang¹; ¹Oak Ridge National Laboratory; ²University of Tennessee; ³University of Florida

Unlike the conventional histogram data collection method, the event-based data acquisition scheme at the Spallation Neutron Source (SNS) records neutrons with an intrinsic timing resolution of 100ns. A novel asynchronous neutron diffraction measurement technique has been demonstrated at VULCAN, the engineering diffractometer at SNS by making use of both neutron scattering and sample environment parameters in time event data acquisition mode. The asynchronous measurement strategy is an entirely new approach to study time-resolved phenomena such as in-situ phase transformation at elevated temperatures, lithiation and delithiation in rechargeable Li-ion batteries, and low cycle fatigue of stainless steel where the relevant time scales are minutes to milliseconds. The ultimate time resolution achievable with this technique is expected to be $<10 \ \mu$ s, which will enable the investigation of fast transition phenomena by neutron scattering. Details of this measurement methodology as well as its application in various scientific cases will be presented.

10:00 AM Break

10:20 AM

Phonon Density of States and High Temperature Thermodynamics of MgB2: *Jorge Munoz*¹; Nikolay Markovskiy¹; Matthew Lucas²; Olivier Delaire³; Chen Li¹; Matthew Stone³; Douglas Abernathy³; Brent Fultz¹; ¹California Institute of Technology; ²Air Force Research Lab; ³Oak Ridge National Lab

Inelastic neutron scattering spectra were measured from 7 to 750 K on polycrystalline MgB₂ and phonon density-of-states (DOS) curves were obtained. The thermal expansion was measured from 300 to 900 K using x-ray diffraction. First-principles calculations were conducted to study the phonon DOS curves and thermal expansion behavior in the quasi-harmonic approximation. The electronic DOS shows a peak at the Fermi level composed predominantly of in-plane boron hybridized states. These states couple strongly to the E_{2g} phonon modes. Quantitative agreement was found between experiment and the quasi-harmonic simulations, suggesting a small role for anharmonicity in most modes. Nevertheless, the modes in the energy range from 60 to 75 meV, which include the E_{2g} modes along the Γ -A direction, have different temperature dependence. This anomaly could be caused by the adiabatic electron-phonon interaction, which induces a broadening of sharp features in the electronic DOS and can alter the electronic screening behavior.

10:40 AM Invited

Phonon Studies with Inelastic Neutron Scattering and First-Principles Simulations: Olivier Delaire¹; ¹Oak Ridge National Laboratory

Inelastic neutron scattering is the preferred technique to measure phonons in materials, with recent advances allowing to fully map out the four-dimensional scattering function S(Q,E) for microscopic dynamics. First-principles calculations of the electronic structure and phonons have also reached a high level of accuracy, allowing for a powerful comparison with experiments. Studies combining these experimental and computational techniques will be presented. In particular, we have identified that the adiabatic coupling of phonons and electronic structure at high temperature significantly affects the thermodynamics in several classes of materials. This effect was investigated in details with temperature-dependent phonon measurements on powders and single-crystals, and with ab-initio molecular dynamics. We also present results on thermoelectric materials, where phonons are important to understand thermal transport, which directly relates to the thermoelectric efficiency. Work was partially supported by the US DOE, Basic Energy Sciences, as part of an Energy Frontier Research Center, DE-SC0001299.



11:10 AM Invited

Phonon Thermodynamics of Binary Fe Alloys: *Matthew Lucas*¹; ¹Air Force Research Laboratory

The phonon density of states gives insight into interatomic forces and provides the vibrational entropy, making it a key thermodynamic function for understanding alloy phase transformations. The significance of phonon thermodynamics is discussed in the context of recent measurements on binary alloys of Fe with Al, Co, Cr, and V. For equiatomic B2 ordered FeAl, the vibrational entropy of vacancy formation counteracts the corresponding change in configurational entropy, destabilizing vacancies at higher temperatures. Changes in the phonon spectrum upon ordering in equiatomic FeCo are accurately captured using the cluster inversion method for measurements on random solid solutions. For FeCr alloys, the positive vibrational entropy of mixing helps to stabilize the random solid solution with respect to the unmixed phase. The change in vibrational entropy upon ordering for equiatomic FeV is found to be positive, which is consistent with recent calculations of the phonon density of states.

11:40 AM

The Temperature Dependence of Phonons in Scandium Fluoride, a Material with Large Negative Thermal Expansion: *Chen Li*¹; Xiaoli Tang¹; Jorge Munoz¹; Brandon Keith¹; Doug Abernathy²; Sally Tracy¹; Benjamin Greve³; Angus Wilkinson³; Brent Fultz¹; ¹California Institute of Technology; ²Oak Ridge National Laboratory; ³Georgia Institute of Technology

It has recently been discovered that cubic scandium tri-fluoride has a negative thermal expansion as large as $1\times10^{-5}/K$ over a temperature range of 100 to 700 K. Inelastic neutron scattering experiments were performed to study the temperature-dependent lattice dynamics of ScF₃ from 7 to 750 K. The measured phonon densities of states (DOS) shows a large non-harmonic behavior in the same range of temperature as the negative thermal expansion. Calculations of phonons with first-principles methods identified the individual modes in the DOS, indicating that the correlated rocking of the structural octahedra reduces the lattice parameter while preserving the cubic structure symmetry. First-principles molecular dynamics simulations showed that large thermal excursions of F atoms cause their neighboring Sc atoms to be drawn together with increasing temperature.

David Pope Honorary Symposium on Fundamentals of Deformation and Fracture of Advanced Metallic Materials: Intermetallics III, Superalloys, and Gum Metal

Sponsored by: The Minerals, Metals and Materials Society, TMS Materials Processing and Manufacturing Division, TMS Structural Materials Division, TMS: High Temperature Alloys Committee, TMS/ASM: Mechanical Behavior of Materials Committee, TMS: Nanomechanical Materials Behavior Committee

Program Organizers: E. P. George, Oak Ridge National Laboratory; Haruyuki Inui, Kyoto University; C. T. Liu, The Hong Kong Polytechnic University

| Tuesday AM | Room: 32A |
|---------------|-------------------------------|
| March 1, 2011 | Location: San Diego Conv. Ctr |

Session Chairs: Ian Baker, Dartmouth College; Takayuki Takasugi, Osaka Prefecture University

8:30 AM Invited

Stability and Structure of Transition Metal C14/C15 Laves Phases: *Masao Takeyama*¹; Shigehiro Ishikawa²; ¹Tokyo Institute of Technology; ²Former graduate student (Currently Sumitomo Metal Co.)

Phase stability and crystal structure change between hexagonal C14 and cubic C15 Laves phases at elevated temperatures has been examined along the pseudo-binary lines of A_2B-C_2B and A_2B-A_2C in Fe-Nb-M and Co-Nb-Cr ternary systems (M: transition metals). In C14-C14 combinations, a continuous solid solution is formed between the two Laves phases in any

system. In C14-C15 combinations, the C14 phase region becomes enlarged extensively toward the counterpart, whereas the C15 region is limited to the binary edge. In C15-C15 combinations, however, the Laves phase region is limited to its binary edge and a large C14 region appears in between. These results suggest that C14 structure is thermodynamically more stable than C15 structure. The higher stability of C14 structure is associated with interaction energy among sublattices. The details will be discussed in terms of the site occupation of M and structure change of the tetrahedral unit in their crystal structures.

9:00 AM Invited

Resemblance and Difference in Mechanical Properties between L1₂ and E2₁**Type Ordered Crystal Structures**: *Yoshisato Kimura*¹; ¹Tokyo Institute of Technology

The ordered crystal structure of E2₁ can be regarded as ternary L1₂ stabilized by an interstitial carbon at the cell center. Objective of the present work, aiming at the heat resistant alloy design, is to understand mechanical properties of E2₁ M₃AlC_{1,x} (M=Fe, Co, Ni) compounds from the viewpoint of resemblance and difference between L1₂ and E2₁ type ordered crystal structures. Single crystals of M₃AlC_{1,x} were prepared by directional solidification using optical floating zone melting and their mechanical properties were evaluated by compression tests. The operative slip systems of E2₁ Ni₃AlC_{1,x} are the same as L1₂ Ni₃Al; octahedral slip at lower temperatures and cube slip at higher temperatures than 1073 K. Only cube slip operates in Fe₃AlC_{1,x} above 1073 K, while octahedral slip operates in a wide temperature range from 77 to 1373 K in Co₃AlC_{1,x} in which the extra ordering of carbon atoms plays quite important role.

9:30 AM Invited

Microstructure Evolution and Solubility Change of Constituent Phases in Mo-Si-B Based Alloys at 1800 Degree C: *Kyosuke Yoshimi*¹; Seong-Ho Ha¹; Kouichi Maruyama¹; ¹Tohoku University

Microstructure evolution of as-cast Mo-rich Mo-Si-B alloys at 1800 degree C was experimentally investigated with referring some projection diagrams of the liquidus surfaces and some equilibrium phase diagrams of the alloys. As-cast microstructures of the alloys were drastically changed by heat treatment at 1800 degree C for 24 h, and thermally stable microstructures were developed during the heat treatment. For example, Mo2B crystallized out during solidification as the primary or secondary phase along with their solidification paths even though the alloy composition lied in the triangle of Mo-Mo3Si-Mo5SiB2. However, the unstable Mo2B was completely decomposed during the heat treatment and contributed to develop uniform, fine microstructures. The compositions of constituent phases after the heat treatment were carefully analyzed by EPMA with some Mo-Si-B alloy standards, and an equilibrium phase diagram in the Mo-rich side of the Mo-Si-B ternary system at 1800 degree C was established.

10:00 AM Break

10:15 AM Invited

Overview of Creep Deformation of Nickel Base Superalloys and Intermetallics: *Dilip Shah*¹; ¹Pratt & Whitney

In comparison to tensile properties determined at high strain rate, diffusion controlled creep deformation is a far more complex process. The primary focus of the development of high temperature materials has been improvement in creep resistance. Creep deformation is not only a measure of temperature capability of the material but also affects other low strain rate deformation such as dwell fatigue and thermal-mechanical fatigue. This presentation provides an overview of creep deformation of nickel base superalloys and intermetallics. It will touch upon a variety of phenomena, such as primary creep, influence of crystal orientation, effects of alloying additions, role of phase instability, ordering, two phase structure and heat treatments. Also, the time has come to pay more attention to artifacts of load controlled creep testing of anisotropic single crystal alloys and to environmental interactions, even for nominal laboratory conditions.

10:45 AM

Localized Shear Deformation in Gum Metal at Ideal Strength: *Shigeru Kuramoto*¹; Tadahiko Furuta¹; Naoyuki Nagasako¹; John Morris²; ¹Toyota Central R&D Labs., Inc.; ²University of California, Berkeley

Experimental results on localized shear deformation in a multifunctional Ti-36Nb-2Ta-3Zr-0.3O alloy (mass%), Gum Metal, are summarized and the mechanism for the shear deformation is considered in relation to elastic softening in C11- C12. Very small value of C11- C12 in the alloy means sufficiently low Peierls stress required for dislocation motion. However, actual deformation strength of the alloy is much higher; resolved shear stress in nanopillars of the alloy has been reported to approach its ideal shear strength during compression test. Results of microstructural analyses in various size scales performed so far support that the key basic process of plastic deformation would be localized shear deformation accompanied by inhomogeneous crystal lattice rotation. The actual shear deformation stress at ideal strength along with elastic softening in the alloy implies that the localized shear deformation involves anisotropic shear melting process by local stress increase in specific crystal lattice orientation.

11:00 AM

Microstructual Characterization and Deformation Behavior of Ideal Strength Metallic Materials: *Tadahiko Furuta*¹; Shigeru Kuramoto¹; Kaveh Edalati²; Zenji Horita²; ¹Toyota Central R & D Labs., Inc.; ²Kyushu University

The plastic deformation of metallic material is based on the dislocation theory, which well explains large difference between the ideal shear strength and the practical strength. We recently found that the actual deformation stress is considered to be closer to their ideal strength in Ti-23%Nb-0.7%Ta-2%Zr-1.20 (in at%) and Fe-18.1%Ni-34.9%Co-9.3%Ti alloys. They are composed of body-centered cubic crystal with lattice softening along specific orientation and have nano-sized obstacles in their microstructures, which can suppress the dislocation motion up to high strength level, possibly near ideal strength. In this study, effects of phase stability on change in microstructure during severe plastic deformation and deformation behavior in both alloys and their deformation characteristics were compared. From these experimental results, requirements for ideal strength deformation will be discussed.

11:15 AM

Non-Planar Deformation as a Dominant Deformation Mechanism Following Low Cycle Fatigue of a Ni-Based Superalloy: *Patrick Phillips*¹; Libor Kovarik²; Raymond Unocic³; Dan Wei⁴; David Mourer⁴; Michael Mills¹; ¹Ohio State University; ²PNNL; ³ORNL; ⁴GE Aviation

Many materials demonstrate strictly planar deformation during low cycle fatigue (LCF), which often takes the form of persistent slip bands. In the general case of Ni-based superalloys, these slip bands consist of paired dislocations traveling on {111} planes. However, extensive electron microscopy characterization has revealed non-planar deformation to be a dominant mode in polycrystalline R104, resulting from ample cross-slipping processes between {111} and {100} planes. Somewhat unexpectedly, this mechanism appears at both low and high temperatures, although the macroscopic material response is quite different. In addition to temperature effects, any deformation dependencies on grain orientation or cycle number will be discussed. Preliminary results comparing dwell fatigue deformation mechanisms to those observed during LCF will also be presented.

11:30 AM

Investigation of Fatigue Crack Growth Mechanisms in a Ni-Based Superalloy: *Clarissa Yablinsky*¹; Katharine Flores¹; Michael Mills¹; James Williams¹; ¹The Ohio State University

Historically, the critical design parameter for Ni-based superalloy turbine blades has been creep resistance. With modern airfoil designs and longer service times, fatigue resistance can also be a limiting factor. In this study, compact tension specimens of monocrystalline Ni-based superalloy René N5 were tested under cyclic loading conditions. Test temperature, environment, frequency, and orientation were varied in order to examine the effects of plastic zone size, recovery, and other time dependant processes on crack growth. Fracture surfaces and microstructures were characterized using a high resolution scanning electron microscope in order to examine crack path selection, fracture topography, and the γ/γ morphology along the crack wake and in the bulk material. Dislocation arrangements were characterized via transmission electron microscopy using site-specific foils prepared by focused ion beam techniques in order to understand the damage mechanisms active during fatigue crack growth.

11:45 AM

Fatigue Life Modeling of Single Crystal Nickel-Base Superalloys: *Clinique L. Brundidge*¹; Tresa M. Pollock²; ¹University of Michigan; ²University of California, Santa Barbara

Factors influencing the fatigue life of a single crystal nickel-base superalloy tested at 538\176C have been examined. The role of cooling rates during solidification has been investigated with the use of a liquid metal cooling (LMC) directional solidification process in comparison to a conventional Bridgman technique. Increases in cooling rates during solidification significantly decrease primary and secondary dendrite arm spacings as well as decrease the size of solidification shrinkage pores. Increases in cooling rates improve the fatigue life by as much as a factor of seven. Fatigue cracks originate from casting porosity, where the size of the largest pores in the samples scales with the secondary dendrite arm spacings. The development of a microstructure-based model to quantify the total life of single-crystals will be discussed.

12:00 PM

The Effect of Temperature on the Microstructure and Mechanical Behavior of Two-Phase Fe₃₀Ni₂₀Mn₂₀Al₃₀ Alloy: *Xiaolan Wu***¹; Ian Baker¹; ¹Thayer School of Engineering, Dartmouth College**

This paper describes the microstructures and mechanical properties of $Fe_{30}Ni_{20}Mn_{20}Al_{30}$ at elevated temperatures. Both post-mortem and in-situ heating transmission electron microscopy (TEM) accompanied by energy dispersive X-ray spectroscopy were used to characterize the microstructures. At temperatures less than 723 K, the alloy $Fe_{30}Ni_{20}Mn_{20}Al_{30}$ consisted of alternating Fe- and Mn-rich B2-ordered, and Ni- and Al-rich L2₁-ordered phases aligned along <100>, which probably formed by spinodal decomposition. At ~723 K, the L2₁-ordered Ni- and Al-rich phase started to disorder to a B2 structure. At ~773 K only two B2 phases were present. Compression tests performed at temperatures up to 873 K at a strain rate of 5×10^{-4} s⁻¹ showed a brittle-to-ductile transition and a large drop in yield strength at ~773 K, which was coincident with the L2₁ to B2 temperature. Also, the deformation mechanism both at room temperature and at ~773 K will be discussed in the paper.

Deformation, Damage, and Fracture of Light Metals and Alloys: Session I

Sponsored by: The Minerals, Metals and Materials Society, MS&T Organization, TMS Light Metals Division, TMS: Chemistry and Physics of Materials Committee, TMS/ASM: Mechanical Behavior of Materials Committee

Program Organizers: Qizhen Li, University of Nevada, Reno; Xun-Li Wang, Oak Ridge National Laboratory; Yanyao Jiang, University of Nevada, Reno

| Tuesday AM | Room: 13 |
|---------------|-------------------------------|
| March 1, 2011 | Location: San Diego Conv. Ctr |

Session Chair: Qizhen Li, University of Nevada, Reno

8:30 AM Invited

Modeling Dislocation Slip Transmission across Alpha-Beta Interface in Ti-Alloy: Chen Shen¹; Ju Li²; *Yunzhi Wang*³; ¹GE; ²University of Pennsylvania; ³Ohio State University

We apply 3D microscopic phase field model to study dislocation transmission across alpha-beta interfaces with residual interfacial dislocations in Ti-alloys. The model employs complex alloy energetics directly from ab



initio calculations, circumventing the need for fitting atomistic potential. We first compute the generalized stacking fault (GSF) energy surface of HCP (alpha) and BCC (beta) Ti. After matching the two GSFs at the alpha-beta interface with Burgers orientation relationship, we perform microscopic phase field simulations. These simulations have been previously checked against the Peierls model calculations and have been shown to agree with the Peierls model results completely. The new calculations in alpha-beta-alpha sandwich configurations reveal intricate dislocation pileup, transmission, storage and reaction mechanisms similar to what have been seen in atomistic simulations and experimental characterizations. A coarse-grained dislocation density based description coupled to continuum elasticity could be developed to predict the overall interface-strengthening behavior of the alloys.

9:00 AM Invited

Deformation and Fracture of Nanostructured fcc Materials under Monotonic and Cyclic Loading: *Diana Farkas*¹; ¹Virginia Tech

We present simulations using embedded atom method (EAM) potentials that investigate the deformation, fracture and fatigue behavior in nanocrystalline fcc materials. The simulations include deformation studies where strain localization and sustained emission of dislocations from the grain boundaries are shown to lead to crack initiation. Cracks nucleate preferentially in weak grain boundaries that are perpendicular to the loading direction. The simulation results also revealed a particular nanoscale mechanism of crack propagation as the main crack links with nano-voids nucleated ahead of the crack tip. Depending on the particular orientation relationships, cracks can also be stopped by grain boundaries. Under applied cyclic loading and show particular mechanisms of crack advance related to damage accumulation.

9:30 AM

Using Ab Initio Calculations in Designing BCC MgLi-X Alloys for Ultra-Lightweight Applications: *Martin Friak*¹; William Counts¹; Dierk Raabe¹; Joerg Neugebauer¹; ¹Max Planck Institute for Iron Research

Body-center-cubic Mg-Li-based alloys are a promising light-weight structural material. In order to tailor the Mg-Li composition with respect to specific industrial requirements, systematic materials-design concepts need to be developed and applied. We have therefore performed a quantummechanical study of fundamental physical properties of bcc MgLi-X substitutional ternaries with solutes from the 3rd row (Na, Al, Si, P, S, Cl) and 4th row transition metal (Sc, Ti, V, Cr, Mn, Fe,Co, Ni, Cu, Zn) elements. The computed properties are used to determine engineering parameters such as (i) specific Young's modulus or (ii) bulk over shear modulus ratio (B/G) differentiating between brittle and ductile behavior. Analyzing these extensive and systematic ab initio data sets we derive chemical trends and explain why none is able to simultaneously improve both specific Young's modulus and ductility (see Counts et al., Acta Materialia, vol. 57, 69 (2009)).

9:45 AM

The Effect of Crystallographic Orientation on Void Growth: A Molecular Dynamics Study: Mehul Bhatia¹; *Kiran Solanki*¹; Amitava Moitra¹; Mark Tschopp¹; ¹Mississippi State University

In ductile materials, fracture involves void nucleation, growth and coalescence. The objective of this research is to understand how crystallographic orientation influences void growth in Al for uniaxial tensile deformation. Molecular Dynamics simulation with Cubical specimens having periodic boundary condition were provided with one embedded spherical void and were subjected to remote uniaxial tension of different crystal orientation. The simulation results show how crystallographic orientation affects the yield stress and void growth corresponding to dislocation nucleation from surface of the void resulting in shear loops in perfect FCC lattice. The effect of crystallographic orientation was evident as very different dislocation patterns/shear loops occurred in the specimen with different orientations. The significance of this research is that atomistic simulations of this type can help to inform continuum void growth models for multiscale models.

10:00 AM Break

10:15 AM Invited

Creep Deformation of Al-Sc-X Alloys: Matthew Krug¹; David Seidman¹; *David Dunand*¹; ¹Northwestern University

Three alloys (Al-0.12Sc, Al-2.9Li-0.11Sc, and Al-5.53Li-0.048Sc-0.0092Yb,at.%) were aged at 325°C to produce coherent, misfitting L12 Al3[Sc(Li,Yb)] nano-precipitates that are coarsening resistant. Compared to Al-0.12Sc, Al-2.9Li-0.11Sc has higher peak-strength, and the time to onset of over-aging is delayed from 24 to 96 h. The aged alloys were crept at 300°C in compression, over minimum steady-state strain rates between 10-9 and 10-4 s-1. The alloys exhibit high apparent stress exponents (n=14–33), indicative of threshold stress behavior. Calculated threshold stresses range between 8 and 20 MPa. The threshold stress normalized by the Orowan stress increases with precipitate size and lattice parameter mismatch due to elastic strains induced in the matrix, and their interactions with dislocations. Comparisons are made with past work on similar Al-Sc-RE alloys, helping to draw conclusions about the benefits of ternary additions to creep- and coarsening-resistant Al-Sc alloys.

10:45 AM Invited

Impression Creep – A Localized Technique for Characterizing Creep Deformation of Materials: *Fuqian Yang*¹; ¹University of Kentucky

The impression test using a flat-ended indenter has been developed to study the time-dependent plastic deformation of materials. In contrast to the sharp-instrumented indentation, the contact area remains constant during the impression allowing a constant average contact stress when subjected to constant loads. Steady-state creep of various materials has been observed. The impression creep tests of a precipitation hardenable Mg-8Zn-4Al-0.5Ca (wt.%) casting alloy were performed in the temperature range of 403–623 K and under the punching stress range of 1.68–60.4 MPa. Using a hyperbolic sine stress law between the steady-state impression velocity and the punching stress, a single activation energy was found to be 77.5 kJ/mol, which is about half of the activation energy for lattice diffusion in Mg. A single mechanism of grain boundary fluid flow was proposed to be the controlling mechanism for the creep behavior of the Mg-8Zn-4Al-0.5Ca alloy under the testing conditions.

11:15 AM

Creep Fatigue Behavior of 319 Aluminum Casting Alloys under Hot Compressive Dwell Conditions: *Xiang Chen*¹; Diana Lados¹; Richard Pettit²; ¹Worcester Polytechnic Institute; ²FractureLab

Fatigue crack growth under Hot Compressive Dwell (HCD) conditions is an important failure mode for many high temperature applications, such as cylinder heads for internal combustion engines. A new testing methodology was developed to study the creep mechanism that accelerates the growth of cracks loaded with a compressive dwell cycle. Tensile residual stress build up at the crack root is considered a key factor contributing to crack growth under HCD conditions. To evaluate this effect quantitatively, stress relaxation and crack growth tests were performed to determine the creep and crack growth responses of the material. A Blunt Compact Tension (BCT) specimen was then analyzed using FRANC2D to determine the stress distribution, and obtain a 2D weight function K-solution. The residual stress distribution is then applied via the weight function to determine residual K that builds up during the operating life of the part. These results will be presented and discussed.

11:30 AM

Room Temperature Creep and Substructure Formation in Pure Aluminum at Ultra-Low Strain Rates: *Junjie Shen*¹; Iketa Ken-ichi¹; Hata Satoshi¹; Nakashima Hideharu¹; ¹Kyushu University

The creep behavior in highly pure aluminum (5N) and industrial pure aluminum (1070) with different grain sizes has been investigated by helicoid spring creep tests at ultra-low strain rates lower than 10-9s-1 and room temperature. Obtained results show that different types of deformation mechanisms are closely related with grain sizes and impurity concentrations: when the average grain size was 24 μ m, the stress exponent, n ~ 1. The

9:00 AM

dominant deformation mechanism was considered to be grain boundary sliding; on the other hand when the average grain size was 1.6 mm, the stress exponent, $n\sim 5$, which was interpreted as dislocation creep. Microstructural observation shows dislocation tangle, cell formation; in an industrial pure aluminum with grain size of 25 μ m, the stress exponent, n=2. Microstructure observations revealed dislocation emission from grain boundary acts as main deformation mechanism and intergranular dislocations tangle, cell formation as coordination mechanism.

11:45 AM

Quantifying the Relationship Between Deformation-Induced Surface Roughness, Grain Orientation, and Strain Localization in Polycrystalline Aluminum: *Mark Stoudt*¹; Joseph Hubbard¹; Adam Creuziger¹; Lyle Levine¹; ¹National Institute of Standards and Technology

Since bulk plastic deformation in polycrystalline materials is strongly dependent on the character of the individual grains, careful examinations of surface morphology and grain orientations with strain can reveal considerable information about the active deformation mechanisms and directly quantify the morphological conditions that promote strain localization. High-resolution topographical analyses, performed *in-situ* on aluminum sheet that was incrementally strained in uniaxial tension, were used to construct maps of the localization potential as a function of strain. These maps were integrated with EBSD measurements of the initial grain orientations to yield a grain-by-grain assessment of the microstructural conditions required to produce the critical surface morphology. The results suggest the relationship between grain orientation and Taylor factors. The methodologies used, and details regarding the nature of the relationships between strain, microstructure, and surface morphology shall be presented and discussed.

Dynamic Behavior of Materials V: Spalling and Dynamic Fracture

Sponsored by: The Minerals, Metals and Materials Society, TMS Structural Materials Division, TMS/ASM: Mechanical Behavior of Materials Committee

Program Organizers: Marc Meyers, UCSD; Naresh Thadhani, Georgia Institute of Technology; George Gray, Los Alamos National Laboratory

| Tuesday AM | Room: 5A |
|---------------|-------------------------------|
| March 1, 2011 | Location: San Diego Conv. Ctr |

Session Chair: George Gray, Los Alamos National Lab

8:30 AM Invited

Dynamic Necking of Structures Submitted to High Strain Rate Loadings: *Alain Molinari*¹; Sébastien Mercier¹; ¹Université Paul Verlaine-Metz

The fragmentation of structures has received a large attention during the last decades. A large effort was recently made to understand the behavior of structures subjected to an intense blast. To ensure integrity of structures, the conditions for the onset of fragmentation as well as for delaying the occurrence of such phenomenon have to be understood. Experiments conducted on rings and cylinders under rapid expansion have shown that the ductility of materials and the fragmentation process are significantly affected by the loading rate. Our scope is to describe by theoretical means the process of multiple necking that leads to the failure of structural elements under dynamic loading (bars, plates, cylinders, rings and hemispherical shells). The effects of material parameters, material inertia, loading conditions and sample geometry are analysed by means of a linearized stability analysis. Results are compared to experimental data.

3-D Modelling of Local and Global Spall Damage in Shocked FCC Multicrystals: *Kapil Krishnan*¹; Leda Wayne¹; Andrew Brown¹; Pedro Peralta¹; Shengnian Luo²; Darrin Byler²; Aaron Koskelo²; ¹Arizona State University; ²Los Alamos National Laboratory

3-D finite element (FE) simulations were used to study effects of microstructure, e.g., grain boundaries (GBs), on spall damage in copper multicrystals. Laser-driven plate impact experiments were conducted at low pressures (2-6 GPa) to capture spall damage at the nucleation stage. The 3-D FE model was developed from serial sectioning of the tested samples. Analysis was performed with ABAQUS/EXPLICIT using anisotropic elasticity and the Steinberg-Guinan (SG) model, where plastic anisotropy was modeled using Hill's anisotropic yield criterion. A damage model based on a cut-off tensile pressure was incorporated for element removal to study interactions between release waves and existing voids. The global damage appeared at the expected spall plane and the difference between target and flyer diameters led to release waves from the corner of the flyer that localized damage zone towards this region. Locally, damage localized near GBs. The FE results were compared with the experimental observations.

9:20 AM

Examination of the Damage and Failure Response of Tantalum and Copper under Varied Shock Loading Conditions: Ellen Cerreta¹; Darcie Dennis-Koller¹; Neil Bourne¹; George Gray¹; *Curt Bronkhorst*¹; Davis Tonks¹; Irene Beyerlein¹; Benjamin Hansen¹; Ricardo Lebensohn¹; ¹Los Alamos National Laboratory

A number of plate impact experiments have been conducted on high purity polycrystalline tantalum and copper samples using graded flyer plate configurations to alter the loading profile. These experiments are designed in a way so that a broad range of damage regimes are probed. The results show that the nucleation of damage primarily occurs at the grain boundaries of the materials. This affords us the opportunity to propose a porosity damage nucleation criterion which begins to account for the length scales of the microstructure (grain size distribution) and the mechanical response of the grain boundary regions (failure stress distribution). This is done in the context of a G-T-N type model for the ductile damage and failure response of both the materials examined. The role of micro-inertial effects on the porosity growth process is also considered.

9:40 AM

Geometric and Microstructural 3-D Characteristics of Incipient Spall Damage in Shock Loaded Cu Multicrystals and Polycrystals: *Andrew Brown*¹; Leda Wayne¹; Kapil Krishnan¹; Pedro Peralta¹; Shengnian Luo²; Scott Greenfield²; Darrin Byler²; Kenneth McClellan²; Aaron Koskelo²; ¹Arizona State University; ²Los Alamos National Laboratory

Spall-induced void structures were analyzed in shock loaded copper samples to determine void size, shape, and spacing distributions. Copper samples (1000 μ m thick) were impacted by laser-driven flyer plates (500 μ m thick) at low pressures (2-6 GPa) to encourage incipient spall damage. Serial sectioning and Electron Backscattering Diffraction (EBSD), along with inplane and through-thickness optical microscopy, were used to create 3-D renditions of the voids and their surrounding microstructure to characterize and compare their local and global geometrical and crystallographic characteristics. Analysis of regions of localized damage indicates that grain boundaries with misorientations between 30° and 50° are preferred sites for intergranular voids, which were typically shaped as sheets following the boundaries. Damage on the spall plane contained a spatial distribution of pores that was statistically uniform, indicating 1-D conditions. Effects of pre-existing plastic deformation on damage sites were also studied using half-hard and annealed samples with similar grain size.



10:00 AM

Instrumented Ring Expansion for the Measurement of High Strain Rate Constitutive and Fracture Behavior: *Jason Johnson*¹; Geoff Taber¹; Gregg Fenton²; Glenn Daehn¹; ¹Ohio State University; ²Applied Research Associates

The study and development of high strain rate constitutive models is pertinent to several fields, yet the test methods utilized to probe this high strain-rate realm are limited in both number and standardization. New technologies have been leveraged to revive an old, under-utilized test method – the axisymmetric expanding ring. The combination of Photon Doppler Velocimetry (PDV) and one of several ring launch techniques allows the successful testing and instrumentation of samples loaded in tension without wave effects at strain rates in excess of 104 s-1. Design and construction of the embodiment of this test at OSU.. Examples of expanding low ductility, modest conductivity metal (hardened steel) and a high conductivity, high ductility material will be discussed in depth. In the former case concurrent numerically modeling of the problem is necessary for accurate constitutive modeling, while simpler methods are acceptable in the latter case.

10:20 AM Break

10:30 AM Invited

The Dependence of Dynamic Spall Strength on Flow Stress and Temperature: Roger Minich¹; ¹LLNL

A statistical void nucleation and growth model is presented that relates the dependence of dynamic spall strength on flow stress and temperature. The model is incorprated in a finite element code and compared to a wide range of plate impact experiments. The model successfully predicts the pressure dependence of the spall strength and emphasizes the role of stress fluctuations in determining the size distribution of nucleated voids. It also predicts the observaton that the spall strength for two different microstructures are comparable when the corresponding flow stresses are comparable. Also, the temperature dependence of the dynamic spall strength is shown to be consistent with data for temperatures even approaching melt.

11:00 AM

Laser-Shock Induced Spalling and Fragmentation in Vanadium: Marc Meyers¹; H. Jarmakani¹; B. Maddox²; C. T. Wei¹; D. Kalantar²; ¹University of California, San Diego; ²Lawrence Livermore National Laboratory

Polycrystalline and monocrystalline vanadium was subjected to shock compression followed by tensile wave release to study spall and fragmentation behavior. The shock pulse was generated by a direct laser drive at energy levels ranging from 11 and 440 J/mm² and initial pulse durations of 3 and 8 ns (approximate initial pressures between 10 and 250 GPa). The effects of target thickness, laser energy, polycrystallinity, and pulse duration were studied. Calculations show melting at a pressure threshold of ~150 GPa. Consistent with the analytical predictions, the recovered specimens and fragments show evidence of melting at the higher energy levels. Spalling in the polycrystals occurred by a ductile tearing mechanism that favored grain boundaries. In the monocrystals, it occurred by a mixture of cleavage fracture along {010} planes and ductile dimple fracture. This lower spall strength in polycrystals contradicts predictions from the Hall-Petch equation. Experimentally obtained fragment sizes were compared with predictions from the Grady-Kipp model. The spall strength of vanadium under laser loading conditions was calculated from both VISAR pullback signals and using the spall thickness and found to be considerably higher than predictions from gas-gun experiments. This higher spall strength is suggestive of a strong time dependence of the phenomenon, consistent with the nucleation and growth kinetics of voids and the strain-rate sensitivity embedded in the Grady theory.

11:20 AM

Micro-CT for the Quantification of 3D Voids within Damaged Structures: *Brian Patterson*¹; Christopher Hamilton¹; Ellen Cerreta¹; Darcie Dennis-Koller¹; Curt Bronkhorst¹; Benjamin Hansen¹; ¹Los Alamos National Laboratory

Micro X-ray Computed Tomography (MXCT) is widely used in the materials community to examine the internal structure of materials for voids and cracks due to damage or casting, or other defects. Most research in this area focuses on the qualitative aspect of the image, simply answering; Are there voids present? Here we present an ongoing study of the quantified incipient spall voids in Cu with different grain sizes, using a gas gun with various velocities. Data analysis packages for MXCT are just now becoming able to dimensionally measure and produce statistics on the voids present. In order to make the size of the features in the 3D image quantifiable, the question, how many radiographs are required to render the object dimensionally accurate in 3D, must be answered. A series of data sets has been collected, varying the number of radiographs collected in order to determine the appropriate number required.

11:40 AM

Shock-Induced Spallation Phenomena in Copper-Niobium Nanolayered Composites: Niraj Gupta¹; Alexander Stukowski²; Michael Baskes³; Srinivasan Srivilliputhur¹; ¹University of North Texas; ²Darmstadt University of Technology; ³Los Alamos National Laboratory

Shock-induced spallation phenomena in Copper-Niobium nanolayered composites conforming to a Kurdjumov-Sach's orientation relation were simulated using molecular dynamics to determine both spallation strength and the nature of void formation. The copper and niobium system is of interest due to its immiscible nature and the orientational relation of the two lattices which creates an interface acting as an effective sink for dislocations and vacancies. The target structures consisted of varying numbers of alternating copper and niobium layers with thicknesses varying from 1 nm to 22 nm. Flyer velocities ranged from 3.5 to 11.5 Å/ps, corresponding to an approximate strain rate of 10^9 /s. Spallation occurs in the vicinity of the Cu-Nb interface, and always in the copper layer. The proposed factors contributing to spallation will be discussed, as well as what effect the layer morphology has on the strength of the target.

12:00 PM

Materials Characterization of Railgun Erosion Phenomena: *Brenda Machado*¹; Lawrence Murr¹; Edwin Martinez¹; Sara Gaytan¹; Sikhanda Satapathy²; ¹University of Texas at El Paso; ²The University of Texas at Austin

Railguns, consisting of a Cu rail-stator system with a moving Al projectile armature, are able to launch large, light-weight (usually Al) projectiles hundreds of miles using a high current pulse creating a comparably large magnetic field. Rail erosion has been a limiting feature. In this research, we have examined the Cu rail surface erosion and mixing of rail and Al projectile debris using optical metallography and scanning electron microscopy. The observations illustrate a unique, elongated starting Cu rail grain structure with a high dislocation density observed by transmission electron microscopy (TEM). The rail surface debris coating exhibits a propensity of porous Al (or gas bubble structure) created by temperatures above the Al melting temperature. TEM representative of the Al/Cu interface illustrates little, if any, alloying. The Al projectile and Cu rail form a dynamically recrystallized zone where small Al and Cu grains (~20 nm diameter) allow for solid-state flow.

Electrode Technology for Aluminium Production: Anode Raw Materials and Green Carbon

Sponsored by: The Minerals, Metals and Materials Society, TMS Light Metals Division, TMS: Aluminum Committee Program Organizers: Alan Tomsett, Rio Tinto Alcan; Ketil Rye, Alcoa Mosjøen; Barry Sadler, Net Carbon Consulting Pty Ltd

| Tuesday AM | Room: 16B |
|---------------|-------------------------------|
| March 1, 2011 | Location: San Diego Conv. Ctr |

Session Chair: Frank Cannova, BP Coke

8:30 AM Introductory Comments

8:35 AM

Property Profile of Lab- Scale Anodes Produced with 180°C Mettler Coal Tar Pitch: Winfried Boenigk¹; Claudia Boltersdorf¹; Falk Lindner¹; Jens Stiegert¹; ¹RÜTGERS Germany GmbH

The PAH- induced toxicity of coal tar pitch decreases with increasing softening temperature. The use of high- melting pitches is however restricted due to operational challenges. One critical limitation is high-temperature mixing. Temperatures up to 300°C were now realised using a novel developed EIRICH mixer. A 180°C Mettler binder pitch resulted in anodes having a higher baked density (+ 0.03 g/cm³). Electrical resistivity and air permeability are reduced whereas compressive strength and Young's modulus are increased. The significantly lower baking loss allows a faster carbonisation process in the low temperature range potentially increasing the throughput of baking furnaces.

9:00 AM

Quality and Process Performance of Rotary Kilns and Shaft Calciners: Les Edwards¹; ¹Rain CII Carbon

Rotary kilns have been used successfully for many years to produce calcined coke for the aluminium industry and they offer a high level of automation, performance and flexibility. Shaft calciners make a high bulk density, coarse particle size product and several papers have been published recently highlighting these benefits. This paper presents a detailed comparison of the merits of these two different calcining technologies from a process and product quality perspective. It addresses several misconceptions about the technologies related to operability, product quality and their ability to handle a wide range of green coke qualities. Both technologies will continue to be used in a complimentary manner in the future.

9:25 AM

Sub-Surface Carbon Dioxide Reaction in Anodes: *Donald Ziegler*¹; ¹Alcoa Primary Metals

Formation of carbon dust in electrolysis is linked to reaction of the anodes with carbon dioxide. The general understanding is that the reaction takes place inside the anodes, below the bath surface and rather more toward the sides of the anodes than the bottom. Given this, a relevant question is the relative importance of transport through the anode compared to its intrinsic reactivity. To provide quantitative answers, a transport-reaction model has been developed. The key finding is that the extent of reaction is insensitive to the permeability. This is because the reaction produces two moles of CO for every mole of CO2 consumed, so that there is a net flow away from the reaction locale. Consequently, fresh reactant must be supplied by diffusion rather than convection. Since these two processes are governed by different material properties, this finding opens the possibility of new approaches to optimization of anode structure.

9:50 AM

Paste Quality Improvements at Alcoa Poços de Caldas Plant: Beatriz Vry¹; Ciro Kato¹; Jeronimo Araujo¹; Fabiano José Ribeiro¹; André Luís Abreu¹; ¹Alcoa

Alcoa Poços de Caldas Soderberg Carbon Plant began its operation in 1965 and after a series of upgrades including the mixer heating system upgrade in 1989, fines control in 2000, mixing temperature optimization in 2004 and installation of coke pre heaters in 2009, the plant now has twice the original production capacity with near world-class paste quality. The benchmark paste quality characteristic is 1.55 g/cc of baked apparent density (BAD), while Poços results are about 1.45 g/cc. The Paste Plant is now challenged to meet Potroom requirements for anode performance (higher loads and dry anode top technology). This paper describes the enablers chosen to improve the baked properties, which includes the optimization of fines production, mixing process and recipe. The quality management system which includes a carbon laboratory with Soderberg baking furnace, sample preparation and baked analysis (BAD, Air Permeability, CO2 Reactivity and Electrical Resistivity) is also described.

10:15 AM Break

10:25 AM

The Vertical Ball Mill for the Grinding of Calcined Petroleum Coke to Improve the Quality of the Anodes in the Aluminium Industry: *Stefan Gosau*¹; Andreas Wolf¹; ¹Claudius Peters Projects GmbH

The carbon fines used in anode production have traditionally been generated using the "horizontal" ball mill concept. For carbon fines, the correct particle size distribution with low variation, and low impurity levels are required to produce high quality anodes. A new vertical ball ring mill concept has been developed based on the results of research on the grinding of calcined petroleum coke. Industrial vertical mills are now in operation in seven anode plants around the world. The benefits seen from the mill include lower capital expenditure, reduced variation in sizing and reduced wear of the mill. Results from the plants, showing reduced pitch level variation, improved anode quality and reduced operating costs will be presented in the paper.

10:50 AM

Prebaked Anode from Coal Extract (2) - Effects of the Properties of Hypercoal-Coke on the Preformance of Prebaked Anodes: *Maki Hamaguchi*¹; Noriyuki Okuyama¹; Nobuyuki Komatsu¹; Jiro Koide²; Keisuke Kano²; ¹Kobe Steel, Ltd.; ²Sumitomo Corporation

Preparation of prebaked anodes utilizing coal solvent extraction technology will be reported. We previously reported that the coal extract prepared from non-hydrogenative extraction of thermal coals using tworing-aromatic solvent (Hyper-coal) is suitable for feedstock for anode coke. It contains very low levels of the impurities such as sulfur, sodium, nickel, and vanadium that are present in the coke normally used in anodes. In this paper, we will describe the results of detailed analyses of the Hyper-coal coke (HPCC), the effects of calcinating conditions of the Hypercoal, and the performance of prebaked anodes prepared from the HPCC.

11:15 AM

The New Generation of Vertical Shaft Calciner Technology: *Jingli Zhao*¹; ¹Jinan Aohai Carbon Products Co.,Ltd.

The vertical shaft calciner is widely applied in China for CPC calcination. Its application, however, is restricted by its lower capacity, less automation and no waste heat recuperation. A new generation of energy saving shaft calciner technology with higher capacity and power generation system has been developed recently and is illustrated in this paper. 75 kt of CPC annual production can be achieved by only one new shaft calciner, the waste heat from which can be recuperated to generate electricity of 28 million kWh. The major invention is calciner structure optimization by computer simulation for better volatile combustion and calciner heat balance, which brings about better CPC quality, higher capacity and provides more energy for power generation. The new shaft calciner technology is flexible to the size distribution and volatile content in the green coke and applicable for the pulverous coke and the coke with high volatile content.



Property Enhancement Sponsored by: The Minerals, Metals and Materials Society, TMS Structural Materials Division

Program Organizers: Tongguang Zhai, University of Kentucky; Zhengdong Long, Kaiser Aluminum; Peter Liaw, University of Tennessee

| Tuesday AM | Room: 31C |
|---------------|-------------------------------|
| March 1, 2011 | Location: San Diego Conv. Ctr |

Session Chairs: Peter Liaw, University of Tennessee; E-Wen Huang, National Central University

8:30 AM

Monitoring and Characterization of the Fatigue Response of Nano-Crystalline Mg Composites Reinforced with Ti2AlC: *Antonios Kontsos*¹; Kavan Hazeli¹; Babak Anasori¹; Theodoros Loutas²; Michel Barsoum¹; ¹Drexel University; ²University of Patras

Herein we report on the mechanical and fatigue properties of nanocrystalline Mg-matrix composites reinforced with a Ti2AlC powder, fabricated by pressureless spontaneous melt infiltration of porous Ti2AlC preforms. Careful monotonic and cyclic tensile and compression experiments, combined with continuous acoustic emission (AE) monitoring are used to obtain vital information pertinent to the initiation and evolution of deformation and damage mechanisms related to this composite. The fatigue response is shown to be excellent over an extended period of time during which the recorded and extracted AE features are noticeably different from the initial and final stages of fatigue life. These results combined with the observed high damping are consistent with, and can be explained by invoking the formation and annihilation of incipient kink bands. The latter are fully reversible dislocation-based defects consisted of parallel coaxial dislocations formed on easy slip planes of kinking non-linear elastic solids such as Ti2AlC and Mg.

8:50 AM

Effects of Ultrasonic Nanocrystal Surface Modification on Fatigue Behavior of SUS316 Austenitic Stainless Steel Tube for Stents: *Auezhan Amanov*¹; Young Sik Pyun¹; Jun Hyong Kim¹; Hak Du Kim¹; Sang Ho Kim²; Chae Jong Park²; ¹Sun Moon University; ²M.I. Tech Co., Ltd.

The present paper describes the effect of Ultrasonic Nanocrystal Surface Modification (UNSM) treatment on fatigue behavior of SUS316 austenitic stainless steel tube for stents which is inserted into clogged heart, superficial femoral, carotid, and renal arteries. The surface hardness, surface integrity and compressive residual stress were compared before and after UNSM treatment. The fatigue test under room temperature is under carrying out and their results will be compared before and after UNSM treatment also. In addition, the possibility of replacement the expensive Co-Cr alloy tube by the UNSM treated SUS316 tube will be analyzed.

9:10 AM

Increasing the Fatigue Life of SAE52100 Steel by Ultrasonic Nanocrystal Surface Modification: *Jong Soon Im*¹; Young Sik Pyun²; Auezhan Amanov²; Sung Jae Lee¹; Jun Hyong Kim²; Chang Min Suh³; ¹ILJIN GLOBAL; ²Sun Moon University; ³Kyungpook National University

To increase the fatigue strength of slim bearing rings, the Ultrasonic Nanocrystal Surface Modification (UNSM) treatment was applied to rotary bending fatigue test specimens which are made of bearing steel SAE52100. XRD analysis shows that the structure of subsurface layer has become a nanograin structure till 100 μ m depth from the top surface. Surface structure and nano grain refinement were analyzed and compared before and after UNSM treatment by EBSD analyses as well as fatigue crack growth behavior of UNSM-treated specimens was compared with that of original specimens

which had not been UNSM-treated. It was also revealed from the surface analyses that surface hardness was increased by 20% and compressive residual stress was also induced up to 900 MPa of the UNSM-treated surface which are the main phenomena in prolonging fatigue life of bearings. RCF and friction characteristics after UNSM treatment were also explained.

9:30 AM

140th Annual Meeting & Exhibition

Research on HCF Tests and Damage Model of TC11 Alloy Welded Joints: Xiaogang Liu¹; Guo Hai-ding¹; ¹Nuaa

In the paper, the loading controlled fatigue tests of TC11 alloy welded joints have been done; the micro characteristics of fatigue fracture surface have been studied by SEM (scan electron microscope) as well. According to the test results, two types of fatigue source on fracture surface of the welds are found, say, edge fatigue source and internal fatigue source. Then S-N curve of the two types are obtained respectively. The fatigue life of the edge fatigue source is 35-65% longer then that of the internal fatigue source. Moreover, based on the gray distribution of the fracture surface's SEM imagines, the fractal dimension of fatigue source rejoin on fracture surface has been calculated by box counting method, the relationship between fractal dimension and fatigue life is analyzed. Finally, a fractal damage model which concern macro and micro damage is established based on the combination of damage mechanics theory and fractal theory.

9:50 AM

Residual Stresses in Alloy CF8C Plus Coated with Iron Aluminide: *Deepak Kumar*¹; Sebastien Dryepondt¹; Philip Maziasz¹; Bruce Pint¹; Beth Armstrong¹; Edgar Curzio¹; ¹Oak Ridge National Laboratory

CF8C plus is an economic, cast austenitic stainless steel that has creep resistance comparable to state-of-the-art wrought stainless steel and Nibase alloy, such as alloy 617, but does not require any post processing heat treatments. In this paper we discuss the evolution of residual stresses when this alloy is coated with aluminide coatings applied by slurry-coating and pack cementation processes with the objective of improving its oxidation resistance. The near surface and bulk residual stresses during heating/ cooling of the coated samples were determined by x-ray and neutron diffraction techniques for temperatures up to 900□C. Conventional tension-compression strain-controlled fatigue experiments were conducted on the bare and coated samples to assess the effect of residual stresses on the fatigue strength.

10:10 AM Break

10:20 AM

Fatigue Behavior of Al 6082-T4 and Al 7075-T73 after Ball Burnishing: *Yasser Ahmed*¹; Mansour Mhaede²; Lothar Wagner²; ¹German University in Cairo; ²Institute of Materials Science and Engineering (IWW), TU of Clausthal

The effect of ball burnishing on the rotating beam fatigue strength of age-hardened 6082-T4 and 7075-T73 aluminum has been investigated. Deep rolled specimens were cyclically deformed at room temperature using push-pull stress controlled fatigue and compared to the electrically polished condition as a reference, Also Shot peened condition give better results compared to electrically polish. Optimization curve was produced for both SP and BB conditions, due to this optimization shot peened with Almen intensity of 0.2 mmA for both alloys was used. For ball burnishing (deep rolling) 40 bars was used for 6082-T4 and 75 bars for 7075-T73 by deep rolling tool HG13. The observed improvements were from about 45% for Al 6082-T4 while it was the double for Al 7075-T73 compared to electrically polish, while the improvement of fatigue for BB condition compared to SP was 5% for Al 6082-T4 and 28 % for Al 7075-T73. Data analysis shows that the fatigue behavior in these alloys affected by surface treatment. It was found that deep rolling can dramatically enhance the fatigue behavior of aluminum alloys as compared to the shot peening and polished condition due to near surface compressive residual stresses as well as work hardening states and increased hardness induced by mechanical surface treatment (deep rolling).

10:40 AM

High Temperature Fatigue Behavior of Laser Shock Peened IN718Plus Superalloy: Vibhor Chaswal¹; S Mannava¹; Dong Qian¹; Vijay Vasudevan¹; Kristina Langer²; ¹University of Cincinnati; ²Wright Patterson Air Force Base

Service temperature fatigue testing is conducted on 2.5 and 5mm thick IN718Plus aeroengine superalloy after laser shock peening(LSP) with a double side patch overlay of 2.5mm spots at 5 to 8 GW/sq.cm using pulsed Nd:glass laser. Initially thermal relaxation of through thickness compressive residual stresses is established using conventional and Synchrotron X-Ray Diffraction. High temperature(HT) fatigue tests are then conducted at R=0.1 and monitored with an HT clip-on strain gauge and AC potential drop(ACPD). Subsequent fatigue induced residual stress relaxation is determined using a dedicated XRD system and correlated with nano and micro-indentation. While conditions for crack initiation and branching are investigated using scanning electron microscopy, ACPD is used to study final fracture. Microstructural evolution of Untreated, LSP treated, LSP + Fatigued samples is characterized using optical and Transmission electron microscopy. Based on dislocation substructures and precipitate morphologies that offer highest strengthening and fatigue resistance, optimum LSP parameters are recommended.

11:00 AM

Mechanical Properties and Four-Point-Bending Fatigue Behaviors of Non-Heat Treated and Carburized Low-Carbon Steels for Load-Chain Materials: *Wei Wu*¹; Gongyao Wang¹; David Huber²; Peter Hogan²; Rodney Reynolds²; Chris Hale²; Lee Whitted²; Joe Eudy²; John Stewart²; Jules Raphael³; Doug Fielden¹; Peter Liaw¹; ¹The University of Tennessee; ²Columbus McKinnon Corporation; ³J R Technical Services

The low-carbon steels, 10B22, 4615, and 4720, are used in electric hoists as load-chain materials. The mechanical properties of non-heat treated and carburized low-carbon steels were investigated. Four-point-bending-fatigue tests were conducted on cylindrical specimens to examine the fatigue behaviors of non-heat treated and carburized low-carbon steels at different stress levels. The four-point-bending-fatigue tests were performed at a stress ratio of 0.1 and a frequency of 10 Hz with a sinusoidal waveform. The fatigue results showed that the fatigue-strength of the carburized 10B22 steel was the highest at the reference cycles, 10⁷. Scanning-electron microscopy (SEM) fractography of tensile samples demonstrates the typical ductile fracture of the non-heat treated steels at room temperature. However, the mixture of the fracture mechanisms can be seen in the carburized steels; the ductile fracture at the core and the intergranular fracture in the hard layer were observed.

11:20 AM

Sustained Peak Low Cycle Fatigue: The Role of Coatings: *Britta Laux*¹; Tresa Pollock¹; ¹University of California, Santa Barbara

Turbine airfoil durability is often limited by low cycle fatigue, particularly when the cycle contains a compressive hold at elevated temperature. The initiation and growth of cracks in a single crystal superalloy have been studied during strain controlled fatigue at 1093\176C with a cycle that contained a 120s compressive hold. Samples which were fabricated from the SX nickel base superalloy Rene N5 were cycled in the uncoated condition and with aluminide coatings. All cracks initiated at sample surfaces and grew in a plane normal to the applied stress in the early stages of fatigue. Crack tips contained a layer of oxide. The growth process continued by a combined process of oxidation and creep. The role of the coating in this failure process is considered in the context of a model developed for crack growth during sustained peak low cycle fatigue.

11:40 AM

S-N Fatigue and Fatigue Crack Propagation Behaviors of High Mn Steels: *HyunJung Lee*¹; Jakie Kwon²; Youngju Kim²; Sangshik Kim¹; ¹Gyeong Sang National Univ.; ²Korea Institute of Geoscience and Mineral Resources

The increasing concern on safety and economical issues in shipbuilding industry requires new steels with better fatigue behaviors. The efforts to increase yield strength of steel would increase S-N fatigue life, but may decrease the resistance to fatigue crack propagation (FCP). In the present study, both S-N fatigue and FCP behaviors of high manganese steels were examined and compared to those of pearlite+ferrite and bainite steels. The S-N fatigue and FCP tests were conducted on high manganese steels, the microstructures of which were dominantly either martensitic or austenitic, at an R ratio of 0.1 and along L-T and T-L. It was found that the microstructure and yield strength affected both of fatigue behaviors of high Mn steels. Fatigue crack paths and fracture surfaces demonstrated that the crack tortuosity varied with different microstructure. The present study showed that yield strength alone could not explain the S-N fatigue behavior of steel specimens.

12:00 PM

High Cycle Fatigue Behavior of Shot-Peened Steels: *Alan Plumtree*¹; Mehdi Mirzazadeh¹; ¹University of Waterloo

The uniaxial fatigue behavior of four shot-peened engineering steels heat treated to the same hardness was investigated. Following long life (107) cycling under fully reversed (R=-1) uniaxial loading conditions, cyclic softening of the surface was accompanied by a decrease in the depth of surface hardness. Neither cyclic softening nor hardening occurred in non shot-peened steels cycled under the same conditions. The greatest amount of cyclic softening occurred in the two(0.4C and 0.7C)shot-peened hot rolled steels, whereas the fatigue limit of a 0.5C powder metallurgical steel increased 14.0%. However, the fatigue limit of a shot-peened heat treated and tempered steel(0.5C) decreased 12.0% due to the relaxation of internal stresses. In general, the beneficial effects of shot-peening, such as those due to compressive residual stresses and work hardening balanced the effects of surface roughness. Crack initiation occurred below the surface.

Friction Stir Welding and Processing VI: Aluminum and Magnesium Alloys I

Sponsored by: The Minerals, Metals and Materials Society, TMS Materials Processing and Manufacturing Division, TMS: Shaping and Forming Committee

Program Organizers: Rajiv Mishra, Missouri University of Science and Technology; Murray Mahoney, Retired from Rockwell Scientific; Yutaka Sato, Tohoku University; Yuri Hovanski, Pacific Northwest National Laboratory; Ravi Verma, General Motors

| Tuesday AM | Room: 5B |
|---------------|-------------------------------|
| March 1, 2011 | Location: San Diego Conv. Ctr |

Session Chair: Yutaka Sato, Tohoku University

8:30 AM

Microstructure and Mechanical Properties of Friction Stir Welded (FSW) AA5454-Joints: Xavier Lang¹; Dietmar Eifler¹; *Guntram Wagner*¹; ¹University of Kaiserslautern

The industrial application of friction stir welding as a high quality joining process requires the understanding of the influence of the FSW process on the developing microstructure and the resulting mechanical properties. The present work provides a comparison of FSW butt welds of the aluminum alloy AA5454 in the states O and H22. The influence of the friction stir welding process on the microhardness profile in the joining areas and the changes of the grain size in the different welding zones in relation to the base material will be described in detail. Furthermore it will be shown that the ultimate tensile strength, the yield strength and the total elongation after friction stir welding are nearly identical independent of the initial state of the investigated Al-alloys. Finally the fatigue behavior of welded AA5454 in the states O and H22 will be discussed.



8:50 AM

The Effect of Friction Stir Welding on the Dispersoid Particles of Aluminium Alloy 2195: *Roy Crooks*¹; Jorge dos Santos²; Kati Savolainen³; Hannu Hänninen³; ¹Black Laboratories, L.L.C.; ²GKSS-Research Centre GmbH; ³Aalto University

Grain coarsening is observed in friction stir welded nuggets of AA2195 after post-weld anneals. One factor which may contribute to this behaviour is the modification of dispersoid particle distributions by friction stir welding (FSW). High volume fractions of small particles are desirable for impeding grain boundary motion, recrystallization and grain growth. The most effective dispersoid in this alloy is the coherent precipitate, Al3Zr, which is subject to loss of coherency during dynamic recrystallization and a consequent reduction in Zener drag. Loss of coherency implies an increase in the critical particle size and dissolution of particles below that size. The dispersoid distributions of the base plate were compared to those of the advancing side of the as-welded plate. The effect of FSW on the particle size distributions in FSW AA2195 was studied using small angle x-ray scattering (SAXS). Morphology and coherency changes of Al3Zr particles were studied by transmission electron microscopy.

9:10 AM

Microstructural Characteristics of Sc-Modified Al-Zn-Mg-Cu Alloy Extrusions Joined by Friction Stir Welding: *Carter Hamilton*¹; Stanislaw Dymek²; Oleg Senkov³; ¹Miami University; ²AGH University of Science and Technology; ³UES, Inc

Extruded and T6 tempered plates of a Sc-modified Al-Zn-Mg-Cu alloy were joined by friction stir welding (FSW) at a constant weld velocity and various pin rotation speeds (PRS). At low PRS, hardness decreased from each edge of the weld to a local minimum at the weld center; however, at high RPS, the hardness initially decreased from each edge of the weld, but then rose toward the weld center. The transition in the hardness profile was related to different heating and cooling conditions during FSW. In particular, the peak temperature during FSW increased from ~250°C to 450°C as the PRS increased from 175 to 400 rpm. Differential scanning calorimetry of baseline and welded samples revealed that the volume fraction of GP zones and η' particles within the weld regions strongly depended on the weld conditions. For FSW heating rates, secondary phase dissolution/precipitation temperatures are in proximity to the welding temperatures.

9:30 AM

AGG Suppression in Friction-Stir-Welded, Spun-Formed Al-Li 2195 Materials: Stephen Hales¹; Wesley Tayon¹; ¹NASA

Currently, the Al 2219 dome caps for cryogenic propellant tanks are welded assemblies, where multiple panels are contoured to shape, heat treated, and joined. A new, single-piece fabrication approach being explored involves spin forming to final shape of Al-Li 2195 flat plates, which have been friction stir welded (FSW'd) together. The approach requires postforming heat treatment to the T8 temper for service properties. Processing for the T8 condition involves solution heat treatment (SHT), cold water quenching, cold stretching and aging. The occurrence of abnormal grain growth (AGG) during SHT of 2195 FSW'd material has been problematic from the perspective of service properties. The objective of this work was to suppress AGG during SHT by post-forming thermal processing alone. Constraints on the experimental design included applicability to large, complex-shaped, thin-walled domes and the capabilities of commercial heat treatment facilities. In this presentation, the experiments conducted are outlined and research results discussed.

9:50 AM

Analysis of Temperature and Residual Stress Evolution during Friction Stir Welding of Aluminum 7075-T6: Yunfeng Cao¹; Tyler Davis¹; *Yung Shin*¹: ¹Purdue University

In friction stir welding (FSW), it is well understood that the temperature can have a significant effect on the resultant weld quality. It is therefore necessary to examine the temperature evolution during FSW. In this work, a three dimensional model based on finite element analysis is used to investigate the temperature history and thermo-mechanical process in the welding of aluminum alloy 7075-T6. The temperature history of the workpiece and the residual stress of the welded plate are measured by an infrared camera and the X-ray diffraction technique, respectively. The measured results are compared with the model predictions and a correlation between temperature and residual stresses is established. To achieve desirable residual stresses of the welded plate, a laser shock peening (LSP) process is subsequently applied on the workpiece. A complete LSP model is employed to predict the residual stresses after LSP and predictions are compared with experimental results.

10:10 AM

Measurement of Residual Stress in Friction Stir Weld Joints: *Adrian DeWald*¹; Michael Hill²; Murray Mahoney³; ¹Hill Engineering, LLC; ²University of California, Davis; ³Consultant

Friction stir welding (FSW) is currently being used to join materials from plastics to high-strength steels in industries including automotive, aircraft, and shipbuilding. FSW employs a non-consumable pin that rotates at moderate speeds, which is plunged into the butting edges of the work pieces to be joined. Although the temperatures attained during FSW are relatively low compared with conventional fusion welding techniques, residual stresses still develop during FSW. The magnitude and distribution of these residual stresses can be detrimental to performance. This paper investigates the residual stresses generated by friction stir welding in a variety of materials including HSLA-65 steel, AA 2195, and AA 7075. Residual stress measurement data were obtained using the contour method and the slitting method. Using the contour method, residual stresses are obtained through the plate thickness for both the longitudinal and transverse orientations.

10:30 AM

Development of Tatsumaki Friction Stir Welding: Seung Hwan C. Park¹; Satoshi Hirano¹; Shinichi Kaga²; Mitsuru Onose²; Noriaki Tominaga²; Yasutsugu Yoshimura²; ¹Hitachi Ltd.; ²Mitsubishi-Hitachi Metals Machinery, Inc.

The authors have developed a double-sided friction stir welding (FSW) technology that consists of a dual-tool rotating mechanism arranged in face-to-face relation on the front and back surfaces of the joint. One rotating tool has a probe that protrudes from the shoulder, while the other rotating tool has a recess formed in the shoulder. The probe is inserted into the recess for receiving the probe during the FSW. With the shoulders pressed against both surfaces of the joint, the rotating tools move along the joint line. The main advantage of this process is the application of a wide range of weld thicknesses and high speed welding by controlling the motor power consumption. In this study, the effect of tool geometry on weld thickness, and its' possible application to continuous rolling system is described.

10:50 AM Break

11:00 AM

The Role of Plastic Deformation in Suppressing Abnormal Grain Growth in Friction Stir Welded Al-Li 2195: *Eric Hoffman*¹; Robert Hafley¹; Marcia Domack¹; Ravi Shenoy²; Wesley Tayon¹; Jessica Robinson¹; ¹NASA Langley Research Center; ²Lockheed Martin Space Systems

Traditional methods for producing large scale dome end caps for cryogenic propellant tanks utilize a multi-piece welded gore construction. To reduce the mass and fabrication costs and increase the reliability for these domes, a novel near-net manufacturing process is being explored in which a single-piece dome is spin formed from an Al-Li 2195-OM temper blank. The blank is friction stir welded (FSW) together from two commercial Al-Li 2195-OM temper plates to overcome plate size limitations. This manufacturing approach requires post-forming heat treatments to develop the required T8 temper properties. Abnormal grain growth (AGG) was observed in the FSW after solution heat treatment (SHT) and resulted in degraded mechanical properties. In this study, samples of FSW Al-Li 2195 were subjected to plastic deformation introduced by cold working and laser peening. The minimum level of cold work and laser peening intensity required to suppress AGG during SHT was determined.

11:20 AM

The Effect of Dispersoid Modification on Abnormal Grain Growth in Friction Stir Welded Al-Li 2195: *Roy* Crooks¹; Ravi Shenoy²; Wesley Tayon³; Marcia Domack³; ¹National Institute of Aerospace; ²Lockheed Martin Space Systems; ³NASA Langley Research Center

Friction stir welded (FSW) AA2195 plates have been spun formed into large domes used as end caps for cryogenic tanks for space launch vehicles. After FSW, the plates are annealed, spun, solution treated and aged to peak strength. Solution heat treatment of the FSW and spun formed plates may result in excessive growth of nugget grains, particularly near the advancing side interface. Several factors are related to this growth, including stored strain energy, grain size and dispersoid particle size distributions. Samples of FSW AA2195 were studied after FSW and annealing to quantify the microstructural factors contributing to grain growth during the solution heat treatment. Electron backscattered diffraction (EBSD) systems in a scanning electron microscope (SEM) and in a transmission electron microscope were used. Heat treatments developed to modify these factors were assessed.

11:40 AM

Friction Stir Welding of 25 mm Thick Al 6061-T651 Plates: *Guru Dinda*¹; Douglas Grant¹; Matthew Scheid¹; Ashish Dasgupta¹; Sudip Bhattacharya²; Jyoti Mazumder²; ¹Focus: HOPE; ²University of Michigan

Friction stir welding (FSW) was invented in 1991 by The Welding Institute as a solid-state joining method for a variety of metals and alloys, in particular aluminum alloys. Since the early discovery, FSW of aluminum alloys have been extensively investigated. However, very little work is reported on FSW of thick Al plates in the open literature. The objective of this work is to optimize the process parameters such as travel speed, forge force, rotational speed and tilt angle for butt welding of 25 mm thick Al 6061-T651 plates with a view to produce welds without any defects. A comprehensive design of experiments was conducted to establish a process parameter window for welding 25 mm thick Al 6061-T651 plates of various sizes. The weld quality was assessed via optical microscopy, SEM, XRD, microhardness and tensile testing. The effect of process parameters on the resulting weld properties was analyzed using statistical techniques.

12:00 PM

Effects of Forge Axis Force and Backing Plate Boundary Condition on FSW of AA6056: *Piyush Upadhyay*¹; Anthony Reynolds¹; ¹University of South Carolina

For a given set of welding parameters forge axis force can also have a significant effect on stir zone temperature, torque, and in-plane forces. Typically, for a given set of welding parameters, an FSW user chooses an appropriate but arbitrary forge axis force a posteriori based on weld surface quality. This qualitative adjustment of forge axis force can be affected by thermal boundary conditions that are applied to the work-piece. We seek to understand the effects of forge axis force coupled with the thermal boundary condition at the bottom of the work-piece on AA 6056 (4.2mm thick) plate. Forge axis force and backing plate conductivity are varied while holding other parameters constant. Resulting temperature, torque and in-plane forces are analyzed and correlated with the varied parameters. The result demonstrates that for the given gage thickness, metallurgically significant temperature variation can be achieved without changing the rotation/translation speed.

12:20 PM

Friction Stir Welded "A" Frame For Duel Function Test Fixture: *Alan Handyside*¹; Farzad Baratzadeh¹; Jeff Buller¹; Hamid Lankarani²; Blair Carlson³; Dwight Burford¹; ¹National Institute for Aviation Research; ²Wichita State University; ³General Motors Corporation

Advancements in friction stir welding (FSW) pin tool and joint design have been used to develop an automotive and aerospace test fixture . The fixture was designed and built for a case study analyzing functionality of an advanced bumper / crash box fabricated by FSW. The fixture "A" frame is fabricated using FSW of AA6063-T6 and AA6061-T6. The fixture is used as drop tower for constant acceleration tests and with crash sled for constant velocity tests. Butt welds, similar to those developed and tested for the crash box / bumper, were incorporated into the fixture. FEA simulations on the "A" frame, including FSW joints, were used for analysis. Tensile test coupons made by FSW were prepared to determine weld parameters, parent and weld material properties. Summary of FSW process development is presented along with weld coupon test results. An overview of fixture function and preliminary fixture test results is presented.

12:40 PM

Investigation of Lazy S Feature in Self Reacting Tool Welds in 2024-T4 Aluminum: *Karl Warsinski*¹; Michael West²; Jim Freeman³; Todd Curtis²; ¹Michigan Technological University; ²South Dakota School of Mines and Technology; ³MTS Systems Corporation

The current research is an examination of the "Lazy S" feature found in self-reacting tool (SRT) friction stir welds. The research objectives are to characterize the feature using scanning electron and optical microscopy and determine its effect on the mechanical properties of the welded material. Welds were conducted in 2024-T4 aluminum. Welding parameters were varied in an attempt to influence the size and location of the feature. Tensile tests were performed on each weld and were correlated with the total length of the feature. Preliminary results indicate that there is a correlation between decreasing feature length and decreasing tensile strength.

Frontiers in Solidification Science: Experimental Studies

Sponsored by: The Minerals, Metals and Materials Society, TMS Electronic, Magnetic, and Photonic Materials Division, TMS: Chemistry and Physics of Materials Committee, TMS: Solidification Committee

Program Organizers: Jeffrey Hoyt, McMaster University; Daniel Lewis, Rensselaer Polytechnic Institute

| Tuesday AM | Room: 6E |
|---------------|-------------------------------|
| March 1, 2011 | Location: San Diego Conv. Ctr |

Session Chair: To Be Announced

8:30 AM Invited

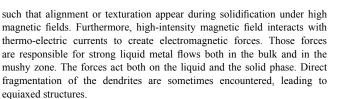
Simulation of Dendritic Growth Observed in Synchroton X-ray Video Experiments: *Christoph Beckermann*¹; Pierre Delaleau¹; Ragnvald Mathiesen²; Lars Arnberg²; ¹University of Iowa; ²NTNU

A mesoscopic model is developed to simulate microstructures observed in situ by X-ray video microscopy during directional solidification of Al-Cu alloys in a Hele-Shaw cell. In the model, a volume-averaged species conservation equation is solved to obtain the solute concentration and solid fraction fields, and an analytical stagnant film model is used to predict the motion of the dendrite envelopes. Good agreement is found between the measured and predicted dendrite envelope shapes, solid fractions, and solute concentration fields. The predicted size of the mushy zone and the extent of the undercooled melt region ahead of the columnar front agree well with the in situ experimental observations. The simulation results show quantitative agreement with internal solid fraction variations measured from the radiographs. The model is also able to realistically simulate a primary dendrite trunk spacing adjustment that was observed in one of the experiments.

9:00 AM Invited

Solidification of Metallic Alloys under Magnetic Fields: *Yves Fautrelle*¹; Xi Li¹; Olga Budenkova¹; Bachir Saadi¹; Zhongming Ren¹; ¹Grenoble Institute of Technology

Polyphase AC magnetic fields are used usually to generate either liquid metal stirring or electromagnetic vibrations. The electromagnetically-driven flows promote segregations and influence their distribution. The flow may also promote the CET thanks its effects on both the temperature and solute fields as well as the possible fragmentation mechanism. As far as DC magnetic fields are concerned, it was known that they usually exert a damping of the bulk fluid flows. Nevertheless, due to crystal anisotropy magnetic effects



140th Annual Meeting & Exhibition

9:30 AM Invited

Two-Phased Spiral Dendrites: *Silvere Akamatsu*¹; Mikael Perrut²; Sabine Bottin-Rousseau¹; Gabriel Faivre¹; ¹CNRS - UPMC; ²ONERA

We report for the first time experimental observations of a steady crystal growth shape called two-phased spiral dendrite in real-time directional solidification of a transparent SCN-DC base nonfaceted ternary alloy in glass-wall samples. Spiral dendrites arise from a ternary-component driven eutectic-cell instability of a two-phased solid. They exhibit an overall parabolic shape, and a lateral branching. Coupled growth occurs continuously from a spiral pattern on the tip, and delivers two intricate helices. The spiral step and the tip radius of curvature vary approximately as the reciprocal of the square root of the solidification rate, and fall close to the minimum-undercooling spacing of binary SCN-DC. The spiral geometry is compatible with a growth of the lamellae perpendicular to the solidification front envelope. In contrast to the one-phased dendrite, the growth direction of spiral dendrites is not determined by any surface tension anisotropy, and is initial-condition dependent.

10:00 AM Break

10:15 AM Invited

Universality and the Pinch-off of Rods by Capillarity: L. Aagesen¹; A. Johnson¹; J. Fife¹; *Peter Voorhees*¹; M. Miksis¹; S. Poulsen²; E. Lauridsen²; F. Marone³; M. Stampanoni³; ¹Northwestern University; ²Riso Laboratory for Sustainable Energy; ³Swiss Light Source

The detachment of secondary dendrite arms during solidification processing has a significant influence on the resulting microstructure. To understand the fragmentation process when it is driven by capillarity, we examine the evolution of the interfacial morphology of liquid and solid rods in an Al_15 wt.% Cu alloy. Interfacial energy induces a rod develop undulations by the well-known Rayleigh instability. These undulations increase in amplitude and lead to pinching. We show theoretically that sufficiently close to the pinching event the interfacial morphology becomes universal; the interface shape is independent of the initial morphology of the rod-like phase and material system, and its evolution is described by a power law in time. We test this prediction using insitu x-ray tomography and find an excellent agreement between theory and experiment in both the morphology and the kinetics of the pinching process. The implications of this result to various solidification processes will be discussed.

10:45 AM Invited

Directional Growth Structures in Univariant Eutectics: *Ralph Napolitano*¹; ¹Iowa State University

Directional solidification and serial milling are employed here to investigate the three-dimensional features of multiphase microstructures in Al-Cu and Al-Cu-Ag alloys, focusing on univariant two-phase structures in the ternary. The relationships between local eutectic phase topology, crystallographic orientation/misorientation, eutectic fault configuration, faulted domain structure, and grain structure, relative to the constraints of specimen geometry and applied thermal field, are examined.

11:15 AM

Nucleation Catalysis Potency of Ceramic Nanoparticles in Aluminum Matrix Nanocomposites: Michael De Cicco¹; John Perepezko¹; Lih-Sheng Turng¹; Xiaochun Li¹; ¹University of Wisconsin-Madison

The nanoparticles in metal matrix nanocomposites (MMNCs) were shown to catalyze nucleation of solidification. Nanoparticles of SiC, TiC, and γ -Al₂O₃ were dispersed in an aluminum alloy A356 matrix using an ultrasonic processing technique. The droplet emulsion technique was used to examine the undercooling in each matrix-nanoparticle system. Despite

their small sizes, the nanoparticles demonstrated the ability to significantly reduce the necessary undercooling for nucleation. In general, the degree of undercooling in the MMNCs containing SiC, TiC and γ -Al₂O₃ was in agreement with the free growth undercooling. The nucleation catalysis by the nanoparticles resulted in significantly refined microstructures. The grain refining effectiveness of nanoparticles was also examined in pure Al and Al-10Mg using TiC_{0.7}N_{0.3} nanoparticles. In both pure Al and Al-10Mg the nanoparticle addition significantly reduced the average grain size of the matrix. Comparison was made to the commonly used Al-5Ti-B grain refiner. At the addition levels used, the nanoparticles were more effective than the Al-5Ti-B grain refiner.

Hume-Rothery Symposium Thermodynamics and Diffusion Coupling in Alloys - Application Driven Science: Diffusion Coefficients and Thermodynamics

Sponsored by: The Minerals, Metals and Materials Society, TMS Electronic, Magnetic, and Photonic Materials Division, TMS: Alloy Phases Committee

Program Organizers: Zi-Kui Liu, The Pennsylvania State University; Larry Kaufman, CALPHAD, Inc.; Annika Borgenstam, Royal Institute of Technology; Carelyn Campbell, NIST

| Tuesday AM | Room: 31A |
|---------------|-------------------------------|
| March 1, 2011 | Location: San Diego Conv. Ctr |

Session Chairs: Yongho Sohn, University of Central Florida; Gary Shiflet, University of Virginia

8:30 AM Invited

Influence of Thermodynamic Forces on Diffusion in Melts: Axel Griesche¹; Juergen Horbach²; Andreas Meyer²; ¹Federal Institute for Materials Research and Testing (BAM); ²German Aerospace Center (DLR)

We report about diffusion measurements and molecular dynamic simulations in Al-Ni and Al-Cu melts. Capillary methods were used to measure Ni and Cu self diffusion and to measure interdiffusion. The combination of the capillary set-up with X-ray radiography allowed in-situ detecting of convective contributions to the interdiffusion transport by tracking the time dependence of diffusion. Thus, the determination of the interdiffusion coefficient can be restricted to convection-free experiment times resulting in an increased accuracy of the measured interdiffusion coefficient. Additionally, quasielastic neutron scattering was used to measure convection-free Ni and Cu self diffusion. Molecular dynamics simulations were used to determine all diffusion coefficients and the thermodynamic factor. The comparison between experiment and simulation shows an excellent agreement of the interdiffusion is enhanced by thermodynamic forces with a maximum around the stoichiometric composition.

9:00 AM Invited

Atomic Bond Defects; Thermodynamics and Diffusion in Metallic Glasses: Gary Shiflet¹; Aiwu Zhu¹; S. Joseph Poon¹; ¹University of Virginia

Diffusion in metallic glasses and deeply undercooled liquids will be atomistically developed and analyzed using the concept of 'atomic bond deficiency', i.e., cooperative movements of multiple adjacent atoms. Diffusion in metallic glasses and supercooled liquids is a fundamental process that controls the glass formability, thermal stability and viscosity and, to some extent, affects their ductility. Experimental measurements indicate that diffusion in amorphous metals is a thermal activation process with many similarities to crystalline solids, including: simple Arrhenius temperaturedependence of coefficient D; atomic size effect of diffusing species; and the annealing effect of quenched states. However, amorphous metal diffusion is significantly different from crystals, quantitatively in particular, as indicated in: a much larger slope of the Q versus the logarithm of Do, and more pronounced positive size effects of diffusing atoms on Q. Comparisons with previous experimental data and rationalization with seemly confusing disparate results will be presented and explained.

9:30 AM Invited

Application of Thermodynamic and Kinetic Modeling to Diffusion Simulations in Nickel-Base Superalloy Systems: Anders Engström¹; *Henrik Larsson*¹; Johan Bratberg¹; Lars Höglund¹; Paul Mason²; ¹Thermo-Calc Software AB; ²Thermo-Calc Software Inc

This paper presents a brief review, followed by some new results from recent diffusion simulations in Ni-base superalloy systems, performed by means of a thermodynamic and kinetic modelling approach as taken in the commercial finite-difference code DICTRA. The DICTRA code solves the multi-component diffusion equations, combining assessed thermodynamic and kinetic data in order to determine the full composition dependent interdiffusion matrix. The link between fundamental physics based models and critically assessed data allows simulations to be performed with realistic conditions and data on alloys of practical importance. Emphasis in this paper is on modelling and simulation of interdiffusion occurring between NiAl coatings and different Ni-base superalloy substrates. For this purpose we have used the so-called homogenization approach to diffusion in multi-phase systems, recently implemented into the DICTRA software. The simulation results obtained are validated against experimental data, and the agreement is very satisfactory given the complexity of the problem.

10:00 AM Break

10:20 AM Invited

Selected Observations from Interdiffusion Study in U-Mo-Al System: *Yongho Sohn*¹; Emmanuel Perez¹; Bo Yao¹; Ashley Ewh¹; Dennis Keiser, Jr.²; ¹University of Central Florida; ²Idaho National Laboratory

Interdiffusion and microstructural development in the U-Mo-Al system with several additional alloying additions was examined using solidto-solid diffusion couples in the temperature range of 500 to 600C. In ternary U-Mo (7-12 wt.%) vs. Al diffusion couples annealed at 600°C for 24 hours, interdiffusion microstructure varied of finely dispersed UAl3, UAl4, U6Mo4Al43, and UMo2Al20 phases while the average composition throughout the interdiffusion zone remained constant at approximately 80 at.% Al. The addition of Si (up to 5 wt.%) in Al significantly reduced the thickness of the intermetallic layer by changing the constituent phases within the interdiffusion zone. The formation of (U,Mo)(Al,Si)3 with relatively large solubility for Mo and Si was observed. Concurrently, the UAl4 and U6Mo4Al43 phases with poor irradiation behavior were absent. Additional efforts to reduce the growth kinetics of the complex intermetallic layer including alloying additions to the U-Mo alloy and diffusion barriers such as Zr and Nb are presented and discussed.

10:50 AM Invited

Analysis of the Influence of Vacancy-Solute Interaction on Diffusion of Atomic Monomers and Clusters: Piotr Warczok¹; Jaroslav Zenisek²; Ernst Kozeschnik¹; ¹Vienna University of Technology; ²Materials Center Leoben Forschung GmbH

In the present paper, we investigate the dependence of the diffusional mobility of single solute atoms as well as clusters of atoms on the vacancysolute binding characteristics with the Monte Carlo (MC) method. Existing work, mainly based on first-principles calculations and atomistic simulations, is reviewed first. Then, we compare these results to our simulations performed with MC and explore these effects in the light of macroscopic diffusive fluxes and atomic clusters movement in the sense of Brownian motion. Finally, we propose a numerical method for incorporation of the movement and potential collisions of clusters in a precipitation kinetics framework.

11:20 AM

Characterization of Phase Formation and Diffusion Behavior of the Cu-Zn Binary System: *Christopher Eastman*¹; John Kuper¹; Ji-Cheng (J.-C.) Zhao¹; ¹The Ohio State University

Diffusivity data are limited for the Cu-Zn binary system and it is still questionable whether β ' undergoes a eutectoid decomposition at low temperatures. Zinc is a widely used element in copper alloys; therefore

the diffusion coefficient of Zn in Cu will be useful for simulating phase precipitation in Cu alloys. This paper characterizes phase formation and diffusion behavior in the Cu-Zn binary system through the use of infinite diffusion couples, transient liquid phase diffusion couples, solid-liquid conical diffusion couples by immersion of a Cu cone into molten Zn, and U.S. pennies which consist of a Zn core and an electroplated Cu outer layer. Heat treatments for different durations and at several temperatures were used to characterize the diffusion behavior of the Cu-Zn binary system. Optical microscopy, electron dispersive spectroscopy (EDS) and electron probe microanalysis were used to obtain composition profiles in order to extract the diffusivity values.

11:50 AM

Interdiffusion Investigation of Mo and Zr in Fe, Fe-Cr and Fe-Ni-Cr Alloys at 650, 750, and 850°C: *Ashley Ewh*¹; Judith Dickson¹; Bulent Sencer²; John Kennedy²; Yongho Sohn¹; ¹University of Central Florida; ²Idaho National Laboratory

Interdiffusion between molybdenum or zirconium and iron alloys was studied using various solid-to-solid diffusion couples. The couples were assembled with disks of Mo, Zr, Fe, Fe-15Cr, and Fe-15Cr-15Ni, in wt.%, and were isothermally annealed at 650, 750, and 850°C for 45, 30, and 15 days, respectively. Following the diffusion anneal, the couples were water quenched to maintain the high temperature microstructure and were crosssectioned for analysis. Microstructural observations of the interdiffusion zone were made via optical and scanning electron microscopy. Intermetallic layer phase constituents were identified using a combination of energy dispersive spectroscopy and transmission electron microscopy. Concentration profiles were also determined via electron probe microanalysis and were used to determine relevant interdiffusion coefficients of the individual components. The development and growth kinetics of the intermetallic phases developed in these couples are discussed with regard to the phase diagrams and compared with previous literature.

ICME: Overcoming Barriers and Streamlining the Transition of Advanced Technologies to Engineering Practice -- The 12th MPMD Global Innovations Symposium: Emerging and Fundamental Techniques and the Advancement of ICME in Industry

Sponsored by: The Minerals, Metals and Materials Society, TMS Materials Processing and Manufacturing Division *Program Organizers:* Paul Mason, Thermo-Calc Software Inc; Mei Li, Ford Motor Company; James Warren, National Institute of Standards and Technology; Jeff Simmons, AFRL

Tuesday AM March 1, 2011 Room: 7A Location: San Diego Conv. Ctr

Session Chair: Mei Li, Ford Motor Company

8:30 AM

Modeling and Simulation of Mechanical Properties of Magnesium Alloy Wheel Casting for Automobile: Liang Huo¹; *Zhiqiang Han*¹; Xunming Zhu²; Junpeng Duan²; Aimin Wang²; Baicheng Liu³; ⁻¹Key Laboratory for Advanced Materials Processing Technology (Ministry of Education), Department of Mechanical Engineering, Tsinghua University; ²WANFENG Magnesium Co. Ltd., WANFENG Auto Holding Group; ³State Key Laboratory of Automotive Safety and Energy, Department of Automotive Engineering, Tsinghua University

Modeling and simulation have become a powerful tool in optimizing casting process and predicting component microstructure. However, a further step is desirable for engineers to predict the mechanical properties based on the casting process and microstructure simulation, so as to optimize the structure of casting component and reduce the developing time. In



the present paper, the mechanical properties of a magnesium alloy wheel casting for automobile were predicted by integrating the model of as-cast microstructure with the model of tensile strength, as well as the simulation of mold filling process and temperature field during solidification. Considering the grain size variation due to different cooling rate, tensile strength was predicted based on Hall-Petch equation. The distribution of grain size and the variation of the tensile strength of the magnesium alloy wheel were predicted by the present model. Metallographic examination and mechanical property test were performed for validation.

8:50 AM Invited

Engineering Grain Boundary Populations and Connectivity in Polycrystalline Structures: *Gregory Rohrer*¹; Herbert Miller¹; ¹Carnegie Mellon University

Efforts to control the populations of grain boundaries in polycrystals, and the structure sensitive properties that are linked to the grain boundary network structure, are usually referred to as grain boundary engineering. In this paper, I will review progress in understanding the mechanisms by which grain boundary populations and connectivity change during processing. Both the relative populations of different grain boundaries, and their connectivity, have been measured in Ni before and after repeated thermomechanical processing. When the observations are compared to recently measured grain boundary energies, it is observed that higher energy boundaries in the network are replaced by lower energy boundaries. A model for the evolution of the grain boundary populations will be presented. Finally, homology metrics are used to evaluate changes in the connectivity of grain boundaries as a function of processing.

9:15 AM

The Development of Tools for the Prediction of the Tensile and Fracture Toughness Properties in a/ß Titanium alloys: *Santhosh Koduri*¹; Peter Collins²; Hamish Fraser¹; ¹The Ohio State University; ²University of North Texas

The development of tools to predict the mechanical properties based upon compositional and microstructural inputs in multi-component, multiphase Ti-based alloys represents a significant challenge and a key element of Integrated Computational Materials Engineering. One such solution is the development of high-fidelity databases and the subsequent application of non-linear modeling tools such as neural networks based upon a Bayesian framework to extract the underlying composition-microsructure-property relationships. This talk will highlight the development of such rules-based models for the prediction of the tensile and fracture toughness properties of Ti6Al4V at room temperature. These models have been successfully used to isolate the influence of the individual microstructural features on the mechanical properties, potentially providing the basis for the development of more robust phenomenological models.

9:35 AM

Quantifying Interface Energetics and Kinetics using Atomic-scale Simulations: Moneesh Upmanyu¹; ¹Northeastern University

Predictive capabilities of microstructural evolution models are extremely sensitive to their properties, in particular their energetics and kinetics. In polycrystalline microstructures, the interfacial properties are set at the atomic-scale, necessitating the need for i) techniques that extract these properties for individual interfaces with well-known degrees of freedom, and ii) multiphysics integrated efforts that transfer of these properties to largerscale evolution models. In this talk, I will present progress in computational frameworks that allow efficient extraction of interface free energies, stiffness and mobilities as relevant for fundamental annealing phenomena. A focus will be on techniques that allow us to quantify the effect of solutes for homophase interfaces such as grain boundaries. The relevance for ICMEbased efforts will be discussed.

9:55 AM Invited

Integrated Computational Materials Design and Qualification: Making CyberSteel Fly: Greg Olson¹; ¹Northwestern University

The numerical implementation of established materials science principles in the form of purposeful engineering tools has brought a new level of integration of the science and engineering of materials. Parametric materials design integrating materials science, applied mechanics and quantum physics within a systems engineering framework has brought a first generation of designer "cyberalloys" that have now entered successful commercial applications, and a new enterprise of commercial materials design services led by QuesTek Innovations LLC has steadily grown over the past decade. The success of materials design established a basis for the DARPA-AIM initiative which broadened computational materials engineering to address acceleration of the full materials development and qualification cycle. The recent flight qualification of the Ferrium S53 CyberSteel for aircraft landing gear demonstrates the power of the integrated computational design + AIM methodology.

10:20 AM Break

10:35 AM Invited

3-D Modeling of Machining Distortions of Aerospace Components: Shesh Srivatsa¹; ¹GE Aviation

Aircraft engine and airframe structural components that are machined from forgings represent a significant cost of both military and commercial aircraft. Typical component applications are rotating disks in aircraft engines and structural components in airframes. The buy-to-fly weight ratio, which is the ratio of the forged material weight to the finished part weight, is typically between 4 and 10 for such components. The excess material is removed by various machining operations, which are a major contributor to the cost of forged components. Machining distortions are a problem with most forged components which are quenched rapidly in order to generate the required mechanical properties. Distortion can be caused by material bulk stresses resulting from heat-treating operations, or from local near-surface machining-induced stresses. Typically additional machining operations and setups are added in a time-consuming and costly trial-and-error approach to minimize the effects of part distortion. Manufacturing residual stresses can adversely impact the behavior of the components during service. There is a need to understand the effects of heat treating and machining on distortion and to predict, minimize, and control these distortion-related processes. The objective of this program is to establish a modeling method that accurately predicts distortion during machining of 3-D shaped forgings used in aircraft engines and airframe structures. Prediction and validation of machining distortions due to bulk and surface residual stresses will be presented. This program is funded by the USAF Metals Affordability Initiative (MAI).

11:00 AM Invited

A Case for ICME - Ti Alloy Design Tool Development at Boeing: *Donald Shih*¹; ¹The Boeing Company

Titanium structures are critically important to Boeing. Advanced Ti alloys, e.g. lighter alloys and tougher/ stronger alloys are needed. But it commonly takes too long to develop such an alloy. New design concept and methodology that sharply reduce this cycle duration are a must. Atomic modeling, multiscale simulation and data-mining are proven useful to achieve such goals in other materials. However, they have not been applied in Ti alloys, mainly due to many key challenges. Boeing, with our academic partners, has been developing the concept and methodology to overcome these challenges using the ICME approaches. As a key part of multiscale modeling and simulation in the lighter Ti alloys and tougher/ stronger alloys design effort, DFT based first-principles and phase diagram calculations have been conducted. This presentation will give a case study of using of multiscale modeling and simulation and validation for Ti alloy design tool development will be presented.

11:25 AM Invited

Application of Computational Modeling during Processing of Stainless Steels: Ashish Patel¹; ¹Carpenter Technology Corporation

These days process and alloy modeling is gaining prominence, largely due to the urgency in developing new alloys and optimizing the processes that are used in manufacturing these alloys. Currently, there are numerous efforts in both academia and in within the industry to model the effect of alloying elements on microstructure and to get an insight on the effect of processing parameters on properties of high performance alloys. This talk will provide a brief overview of the commonly used processing techniques used during manufacturing of high performance alloys followed by illustrations of typical outcomes from models used to simulate the entire processing sequence for manufacturing high nitrogen austenitic steels. The nitrogen solubility is determined from a CALPHAD based model, a CFD based model is used to simulate the melting and casting, an analytical model for simulating the heat treatment followed by a FEM based simulation for the thermo-mechanical processing.

11:50 AM Invited

Fast Acting Models for Materials-Centric Engineering Design: *Triplicane Parthasarathy*¹; Y.S. Choi¹; R. Goetz²; D. Furrer²; R. John³; R. Dutton³; ¹UES, Inc.; ²Rolls Royce Engines; ³Air Force Research Laboratory

Engineering design of turbine disks with complex heat treatment or heat treatment gradients are of interest in pushing the envelope of turbine disks in future aircraft design. The use of such complex process designs make it essential to incorporate material-centric models within the design space. UES has been working in collaboration with Rolls Royce, under Air Force funding, to develop fast acting models that are based on mechanism based higher order models towards property predictions from either microstructural inputs or heat treatment inputs. Results on these efforts are presented and implications discussed.

Magnesium Technology 2011: Alloy Design/ Development; Grain Refinement and Severe Plastic Deformation

Sponsored by: The Minerals, Metals and Materials Society, TMS Light Metals Division, TMS: Magnesium Committee Program Organizers: Wim Sillekens, TNO Science and Industry; Sean Agnew, University of Virginia; Suveen Mathaudhu, US Army

Research Laboratory; Neale Neelameggham, US Magnesium LLC

| Tuesday AM | Room: 6F |
|---------------|-------------------------------|
| March 1, 2011 | Location: San Diego Conv. Ctr |

Session Chairs: Matthew Barnett, Deakin University; Suveen Mathaudhu, US Army Research Office

8:30 AM

Effect of Zn/Gd Ratio on Phase Constitutions in Mg-Zn-Gd Alloys: Song Zhang¹; *Guangyin Yuan*¹; Chen Lu¹; Wenjiang Ding¹; ¹Shanghai Jiao Tong University

The phase constitutions of Mg-Gd-Zn alloys in the Mg-rich corner were investigated using XRD, SEM and TEM. The effect of Gd/Zn ratio and contents of Gd, Zn element on the phase constitutions of Mg-Zn-Gd alloys were studied. Critical contents of Gd and Zn for the formation of long period stacking ordered (LPSO) structure and X phase in the Mg-Gd-Zn system in the Mg-rich corner have been confirmed using conventional cast process. When Zn%-Gd% =0, LPSO structure and W phase were formed in Mg-Gd-Zn alloys. When Zn%-Gd% =0.5%, only W phase was found in the alloys. When Zn%-Gd% =1%, I phase and W phase were observed in the alloys.

8:50 AM

Optimization of Magnesium-Aluminum-Tin Alloys for As-Cast Microstructure and Mechanical Properties: Xiaoyu Kang¹; *Alan Luo*²; Penghuai Fu¹; Zhenzhen Li¹; Tianyu Zhu¹; Liming Peng¹; Wenjiang Ding¹; ¹National Engineering Research Center of Light Alloys Net Forming and State Key Laboratory of Metal Matrix Composite, Shanghai Jiaotong University; ²General Motors Research & Development Center

The microstructure and mechanical properties of as-cast Mg–Al-Sn alloys have been investigated using computational alloy design and experimental approaches. The as-cast microstructure of Mg-Al-Sn alloys consists of a-Mg, Mg17Al12 and Mg2Sn phases. The volume fractions of Mg17Al12 and Mg2Sn phases increase with increasing Al/Sn contents, and show good agreement between computational thermodynamics modeling and the experimental results. Generally, the yield strength of as-cast alloys increases with Al/Sn alloying contents, while the ductility decreases. This study has confirmed an earlier development of Mg-7Al-2Sn alloy and led to a promising new Mg-7Al-5Sn alloy with significantly improved strength and ductility compared to commercial alloy AZ91 (Mg-9Al-1Zn).

9:10 AM

Thermodynamic Analysis of As-Cast and Heat Treated Microstructures of Mg-Ce-Nd Alloys: Mark Easton¹; Suming Zhu¹; Mark Gibson²; Jian-Feng Nie¹; Joachim Groebner³; Artem Kozlov³; *Rainer Schmid-Fetzer³*; ¹CAST CRC, Monash University; ²CAST CRC, CSIRO, Clayton; ³Clausthal University of Technology

The phase relationships in the Mg-rich corner of the Mg-Ce-Nd system have been investigated through the evaluation of selected compositions in the as-cast and heat treated condition. Consistent thermodynamic CALPHADtype assessments have also been generated for the Mg-Ce-Nd system. It is shown that this system reveals a significant degree of metastability under technologically relevant solidification conditions (i.e. permanent-mould or high pressure die casting). This is simulated in thermodynamic calculations by suppression of the RE5Mg41 phase and reasonable agreement is found with the as-cast microstructures. After heat treatment these microstructures transform, depending on alloy composition, into phase assemblies consistent with the calculated stable equilibrium phase diagram. It is the elucidation of such metastable phase formation and the subsequent transformation from the as-cast to the heat treated state that is a particular strength of the thermodynamic approach and which makes it a powerful tool for alloy development.

9:30 AM

Compressive Strength and Hot Deformation Behavior of TX32 Magnesium Alloy with 0.4% Al and 0.4% Si Additions: *Pitcheswara Kamineni*¹; YVRK Prasad²; Suresh Kalidass¹; Chalasani Dharmendra¹; Norbert Hort³; Karl Kainer³; ¹City University of Hong Kong; ²processingmaps.com; ³GKSS Research Centre

Mg-3Sn-2Ca (TX32) alloy has good corrosion and creep resistance. In this paper, the influence of additions of 0.4%Al and 0.4%Si on its compressive strength and hot working characteristics is reported. It is observed that the compressive strength at higher-temperature dropped significantly. By comparing with the alloy having only 0.4% Al, it is clear that the Si addition is responsible for this deterioration. The hot working behavior as characterized by processing maps revealed that TX32 exhibits two domains of dynamic recrystallization occurring at (1) 300–350 °C and 0.003–0.001 s⁻¹, and (2) 400–500 °C and 0.003–0.3 s⁻¹. In Al and Si containing TX32, both the domains moved to higher temperatures and the flow instability is reduced. In both the domains, the apparent activation energy is higher than that for self-diffusion in magnesium implying that there is a significant contribution from the back stress generated by the hard particles.

9:50 AM

An Analysis of the Grain Refinement of Magnesium By Zirconium: Partha Saha¹; *Srinath Viswanathan*¹; ¹University of Alabama

A Design of Experiments approach was used to conduct a systematic study of the grain refinement of magnesium by zirconium: variables included the amount of zirconium, the pouring temperature, and the settling time prior to



casting. Optical microscopy was used to measure the grain size. TEM was used to identify particles that are likely nucleation sites. The TEM results show that a range of particle sizes are likely substrates and that particles which are likely nucleation sites are faceted. Sample dissolution followed by SEM was used to characterize particle size and morphology while an AccuSizer 770 was used to measure particle size distributions, both in the master alloy and grain refined samples. While only 1 to 3% of the total particles serve as nucleation sites, a comparison of the grain density vs. faceted particle density shows close agreement, suggesting that only faceted particles are likely nucleation sites.

10:10 AM

Study on the Grain Refinement Behavior of Mg-Zr Master Alloy and Zr Containing Compounds in Mg-10Gd-3Y Magnesium Alloy: *Guohua Wu*¹; Ming Sun¹; Jichun Dai¹; Wenjiang Ding¹; ¹Shanghai Jiao Tong University

The effects of Mg-Zr master alloy and potassium fluozirconate (K_2ZrF_6) salts mixture (KSM) on the grain refinement behavior are studied. The results show that the Mg-10Gd-3Y alloy is well refined by Mg-Zr or KSM. The characteristic microstructure feature of the alloy refined by Mg-Zr master alloy is the Zr-rich cores that exist in most grains, while the Zr-rich cores are not observed in the alloy refined by KSM. It is suggested that the grain refinement mechanisms of zirconium in the two cases are different: the Zr released from Mg-Zr master alloy works by generating heterogeneous nucleation, while the Zr reduced from the in-situ reaction between Mg melt and K_2ZrF_6 works by restricting grain growth. Compared with the Mg-30. wt%Zr master alloy, the KSM refiner shows much longer fading time during smelting.

10:30 AM Break

10:50 AM

The Effect of Rare Earth Elements on the Texture and Formability of Asymmetrically Rolled Magnesium Sheet: *David Randman*¹; Bruce Davis¹; Martyn Alderman²; Govindarajan Muralidharan³; Tom Muth³; William Peter³; Tom Watkins³; Odis Cavin³; Edward Kenik³; ¹Magnesium Elektron North America; ²Magnesium Elektron; ³Oak Ridge National Laboratory

The lack of formability is a serious issue when considering magnesium alloys for various applications. Standard symmetric rolling introduces a strong basal texture that decreases the formability; however, asymmetric rolling has been put forward as a possible route to produce sheet with weaker texture and greater ductility. It has also been shown in recent work that weaker textures can be produced through the addition of rare earth elements to magnesium alloys. Therefore, this study has been carried out to investigate the effect of rare earth additions on the texture changes during asymmetric rolling. Two alloys have been used (AZ31B and ZEK100. The effect that the rare earth additions have on the texture of asymmetrically rolled sheet and the subsequent changes in formability will be discussed.

11:10 AM

Improvement of Strength and Ductility of Mg-Zn-Ca-Mn Alloy by Equal Channel Angular Pressing: *Mingyi Zheng*¹; ¹Harbin Institute of Technology

Mg–Zn–CaMn alloys are low cost and have good creep resistance, high strength and excellent biocompatibility. In this research, equal channel angular pressing (ECAP) was performed on the as-extruded Mg- 5.25wt%Zn - 0.6wt%Ca - 0.3wt%Mn magnesium alloy at 250°C and 300°C for 4 passes, respectively. With the decreasing of ECAP temperature, the grain size was reduced. After ECAP at 250°C for 4 passes, extremely fine grains with the average grain size of about 0.8 micrometer are formed. High UTS of 323 MPa and elongation to failure of 23% were achieved in the specimen ECAPed at 300°C, which was resulted from the fine grains, fine dispersed precipitates and the textures in which the basal plane is oriented parallel to the extrusion direction. While the specimens processed at 250°C have textures with the basal planes inclined at about 45° to the extrusion direction, leading to the lower yield strength.

11:30 AM

Deformation Behavior of a Friction Stir Processed Mg Alloy: *Qi Yang*¹; Sergey Mironov²; Yutaka Sato³; Kazutaka Okamoto⁴; ¹Hitachi America, Ltd.; ²Department of Materials Processing, Graduate School of Engineering, Tohoku University ; ³Department of Materials Processing, Graduate School of Engineering, Tohoku University; ⁴Hitachi Research Laboratory, Hitachi Ltd.

Friction stir processing, as a derivative of friction stir welding, in which a non-consumable tool imparts severe plastic deformation to metallic materials, has been used for grain refinement and therefore ductility improvement. In this talk, deformation behavior of a friction stir processed Mg alloy is addressed. Analyses of grain size and crystallographic texture are made to interpret the characteristics of strength and ductility of friction stir processed Mg alloy are compared with those of a friction stir processed 5083 Al alloy.

11:50 AM

Effect of Heat Index on Microstructure and Mechanical Behavior of Friction Stir Processed AZ31: Wei Yuan¹; Rajiv Mishra¹; ¹Missouri University of Science and Technology

Friction stir processing modifies the microstructure and properties of metals through intense plastic deformation. The frictional heat input affects the microstructure evolution and resulting mechanical properties. 2 mm thick commercial AZ31B-H24 Mg alloy was friction stir processed under various process parameter combinations to investigate the effect of heat index on microstructure and properties. Recrystallized grain structure in the nugget region was observed for all processing conditions with decrease in hardness. Results indicate a reduced tensile yield strength and ultimate tensile strength compared to the as-received material in H-temper, but with an improved hardening capacity. The strain hardening behavior of friction stir processed material is discussed.

12:10 PM

Strengthening Mg-Al-Zn Alloy by Repetitive Oblique Shear Strain: *Toshiji Mukai*¹; Hidetoshi Somekawa¹; Alok Singh¹; Tadanobu Inoue¹; ¹National Institute for Materials Science

Enhancing fracture toughness and/or ductility is requirement for reliability in structural application. It has been reported that the grain refinement is one of the possible ways to enhance the strength without losing the ductility. In this study, severe plastic working by caliber rolling has been demonstrated to refine the grain structure of a commercial AZ31 Mg-Al-Zn alloy effectively at a commercial processing speed with the formation of fine sub-grains in a sub-micro-meter scale and resulted in a high yield stress of more than 400 MPa. A simultaneous operation of oblique shear strain weakened the basal texture compared to that of the initial as-extruded alloy, and resulted in tensile ductility comparable to that of the commercially extruded alloy, and showed a higher asymmetry ratio of yield stress in compression/tension (0.82) than that of the as-extruded alloy (0.57).

Magnetic Materials for Energy Applications: Nd-Fe-B Sintered Magnets

Sponsored by: TMS Electronic, Magnetic, and Photonic Materials Division, TMS: Energy Conversion and Storage Committee, TMS: Magnetic Materials Committee; JSPS 147th Committee on Amorphous and Nanocrystalline Materials; Lake Shore Cyrotronics, Inc.; AMT&C

Program Organizers: Victorino Franco, Sevilla University; Oliver Gutfleisch, IFW Dresden; Kazuhiro Hono, National Institute for Materials Science; Paul Ohodnicki, National Energy Technology Laboratory

| Tuesday AM | Room: 11A |
|---------------|-------------------------------|
| March 1, 2011 | Location: San Diego Conv. Ctr |

Session Chair: George Hadjipanayis, University of Delaware

8:30 AM Invited

Materials for Motors of Hybrid Automobiles: *Shigeru Konda*¹; ¹Toyota Motor Corp., Inc.

It has passed over one hundred year after vehicle with gasoline engine had been released. Currently, environmental issues, such as global warming, greenhouse gas and so on, has been discussing. To realize the sustainable mobility society, Hybrid vehicle could be one of the good candidates as ecofriendly car. In this speech, the benefit of Hybrid vehicle could be described. Simultaneously, the needs and expectation for materials would be explained.

8:55 AM Invited

Application of Nd-Fe-B Magnets to the Megawatt Scale Generator for the Wind Turbine: *Takehisa Minowa*¹; ¹Shin-Etsu Chemical Co. Ltd.

Wind power generation is cost effective compared to solar energy generation. Although energy efficiency increases with the size of generators, this makes the generator too heavy for installment. One solution is to use Nd-Fe-B based permanent magnets to make the generator smaller and lighter. Various technologies for wind power generators such as interior permanent magnet (IPM) motors and surface permanent magnet (SPM) motors have been proposed, but the best system has not been determined yet. In this talk, I will overview the technological trend and the required properties of permanent magnets for wind power generation.

9:20 AM Invited

Enhancement of Coercivity of Nd-Fe-B Sintered Magnets by Grain Boundary Modifications: *Kazuhiro Hono*¹; Tadakatsu Ohkubo¹; ¹National Institute for Materials Science

Interest in the coercivity mechanism of Nd-Fe-B based permanent magnets has recently been revived in Japan due to the increasing demand for Dy-free Nd-Fe-B magnets for traction motors of (hybrid) electric vehicles, (H)EV. In the current Nd-Fe-B sintered magnets for the traction motors, 30% of Nd is substituted with Dy to use the increased anisotropy field of the (Nd,Dy)2Fe14B phase, but the natural aboundance of Dy is only 10% of Nd. Thus, we are looking for a way to increase the coercivity of the Nd-Fe-B magnets with lower amount of Dy. For this purpose, we investigate the microstructure-coercivity relationships of Nd-Fe-B magnets by investigating the microstructures of commercial and experimental sintered magnets and hydrogen disproportionation desorption recombination (HDDR) powder by HRSEM, TEM and atom probe tomography (APT). In this talk, we will overview our recent work on the enhancement of coercivity of Nd-Fe-B based magnets by grain boundary modifications.

9:45 AM Invited

Novel Approaches to Microstructural Characterisation in NdFeB Materials: *Thomas Woodcock*¹; Nora Dempsey²; Dominique Givord²; Stefan Zaefferer³; Oliver Gutfleisch¹; ¹IFW Dresden; ²Institute Neél, CNRS-UJF; ³Max Planck Institute for Iron Research

NdFeB sintered magnets have recently found important new applications in electric motors for hybrid electric vehicles and generators for wind

turbines. Magnet grades with Dy additions are typically used for such applications and this incurs a significant cost penalty. Much research effort has therefore recently been put into reducing the Dy content or eliminating Dy in NdFeB sintered magnets for high temperature applications. In addition to various experimental routes toward this, novel approaches yielding detailed microstructural characterisation are required in order to bring greater understanding of coercivity mechanisms. Recent developments include the use of aberration-corrected TEM to obtain highest spatial resolution images and the application of electron backscatter diffraction (EBSD) to obtain crystallographic orientation data on a local scale from all the phases present in the microstructure. The combination of EBSD and EDX with high resolution serial sectioning yields 3D orientation and chemical data which will also be discussed.

10:10 AM Invited

Modeling of Magnetization Reversal in Nd-Fe-B Based Sintered Magnets: *Thomas Schreft*¹; Simon Bance¹; Harald Oezelt¹; Gino Hrkac²; ¹St. Poelten University of Applied Sciences; ²University of Sheffield

High remanent, sintered Nd-Fe-B magnets are a key material for energy saving technology. We study the magnetization reversal mechanism using a multi-scale approach. Atomistic simulations give the local distortion of the Nd2Fe14B crystal structure near grain boundaries and triple junctions. This translates into a change of the magneto-crystalline anisotropy. The thickness of the distorted region which shows a magnet-crystalline anisotropy that is considerably smaller than in the bulk depends on the composition of the intergranular phase and ranges from 0.6 nm to 1.8 nm. Taking into account these local defects, we apply finite element micromagnetics. The simulations show how reversed domains are nucleated near triple junctions. Domains expand over several grains. Domain walls are equally located at grain boundaries or go through the grains. The simulations show cascade type demagnetization in well-aligned sintered magnets.

10:35 AM

Theoretical Investigation on Formation Mechanism of fcc-NdOx in Nd/ Nd-Fe-B Interface: *Ying Chen*¹; Satoshi Hirosawa²; Shuichi Iwata³; ¹Tohoku University; ²NEOMAX Co., Hitachi Metals, Ltd.; ³The University of Tokyo

The disordered fcc-NdOx phase formed at the interface of Nd/Nd-Fe-B is believed to take an important role in coercivity generation, and its appearance directly influenced by the oxygen concentration. To understand the formation mechanism and properties of this particular Nd oxides phase, the ground state stability analysis for a whole oxygen concentration in Nd-O has been performed based on LSDA + U calculations. It is revealed that at low oxygen concentration, the system tends to separate into dhcp-Nd and NdO-NaCl or NdO-ZnS, whereas at oxygen concentration over 50%, the Nd₂O₃ becomes most stable. Further investigation is focused on the relation among Fluorite-NdO₂, C-type(cl80)-Nd₂O₃ and ZnS-NdO which have same fcc-frame of cations and vary in configurations of oxygen anions due to introducing oxygen vacancies. Formation energies, electronic structures for various oxygen vacancies configurations are calculated along this line.

10:50 AM

NdFeB Thick Films for Micro-System Applications: Nora Dempsey¹; Mikhail Kustov¹; Daniel O'Brien¹; Yuepeng Zhang¹; Luiz Zanini¹; Georgeta Ciuta¹; Frederic Dumas-Bouchiat¹; Dominique Givord¹; ¹Institut Néel CNRS/UJF

For the same reasons (high magnetisation and high coercivity) that NdFeB based magnets are widely used in bulk applications such as hybrid and all electric vehicles and wind turbines, they have much potential for use in magnetic micro-systems. In addition, since the force exerted by a magnet depends of the field gradient it produces, a reduction in its size leads to an increase in the volume forces it exerts. Consequently, much effort has been put into the fabrication of NdFeB in film form. In this work we will present different aspects concerning their eventual use in micro-systems, namely their patterning at the micron-scale, the local characterisation of the magnetic fields they produce and the characterisation and control of strain in the films. Such films may be used in the generation of energy at the micron scale

(micro-generators) and to improve the efficiency of energy consumption at the macro-scale (micro-sensors, micro-actuators).

11:05 AM Break

Magnetic Materials for Energy Applications: Magnetostrictive Materials

Sponsored by: TMS Electronic, Magnetic, and Photonic Materials Division, TMS: Energy Conversion and Storage Committee, TMS: Magnetic Materials Committee; JSPS 147th Committee on Amorphous and Nanocrystalline Materials; Lake Shore Cyrotronics, Inc.; AMT&C

Program Organizers: Victorino Franco, Sevilla University; Oliver Gutfleisch, IFW Dresden; Kazuhiro Hono, National Institute for Materials Science; Paul Ohodnicki, National Energy Technology Laboratory

| Tuesday AM | Room: 11A |
|---------------|-------------------------------|
| March 1, 2011 | Location: San Diego Conv. Ctr |

Session Chair: Michael McHenry, Carnegie Mellon University

11:20 AM

Magnetostrictive Behavior of Fe-W Alloy Single Crystals: *Gavin Garside*¹; Chai Ren¹; Biswadeep Saha¹; Meenakshisundaram Ramanathan¹; Sivaraman Guruswamy¹; ¹University of Utah

A systematic examination of change in magnetostriction as a function of W content in the range of 0 to 10 at.% is presented in this paper. Fe-W alloy single crystals were prepared using vertical Bridgman growth technique. Single crystal samples with [001]-orientation were prepared with faces within 0.5 degrees from [001] orientation. The samples were annealed in the alpha-phase region and quenched. Longer annealing times and higher annealing temperatures increase the magnetostriction values obtained. Rapid increase in magnetostriction is observed with W additions of up to 4.4 at.% W. This is followed by a much slower increase with W content. This behavior is associated with the propensity for second phase formation at higher W contents in these alloys. *Support of this work by NSF-DMR under the award DMR-0854166 is gratefully acknowledged.

11:35 AM

Investigation of DO₃ and B2 Type Ordering in Quenched Magnetostrictive Fe-27.5 at.% Ga Alloy Single Crystals: *Chai Ren*¹; Gavin Garside¹; Biswadeep Saha¹; Meenakshisundaram Ramanathan¹; Sivaraman Guruswamy¹; ¹University of Utah

FeGa alloys with large low-field magnetostriction are attractive candidates in energy conversion and harvesting applications. The structural ordering in magnetostrictive Fe-27.5 at.% Ga alloy single crystals that were annealed in the alpha region and quenched was investigated using x-ray diffraction. The annealing temperatures used were 1100 and 1150 degree C. XRD examination as a function of depth in [100] or [111] oriented Fe-Ga samples show dominant existence of DO₃ type ordering arrangement on the top surface to B2 type ordering arrangement in the interior regions of the sample. The detailed examinations of scattering peaks in the XRD patterns suggest that the nature of short-range and long-range ordering present is influenced by sample size and thermal history. Thus sample size and shape will influence magnetostriction measurements. The observations are of importance in magnetostrictive device design. *Support of this work by NSF through the award DMR-0854166 is gratefully acknowledged.

11:50 AM

Influence of Plastic Deformation on the Magnetostrictive Behavior of [001]-oriented Fe-Ga Alloy Single Crystals: *Biswadeep Saha*¹; Gavin Garside¹; Meenakshisundaram Ramanathan¹; Chai Ren¹; Sivaraman Guruswamy¹; ¹University of Utah

Structural ordering, defects and second phases can influence the magnetostrictive behavior in Fe-Ga and other Fe-based magnetostrictive

alloys. In this study, the influence of dislocations on the magnetostrictive behavior of [001]-oriented Fe-20 at.% Ga single crystal is examined. Dislocation arrays were introduced through controlled deformation of rectangular parallelepiped single crystal samples with the faces oriented to within 0.25 degrees off the <100> orientation. Alloy single crystals were obtained through vertical Bridgman growth process. The crystals were plastically deformed to predetermined strain level. Magnetostriction measurements as well as TEM and x-ray examinations were performed prior to and after deformation. Results obtained show that deformation decreases magnetostriction values appreciably.*Support of this work by NSF-DMR through the award DMR-0854166 is gratefully acknowledged.

12:05 PM

Enhanced Magnetoimpedance Effect in Co89Zr7B4 Ribbon/Fe80Ni20 Bilayer Structures: N. Laurita¹; A. Chaturvedi¹; A. Leary²; P. Jayathilaka¹; C. Bauer¹; Casey W. Miller¹; M.H. Phan¹; M.E. McHenry²; *H. Srikanth*¹; ¹University of South Florida; ²Carnegie Mellon University

We report the large enhancement of the magnetoimpedance (MI) effect in CoFe89Zr7B4 amorphous ribbon/Fe80Ni20 bilayers. The amorphous ribbons were prepared by rapid quenching. Atomic force microscopy indicate roughnesses for the free and wheel-side ribbon surfaces of 3-6 nm and 150-200 nm, respectively. 100 nm Fe80Ni20 layers were sputtered onto the ribbons; one sample was coated in zero field, another in 200 Oe applied transverse to the length. Magnetoimpedance measurements were carried out along the ribbon axis in applied dc magnetic fields up to 120 Oe over a frequency range of $0.1 \sim 13$ MHz. We find that the MI effect is largely enhanced in the Fe80Ni20-coated ribbons. The 200 Oe-deposited sample shows the largest effect (19%), which is about twice that of the bare ribbon (11%). Our studies provide strong evidence for enhancing the MI effect in layered structures for sensor applications. Support: NSF-DMMI (HS). NSF-ECCS (CWM).

Massively Parallel Simulations of Materials Response: Session III

Sponsored by: The Minerals, Metals and Materials Society, TMS Materials Processing and Manufacturing Division, TMS Structural Materials Division, TMS/ASM: Computational Materials Science and Engineering Committee, TMS: High Temperature Alloys Committee *Program Organizers:* Diana Farkas, Virginia Tech; Susan Sinnott, University of Florida

| Tuesday AM | Room: 1A |
|---------------|-------------------------------|
| March 1, 2011 | Location: San Diego Conv. Ctr |

Session Chair: To Be Announced

8:30 AM Invited

Ultra-Large Scale Simulations of Deformation and Failure of Biological Protein Materials: Markus Buehler¹; ¹Massachusetts Institute of Technology

Deformation and failure of biological protein materials are critical to our understanding of injuries, disease state, and to reverse-engineer the functional design of biological materials. I will present a survey of recent materiomics studies in our laboratory based on ultra-large scale simulations using LAMMPS. The talk will include a discussion of investigations of intermediate filament fibrils and networks, beta-sheet structures as found in spider silk and amyloids, as well as collagenous tissues that form the structure of tendon and bone. Case studies will be presented that illustrate size effects in protein materials, flaw-tolerance mechanisms, and applications of materials science to genetic diseases, showing how structural defects at the molecular level can have profound effects at the material behavior at larger scales. A detailed analysis will be presented to explain how biological materials overcome the limitations of their building blocks, often functionally inferior, and yet display remarkable functional properties.

8:55 AM Invited

Multilevel Atomistic Modeling of Grain Boundaries and Nanocrystals: Garritt Tucker¹; Shreevant Tiwari¹; *David McDowell*¹; ¹Georgia Institute of Technology

Deformation in nanocrystalline metals involves interface-mediated processes that depend on grain boundary network and structure, with atom shuffling/GB sliding/migration and dislocation nucleation as competing modes. As a step towards informing statistical descriptions of initial yield and plastic flow, and setting the stage to quantify percolation and scaling relations, we apply recently developed volume-averaged metrics of continuum kinematic quantities as post-processing "filters" to results of atomistic simulations of deformation using the LAMMPs MD code, computing vorticity, Green strain, dilatation, and lattice microrotation fields within nanocrystalline copper at a temperature of 10K. The results provide a new, alternative perspective into the role of competing deformation mechanisms as a function of boundary type in bicrystals and mean grain size in nanocrystals. Our results indicate potential utility of these continuum metrics in interpreting the wealth of information arising from atomistic simulations of nanocrystalline ensembles.

9:20 AM Invited

Quantitative Studies of Nanoindentation: Coupled Experiments and Modeling: Lyle Levine¹; Richard Wagner¹; Li Ma¹; Francesca Tavazza¹; Chandler Becker¹; Douglas Smith¹; Dylan Morris¹; David Bahr²; Stefhanni Jennerjohn²; ¹National Institute of Standards and Technology; ²Washington State University

Nanoindentation's ability to probe the local plastic mechanical properties at the surface of almost any specimen has made it the most widely used experimental technique for making such measurements at the nanoscale. However, standard test methods are limited and full traceability to primary reference standards is lacking. At low indentation loads, numerous potential experimental problems exist, including non-traceable force calibration at the nN level, uncharacterized irregular indenter tip shapes, and structural heterogeneities both on and below the sample surface. Similarly, attempts to back out quantitative mechanical properties often suffer from overreliance on the Hertzian approximation and inaccurate boundary conditions for simulations. Example measurements and simulations (using FEA and LAMMPS-MD) for both new and heavily used indenters will be used to illustrate these problems for metal specimens. Finally NIST's recent efforts to provide quantitative experimental and modeling support for this valuable experimental technique will be described.

9:45 AM Invited

Nanostructurally Small Cracks (NSC): Atomistic Modeling of Fatigue: Mark Horstemeyer¹; G. Potirniche²; S. Kim¹; T. Tang¹; Diana Farkas³; ¹Mississippi State University; ²Univ. Idaho; ³Virginia Tech

Molecular Dynamics simulations using EAM and MEAM potentials were conducted to study nanoscale fatigue cracks in nickel and copper crystals. Simulation results revealed that the cyclic plastic deformation at the crack tip was the main influencing factor for fatigue crack growth. Two main nanoscale mechanisms of crack propagation were observed: (1) the main cracks linked with the voids nucleated in front of crack tip due to high dislocation density generated by the cyclic loading; and (2) the main cracks broke the atomic bonds in the crack plane without much plasticity. For the bicrystals and polycrystals, the grain boundaries exerted resistance to the crack propagation. Fatigue crack growth rates for nanocracks were computed and compared with growth rates published in the literature. The atomistic simulations indicated that reversible plastic slip along the active crystallographic directions at the crack tip was responsible for advancing the crack during applied cycling.

10:10 AM Break

10:25 AM

Atomistic Predictions of Age Hardening in Al-Cu Alloys: Chandra Veer Singh¹; Derek Warner¹; ¹Cornell University

A large class of commercial alloys derive their strength from precipitation hardening. In many alloys, such as Al-Cu, hardening is a complex function of time and temperature as the precipitation process involves several types of competing metastable precipitates. Here we combine analytic models for microstructural kinetics with large-scale atomistic simulations (LAMMPS) of dislocation-precipitate and dislocation-solute interactions to examine the precipitation hardening process in an Al-Cu alloy. We compute the critical stresses for dislocations to overcome both GP zones and theta" precipitates directly from atomistic simulations and use an improved Labusch model with atomistically computed interaction energies to calculate solute hardening. Combining strengthening effects, age hardening curves are then formulated and compared with experiments. By comprehensively examining the entire age hardening process, insight can be gained into the strengths and weaknesses of both common kinetics models and potential based atomistic simulations for broad application.

10:45 AM

Massively Parallel Molecular Statics Simulations of the Percolation of Dislocations through a Random Array of Forest Dislocation Obstacles in FCC Nickel: *Satish Rao*¹; Dennis Dimiduk²; Jaafar El-Awady³; Triplicane Parthasarathy¹; Michael Uchic²; Christopher Woodward²; ¹UES Inc.; ²Air Force Research Laboratory; ³Johns Hopkins University

This talk presents results from massively parallel molecular statics simulations, using LAAMPS with ~ 10,000 processors, of the percolation of dislocations through a random array of forest dislocation obstacles in face-centered cubic Nickel. A single gliding dislocation and 540 forest dislocations are inserted into a 0.6μ m by 0.3μ m by 0.3μ m rectangular parallelepiped cell aligned along the [1-10], [11-2] and [111] directions, containing ~1 - 2 billion atoms. The behavior of the percolating dislocation under pure shear stresses applied on the (111) plane are simulated. Details of the percolating wave front and the critical stress required for percolation are obtained from the simulation results. These atomistic results representing the critical percolation stress for dislocations are compared with previous dislocation dynamics and point-obstacle pinning simulation results.

11:05 AM

Atomic Scale Deformation Mechanisms of Amorphous Polyethylene under Tensile Loading: *Mark Tschopp*¹; Jean-Luc Bouvard¹; Don Ward²; Mark Horstemeyer¹; ¹Mississippi State University; ²Sandia National Laboratory

Thermoplastic polymers, such as polyethylene and polypropylene, play an important role in components. However, to date, the molecular deformation behavior at an atomistic level involves coarse-graining potentials, such as the Dreiding potential. The objective of this research is to study the deformation mechanisms in full-atom amorphous polymer systems at the atomic scale under various loading conditions. We generated the amorphous structures and then used molecular dynamics simulations to equilibrate/deform the 3D periodic simulation cell. Various parameters like chain length, number of chain, strain rate were taken into consideration mechanisms. Additionally, we analyzed how the energy associated with bond length, bond angle, dihedral angle, and non-bonding interactions evolved as a function of strain. The significance of this research is that understanding the deformation behavior at the atomic scale is vital to predicting bulk mechanical behavior via higher scale models.

11:25 AM

Energy of Slip Nucleation and Transmission at Grain Boundaries: Michael Sangid¹; Huseyin Sehitoglu¹; ¹University of Illinois, Urbana-Champaign

Grain boundaries (GBs) provide a strengthening mechanism in engineering materials by impeding dislocation motion. In a polycrystalline material,



there is a wide distribution of GB types with characteristic slip transmission and dislocation nucleation behaviors. There is a strong need to quantify the energy barriers of the individual GBs. We introduce a methodology to calculate the energy barriers during slip-GB interaction, in concurrence with the general stacking fault energy curve for slip in a perfect FCC material. By doing so, we calculate the energy barriers for slip transmission and nucleation from various classifications of GBs. The character and structure of the GB plays an important role in impeding slip within the material. From this analysis, we show that there is a strong correlation between the energy barrier and static interfacial boundary energy. The results have profound implications in understanding mechanical response influenced by the underlying grain boundary characters.

11:45 AM

Molecular Dynamics Investigations of Polyurethane-Chrome Oxide Interfaces: Susanne Opalka¹; Kenneth Smith¹; ¹United Technologies Research Center

Polyurethane-chrome oxide atomic-scale interfacial interactions were simulated with the LAMMPS molecular dynamics code to generate fundamental understanding of adhesion phenomena for component design and optimization. This modeling capability was implemented sequentially at several levels, creating models based upon experimentally-known material properties and validating modeling results with experimental tests. First, polymer models were refined by tuning both polymer characteristics and atomic force field parameters to achieve agreement with measured polymer thermal and mechanical properties. Then, hybrid force field parameters for the interactions of key polyurethane functional groups with the passivated chrome surface layer were customized to match interfacial surface tension measurements. Finally, virtual adhesion tests were conducted on conditioned polyurethane-chrome oxide interface models for comparison with nanoscale pull-test experimentation. The validated models will be used for molecular dynamics investigations of viscoelastic phenomena in a moving polyurethane-chrome oxide contact leading to material friction, wear, and transfer.

12:05 PM

Tendency of Cooperative Grain Boundary Sliding in Nanocrystalline Materials: *Shreevant Tiwari*¹; David McDowell¹; ¹Georgia Institute of Technology

The objective of this research is to identify the tendency of cooperative grain boundary (GB) sliding, leading to grain rotation in nanocrystalline metals. We use molecular dynamics (MD) simulations to uniaxially deform 3D nanocrystalline Cu ensembles in the elastic regime and visualize, for each grain, the rotational component of the atomic displacement vector field relative to the grain center. Our results suggest that the rotational component of the relative displacement is more pronounced in regions near certain preferred GBs and triple junctions, and that the extent of rotation in these favored boundary regions increases with temperature, thereby hinting at a thermally activated, cooperative GB sliding mechanism. Additionally, the rotational displacement field used as a part of this work can potentially help resolve GB sliding from a background of several other competing deformation mechanisms, and augment existing metrics of atomistic deformation kinematics.

Materials for the Nuclear Renaissance II: Next Generation Reactors

Sponsored by: The Minerals, Metals and Materials Society, TMS Structural Materials Division, TMS/ASM: Corrosion and Environmental Effects Committee, TMS/ASM: Nuclear Materials Committee

Program Organizers: Raul Rebak, GE Global Research; Brian Cockeram, Bechtel-Bettis; Peter Chou, Electric Power Research Institute; Micah Hackett, TerraPower, LLC

| Tuesday AM | Room: 4 |
|---------------|-------------------------------|
| March 1, 2011 | Location: San Diego Conv. Ctr |

Session Chair: Brian Cockeram, Bechtel Bettis

8:30 AM Introductory Comments

8:35 AM

On the Prospects for Developing Advanced Alloys that Are Immune to Irradiation: Challenges and Opportunities: *G. Robert Odette*¹; Takuya Yamamoto¹; ¹University of California, Santa Barbara

The approaches to developing alloys that are highly resistant to irradiation damage at high displacement damage (dpa) and helium levels are discussed. Nanostructured ferritic alloy class (NFAs) is the leading candidate for such irradiation tolerance. NFAs are Fe-Cr based ferritic stainless steels that contain an ultrahigh density of Y-Ti-O nanofeatures (NFs). The NFs are remarkably thermally stable and provide outstanding high temperature properties and remarkable tolerance to displacement damage as well as the degrading effects of transmutation product helium. The results of recent in situ injection experiments show that the NFs trap helium in ultrafine scale interface bubbles. The helium bubbles are effective sinks for point defects as well as additional helium, and at high densities can suppress almost all manifestation of radiation damage. It is argued that NFAs can be tailored to effectively transform helium from a liability to an asset, possibly leading to near immunity to irradiation damage.

8:55 AM

A Multi-Layer Approach to a Stable Alpha Alumina Barrier Layer on Alloy 617: *Elizabeth Clark*¹; James Yang¹; Gokce Gulsoy²; Deepak Kumar²; Gary Was²; Carlos Levi¹; ¹University of California, Santa Barbara; ²University of Michigan

Alloy 617 is a candidate material for heat exchangers in the GenIV very high temperature nuclear reactor concept. However, impurities in the He may lead to degradation by oxidation, carburization or decarburization of the alloy with deleterious effects on its structural integrity. Alpha-alumina is attractive as a protective barrier layer, but to assure that this phase forms (rather than transient aluminas) in the low pO₂ environment at the use temperature (T≤1000°C), surface modification is required. Lifetime requirements also demand stability of the modified surface layers against interdiffusion with the substrate, and the ability of the oxide to re-form in the event of cracking or spallation due to thermo-mechanical stresses in the prospective applications. This presentation will discuss concepts involving alloy 617 with combinations of aluminization and/or cladding, their oxidation and interdiffusion behavior, and preliminary results on their response to exposure to He with CO/CO₂ ratios conducive to carburization.

9:15 AM

Order-Disorder Transformation in a Ni-Cr-Mo Alloy: Amit Verma¹; *Jung Singh*¹; Mahadevan Sundararaman¹; Nelia Wanderka²; ¹Bhabha Atomic Research Centre; ²Helmholtz-Zentrum Berlin für Materialien und Energie GmbH

Ni-Cr-Mo alloys are potential candidates for structural materials application for high temperature reactors. These alloys form a long-range order (LRO) precipitates, Ni2(Cr,Mo) (Pt2Mo type structure), in the intermediate temperature range. The evolution of ordered precipitates has

10:45 AM

been investigated in a Ni-Cr-Mo alloy using resistivity and transmission electron microscopy (TEM). The relative change in resistance as a function of temperature could be divided into 5 regimes, which could be attributed to different microstructural states. TEM investigations revealed the presence of two types of short-range order (SRO) in solution treated and quenched state: a { $1 \frac{1}{2} 0$ } type SRO and a 1/3 {110} type SRO of Pt2Mo type. The formation of the LRO could be identify to initiate at { $1 \frac{1}{2} 0$ } SRO which transformed first to 1/3 {110} type SRO followed by LRO transition. The SRO state also had an important influence on the kinetics of the transformation.

9:35 AM

Creep Characteristics of a Grade 91 Steel: *Triratna Shrestha*¹; Mehdi Basirat¹; Zachary Wuthrich¹; Indrajit Charit¹; Gabriel Potirniche¹; Karl Rink¹; ¹University of Idaho

Modified 9Cr-1Mo (Grade 91) steels are being considered as a potential candidate material for reactor pressure vessel applications for the Very High Temperature Reactor (VHTR). This research has been focused on studying the tensile creep behavior of as received and welded Grade 91 steel as a function of temperature (500–700 oC) and stress levels (50–200 MPa). The creep testing on the monolithic materials revealed a deformation regime with a stress exponent of ~10 at the higher stress levels. Microstructural analysis using transmission electron microscopy (TEM) is being carried out on the specimens before and after the creep deformation. TEM results will be correlated with the creep parametric dependencies to elucidate the underlying creep mechanisms.

9:55 AM

Microstructural Characterization of Nuclear Grade Graphites: *Joshua Kane*¹; Karthik Chinnathambi¹; Rick Ubic¹; Darryl Butt¹; ¹Boise State University

Nuclear graphite is a prime candidate material for application in Generation IV Very High Temperature Reactor (VHTR) cores because of its high temperature thermo-mechanical properties, resilience to neutron absorption, and chemical resistance. Irradiation induced damage and creep are considered two primary degradation mechanisms for graphite and therefore major life-limiting issues for the VHTR core. This work reports preliminary transmission electron microscopy results of the microstructure characterization of Generation IV VHTR candidate virgin graphite grades PCEA and NBG-18 as well as historical grades IG-110 and PGX. Various microstructural features such as filler, binder, and quinoline insoluble particles have been identified for each grade and compared. Studies are currently underway to identify and analyze dislocations and pinning sites considered, in many theories, essential to irradiation creep in graphite.

10:15 AM Break

10:25 AM

Evaluation of Nanofeature Evolution in the Sequence of Atomization to Consolidation Steps in Processing a Fe14Cr3W0.4Ti0.2Y Alloy: *Nicholas Cunningham*¹; Erich Stergar¹; Auriane Etienne¹; G. Robert Odette¹; Yuan Wu¹; Brian Wirth²; Stuart Maloy³; ¹UC Santa Barbara; ²UC Berkeley; ³Los Alamos National Laboratory

Nanostructured ferritic alloys (NFAs) contain an ultrahigh density of Y-Ti-O nanofeatures (NFs) that provide outstanding high temperature properties and remarkable tolerance to irradiation damage. NFA powders were produced by gas atomization from a melt containing Fe-14%Cr-3%W-0.4%Ti-0.2%Y. Electron probe microanalysis (EPMA), atom probe tomography (APT), small angle neutron scattering (SANS), transmission electron microscopy (TEM) and microhardness measurements were used to characterize the NFA in the as-atomized, ball milled, ball milled and annealed and hot isostatic pressed (HIP) consolidated conditions. Y is phase separated in the as atomized powders. However, attritor milling for 20 to 40 h mixes the Y and introduces O. Subsequent powder annealing and consolidation treatments, typically at 1150°C, result in the precipitation of a high density of NFs. All the annealed powder variants and consolidated alloys show a bimodal grain size distribution, but APT shows the presence of NFs in both large and small grains.

Spatially-Dependent Cluster Dynamics Modeling of Vacancy and Interstitial Cluster Evolution in Ferritic/Martensitic Fe-Cr Alloys: *Thibault Faney*¹; Aaron Kohnert¹; Brian Wirth¹; Djamel Kaoumi²; Arthur Motta³; ¹UC Berkeley; ²USC; ³Penn State University

Computational materials modeling will investigate the mechanisms controlling microstructural evolution in ferritic/martensitic alloys following high dose, high temperature radiation exposure. The aim of this study is to understand and predict primary defects production and defects diffusion, clustering and interaction in a thin foil heavy ion irradiation of ferritic/ martensitic steels. The model involves spatially dependent rate theory, or cluster dynamics, equations that describe the evolution of self-interstitial (mainly interstitial loops) and vacancy clusters (voids) in ferritic-martensitic steels under irradiation. The key parameters that are input to the model are determined from a combination of atomistic materials modeling and available experimental data. A new cascade dynamics model from molecular dynamics has been implemented which improves the accuracy of the results, as well as adaptive time stepping methods which allow to simulate up to higher doses. The Modeling predictions are compared with experimental results obtained at the IVEM facility in Argonne National Laboratory.

11:05 AM

Experimental and Modeling Studies on the Effects of a Wide Range of Flux on the Microstructures and Mechanical Properties of RPV Steels – Predicting Low Flux High Fluence Embrittlement: *Takuya Yamamoto*¹; G. Robert Odette¹; Nicholas Cunningham¹; Douglas Klingensmith¹; Randy Nanstad²; ¹Univ. California Santa Barbara; ²Oak Ridge National Laboratory

Transition temperature shifts (TTS) of reactor pressure vessels (RPV) steels must be predicted at extended life fluences that are far beyond the existing surveillance database. High fluences can be achieved only in test reactors at fluxes that are much higher than under vessel service. TTS are primarily caused by nm-scale hardening features including: a) thermally stable defect solute matrix features; b) thermally unstable matrix defects; c) and Cu-Mn-Ni rich precipitates. Flux affects both the concentrations and balance of these features, thus, the TTS for a given alloy and irradiation condition. We present a database and analysis of irradiation hardening and the evolution of the nm-scale features for a large set of alloys for a very wide range of fluxes and fluences in both the as-irradiated and annealed conditions. The database and analysis is used to develop a physically based model for predicting TTS at high fluence and low flux.

11:25 AM

Material Constraints on Accelerator Driven Sub-Critical Molten Salt Thorium Reactors: John Wallace¹; Ganapati Myneni²; ¹Casting Analysis Corp; ²Thomas Jefferson Nat. Accelerator Facility

The development of linear superconducting accelerators has progressed so efficient and reliable machines can be used for neutron spallation sources. Future materials advances in these machines can be expected to improve their operating efficiencies. These hinge on understanding hydrogen and coatings in the niobium superconducting resonant cavities which provide the accelerating fields. Other than basic research these machines open the possibility of controlling thorium fission reactors as a heat sources for power generation and PWR nuclear waste digestion. This compact reactor is examined for long term materials stability both in the interface region of the spallation source, the long term integrity of the internal graphite structures and nickle based containers and piping. Historically there is limited data on materials degredation in the molten salt environment for periods of 40 years. Accelerated testing and monitoring of material degradation in a range of environments will be discussed along with preliminary experiments.

11:45 AM

Stress Corrosion Cracking Behavior of Ferritic and Austenitic Stainless Steels in High Temperature Water: *Raul Rebak*¹; Peter Andresen¹; ¹GE Global Research

Austenitic stainless steels such as type 304 and 316 are used widely as core internals components in light water reactors. Under certain operation conditions these materials may be susceptible to stress corrosion cracking



and irradiation assisted stress corrosion cracking. Irradiation may produce hardening and alter the local chemistry of the alloys, which may increase their susceptibility to environmentally assisted cracking. Ferritic stainless steels are less susceptible to irradiation damage such as void swelling than the austenitic cousins. Ferritic stainless steels also offer higher thermal conductivity and lower expansion coefficients. Little is known however about the stress corrosion cracking behavior of ferritic steels in high temperature water. Crack propagation rate studies were conducted using four types of ferritic steels in high purity water at 288°C containing dissolved oxygen or dissolved hydrogen. The cracking susceptibility results obtained with the ferritic steels are compared with literature data for austenitic stainless steels.

12:05 PM

Mechanical Properties of Advanced NF616 Steel: Mikhail Sokolov¹; Lizhen Tan¹; ¹ORNL

Fracture toughness, Charpy impact and tensile properties of advanced ferritic-martensitic 9Cr-1.8WNbV steel NF616 were characterized in the wide temperature range from room temperature to 650C. This steel is one of the candidates of high-temperature structural materials in the next generation nuclear systems. Tensile properties are similar in transverse and longitudinal orientations. Strength was decreasing with increase of test temperature. This alloy exhibited considerable fracture toughness properties up to 650C. In addition, thermomechanical treatment is being developed on the asreceived NF616. Preliminary results of Vickers microhardness and tensile tests showed enhancement in microhardness and both strength and ductility compared to the as-received NF616. Microstructural characterization is being performed to explain the properties enhancement induced by the thermomechanical treatment. The effects of thermomechanical treatment on fracture toughness will be discussed as well.

Materials in Clean Power Systems VI: Clean Coal-, Hydrogen Based-Technologies, and Fuel Cells: Materials for Gasification and Turbines II

Sponsored by: The Minerals, Metals and Materials Society, TMS Electronic, Magnetic, and Photonic Materials Division, TMS Structural Materials Division, TMS/ASM: Corrosion and Environmental Effects Committee, TMS: Energy Conversion and Storage Committee, TMS: High Temperature Alloys Committee *Program Organizers*: Xingbo Liu, West Virginia University; Zhenguo "Gary" Yang, Pacific Northwest National Laboratory; Jeffrey Hawk, U.S. Department of Energy, National Energy Technology Laboratory; Teruhisa Horita, AIST; Zi-Kui Liu, The Pennsylvania State University

| Tuesday AM | Room: 33C |
|---------------|-------------------------------|
| March 1, 2011 | Location: San Diego Conv. Ctr |

Session Chair: Jeffrey Hawk, U.S. Department of Energy, National Energy Technology Laboratory

8:30 AM Invited

Gas Turbines of the Future: Hydrogen and Oxy-Combustion Environments: *Jeffrey Hawk*¹; Gordon Holcomb¹; ¹U.S. Department of Energy

Materials issues related to higher efficiency power plants, like hydrogen or oxy-fuel fired gas turbines, require materials with higher temperature capability than the current generation of turbines. Research to extend the usable critical temperature of nickel superalloys has focused on maintaining the strength and integrity of grain boundaries and the interface between the grain boundary phases (carbide and/or TCP) and the matrix, as well as improving the long-term stability of fine strengthening precipitates at the use temperature. Concurrent with achieving these goals is to understand how temperature, stress, and environment affect grain boundary, matrix and surface/coating interface stability as a consequence of exposure to the gas turbine environment. This presentation will focus on specific features of the microstructure and how these features are affected due to exposure to an oxy-combustion type environment. The affect on low cycle fatigue will be discussed as well as the fracture morphology.

8:55 AM

Tempered Martensitic Ferritic Steel Alloy Development for Ultrasupercritical Steam Applications: Christopher Cowen¹; Jeffrey Hawk¹; Paul Jablonski¹; ¹United States Department of Energy

Advanced 9-12% Cr tempered martensitic ferritic steels form the majority tonnage of components used in coal fired power plants that operate in the temperature range of 570-620°C. Computational and experimental alloy development efforts at NETL are focused on increasing the temperature capability of this class of alloy to 650°C in order to increase power plant efficiency while simultaneously decreasing the cost of construction and carbon footprint. This presentation focuses on microstructural stability issues and preservation of strengthening mechanisms that are keys to the successful development of advanced 9-12% Cr steels that meet minimum creep life requirements at 650°C for 100,000 hours and 100 MPa. Compositional, thermo-mechanical, weldability, and inspectability requirements for advanced 9-12% Cr steels are also discussed. Microstructural development and creep behavior determined in tandem for the newly developed NETL alloys as well as for COST E, B2, and FB2 alloys is presented.

9:15 AM Invited

Accelerating High-Performance Materials Design: An Integrated Computational and Experimental Approach: *Michael Gao*¹; De Nyago Tafen¹; Kaisheng Wu¹; Rongxiang Hu¹; Vijay Jain¹; Omer Dogan¹; Jeff Hawk¹; Chris Cowen¹; Paul Jablonski¹; Michael Widom²; ¹NETL; ²Carnegie Mellon University

In order to reduce harmful environmental emission from coal-fired power plants, National Energy Technology Lab has developed various highperformance materials. For example, high-temperature structural alloys based on Cr and Nb for components to be used in oxy-fuel or hydrogen combustion turbines; crystalline and non-Pd amorphous membrane alloys for hydrogen separation; ferritic Fe-based alloys capable of use at 650°C in advanced combustion systems to reduce the amount of CO2 emission. We have adopted an approach that integrates computer simulations with critical experiments to accelerate new materials design. Balancing structureproperty relationship require delicate tradeoffs and compromises by manipulating alloy system and composition, microstructure, coatings, and materials processing. During this talk, we will present ongoing research effort implementing this approach to design high-performance materials, using combination of computer simulation techniques such as first principles calculations, Molecular Dynamics simulations, CALPHAD modeling, microstructure simulations using phase field, and mechanical property simulations using discrete FFT.

9:40 AM Invited

Effect of Oxy-Firing on Fireside Corrosion Rates: Michael Bestor¹; Bruce Pint¹; ¹Oak Ridge National Laboratory

Oxy-firing has been suggested as a method to reduce NOx emissions and capture CO2 from coal-fired power plants. This process involves recirculating the flue gas and will increase the CO2, and likely the H2O and SO2 concentrations, in the boiler. In order to understand the role of substrate chemistry on corrosion behavior, commercial and model alloys are being exposed in standard fireside corrosion tests with and without synthetic ash. The gas composition is varied to reflect air-firing and various oxy-firing scenarios. The current testing was performed at 600°C with ferritic steels the primary focus; however, austenitic steels and Ni-base alloys also were exposed with the former showing the lowest corrosion attack. Research sponsored by the Office of Fossil Energy, Advanced Research Materials Program, U. S. Department of Energy.

10:00 AM Break

10:15 AM Invited

Oxidation Kinetics Modeling Applying Phase Field Approach: *Youhai Wen*¹; Long-Qing Chen²; Jeff Hawk¹; ¹National Energy Technology Laboratory; ²Penn State University

Components in high temperature fossil energy applications are usually exposed to an aggressive environment containing H2O, CO, CO2 CH4, and O2. As service temperature of advanced fossil energy systems increase, chemical reaction rates will increase exponentially and environmental attack will become much more of a concern to designers and in life prediction models. In this work, a general phase-field model is formulated to model the oxidation kinetics. This model can be used to simulate the temporal evolution of oxide thickness and oxygen profile under various conditions such as microstructure dependent diffusivities and simultaneous scale formation and exfoliation. The long term goal of this project is to develop a quantitative tool to predict oxidation kinetics under realistic environmental conditions for certain materials. Pathway of achieving this goal will be discussed.

10:40 AM

Cyclic Oxidation Behavior of HVOF MCrAIY Coatings Deposited on La- and Y-Doped Superalloys: Michael Bestor¹; Allen Haynes¹; Bruce Pint¹; ¹Oak Ridge National Laboratory

One suggested strategy for improving the performance of thermal barrier coating (TBC) systems used to protect hot section components in gas turbines is the addition of low levels of dopants to the Ni-base superalloy substrate. For the more aggressive environment expected for coal-derived, synthesis gas-fired turbines, this strategy may be effective in retaining TBC durability. To quantify the benefit of these dopants, coupons of three commercial alloys with different Y and La contents were coated with the same commercial NiCoCrAlYHfSi bond coating by high velocity oxygen flame spraying. Coupons were oxidized in cyclic tests at 1050°, 1100° and 1150°C and the oxidation rate and alumina scale adhesion were compared in an effort to better understand the benefit of superalloy dopants. This research was sponsored by the U.S. Department of Energy, Office of Coal and Power R&D, Office of Fossil Energy, (R. Dennis program manager).

11:00 AM

An Investigation on Hot Corrosion Resistance of Plasma Sprayed YSZ-Ceria TBC in Na2SO4+V2O5 at 1050 °C: Mohsen Saremi¹; *M.H. Habibi*¹; ¹University of Tehran

Thermal Barrier Coatings are subjected to spallation and destabilization due to oxidation and hot corrosion. In this research, the hot corrosion behaviors of three types of composite coatings were investigated: (1) Conventional YSZ, (2) YSZ+CeO2 (the composite layer of Ceria and YSZ), (3) CeO2/YSZ (The over layer of Ceria on YSZ). The treated samples were characterized using XRD and SEM equipped with EDS. Based on the microscopic observations, the formation of YVO4 crystals and YSZ spallation, and the amount of phase transformations of tetragonal ZrO2 to monoclinic, were the criteria for evaluating the resistance of composite coatings. It was observed that CeO2/YSZ the best resistant coating against hot corrosion test while conventional YSZ was the least among the three coatings. It was shown that the interaction of V2O5 with yttria resulted in formation of YVO4 which is detrimental to YSZ because of its accelerated destabilization.

11:20 AM

An Investigation of the Electrochemical Properties of 3 Types PVD Coated on STS304: *Min-Seok Moon*¹; Woo KeeDo²; Chan-Won Kwak³; Sang-Hyuk Kim²; Joon-Hyuk Song¹; Je-Ha Oh¹; ¹Chonbuk National University, Jeonju Institute of Machinery Carbon Composites; ²Chonbuk National University; ³Se-Won Hard Facing Co., Ltd.

In the PEM fuel cell need to reduced weight and total fabrication cost of a fuel cell stack, and increased durability during the operating condition. Typically bipolar plates are a key component of PEMFC and other Fuel cells. In order to reduce both the weight and cost of the bipolar plates, nowadays consider attention is being paid to developing metallic bipolar plates to replace dense graphite. In this study, try to 3 types Nitride coating process on an austenitic stainless steel (STS304) using a PVD technology (plasma enhanced reactive evaporation) to increase the corrosion resistance of the STS304. Contact angle, SEM, and potentiodynamic tests were used to characterize the 3 types Nitride coating process on the STS304. This study is focus on the best PVD nitride coating process for the corrosion resistance in the PEMFC operating conditions, and could potentially be used in PEMFCs as a bipolar plate material requirement.

11:40 AM

Gaseous Hydrogen Embrittlement of Pipeline Steels: Nicholas Nanninga¹; Yaakov Levy²; Andrew Slifka¹; ¹NIST; ²NRCN

The tensile properties of x52, x65, x80 and x100 pipeline steels have been measured in a high pressure (13.6 MPa), high purity, hydrogen gas environment. Significant losses in elongation to failure and reduction in area were measured when testing in hydrogen compared to air (NTP), and these changes were accompanied by major changes in fracture morphology. For hydrogen charged specimens, surface crack initiation and growth was the primary failure mechanism, compared to a typical cup-and-cone failure for specimens tested in air. In addition to baseline characterization of the effects of strength and microstructure, several tests were conducted on the x100 alloy to determine the effects of strain rate and hydrogen gas pressure. Losses in ductility were observed with increases in pressure (up to 68 MPa) and decreases in strain rate, though a plateau in the effects of these variables was evident for the x100 alloy.

Materials Processing Fundamentals: Powders and Composites

Sponsored by: The Minerals, Metals and Materials Society, TMS Extraction and Processing Division, TMS: Process Technology and Modeling Committee

Program Organizers: Prince Anyalebechi, Grand Valley State University; Srikanth Bontha, Temple University

| Tuesday AM | Room: 12 |
|---------------|-------------------------------|
| March 1, 2011 | Location: San Diego Conv. Ctr |

Session Chair: Prince Anyalebechi, Grand Valley State University

8:30 AM

Exploratory Research in Reactive Spark Plasma Extrusion: *P Mehra*¹; K. Morsi¹; ¹San Diego State University

Spark plasma sintering has gained a considerable amount of attention over the past decade, due to its rapid sintering rates, and low temperature requirements, but has so far been usually limited to the production of simple geometries. The present paper examines the current-activated production of extended geometries through the process of spark plasma "extrusion". Of interest in the present study is exploratory research into the effect of electrical current activation on the reactive consolidation of powder systems to form intermetallic materials.

8:45 AM

Preliminary Investigations of the Effect of Particle Size and Tip Size in the Current Activated Tip-Based Sintering (CATS) of Nickel Powder Compacts: A. El-Desouky¹; K. Morsi¹; K.S. Moon¹; S.K. Kassegne¹; ¹San Diego State University

Current Activated Tip-based Sintering (CATS) is a new process for the powder-based fabrication of macro, micro and possibly nano-scale features and shapes. This new and unique process enables selective sintering of powders by localizing electrically activated sintering conditions through a stationary or moving electrically conducting tip. We present preliminary experimental results on the effect of tip size in the CATS process as well as the effect of initial powder particle size on the sintering behavior of nickel powder.



9:00 AM

Determination of the Spark Plasma Sintering Fundamental Densification Mechanisms by Novel Cyclic Loading Approach: *Wei Li*¹; William Bradbury¹; Joanna McKittrick¹; Randall German²; Eugene Olevsky²; ¹University of California San Diego; ²San Diego State University

Determination of fundamental densification mechanisms during spark plasma sintering (SPS) of particulate materials is critical in analyzing defect formation and density evolution. A new cyclic loading approach is applied to determine the dominant mechanism of material transport during SPS. The advantage of the cyclic loading technique is that only one experimental run is needed to determine the constitutive properties of a powder material for any given heating schedule, and no interrupted tests taking into account the grain growth kinetics are necessary. This methodology is employed for sintering compacts pressed from metal (pure spherical copper) and ceramic (alumina) powders. SPS experiments with different heating rates are conducted with the application of different load levels. The step-wise pressure cyclogram is utilized during processing. The determined material constitutive parameters serve as a basis for a full-scale modeling of spark-plasma sintering process.

9:15 AM

Exploratory Investigations in Reactive Current Activated Tip-based Sintering (CATS): *A Numula*¹; K. Morsi¹; K.S. Moon¹; S.K. Kassegne¹; ¹San Diego State University

Current Activated Tip-based Sintering (CATS) is a new process for the powder-based manufacturing of macro, micro and possibly nano-scale features and shapes. CATS enables the selective sintering of powders by localizing current activation conditions through an electrically conducting small tip (either in the stationary or moving mode). This paper presents preliminary experimental results on the CATS of reactive mixtures of Ni/Al powder to form nickel aluminide intermetallics. Preliminary investigations on the effect of current on the reaction characteristics is discussed.

9:30 AM

Microstructural Evolution of Cu, Ni and Al Powder Particles Processed by Cold Spray: *Yu Zou*¹; Eric Irissou²; Jean-Gabriel Legoux²; Stephen Yue¹; ¹McGill University; ²Industrial Materials Institute (IMI), National Research Council Canada (NRC)

Cold spray is a relatively new coating technology by which coatings can be produced using high-velocity impact of powder particles without significant heating introduced. Micron-sized pure Cu, Ni and Al powder particles were processed by the cold spray, respectively. Microstructural evolutions of these particles were investigated using electron backscatter diffraction and transmission electron microscopy. The results show that non-uniform microstructures with elongated grains/subgrains in the size of microns, equaxied grains in sub-microns and nanocrystalline grains appear in as-sprayed materials. Moreover, deformation twins in nano-scale are observed in the cold sprayed Cu. Formation of these structures is explained by high strain-rate deformation with the dynamic recovery/recrystallization in the complex thermo-mechanical process during cold spray.

9:45 AM

Elucidating Microstructure Formations in Ta(x)C(1-x) at Various Carbon Contents: Robert Morris¹; *Gregory Thompson*¹; ¹University of Alabama

TaC has a melting temperature near 4000oC and can precipitate out Ta-rich carbide precipitates with similar high melting temperatures. This offers the ability to engineer the microstructure for thermomechanical loading. A series of tantalum carbides have been hot isostatic pressed (HIP) from constituent TaC and Ta powders. Depending on carbon content various microstructures could be processed. These include equiaxed single phase TaC or Ta2C grains, equiaxed TaC grains which encased a hatch-pattern of Ta4C3 laths, or acicular grains with very fine laths of TaC/Ta4C3/Ta2C running parallel to the major axis of the grain. To elucidate the microstructure formation mechanisms, a HIP diffusion couple of TaC – Ta metal powders was prepared. The HIP couple revealed the entire span of microstructures. The location of specific microstructures in relationship to the initial powder states provided insights

into the precipitation and reactions from which specific phases and grain morphologies formed.

10:00 AM Break

10:15 AM

Fabrication, Characterization and Comparison of Spinel ZnFe2O4 Obtained by Sonochemestry Way and Ceramic Way: Oscar Restrepo¹; Edgar Chavarriaga¹; Juan Montoya¹; Leidy Jaramillo¹; Miguel Hernández¹; ¹National University of Colombia

This paper provides an analysis of ZnFe2O4 spinel type ceramic pigment obtained by the alternative manufacturing method sonochemistry and the ceramic way. The method sonochemestry appears as an attractive method with enormous advantages in ceramic chemistry, that is why in the synthesis of compounds of industrial interest is emerging as a possible route. The objective is to evaluate the influence that can produce the particle size with optical properties, which are of interest in ceramic pigments industry, also make a comparison with the ceramic way from colorimetric and physical properties. The methods used to characterize the ceramic pigments were x-ray diffraction (XRD), scanning electron microscopy (SEM) and UV-VIS spectrophotometry.

10:30 AM

Properties and Performance of Composites Based on Superrefractories Cements: *Ilyoukha Nickolai*¹; Timofeeva Valentina¹; Schabanov Alexander¹; ¹Academic Ceramic Center

Superrefractories cements (1800-2700°C) is a new refractory insulating material and objective of this work is to enlarge our knowledge about this new product and to search solutions for problems the industry is fasing. Based on this target, we realized several test to find answers to important questions about the application of this product in severe industrial conditions and to analyze how this material performs in high temperatures. High temperature composites and coatings based on superrefractories cements are meant to protect units from influence of temperature more than 2000°C and used for manufacturing monolithic lining, crucibles used in the melting of pure metals, including alloys on rare-earth elements, for closing one of ceramic modules of fire wall, in refractory lining of quartzglasstanks, petrochemistry reactors, in burial of radiation fuel by extreme environments in nuclear reactors.

10:45 AM

Predicting the Mechanical Properties of Aluminium-SiC Functionally Graded Materials Processed by Centrifugal Rotation Method: *Veerarajkumar Aparna*¹; Savita Kaliya Perumal Veerapandian¹; ¹College of Engineering, Guindy, Anna University

Materials characterized by variation in composition and structure gradually over volume, resulting in corresponding changes in properties are defined as functionally graded materials(FGM). Al-SiC FGM's were obtained by centrifugal rotation of die in a muffle furnace. The paper develops a reliable model to predict the functional gradient to the analyzed systems. The wear properties were studied using the pin-on tester. A fem code is employed to estimate the effective elastic properties along the gradient distribution. The obtained values were compared with the theoretical calculation acquired by the rule of mixtures. The results revealed that the properties were significantly influenced by the graded distribution of SiC in the matrix. The resultant FGM's were carefully characterized, a great attention devoted to micro structural investigation.

11:00 AM

Improvement on the Tribological Characteristics of Particulate Copper Silicon Carbide Composites: David Esezobor¹; Atinuke Oladoye¹; ¹University of Lagos

Particulate Cu-SiC composites find applications as wear and heat resistant materials in electrical sliding contacts such as in homopolar machines, railway overhead current collector systems where high electrical/ thermal conductivity combined with good wear properties is required. However, challenges occur during machining due to the presence of hard reinforcement in the matrix this may lead to high turnover of tool wear and

poor surface finish. The adoption of near- net shape technology to produce such hard-to-machine metal matrix composites and subsequent finish machining with its attendant cost has reported limited success. This paper critically appraises the challenges and opportunities in the improvement of tribological characteristics of particulate Cu-SiC composites and identifies low cost reinforcement material that could be used to improve its tribological characteristics.

11:15 AM

Study on Preparation of High-Purity Magnesium Carbonate Whisker from Low-Grade Magnesite: *Caiyun Lu*¹; Min Chen¹; Jingkun Yu¹; ¹Northeastern University

Mg(HCO3)2 solution was prepared through light burning, hydrous carbonation by using low-grade magnesite as the raw materials, and then the impurities were removed by using activated carbon as adsorbent. In this paper, the effect of different additives on the morphology of Mg(HCO3)2 pyrolytic products and the effect of the heating rate on the morphology of the obtained magnesia were studied. The XRD result showed that the main components of Mg(HCO3)2 pyrolytic products were 3MgCO3•Mg(OH)2•3H2O and MgCO3•3H2O, which contained less impurities such as CaO<0.04% and TFe<0.02% after adsorbing the impurities by activated carbon. SEM results showed that the morphology of magnesium carbonate was highly dependent to the preparation conditions, Namely, without any additive, the flake-like pyrolytic product was obtained, petal shaped pyrolytic product was prepared with potassium dihydrogen phosphate additive, spherical pyrolytic product was obtained with ammonium carbonate additive, and whisker pyrolytic product was obtained while soluble magnesium salts was added, because the additives hindered the growth of crystals in one direction, while promoting the directions of crystal growth to without obstruction. The calcining system had a direct impact on the morphology of magnesia converted from the whisker precursor, while the calcining temperature was elevated at 50-min-1, magnesia powder was obtained, while the calcining temperature was elevated at 2 -min-1, most magnesia maintained whisker morphology, because the decomposition of magnesium carbonate was divided into three stages, the calcination product could keep whisker morphology as precursor through control the decomposing speed.

11:30 AM

Preparation of Metal Cobalt Powder by Coprecipitation and Heat Decomposition Method: *Xue Ping*¹; Guo Xueyi²; Tian Qinghua²; Liang Sha²; ¹Jianghan University; ²central south university

This research provides a novel method to prepare the metal cobalt powder. This method prepared the precursor powder of Co(OH)x(CO3)y by the conventional chemical precipitation, the phase analysis made by X-ray and the infrared spectrum proved that component of the precursor powder was Co(OH)x(CO3)y adsorbing NH4+ and Cl- and the organic functional group. The precursor powder was prepared for metal cobalt powder through heat decomposition. Based on DSC-TGA analysis, influence of additive reagent and temperature factor to prepare for the cobalt powder were observed in heat decomposition. The results show when the amount the additive reagent is 63.64%, calcination temperature is 500 oC, all the product is metal cobalt, and the properties are fine.

Microstructural Processes in Irradiated Materials: Microstructure Evolution: Modeling

Sponsored by: The Minerals, Metals and Materials Society, TMS Structural Materials Division, TMS/ASM: Nuclear Materials Committee

Program Organizers: Gary Was, University of Michigan; Thak Sang Byun, Oak Ridge National Laboratory; Shenyang Hu, Pacific Northwest National Laboratory; Dane Morgan, UW Madison; Yasuyoshi Nagai, Tohoku University

| Tuesday AM | Room: 3 |
|---------------|-------------------------------|
| March 1, 2011 | Location: San Diego Conv. Ctr |

Session Chairs: Yuri Osetsky, Oak Ridge National Laboratory; Shenyang Hu, Pacific Northwest National Laboratory

8:30 AM Invited

Simulations of Voids and Gas Bubbles in Irradiated Materials: *Marius Stan*¹; Shenyang Hu²; ¹Argonne National Laboratory; ²Pacific Northwest National Laboratory

The irradiation of nuclear reactor structural materials leads to the formation of voids that cause swelling while in nuclear fuels the accumulation and transport of fission products leads to the formation of gas bubbles that decrease the thermal transport. We review computer simulation techniques for predicting the evolution of voids and gas bubbles. To illustrate the challenges, we discuss phase-field simulations of the nucleation and growth of voids and gas bubbles, focusing on the role of the self-interstitial atoms and vacancies. The simulations show that a high rate of generating interstitials during displacement cascades delays the formation of void lattices. Phase field simulations of UO2 show that gas bubble nucleation is favored at grain boundaries due to the trapping of fission products and the high mobility of vacancies and gas atoms. The effective thermal conductivity strongly depends on the bubble volume fraction but weakly on the morphology of the bubbles.

9:10 AM

Modeling the Helium Transport, Fate in Tempered Martensitic Steels and Nanostructured Ferritic Alloys – Consequences to Void Swelling: *Takuya Yamamoto*¹; G. Robert Odette¹; ¹Univ. California Santa Barbara

A rate theory cluster dynamics model that tracks helium transport and partitioning to, and recycling between, matrix sites, precipitates, dislocations and grain boundaries is applied to treat precipitation of helium bubbles in a tempered martensitic steel, F82H, and a nanostructured ferritic alloy, MA957. The model uses kinetic and thermodynamic parameters derived from atomistic simulations. The predictions are shown to be in good agreement with data from in-situ He implantation experiments. Recently, the model has been extended to treat void nucleation and growth. The model predicts significant swelling in F82H, even with conservative parameters: following an incubation dose of ~ 20 dpa at 40 appm He/dpa and 500°C swelling reaches 3.2 % at 100 dpa and 16.6 % at 200 dpa. The predictions of a more detailed and improved model will be compared to the in-situ He implanter experiment up to 25 dpa and 1250 appm He.

9:30 AM

Modeling He Behavior in Tungsten: Relevance of the Implantation Model: Marc Hou¹; *Charlotte Becquart*²; Andree De-backer²; Christophe Domain³; Christophe Ortiz⁴; ¹Physique des Solides Irradiés et des Nanostructures CP234; ²UMET, UMR 8207, EM2VM; ³EdF, R&D, EM2VM; ⁴Laboratorio Nacional de Fusión por Confinamiento Magnético, CIEMAT

The binary collision approximation code Marlowe, and object kinetic Monte-Carlo simulations parameterized on Density Functional Theory (DFT) data have been used to investigate the fate of He atoms implanted in tungsten. The He atoms and the associated damage have been introduced either at random in the tungsten matrix or according to distributions provided by Marlowe, taking into account the crystalline nature of the matrix or considering it as an amorphous structure. The results indicate that



in order to reproduce the experimental results, one has to model properly the implantation sequence. They furthermore underline the significant contribution of the crystalline nature of the matrix.

9:50 AM

Stability and Evolution of He Clusters and Complex Defect Clusters Investigated by Ab Initio Calculations and OKMC Simulations in Tungsten: *Charlotte Becquart*¹; Andree De Backer¹; Christophe Domain²; ¹UMET, UMR 8207, EM2VM; ²EdF, R&D, EM2VM

Understanding and predicting the behavior of helium in metals is an important issue in particular in the context of materials used in fusion reactors nowadays. Indeed in these conditions, two sources of He are present: transmutation and implantation from the plasma. In tungsten, which is a candidate for the divertor in fusion reactors, theoretical and experimental results indicate that helium is very mobile already below room temperature and can form He clusters very easily. We have used state of the art ab initio calculations to investigate the stability of He clusters associated or not with point defects in tungsten as well as impurities. Small He clusters are mobile and one notable result is that the smallest ones exhibit a 1D motion at low temperatures. The consequences on the evolution of the microstructure under irradiation conditions will be discussed in the framework of an object kinetic Monte Carlo model.

10:10 AM

Mesoscale Simulation of Irradiation-Induced Gas Bubbles: Evolution and Impact on Macroscale Properties: *Paul Millett*¹; Anter El-Azab²; Michael Tonks¹; ¹Idaho National Laboratory; ²Florida State University

Nuclear materials used in fission and fusion applications can be subjected to simultaneously high displacement rates as well as gas production rates. The characteristics of the resultant gas bubble structure, i.e. internal gas density, bubble number density, and bubble distribution, are strongly dependent on the relative defect production rates as well as microstructure (e.g. grain size). Here, we implement a phase-field model capable of capturing multicomponent defect (vacancies, self-interstitials, and gas atoms) diffusion, bubble nucleation and growth, and bubble/grain boundary interactions to investigate these processes throughout time and for varying irradiation conditions. Furthermore, we have utilized this simulation capability to develop models of bubble percolation and the effective thermal transport across heterogeneous microstructures. Interestingly, thermal conductivity is found to be strongly dependent on the relative distribution of intergranular versus intragranular bubbles. This research was supported by the Nuclear Energy Advanced Modeling and Simulation (NEAMS) program within DOE-NE.

10:30 AM Break

10:50 AM

Simple Concentration-Dependent Pair Interaction Model for FeCr Alloys with Vacancy Supersaturation: *Enrique Martinez Saez*¹; Maximilien Levesque²; Frederic Soisson²; Maylise Nastar²; Chu Chun Fu²; ¹LANL; ²CEA-Saclay

FeCr alloys are foreseen as strong candidates for fission and fusion applications as matrix for structural materials. A lattice pair interaction model based on the RedLich-Kister polynomial is presented. The interaction coefficients have been fitted to ab-initio data. The model captures the complex thermodynamics of the system, including the short-range order found experimentally for low Cr concentrations. The broken-bond model has been implemented into the synchronous parallel kinetic Monte Carlo algorithm [J. Comp. Phys. 227 (2008) 3804-3823] so to be able to extend the size of the system and therefore the statistics of the calculation as well as the total time studied. Correlation length and precipitate number density of voids and a' precipitates have been studied as well as their shape and size distributions and the results compared to the experimental results available in the literature. We have found a very good agreement between the kinetic model and the experiments.

11:10 AM

Atomistic Study of Interstitial Migration in the Proximity of a Helium Bubble in the Fe-Cr System: *Jeffery Hetherly*¹; Alfredo Caro¹; ¹Los Alamos National Laboratory

We investigate the effect that helium bubbles have on the diffusion of self interstitials in Fe-Cr alloys using atomistic techniques. Different bubble pressures and bubble locations (bulk versus grain boundaries) are explored. The results are interpreted in terms of the sink capture efficiency of a bubble for interstitials and the anisotropy if interstitial diffusion in the presence of a stress field. Coated bubbles, either depleted or enriched in solute, are also of interest and are expected to give a different behavior than plain voids.

11:30 AM

Microstructure Evolution of Two Model Ferritic/Martensitic Steels Irradiated with Ions In-Situ in a TEM: *Djamel Kaoumi*¹; Jimmy Adamson¹; Athur Motta²; Mark Kirk³; ¹The University of South Carolina; ²The Pennsylvania State University; ³Argonne National Laboratory

Two model steels (one ferritic/martensitic(Fe12Cr0.1C) and one fully martensitic(Fe9Cr0.1C)) were custom-made with the intent of reproducing the type of starting microstructure of F/M steels, but without the complications of additional alloying elements. The alloys were irradiated with 1-MeV Krions at 25°C, 200°C, 300°C to doses up to 10 dpa in-situ in a TEM. The microstructure evolution was followed and characterized at successive doses in terms of defect formation, black dot density, number density of defect clusters, and stability of as-fabricated microstructure using weak-beam dark-field imaging and g.b analysis. The effect of the irradiation temperature on the damage density and on the stability of the initial microstructure is assessed. The overall goal is to determine directly the spatial correlation of the time evolution of the irradiation-induced defect structures with the pre-existing alloy microstructure and to compare with calculations based on rate-theory modelling. The results are summarized in this paper.

11:50 AM

Atomic-Scale Features of Strengthening Due to Impenetrable Obstacles in Iron: Yury Osetskiy¹; Roger Stoller¹; ¹ORNL

Oxide dispersion strengthened (ODS) alloys are considered as promising structural materials and therefore are under study by different experimental, theoretical and modeling techniques. In this presentation we report the first results of an extensive atomic-scale study of mechanical properties of materials containing impenetrable obstacles simulating ODS particles. We have considered rigid spherical coherent precipitates embedded into bcc-iron matrix. At the first stage we simulated a $\frac{1}{2}$ <111> edge dislocation gliding in the plane intersecting precipitates of diameter from 1 to 6nm at different distances to their equator. Different interaction mechanisms were observed depending on the dislocation glide plane position and temperature. The conditions of maximum strength were investigated and the results were discussed in the view of existing experimental data.

12:10 PM

Mobility of Low Energy Boundaries in FCC Copper during Irradiation: James Belak¹; Bryan Reed¹; Ming Tang¹; Joel Bernier¹; Vasily Bulatov¹; Thomas LaGrange¹; Mukul Kumar¹; ¹Lawrence Livermore National Laboratory

The mobility of ideal low energy boundaries (e.g. Sigma 3) in FCC copper has proven difficult to study using molecular dynamics due to the long timescales involved. However, by introducing a small vicinal step or shear along the boundary (to nucleate a stepped region), these low energy boundaries readily move. Here we quantify the mobility of Sigma 3 boundaries in FCC copper as a function of vicinal angle and local boundary shear stress. These simulations are used to drive the boundary through regions of irradiation damage (vacancies, interstitials and defect clusters). The defect field initially enhances the step density and mobility, which saturates as the boundary roughens. The simulation results are used to parameterize a simplified model of boundary mobility during irradiation. *Work performed under the auspices of the U.S. DOE by LLNL under Contract DE-AC52-07NA27344 and supported by the U.S. Department of Energy, Office of Basic Energy Sciences.

Neutron and X-Ray Studies of Advanced Materials IV: Complex Materials

Sponsored by: The Minerals, Metals and Materials Society, TMS Structural Materials Division, TMS/ASM: Mechanical Behavior of Materials Committee, TMS: Chemistry and Physics of Materials Committee

Program Organizers: Rozaliya Barabash, Oak Ridge National Laboratory; Xun-Li Wang, Oak Ridge National Laboratory; Jaimie Tiley, Air Force Research Laboratory; Peter Liaw, The University of Tennessee; Erica Lilleodden, GKSS Research Center; Brent Fultz, California Institute of Technology; Y-D Wang, Northeastern University

| Tuesday AM | Room: 10 |
|---------------|-------------------------------|
| March 1, 2011 | Location: San Diego Conv. Ctr |

Session Chairs: T.-C. Chiang, University of Illinois at Urbana-Champaign; Yang Ren, APS

8:30 AM Keynote

From Structure to Nano-Structure: Materials Research with X-Rays and Neutrons: *Gernot Kostorz*¹; ¹ETH Zurich

X-rays and neutrons have served as probes for the study of structural and dynamic properties of materials for a long time. Improvements in X-ray and neutron sources and user-oriented research facilities continue to enhance possibilities for increasingly sophisticated experimentation. Some applications of neutron and X-ray scattering – diffraction, diffuse and smallangle scattering – will be presented, with emphasis on recent developments and combination with other methods.

8:55 AM Invited

Diffuse Scattering as an Aid to the Understanding of Polymorphism in Pharmaceuticals: *Richard Welberry*¹; Darren Goossens¹; Eric Chan¹; Aidan Heerdegen¹; ¹Australian National University

Polymorphism occurs when the same molecular compound can crystallise in more than one distinct crystal structure. Its study is a field of great interest and activity. This is largely driven by its importance in the pharmaceutical industry but polymorphism is also an issue in the pigments, dyes and explosives industries. The polymorph formed by a compound generally exerts a strong influence on its solid-state properties. The polymorphic form of a drug molecule may affect ease of manufacture and processing, shelf-life and most significantly, the rate of uptake of the molecule by the human body. They can even vary in toxicity; one polymorph may be safe, a second may be toxic. In this paper we show how diffuse scattering experiments coupled with Monte Carlo computer modeling can aid in the understanding of polymorphism. Examples of the two common pharmaceuticals benzocaine and aspirin, both of which are bimorphic, will be discussed.

9:15 AM Invited

Modeling Diffraction from Thin Film Structures: *I Noyan*¹; Andrew Ying¹; Braxton Osting¹; Conal Murray¹; ¹Columbia University

We present a rigorous model of kinematic diffraction of a coherent, monochromatic, X-ray beam, focused by a Fresnel zone plate onto a thin, perfect, single-crystal layer. In this model, we first calculate the coherent wave emanating from an ideal zone plate equipped with a direct-beam stop and order sorting aperture. Then, we compute the diffraction of the focused wavefront by a thin silicon film positioned at the primary focal spot. Finally, we propagate the diffracted wavefront to the position of an area detector, and map the intensity distribution in the detector plane. Our model showed that the data analysis of kinematic diffraction patterns obtained from area detectors have some differences from traditional radial scans. These differences were verified through experiments.

9:35 AM Invited

Multiple Diffraction in Quasicrystals: *Walter Steurer*¹; Changzeng Fan¹; ¹ETH Zurich

Multiple diffraction takes place when a crystal is oriented in a way that more than one set of atomic planes is in a position to diffract the incoming monochromatic radiation simultaneously. Because of the interaction between the excited reflections, the total amount of intensity will be redistributed among them. Multiple diffraction is omnipresent during a diffraction measurement on a quasicrystal as a result of its dense set of Bragg reflections. It can bias weak Bragg intensities, which are the key to the solution of the structure of quasicrystals. A complete understanding of multiple diffraction in quasicrystals will help us to get more accurate data sets. Therewith, quasicrystal structure refinement can be substantially improved. Here we report the first results of our study on multiple diffraction in quasicrystals and its influence on quasicrystal structure analysis.

9:55 AM Invited

Development of Ultrasmall-Angle X-Ray Scattering / X-Ray Photon Correlation Spectroscopy (USAXS/XPCS) for In Situ Studies of Equilibrium and Non-Equilibrium Dynamics over Extended Length and Time Scales: Jan Ilavsky¹; Andrew Allen²; Fan Zhang²; Lyle Levine²; Alec Sandy¹; Gabrielle Long¹; ¹APS, Argonne National Laboratory; ²National Institute of Standards and technology

Scattering and imaging techniques are applicable in static microstructural studies over the full nanometers-to-micrometers feature size range. The dynamics of materials, especially their response to abrupt changes in the sample environment, is on the other hand the domain of the X-ray photon correlation spectroscopy (XPCS). However, existing XPCS facilities are limited to microstructure length scales smaller than about 50 nanometers, thus eliminating large classes of materials that are of major technological importance. We have developed combined ultrasmall-angle X-ray scattering /X-ray photon correlation spectroscopy (USAXS/XPCS) technique to probe the slow equilibrium and non-equilibrium dynamics of optically opaque materials with prominent scattering features in the range 100 nm to several micrometers, i.e., between the ranges of dynamical light scattering and conventional XPCS. Presented example of USAXS-XPCS capabilities will be study of equilibrium dynamics of colloidal dispersions at various volume concentrations as a function of temperature.

10:15 AM Invited

X-ray Studies of the Lattice Dynamics of Cr across Its Antiferromagnetic Transition: *Tai Chiang*¹; Ruqing Xu¹; Mary Upton²; Hawoong Hong²; ¹University of Illinois; ²Argonne National Laboratory

Spin-lattice coupling is a classic topic in solid state physics. While generally weak, it is relevant to the basic physics of how elementary excitations interact. A striking case is the Neel transition at Tc = 311 K in chromium. Ultrasonic measurements revealed a substantial, anomalous softening in the elastic constants near Tc. However, this anomaly has not been detected by neutron scattering. To clarify this issue we have carried out both inelastic x-ray scattering (IXS) and x-ray thermal diffuse scattering (TDS) measurements of this system. IXS scans at several selected regions in reciprocal space did not find significant changes in phonon frequencies, in agreement with prior neutron scattering results. However, TDS measurements near a Brillouin zone center, where IXS measurements had difficulties, revealed an anomalous behavior of the phonons. Our findings suggest that the spin-lattice coupling in chromium is dominated by long-wavelength interactions.

10:35 AM Invited

Diffuse X-Ray Scattering of Bulk Au-50 at.% Pd and a Ni-23 at.% Pt(100) Surface: Bernd Schoenfeld¹; ¹ETH Zurich

Experimentally no ground state structure is known for bulk Au-Pd, but a series of structures were suggested by electronic structure calculations. In search of plausible superstructures, diffuse x-ray scattering from single crystalline Au-50 at.% Pd was taken for a quenched state of thermal equilibrium. Maxima in short-range order scattering are seen at $2k_F$ positions, repeatedly found with Au or Cu based alloys. Using the effective



pair interaction parameters, the existence of the suggested structures close to 1:1 stoichiometry is addressed, based on the values of the respective ordering energies. In the course of the ongoing research to characterize the near-surface microstructure of Ni-Pt by grazing incidence diffraction, Ni-23 at.% Pt(100) was measured at 970 K. In contrast to the (110) surface previously investigated, the (100) near-surface regime is connected with strong order leading to strong crystal truncation rods through 100 positions. A tetragonal model is applied to analyze diffuse scattering.

10:55 AM Break

11:05 AM Keynote

Diffraction from Nanocrystalline Materials: Reciprocal Space versus Direct Space Methods: Paolo Scardi¹; Matteo Leoni¹; Luca Gelisio¹; Alberto Leonardi¹; ¹University of Trento

Diffraction Line Profile Analysis (LPA) is commonly employed in the characterization of nanocrystalline materials, to gather information on nanocrystal size and shape, lattice defects and atomic-scale distortions. Despite the popularity of LPA in most nanomaterial studies, the applicability of traditional methods based on the reciprocal space approach down to the characteristic dimensions of a few nanometers is not so straightforward, and should be questioned when non-crystallographic structures are involved. The intrinsically discrete nature of the matter on the nanoscale is better described by direct space methods, like those based on the Debye equation. However, the change of paradigm - from reciprocal to direct space - opens new challenges in LPA, to develop computationally effective methods and to obtain a better understanding and representation of the real structure of nanocrystals.

11:30 AM Invited

Doing Neutron Scattering Science with the Multi-Axis Crystal Spectrometer at the NCNR: Jose Rodriguez-Rivera¹; ¹University of Maryland/NIST Center for Neutron Resarch

The Multi-Axis Crystal Spectrometer at the NIST Center for Neutron Research began commissioning operation on 2009 and is in the user program since January 2010. With a Energy range up to 20meV, the high neutron flux, up to 5×10^{8} neutrons/cm2/s will open new areas of condensed matter physics to exploration through inelastic neutron Scattering. The high neutron flux is obtained by using a doubly focusing monochromator subtending a solid angle of up to 0.005 Sr to the cold neutron source. The detector system consist of an array of 20 channels. Each detector channel is built around a vertically focusing double crystal analyzer. The MACS instrument is particularly powerful for probing the wave vector dependence of inelastic neutron scattering in select ranges of energy transfer to access the dynamic structure of fluctuating systems. The first experiment shows the instrument capabilities and opens a new horizon for neutron scattering science.

11:50 AM

Diffraction Measurements to Identify Structural Changes In Li[Li1/3-2x/3NixMn2/3-X/3]O2 (x=1/5) Cathode Materials for Lithium Ion Batteries: *Christopher Fell*¹; Shirley Meng²; Jacob Jones¹; ¹University of Florida; ²Unversity of California San Diego

The lithium-excess layered oxide compounds Li[NixLi1/3-2x/3Mn2/3-x/3] O2 (0 < x < 1/2) are of great interest as a new generation of positive electrode materials for high energy density lithium-ion batteries. Following lithium deintercalation and the associated oxidation of Ni2+ to Ni4+, lithium may continue to be extracted from this material despite the fact that all the manganese and nickel ions are in their fully charged (+4) oxidation state. In order to understand the electrochemical processes in Li[Li0.2Ni0.2Mn0.6] O2, we investigated the structural changes in the bulk material quantitatively using synchrotron x-ray and neutron diffraction. Synchrotron X-ray diffraction data of electrochemically cycled electrode materials show an expanded c/a lattice ratio, peculiar cation migration and growth of a second phase. Neutron diffraction data following chemical delithiation confirms that not only the Li ions but the transition metal ions (i.e. Ni) are dynamically migrating during the delithiation process.

12:00 PM Invited

Site Occupation of Atoms in Crystal Lattice Determined by High-Pressure X-Ray Diffraction Technique: *Zhihua Nie*¹; Yandong Wang¹; Zhenwei Huang²; Dongmei Liu²; Qiaoshi Zeng³; Wenge Yang³; Yang Ren⁴; ¹Beijing Institute of Technology; ²Northeastern University; ³Carnegie Institution of Washington; ⁴Argonne National Laboratory

Both mechanical and functional behaviors of alloys rely greatly on their crystal lattice structure and lattice-site occupation (LSO) of atoms. The detailed LSO of added alloying elements in a crystalline phase can only be determined through the Rietveld refinement by fitting a theoretical line profile to experimental X-ray or neutron diffraction data or constructing the atomic pair distribution function in the real space. However, so far it is impossible to obtain the accurate information on the LSO of specified atoms with less difference in scattering factor between the alloying element and fundamental constitutive elements. Here we present a new method for determining the LSO through the change in lattice parameters and phase transition behavior under hydrostatic pressure by in-situ XRD, in comparison with that obtained by the first-principles calculations considering different LSOs of atoms. This method is successfully demonstrated through the high pressure XRD experiments of a NiCoMnIn magnetic-field-driven alloy.

12:20 PM Invited

In situ Neutron Diffraction Studies of Phase Transformations in Shape Memory Alloys: Raj Vaidyanathan¹; ¹UCF

We report on in situ neutron diffraction measurements performed on NiTi-based shape memory alloys during selected combinations of heating, cooling and mechanical loading at Los Alamos National Laboratory. The choice of alloy systems is motivated by the temperature range at which they exhibit phase transformations that result in the shape memory effect - from below room temperature for NiTiFe alloys and near room temperature for NiTi alloys to above room temperature for NiTiPd alloys. Micromechanical and microstructural changes, i.e., texture, strain and phase volume fraction evolution were quantified for the cubic B2 to trigonal R to monoclinic B19' phase transformations in NiTiFe, the cubic B2 to orthorhombic B19 phase transformation in NiTi and the cubic B2 to orthorhombic B19 phase transformation in NiTiPd. The implications of these results for engineering shape memory alloys with useful ternary and quaternary elemental additions for aerospace applications is presented.

12:40 PM Invited

Temperature Dependence of Diffuse Scattering in PZN: Darren Goossens¹; Ross Whitfield¹; T. Welberry¹; ¹Australian National University

Structural disorder appears to relate to the useful physical properties of ferroelectrics and relaxors. One such material is PZN, $PbZn_{1/3}Nb_{2/3}O3$. To explore what aspects of the disorder are specific to the polarised state, the temperature dependence of diffuse scattering in PZN has been investigated. Data were collected using both neutron and X-ray single crystal experiments in a range of temperatures from 100K to 500K. It has been found that some features, like the diffuse scattering from the B-site ordering, remain unchanged with change of temperature in terms of both intensity and peak shape. However, other diffuse scattering features evolve with T, for example the size-effect scattering around the Bragg peaks. The size-effect becomes less pronounced with increasing temperature, with the diffuse rods caused by the planer domains change only slightly with temperature.

Pb-Free Solders and Other Materials for Emerging Interconnect and Packaging Technologies: Alloy and Microstructure Development

Sponsored by: The Minerals, Metals and Materials Society, TMS Electronic, Magnetic, and Photonic Materials Division, TMS: Electronic Packaging and Interconnection Materials Committee *Program Organizers*: Indranath Dutta, Washington State University; Darrel Frear, Freescale Semiconductor; Sung Kang, IBM; Eric Cotts, SUNY Binghamton; Laura Turbini, Research in Motion; Rajen Sidhu, Intel Corporation; John Osenbach, LSI Corporation; Albert Wu, National Central Univ, Taiwan; Tae-Kyu Lee, Cisco Systems

| Tuesday AM | Room: 7B |
|---------------|-------------------------------|
| March 1, 2011 | Location: San Diego Conv. Ctr |

Session Chairs: Darrel Frear, Freescale Semiconductor; Thomas Bieler, Michigan State University

8:30 AM Invited

Structure and Transformation in Sn-Rich Sn-In Solders: John Morris¹; Kyu-Oh Lee²; Fay Hua²; ¹University of California Berkeley; ²Intel Corporation

Of the Pb-free solders, Sn-rich InSn is unusually interesting in its structural and mechanical properties. The phases found for Sn-rich compositions include the a (diamond) and β (tetragonal) structures of pure Sn, and the \Box (hexagonal) structure of InSn. The β -Sn structure is notable for its complexity, which complicates the properties of all Sn-rich solders. The \Box -InSn structure is notable for its simplicity; in ambient it is a solid solution rather than an ordered compound, and is one of few materials that crystallize in a simple hexagonal structure. Surprisingly, the β - and \Box -structures of InSn have simple crystallographic connections, which not only facilitate transformation between them, but also permit martensitic transformation on cooling or under load. Here we describe the crystallographic relations and explore their influence on the microstructure and properties of Sn(7-13) In solders. Interestingly, transformation-induced plasticity (TRIP) occurs under appropriate conditions, including the first documented example of TRIP-mediated creep.

8:55 AM Invited

Optimization of Pb-Free Solder Joint Reliability from Metallurgical Perspective: *Kejun Zeng*¹; ¹Texas Instruments Inc.

Electronic packages with NEMI recommended Sn3.9Ag0.6Cu solder joints have shown poor performance in BLR tests. To improve package performance in board level drop test, a low Ag content of SnAgCu solder is preferred. On the other hand, the resistance of SnAgCu solder to thermal fatigue is dependant on the Ag content. Packages with low Ag content of SnAgCu solder have poor performance in thermal cycling test. In order for SnAgCu solder joints to perform well in both drop and thermal cycling tests, the key is to have better interfacial reliability. We will discuss how to optimize the Pb-free solder joint reliability by considering the effects of both solder alloys and surface materials on the metal pads. We will demonstrate that it is possible to keep a high content of Ag in the solder to get high resistance to thermal fatigue while the drop performance of the joints is not compromised.

9:20 AM Invited

On the Driving Force for Massive Spalling in Solder Systems: W. M. Chen¹; *C. Robert Kao*¹; ¹National Taiwan University

To identify the driving force for the massive spalling phenomenon, welldesigned experiments were carried out in this study. Copper-doped solder was reacted with Ni to form the Sn-0.6Cu/(Cu,Ni)6Sn5/Ni structure first. The original Sn-0.6Cu solder was then removed and replaced with Sn-0.3Cu, or with fresh Sn-0.6Cu. The swapping of solder to Sn-0.3Cu caused the massive spalling of (Cu,Ni)6Sn5. Without this swapping or in the case of swapping to fresh Sn-0.6Cu, the massive spalling did not occur. The results of this study unequivocally proved that the massive spalling reported in literature was caused by a driving force of pure thermodynamics in nature.

9:45 AM Invited

A Study of the Factors Affecting the ß to a Transition in Solder Alloys: *Christopher Hunt*¹; Davide Di Maio¹; ¹National Physical Laboratory

With introduction of lead-free alloys into harsh conditions, there is some concern that these alloys will undergo the catastrophic solid state β to a transformation. In this transformation, with an equilibrium temperature of 13°C, tin becomes a semiconductor and there is a 27% increase in volume. In this paper techniques that have been developed to monitor the transformation rate based on a time lapse technique and the application of electrical continuity measurements in the bulk tin. A technique for initiating the transformation based on the use of a seed is described. In this paper, various factors affecting the transformation rate were investigated: stress, alloy composition, and nucleating seed. Of very significant interest is the effect of flux and its residues, and that of oxides in influencing the transformation rate.

10:10 AM

Effect of Solidification Temperature on the Microstructure of SnAgCu Solder Joints: Babak Arfaei¹; Eric Cotts¹; ¹Binghamton University

Variations in the microstructure of SnAgCu solder joints resulting from changes in solidification temperatures are examined. Sample and pad size, thermal history and substrate finish all may affect the solidification temperature. Solder joint Sn grain morphology, and intermetallic precipitate size and number, are directly affected by solidification temperature; thus solder joint mechanical properties are strongly influenced by this parameter. The Sn grain morphologies and precipitate microstructures were examined in near eutectic SnAgCu solder joints solidified at undercoolings between ten and eighty degrees. Larger solder joints (e.g. ball grid array, 500 micron diameter) generally solidify at higher temperatures and show a beach ball twinning structure, however through the control of thermal history, the solidification temperature of such large solder joints was reduced thirty degrees. An interlaced twining morphology are reported. Effects on creep and cyclic failure times of SnAgCu solder joints are discussed.

10:30 AM Break

10:40 AM

Effect of the Ternary Quasiperitectic Reaction on the Formation of Microstructure during Freezing of Ternary Pb-Free Solder Alloys: *Doug Perovic*¹; Leonid Snugovsky¹; Polina Snugovsky²; John Rutter¹; ¹University of Toronto; ²Celestica Inc.

The banning of Pb as a toxic material has led to the introduction of ternary solder alloys, such as the SAC series, to replace the traditional Pb-Sn eutectic solder. The addition of a third element to the solder alloy brings with it the possibility of the introduction of ternary solidification reactions, in addition to the usual binary reactions, during freezing of the solder. Such a ternary reaction, known as a quasiperitectic reaction, has been observed in the phase diagrams of certain Pb-free systems. In particular, these are alloy systems in which the phenomenon of "spalling" occurs in joints made with the associated solder alloys. It is the purpose of this paper to show the effect of the ternary quasiperitectic reaction on the formation of Sn-Ag-Cu alloys and Sn-Zn-Cu Alloy on Cu/Ni substrate will be presented.

11:00 AM

Development of SAC3595 Solders Alloyed with Al, Mn, or Zn for High Reliability: *Adam Boesenberg*¹; Iver Anderson²; Joel Harringa²; ¹Iowa State University; ²Ames Laboratory

As a robust replacement for leaded solders that can become environmental toxins, a family of near-eutectic Pb-free solder alloys based on Sn-Ag-Cu (SAC) compositions have shown promise worldwide for electronic assembly. However, reliability issues in divergent assembly methods and aggressive operating environments have arisen. Micro-alloying of Sn-3.5Ag-0.95Cu (wt.%) solder with Al, Mn, Zn was developed for reliable heterogeneous nucleation control in solder joint solidification to address drop impact and



thermal cycling issues. Cu substrate solderability of these SAC3595+X alloys was investigated at concentrations between 0.01-0.25wt% using globule wetting balance tests to quantify any increased oxidation during reflow. Composition dependence of these X additions also was explored in simplified Cu joints by differential scanning calorimetry, microstructure analysis, and X-ray diffraction to determine coupling between undercooling and joint microstructure development on single and multiple reflow cycles. Supported by Iowa State University Research Foundation and Nihon-Superior, Inc., through Ames Lab contract DE-AC02-07CH11358.

11:20 AM

Effect of Gold Content on the Microstructural Evolution of SAC305 Solder Joints under Isothermal Aging: *Mike Powers*¹; Jianbiao Pan²; Julie Silk¹; Patrick Hyland²; ¹Agilent Technologies; ²California Polytechnic State University

Au over Ni on Cu is a widely used printed circuit board (PCB) surface finish, under bump metallization and component lead metallization. It is generally accepted that less than 2-3 weight percent Au in Sn-Pb solder joints will preclude reliability issues associated with the formation of Au based intermetallic compounds. However, the critical limit for Au content in Pb-free solder joints is not well established. This paper investigates the microstructural evolution of SAC305 solder joints with varying Au content under isothermal aging. Three surface mount package platforms with different Au thicknesses on their component leads were soldered to PCB with two different Au thicknesses, in a realistic manufacturing setting. The assembled boards were divided into three groups: one without thermal treatment, one isothermally aged at 125\176 C for 30 days and the third aged at 125\176 C for 56 days. The resulting microstructure of the test groups is compared.

11:40 AM

Rare Earths Addition Effect on Microstructure and Intermetallic Layer Growth Kinetics on Lead-Free Solder Sn-Ag-Bi: *Miguel Neri*¹; Alberto Martinez-Villafañe¹; Caleb Carreño¹; ¹CIMAV, S.C.

Rare earths were added to Sn-Ag-Bi alloy in order to determine its effect on microstructure and Tin-Copper intermetallic layer growth kinetics. There were 3 different sample alloys prepared: Sn-Ag-Bi, Sn-Ag-Bi + Nd, and Sn-Ag-Bi + Pr. These alloys were applied to an electrolytic copper substrate and were given ageing heat treatments at temperatures between 50 to 150 °C at different times of permanence (0, 50, 150, 250 and 500 hours), in order to determine the Tin-Copper intermetallic layer growth kinetics and microstructure evolution on the soldered joints. These samples were prepared by metallographic techniques in order to measure the intermetallic layer thickness, and observe the microstructure thickening depending on temperature and time of ageing heat treatment, using optical microscopy, scanning electron microscopy, and EDS. The intermetallic layer thickness grew by increasing temperature and ageing treatment time, while microstructure was thickening with increasing temperature and ageing treatment time.

12:00 PM

Magnetically-Driven Three-Dimensional Manipulation and Inductive Heating of Magnetic-Dispersion Containing Lead-Free Solders: *Ainissa Ramirez*¹; Xu Huang¹; Joshua Calabro¹; Brian Lewis¹; ¹Yale University

Fundamental to the development of three-dimensional microfabrication is a material that enables vertical geometries. Here we show lead-free solders containing iron dispersions that can be remotely manipulated by magnetic fields to create vertical geometries and thus enable three-dimensional fabrication. These iron dispersions enhance the mechanical properties needed for strong, reliable interconnects, without significantly altering the electrical properties. Additionally, these iron dispersions act as susceptors during electromagnetic induction heating conditions, allowing the rapid melting of these novel materials at lower temperatures than those usually reported for conventional solder. Such capabilities have potential applications in the assembly of temperature-sensitive devices by localizing high temperatures and by reducing the temperature excursions associated with other lead-free solders.

Physical and Mechanical Metallurgy of Shape Memory Alloys for Actuator Applications: Characterization of Shape Memory Alloys: Microstructural Transformation

Sponsored by: The Minerals, Metals and Materials Society Program Organizers: S. Raj, NASA Glenn Research Center; Raj Vaidyanathan, University of Central Florida; Ibrahim Karaman, Texas A&M University; Ronald Noebe, NASA Glenn Research Center; Frederick Calkins, The Boeing Company; Shuichi Miyazaki, Institute of Materials Science, University of Tsukuba

| Tuesday AM | Room: 11B |
|---------------|-------------------------------|
| March 1, 2011 | Location: San Diego Conv. Ctr |

Session Chairs: Ibrahim Karaman, Texas A&M University; Sai Raj, NASA Glenn Research Center

8:30 AM Introductory Comments

8:35 AM Plenary

Hysteresis, Reversibility, and Shape Memory: *Richard James*¹; Vijay Srivastava¹; Yintao Song¹; ¹University of Minnesota

We present some recent measurements of hysteresis, in materials undergoing first order phase transformations, that resulted from a systematic program of tuning of the lattice parameters by changing composition. The lattice parameters were tuned so that a certain non generic condition of compatibility between phases was satisfied. The tuned alloys exhibit thermal hysteresis as low as 2 C by careful bulk measurements, and in all cases less than 6 C. The procedures are effective for broad classes of hard materials undergoing diffusionless transformations, including metals and oxides. Studies of reversibility show improved stability of the transformation, measured by the migration of the hysteresis loop under repeated cycling. Some examples of this tuning in Heusler systems show fascinating convergence of shape memory and magnetism. Using these tuned Heuslers, we demonstrate new devices that 1) convert heat directly into electricity, 2) convert heat directly into kinetic energy.

9:05 AM Invited

Effects of Surface Modifications on Twinning Stress and the Stability of Twin Microstructures of Magnetic Shape-Memory Alloys: Peter Müllner¹; Markus Chmielus²; Cassie Witherspoon¹; Rainer Schneider³; Kari Ullakko¹; ¹Boise State University; ²Boise State University and Helmholtz Centre Berlin for Materials and Energy; ³Beuth Hochschule für Technik and VDI/VDE Innovation and Technik GmbH

Twinning is the primary deformation mechanism in magnetic shapememory alloys (MSMA). Inclusions, precipitates and defects hinder or even prevent twin boundary motion in the bulk of MSMA single crystals. We study the effect of surface damage on the mechanical properties and twin structure of Ni-Mn-Ga single crystals. Surface damage was produced with spark erosion, ion implantation, shot blasting and abrasive wearing. The degree of surface modification was characterized with x-ray diffraction where the broadening of Bragg reflections and of rocking curves was taken as a measure of localized elastic and plastic strains. Surface deformation stabilizes a dense twin-microstructure and prevents twins form coarsening. The density of twins increases with increasing degree of deformation. With increasing surface deformation and twin density, twinning stress and hardening rate increase. The stabilization of a dense twin microstructure prevents damage accumulation in high-cycle magneto-mechanical actuation and is critical for technological applications of MSMA.

9:25 AM Invited

In-Situ Neutron Scattering Studies of Shape Memory Alloy Actuator Materials: *Donald Brown*¹; Bjorn Clausen¹; Thomas Sisneros¹; ¹Los Alamos National Lab

Neutrons are uniquely suited to probe the crystallographic response of materials to external stimuli because of their high penetration, which allows

them to sample the bulk of the material.. This is important for shape memory alloys (SMA's) as surface grains might be expected to behave differently from those in the bulk due to the different constraints. The SMARTS neutron diffractometer at the Lujan Center was built on the philosophy of studying materials under their operating conditions, and this philosophy has been aggressively applied to SMA's. The design of SMARTS allows for determination of the phase fraction, internal stress, and, to a degree, the texture evolution of SMA's under various conditions including tensile, compressive, or cyclic loading while simultaneously controlling temperature and/or magnetic field. This talk will highlight these capabilities, which are available to general users, by describing several examples of recent research on SMA's under multiple environmental conditions.

9:45 AM Invited

Nanocrystalline Shape Memory Alloys: *Thomas Waitz*¹; Wolfgang Pranger²; Clemens Mangler¹; Martin Peterlechner¹; Gerd Steiner¹; Thomas Antretter³; Franz Dieter Fischer³; Peter Müllner⁴; ¹University of Vienna; ²Materials Center Leoben Forschung GmbH; ³Montanuniversität Leoben; ⁴Boise State University

Martensitic phase transformations can be significantly affected by a grain size and specimen size on the micro- and nanoscale. Bulk nanocrystalline shape memory alloys for actuator applications can show large recovery stresses. Thin films and small pillars are promising candidates for actuators for micro- and nanoelectromechanical systems. In the present work, the effect of a grain size at the nanoscale on the martensitic phase transformation is studied using bulk materials processed by severe plastic deformation that include NiTi and high temperature NiTiHf shape memory alloys as well as NiMnGa and high temperature NiFeGaCo ferromagnetic shape memory alloys. Grain refinement causes a suppression of the martensitic phase transformation that can occur in burst like events. Considering a size dependent energy barrier opposing the transformation, the phase stability and unique martensitic morphology of the nanograins is explained.

10:05 AM Break

10:15 AM Invited

New Microscopic Tools Applied for the Study of SMA: *Dominique Schryvers*¹; ¹University of Antwerp

In recent years several new electron microscopic tools have become available for the study of the crystallography and microstructure of functional materials. Atomic crystal structures can be refined with new optimization procedures including dynamic diffraction allowing focusing on nanoscale structures such as metastable Ni4Ti3 precipitates in Ni-Ti SMA. Quantitative analysis of atomic resolution images and spectroscopic data yields three-dimensional views of concentration gradients and strain fields in the matrix surrounding such precipitates while tomographic slice-and-view techniques result in three-dimensional shape and distribution functions for the precipitates. More conventional techniques provide insight in the role of lattice parameter relations between parent and product for the lowering of the hysteresis and energy dissipation and the corresponding twin configurations. Site-specific sample preparation with FIB provides new ways for the study of surface and interior of micro-wires treated by a variety of processes. Examples of these and other applications will be presented.

10:35 AM Invited

Modulated Martensite: Why it Forms and Why it Deforms Easily: Sebastian Fähler¹; ¹IFW Dresden

The high strain up to 10% in magnetic shape memory alloys is only observed in martensitic phases exhibiting modulations. In order to understand the origin of modulated martensites and consequences for the twin boundary mobility we analyze epitaxial Ni-Mn-Ga films as a model system. In agreement with the concept of adaptive martensite modulations are induced by the geometrical constraints at the habit plane. Hence modulated martensite is build from nanotwinned tetragonal martensite. We observe coarsening of these twin variants by doubling of periodicity in discrete steps from the atomic to the micrometer scale. When the activation energy for this process is too high, a second hierarchy of mesoscopic twin boundaries forms.

In contrast to the common, atomically sharp twin boundaries, the complex unit cell of an adaptive phase results in diffuse, mesoscopic twin boundaries. The extraordinarily high mobility of mesoscopic twin boundaries can be attributed to their broad pinning potential

10:55 AM Invited

Transformation Characteristics of Ni-Mn-Ga High Temperature Shape Memory Alloys: Ruben Santamarta¹; *Jaume Pons*¹; Catalina Picornell¹; Eduard Cesari¹; Joan Font²; Joaquim Muntasell²; Ibrahim Karaman³; Dimitris Lagoudas³; ¹University of the Balearic Islands; ²Polytechnical University of Catalonia; ³Texas A&M University

The martensitic transformation (MT) characteristics of several Ni-Mn-Ga alloys with high transformation temperatures (TTs) will be presented. The studied alloys with the highest TTs, ~750K, are unstable; the MT is degraded after a few cycles by intense precipitation of \947' phase or lath-shaped particles similar to the Ni5Al3 phase. Alloys with Ni content close to stoichiometry show an excellent thermal stability upon ageing. For instance, the alloys Ni₅₁₂Mn_{31.1}Ga_{17.7} (TT~485K) and Ni₅₁₂Mn_{33.1}Ga_{15.7} (TT~575K) aged at 770 K for years do not experience any significant change in the TTs. In other alloys, like Ni₅₅₂Mn_{29.1}Ga_{15.7} (TT~665K)and Ni_{58.3}Mn_{15.9}Ga_{25.8} (TT~525K), precipitation of lath-shaped or \947' phases take place after several days at 670K or 770K, respectively. The superelasticity and shape memory characteristics will also be presented both in single phase alloys and in alloys with controlled precipitation of second phases introduced to improve the ductility. Finally, the effects of Cu additions will be discussed.

11:15 AM

Microstructural Instability in NiTi Based Shape Memory Alloy Actuators: Nicholas Jones¹; David Dye¹; ¹Imperial College London

NiTi based shape memory alloy (SMA) actuators offer the potential for simple dynamic components that can reduce aerospace emissions. For these components to be structurally useful, they require a significant bias load. However, despite fabrication of successful demonstrator components, the cyclic instability of the martensitic transformation continues to prevent this technology from transferring into full scale production. The addition of copper can alter the transformation sequence including an orthorhombic martensite, which seems to decrease the rate of cyclic destabilisation. Using synchrotron X-ray diffraction we have studied the behaviour of both a near equiatomic and a copper containing NiTi SMA over several thermal cycles under different uniaxial loads. The martensitic microstructure is found to evolve during cycling and an accumulation of strain is observed, which appears to be driven by accommodation of the applied load. The observed effects are discussed, relating the transformation fundamentals to the instability of the material.

11:30 AM

The R Phase Transformation in Rapidly Solidified Ti-47.3Ni(at%) Alloy Ribbons: *Tae-hyun Nam*¹; Hyo-jung Mun¹; Yinong Liu²; Hong Yang²; Yeonwook Kim³; ¹Gyeongsang National University; ²University of Western Australia; ³Keimyung University

In the present study, Ti-47.3Ni(at%) alloy ribbons with a thickness of $32\pm1\mu$ m were prepared by melt spinning and then microstructures and transformation behavior were investigated by means of transmission electron microscopy(TEM), X-ray diffraction(XRD), electrical resistivity(ER) measurement and differential scanning calorimetry(DSC). Nano-sized Ti2Ni particles with a specific orientation relationship with matrix were observed in as-spun ribbons. The B2-R-B19' transformation occurred in as-spun ribbons and moreover the B2-R transformation was separated clearly from the R-B19' transformation. The two-stage B2-R-B19' transformation behavior was still preserved after annealing the as-spun ribbons at the temperature range from 673 K to 1223 K for 3.6 ks. When the annealing temperature was higher than 973 K, the B2-R and the R-B19' transformations were not separated clearly, which was ascribed to the fact that nano-sized Ti2Ni particles grew and lost the specific orientation relationship with matrix by high temperature annealing.



11:45 AM

Characterization of Nanoscale Precipitates in a Ni-Rich Ni-29.7Ti-20Hf (at.%) High Temperature Shape Memory Alloy: Taisuke Sasaki¹; B. C. Hornbuckle¹; Glen Bigelow²; Ronald Noebe²; Mark Weaver¹; *Gregory Thompson*¹; ¹University of Alabama; ²NASA Glenn Research Center

Though Ni-rich Ni-Ti alloys have superior dimensional stability compared to Ti-rich compositions, after several thermomechanical cycles, retained strain can occur. The ternary addition of Hf has been observed to reduce this effect and has the added benefit of raising the transformation temperatures. The Hf addition has been shown to form nanoscale precipitates; however, little is understood with respect to the microstructure of this fine phase. In this work, we investigated the effect of aging on the transformation temperature and microstructure of an extruded Ni-29.7Ti-20Hf (at.%) alloy. The samples were solution treated at 1050°C for 0.5 hr followed by aging at 550°C for various times. Unlike the recent P-phase reported in NiTiPt, the NiTiHf alloys exhibit a different crystal structure. Transmission electron microscopy and atom probe tomography have been performed to quantify the structure.

12:00 PM End of Session

Polycrystal Modelling with Experimental Integration: A Symposium Honoring Carlos Tome: Hexagonal Materials and Twinning

Sponsored by: The Minerals, Metals and Materials Society, TMS Structural Materials Division, TMS Materials Processing and Manufacturing Division, ASM-MSCTS: Texture and Anisotropy Committee, TMS/ASM: Mechanical Behavior of Materials Committee, TMS/ASM: Computational Materials Science and Engineering Committee

Program Organizers: Ricardo Lebensohn, Los Alamos National Laboratory; Sean Agnew, University of Virginia; Mark Daymond, Queens's University

| Tuesday AM | Room: 6C |
|---------------|-------------------------------|
| March 1, 2011 | Location: San Diego Conv. Ctr |

Session Chairs: Sean Agnew, University of Virginia; Jian Wang, Los Alamos National Laboratory; Irene Beyerlein, Los Alamos National Laboratory

8:30 AM Invited

Role of Stress Fluctuations in the Nucleation of Deformation Twinning in Hcp Metals: *Irene Beyerlein*¹; Anand Kanjarla¹; Carlos Tome¹; Ricardo Lebensohn¹; ¹Los Alamos National Laboratory

We present an experimental and theoretical approach for understanding the statistical nature of deformation twinning in hexagonal close packed (hcp) polycrystals. We first describe statistical studies of {1012} twinning in high-purity Zr and Mg that correlate deformation twinning with certain microstuctural features, such as grain size, grain orientation, and grain boundary misorientation angle. To determine the impact of twinning on aggregate deformation behavior, these metallographic results are combined with a multi-scale constitutive model for hcp metals. The predictions indicate that the amplitude and variation in the stress fluctuations between the grain interior and grain boundary play a crucial role. In light of this, we consider two models, the second-order (SO) VPSC approach (Lebensohn et al., 2007) and Fast Fourier Transform method (FFT) (Lebensohn et al., 2004), both of which account for grain orientation in the calculation of stress states. We report on how the modeling results compare for various cases.

8:55 AM Invited

Orthotropic Strain Rate Potential for Hexagonal Metals: *Oana Cazacu*¹; Ioan Ionescu²; ¹University of Florida; ²LPMTM, University Paris 13

Existing strain rate potentials are applicable only to materials with cubic crystal structure. In this paper, an anisotropic strain rate potential for hexagonal metals is developed. First, an exact dual to the isotropic form of Cazacu et al. (2006) stress potential is derived. Next, this isotropic strain

rate potential is extended such as to account for orthotropic symmetry. The ability of the developed anisotropic strain rate potential to describe the complex behavior of hexagonal metals is demonstrated by comparison with experimental data on titanium.

9:20 AM

Modeling Deformation Twinning with a Binary-Tree Based Polycrystal Model: Sivasambu Mahesh¹; ¹IIT Kanpur

A novel polycrystal model that explicitly accounts for intergranular interactions is described. In this model, the polycrystal is regarded as a binary tree. Leaf nodes of the binary tree represent the grains and successively higher nodes represent increasingly larger sub-aggregates of grains culminating with the root of the tree, which represents the entire polycrystalline aggregate. Traction and velocity continuity conditions are imposed across the interface between the children of each non-leaf node in the binary tree. The present model is employed to model deformation twinning of hcp magnesium and zirconium. Texture predictions from the present model are compared with those obtained using the VPSC model by Dr. Tome' and co-workers, and with experimental observations.

9:40 AM Break

9:55 AM Invited

Effect of Texture on Anisotropic Creep of Zr-2.5Nb Tubes: *Rick Holt*¹; W. Li¹; S. Tracy¹; Ricardo Lebensohn²; ¹Queen's University; ²Los Alamos National Laboratory

We have investigated the anisotropy of thermal creep of cold-worked Zr-2.5Nb tubes for a range of textures and stress states. The tests were performed on internally pressurized thin-wall standard capsules at a stress of 300MPa at 350C. The stress state was modified by applying a load to the ends of the caspsules to give a stress ratio of 0.25<sigma_hoop/sigma_axial<0.75. The tests showed an obvious correlation of creep anisotropy with the texture. A self-consistent visco-plastic polycrystalline model (SELFPOLY) based solely upon crystallographic texture showed a poor correlation with the experimental results. A modified self-consistent model is introduced to take into account different pre-existing anisotropic dislocation distributions from cold-work. The anisotropic dislocation structures are calculated using an elasto-plastic self consistent model (EPSC). Much better agreement with the experimental creep anisotropy is found, indicating that individual dislocation distributions in grains with different orientations are important in controlling the creep anisotropy.

10:20 AM Invited

Atomistic Modeling of Deformation Twinning Mechanisms in Hcp Metals: Jian Wang¹; Irene Beyerlein¹; Carlos Tome¹; ¹LANL

Twin propagation and growth are responsible for the hardening and texture evolution characteristic of Mg alloys subjected to plastic deformation. Propagation, however, does not take place unless it is preceded by twin nucleation. As a consequence, understanding nucleation and accounting for it in material models is a prerequisite for understanding the constitutive response of Mg alloys. Experimental observations indicate that twin formation tends to form in suitably oriented grains, and some studies report a positive grain size effect, wherein twinning appears to form more easily in larger grains. In this talk, some fundamental issues, such as grain boundary structures, twinning dislocations, and nucleation and propagation mechanisms of twins, are discussed. Finally, we propose a comprehensive approach for understanding deformation twinning from atomic-scale to micro-scale. Such approach relies on, and relates, molecular dynamics (MD) simulations, EBSD, and a nucleation model.

10:45 AM

Grain Size and Neighbor Grain Effects on Deformation Twinning: *Rodney McCabe*¹; Irene Beyerlein¹; Carlos Tome¹; ¹Los Alamos National Laboratory

Whether or not twins nucleate and grow in a grain depends on several microstructural characteristics of the grain and it neighbors. Grain orientation is a good predictor of the probability of twinning. However, not all grains of similar orientation exhibit twins, and a considerable fraction of

12:05 PM

observed twins are not of the twin variant with the highest resolved shear stress based on the orientation of the grain and the bulk stress state of the material. Here we examine the role that grain size and neighbor grain attributes (neighbor orientation, grain boundary misorientation) play in this statistical nature of twinning. We examine these effects using large numbers of twin statistics developed using electron backscatter diffraction (EBSD) for {1012} twinning in magnesium, {1012} and {1122} twinning in zirconium, and {130} twinning in uranium.

11:05 AM

Texture Evolution during Themomechanical Processing of Zircaloy-4: *Christabel Evans*¹; David Dye¹; Trevor Lindley¹; David Rugg²; Nicholas Jones¹; ¹Imperial College London; ²Rolls-Royce plc.

Zirconium alloys are widely used for nuclear reactor core internals due to their low neutron absorption cross section and good corrosion resistance. Zircaloy-4 is an alpha-Zr alloy which deforms at room temperature by both slip and twinning. The textures used are engineered so as to optimize service performance. In order to understand how texture can evolve in Zr under a variety of conditions, in situ synchrotron X-ray diffraction compression and tension tests have been performed on rolled Zry-4 under varying strain rates and temperatures up to 550 °C, along with post-hoc EBSD, to understand how the deformation mechanisms change from the texture evolution. The results are interpreted with the aid of Tome's now-famous VPSC model.

11:25 AM

Crystal Plasticity Based Finite Element Simulations of Deformation in AM30 Magnesium Alloy Under Complex Strain Paths: Adel Izadbakhsh¹; *Kaan Inal*¹; Raja Mishra²; ¹University of Waterloo; ²General Motors R&D Center

Deformation of AM30 magnesium alloy subjected to complex strain paths has been simulated using a Crystal Plasticity based Finite Element Method (CPFEM). A new crystal plasticity framework that satisfies equilibrium and compatibility requirements throughout the polycrystal aggregate and incorporates the interaction between twinning and slip through the kinematics of deformation has been developed. The model includes contraction and double twinning mechanisms in addition to basal and non-basal slip and extension twinning. A rate-dependent crystal plasticity constitutive law calibrated with uniaxial tension and compression data at room temperature and at 2000C is implemented in a User defined MATerial subroutine (UMAT) in LS-DYNA. The deformation pattern of AM30 tubes, especially the initiation and propagation of localization during the "Ring Hoop Tension Test", simple shear and pure bending has been simulated. Simulations show that neglecting contraction and double twinning can significantly delay/defer the initiation of localized deformation and its propagation.

11:45 AM

Experimental and Simulation Studies on the Evolution of Rolling Texture in a Two Phase Titanium Alloy: *Nilesh Gurao*¹; Satyam Suwas¹; ¹Indian Instituteof Science, Bangalore

The evolution of deformation texture and microstructure during rolling of a two phase (a+ β) titanium alloy with a nominal composition Ti-13Nb-13Zr has been studied. Two different morphologies, namely, colony and equiaxed, were generated by suitable heat treatments prior to rolling. Microstructural evolution was examined using Electron Back Scatter Diffraction (EBSD) and textures were measured by X-ray diffraction. A characteristic texture evolution was noted in both the HCP a and the BCC β phase irrespective of the different initial morphology. The evolution of higher intragranular misorientations in the β phase indicates that the softer β phase carries most of the strain. Texture evolution was simulated using viscoplastic self-consistent (VPSC) model. The experimental textures were successfully reproduced using VPSC simulations that incorporated the different initial morphologies of both the phases. Hardening Mechanisms upon Profuse Twinning in Pure Magnesium: *Andrew Oppedal*¹; Haitham El Kadiri¹; Carlos Tomé²; James Baird¹; Sven Vogel²; George Kaschner²; Mark Horstemeyer¹; ¹Mississippi State University; ²Los Alamos National Laboratory

Textured hexagonal close packed double-lattice structures show stronger anisotropy than textured single-lattice structures. The reason lies behind the necessity to activate glide twinning and hard slip dislocation modes. Although the mechanisms behind activation of dislocations with nonbasal Burgers vectors are still not fundamentally understood, the effect of twinning on hardening presents the most substantial challenge to polycrystal plasticity modelers. The origin of the increasing strain hardening rate regime (Regime II) upon profuse twinning is still not fundamentally clear. Previous successful attempts to fit stress-strain behavior based on a Hall-Petch effect by twin segmentation led to discrepancies in predicting intermediate textures and/or twin volume fraction evolution. A recent dislocation-based hardening rule incorporated into the Visco-Plastic Self-Consistent (VPSC) model allows slip and twinning to be physically coupled in the simulations. In this paper, we investigate hardening mechanisms in pure magnesium and apply a dislocation based formalism to model anisotropy.

12:25 PM

Micromechanical Model of Metals and Alloys of Low Symmetry Deforming by Slip and Twinning: *Katarzyna Kowalczyk-Gajewska*¹; ¹Institute of Fundamental Technological Research, Warsaw

The micromechanical model of finite plastic deformations of polycrystalline materials of low symmetry, characterized by high specific strength, is presented. As concerns texture evolution the model accounts for appearance of new twin related orientations using a new reorientation scheme called Probabilistic Twin Volume Consistent scheme. It takes into account the history of the deformation process and maintains the volume fraction of reoriented grains at a level consistent with the shear activity of twins contributing to the deformation. Within the proposed framework the hardening rule describing slip-twin interactions is developed. Evolution of critical shear stress for slip due to twin activity is described by the rule accounting for geometrical effects of twin boundaries in reducing main free path distance for dislocations. It also takes into account the lamellar substructure of single grain which evolves during twinning. Model predictions are verified for titanium alluminide intermetallic of near gamma microstructure and magnesium.

Processing and Properties of Powder-Based Materials: Current-Activated and Conventional Sintering

Sponsored by: The Minerals, Metals and Materials Society, TMS Materials Processing and Manufacturing Division, TMS: Powder Materials Committee

Program Organizers: K. Morsi, San Diego State University; Ahmed El-Desouky, San Diego State University

| Tuesday AM | Room: 33A |
|---------------|-------------------------------|
| March 1, 2011 | Location: San Diego Conv. Ctr |

Session Chair: Javier Garay, University of California-Riverside

8:30 AM Introductory Comments

8:35 AM Keynote

Coarsening Models Applicable to Sintering: *Randall German*¹; ¹San Diego State University

Treatments of sintering are analyzed to show grain size is determined by the microstructure contiguity during densification. Grain size determines the sintering rate. Thus, not only do properties pivot around grain size, but the rate of sintering traces to control of the interfaces during sintering. With nanoscale powders there is more demand for controlled coarsening during



sintering. This treatment shows a simple model that links grain growth to interfacial features - pores, liquids, dispersoids, or other second phases. Since sintering converges toward a self-similar grain shape and grain size distribution, most of the relations are fairly simple. Then grain growth rates are predicted based on the faction of each interface and the transport events associated with the evolving solid-liquid-vapor microstructure. Reviews of data from classic experiments to recent nanoscale SPS experiments are used to illustrate the model. Means to densify without extensive coarsening are extracted from the model.

9:05 AM

Challenges in the Scalability of Field Assisted Sintering: *Chris Haines*¹; Darold Martin¹; Deepak Kapoor¹; William Bradbury²; Eugene Olevsky²; ¹US Army ARDEC; ²San Diego State University

Field-Assisted Sintering Technology (FAST) aka Spark Plasma Sintering (SPS) is a revolutionary, game-changing technology which provides the ability to consolidate materials to full density in minutes, as opposed to hours with conventional sintering techniques. To date, most research has reported on sample sizes in the range of a few centimeters to a few inches. In order for the technology to mature as a viable manufacturing technology in the industrial base, significant scale-up is required. Scaling of such a highly energetic sintering technology is not trivial and presents many challenges. We have observed, both experimentally and in our modeling, a significant dependence on factors such as sample dimensions, geometry, and die design on the temperature and current distribution during sintering. These effects can subsequently be seen in the resulting microstructure of the sintered specimens. Proposed solutions to these challenges will be discussed.

9:25 AM

Cryomilled Commercially Pure Ti Consolidated via Spark Plasma Sintering: Osman Ertorer¹; Troy Topping¹; Ying Li¹; Wes Moss²; Enrique Lavernia¹; ¹University of California - Davis; ²TRD

Cryomilled nanocrystalline CP-Ti powders were spark plasma sintered (SPS) using varied process parameters (i.e., heating rate, temperature, pressure, and dwell time) in order to study densification, microstructure, and mechanical behavior. Results were rationalized on the basis of the relevant literature and experimental results, and they reveal a strong dependence on SPS parameters. An interesting finding was that the measured high ductility was accompanied by a moderate strength (YS > 700 MPa, UTS > 840 MPa with elongation to failure values larger than 20%). The strain rate sensitivity of produced samples was also studied. The combinations of microstructure and mechanical response were attributed to the multi-step processing using various SPS parameters as well as to the presence of interstitial solutes introduced during cryomilling.

9:45 AM

Microstructural Characterization of Mechanically Alloyed Lanthana-Bearing Oxide Dispersion Strengthened Steels: *Somayeh Pasebani*¹; Indrajit Charit¹; Kerry Allahar²; Brian Jaques²; Darryl Butt²; James Cole³; ¹University of Idaho; ²Boise State University; ³Idaho National Laboratory

Oxide dispersion strengthened (ODS) alloys are being considered for advanced reactor applications due to their excellent creep and radiation damage resistance imparted primarily due to the presence of fine oxide particles. The objective of this study is to develop a new ODS alloy by mechanical alloying (MA) followed by spark plasma sintering (SPS). Different amounts (0-1 wt.%) of lanthanum oxide were mixed with a base alloy composition of Fe-14Cr-0.9Ti-0.3Mo (in wt.%) and processed via MA for different durations using the stainless steel milling media. Differential scanning calorimetry (DSC) was performed on the MA powders to study the kinetics of any phase transformation occurring. Further, detailed phase analysis was carried out using X-ray diffraction (XRD). Scanning electron microscopy (SEM) was also used to determine the particle size, shape and distribution. SPS will be used to produce the bulk ODS samples and characterized for microstructure and mechanical properties.

10:05 AM

Spark Plasma Sintering of Ultra-Fine Grained and Nanocrystalline WC Based Hard Metals: *Milan Dopita*¹; David Chmelik¹; Anton Salomon¹; C. Sriram²; Hans Seifert¹; ¹Technical University of Freiberg; ²National Institute of Technology Tiruchirappalli

Modern trends in the materials research emphasizing the increase of the materials serving life-time tend to the preparation of the materials with nanocrystalline microstructure as it has been shown that nanocrystalline hard metals have better mechanical properties in comparison to their course-grained counterparts. In our work we focused on sintering of the nanocrystalline WC based hard metals using the spark plasma sintering method. Two types of materials i) WC-Co composites and ii) binderless WC were studied. The main accent was focused on the study of individual sintering parameters (temperature, time and pressure) and their correlations with sintered specimens microstructure and mechanical properties. Sintered specimens were investigated using XRD, SEM/EBSD, TEM/HRTEM, hardness and fracture toughness measurements.We derived favourable conditions for sintering of fully dense nanocrystalline hard metals and proved that the specimens sintered using these conditions have significantly improved mechanical properties in comparison to classical course grained hard metals.

10:25 AM Break

10:35 AM

Preliminary Investigations in Current-Activated Tip-Based Sintering (CATS): Modeling and Experiments: *A. El-Desouky*¹; S.K. Kassegne¹; K.S. Moon¹; K. Morsi¹; ¹San Diego State University

Spark Plasma Sintering (SPS) has emerged as a process with unique advantages such as lower sintering temperatures and shorter holding times than conventional sintering, in addition to the production of materials with unique microstructures and properties. However, the process has been largely limited to the production of bulk materials with simple geometries on a relatively moderate size scale. In this presentation preliminary experimental and modeling results on novel current-activated tip-based sintering (CATS) powder compacts are presented. CATS enables the selective sintering of micro-scale (and potentially nano-scale) features using a moving or stationary (electrically conductive) tip configuration. Preliminary finite element modeling results on current and temperature distributions under typical CATS conditions is also presented, in addition to a discussion on the versatility and extended applications of this new process.

10:55 AM

The Role of Sintering Methods (HP & SPS) on Substructure and Its Correspondence on Creep Properties in Alumina Based Ceramic Materials: *Ebrahim Karamian*¹; Alain Bataille²; Ahmad Monshi³; Ehsan Mohamadi Zahrani⁴; ¹Isfahan University of Technology; ²UMET, Unité Matériaux et Transformations, UMR CNRS 8207, University of Lille Science and Technology; ³Department of Materials Engineering, Isfahan University of Technology; ⁴Department of Materials Engineering, University of British Columbia

Spark plasma sintering method (SPS) is more than a decade to be an interesting alternative to classical densification processes for ceramic materials. Owing to the advantage of rapid heating, the alumina ceramics obtained by SPS have a grain size and density comparable to those of HPed ones. This paper describes the effect of HP & SPS on substructure and its correspondence on creep properties in alumina based ceramic materials. Pure alumina(SM8,Baikowski) was densified SPS at 65 MPa (1200°C) and 45 MPa (1450 °C) by HP(hot pressing). The grain size of the HP alumina was more twice coarser than the grain size of SPS sample . The grain growth is more active during creep of SPS alumina (1300 °C, s =30 MPa) than of HP alumina.Generally,the fineness of SPS materials microstructure shall speed up all processes related to diffusion.So, creep resistance shall be decreased.

11:15 AM

Spark Plasma Sintering of Ferritic Oxide Dispersion Strengthened Alloys: *Kerry Allahar*¹; Jatuporn Burns¹; Brian Jaques¹; Indrajit Charit²; Darryl Butt¹; James Cole³; ¹Boise State University; ²University of Idaho; ³Idaho National Laboratory

Oxide Dispersion Strengthened (ODS) alloys are candidate cladding materials due to their resistance to radiation, thermally induced creep, and swelling. Conventional powder metallurgy consolidation techniques have been primarily used in the development of ferritic ODS alloys with limited application of spark plasma sintering (SPS). Sintering by SPS is achieved by Joule heating using a pulsed DC coupled with uni-axial pressure. Advantages of SPS include faster heating rates, uniform heating condition, lower sintering temperature and shorter dwell time. The influences of SPS processing parameters on the microstructural evolution are presented for two pre-alloyed Fe/Cr/Al and Fe/Cr/Mo powders where the composition of Y2O3 was varied (0 to 0.5%). Parameters included temperature (600 to 1100 oC), dwell time (5 to 30 minutes) and heating rate (50 to 200 oC/min). Characterization of the grain sizes and boundaries was performed using EBSD and SEM and the fate of the ceramic dispersions was studied using TEM.

11:35 AM

Characteristics of Tin/Fe Cermet Fabricated by Mechanical Milling and Pulse Current Sintering: *Hiroyuki Nakayama*¹; Keizo Kobayashi¹; Kotaro Kikuchi²; ¹National Institute of Advanced Industrial Science and Technology; ²SS Alloy Co., Ltd.,

Titanium nitride (TiN) shows poor wettability with various liquid metals, thus the fabrication of TiN based cermets is difficult using conventional sintering. Therefore, in this study, we examined the fabrication of TiN based cermet by mechanical milling and subsequent pulse current sintering. The Fe as a binder phase was selected, because it is one of the most economical elements. The TiN powder (70 mass%) and Fe powder (30 mass%) were mechanically milled for 28.8 ks using planetary ball milling under Ar atmosphere. Subsequently, the milled powder was successfully consolidated using pulse current sintering method at 1473 K for 300 s under 60 MPa. The sintered compact was composed of TiN and Fe defined by X-ray diffraction, and the hardness achieved to HRA 91.5.

Recent Developments in the Processing, Characterization, Properties and Performance of Metal Matrix Composites: Processing, Microstructure and Mechanical Properties I

Sponsored by: The Minerals, Metals and Materials Society Program Organizers: Martin Pech-Canul, Centro de Investigacion y de Estudios Avanzados del Instituto Politecnico Nacional; Zariff Chaudhury, Arkansas State University; Golam Newaz, Wayne State University

| Tuesday AM | Room: 6A |
|---------------|-------------------------------|
| March 1, 2011 | Location: San Diego Conv. Ctr |

Session Chair: Martin Pech-Canul, Cinvestav Saltillo

8:30 AM

Effects of Zr on the Microstructure and Tensile Properties of Al-15%Mg2Si Metal Matrix Composite: Ahmad Razaghian¹; Amin Bahrami¹; *Masoud Emamy*²; Nargues Nemati³; Hamid Reza Jafari Nodooshan⁴; ¹Imam Khomeini International University; ²Center of Excellence for High Performance Materials, School of Metallurgy and Materials, University of Tehran; ³Sahand University of Technology; ⁴Islamic Azad University

The effects of Zr modification on the microstructure and tensile properties of an in situ prepared Al-15%Mg2Si composite have been investigated. Microstructural examinations were conducted by optical and scanning electron microscopy equipped with energy dispersive spectrometry. The optimum amount of Zr was selected as 1 wt. %. It was found that the addition

of Zr reduces the average size of Mg2Si primary particles. Adding Zr also raised both tensile strength (from 240MPa to 300MPa) and elongation values (from 2.4 to 6%). Fractographic examination of the unmodified composite also showed that large Mg2Si particles are responsible for fracture behavior.

8:50 AM

Investigation of Wear Properties of Hot Extruded Al-15wt%Mg2Si In-Situ Metal Matrix Composite: Hamid Reza Jafari Nodooshan¹; *Masoud Emamy*²; Amin Bahrami³; Ashkan Zolriasatein⁴; ¹Islamic Azad University; ²University of Tehran; ³Imam Khomeini International University; ⁴K. N. Toosi University of Technology

In recent years, lightweight metal matrix composites (MMC) have received wider attention for their technological application, such as automotive parts etc. For structural application, the wear properties are considered to be one of the major factors controlling the performance. In this study wear behavior of Al based composites reinforced with in-situ Mg2Si particles have been investigated. The composite was prepared by casting followed by extrusion at various temperatures with different ratio. The wear behavior of sample was investigated using a pin-on-disk technique under an applied load of 10N. In the extruded samples, the composite exhibited superior wear resistance than as cast in-situ composite.

9:10 AM

Microstructural Development of Al–15wt.%Mg2Si in Situ Composite with Be Addition: Mortaza Azarbarmas¹; Masoud Emamy¹; *Jafar Rassizadehghani*¹; Mohammad Alipour¹; Mostafa Karamouz¹; ¹University of Tehran

In this study, the effects of Be additions on the microstructural development of an in situ Al–15wt.%Mg2Si composite were investigated. A study of the specimen's surfaces via scanning electron microscope (SEM) and optical microscope revealed that with increasing Be additions in the composites, the average size of primary Mg2Si particles was reduced, and that the amount of alpha phase surrounding the Mg2Si particles was increased, with a littile change in morphology of this particles. Meanwhile the morphology of pseudo-eutectic phase was changed.

9:30 AM

Microstructural Properties and Wear Behaviour of AlSi9Mg Matrix B4Cp Reinforced Composites: *Fatih Toptan*¹; Isil Kerti¹; Ahmet Sagin¹; Mustafa Cigdem¹; Sibel Daglilar¹; Fatih Yuksel¹; ¹Yildiz Technical University

In the present work, AlSi9Mg alloy matrix composites reinforced with 10, 15 and 20% (wt.) B4Cp were produced by casting route at 850 °C. Titanium-containing flux (K2TiF6) was used to overcome the wetting problem between B4C and liquid aluminium metal. The microstructure of matrix/reinforcement interfaces were investigated with SEM studies. The reaction layer was also characterized with EDS analysis and X-ray mapping. It was found from the microstructural observations by high resolution field emission gun SEM (FEG-SEM) that the wetting improved by the formation of very thin (80-180 nm in thickness) TiC and TiB2 reaction layers. The samples were subjected to pin-on-disc wear tests against AISI 4140 pin under dry sliding conditions. The worn surface was studied through SEM and EDS analysis. It has seen that, wear resistance increased as particle volume fraction increased.

9:50 AM

Modification of Al-Mg2Si In Situ Composite by Boron: Mortaza Azarbarmas¹; Masoud Emamy¹; *Jafar Rassizadehghani*¹; Mostafa Karamouz¹; Mohammad Alipour¹; ¹University of Tehran

In this work, the effects of B additions on the microstructural development of an in situ Al–15wt.%Mg2Si composite were investigated. It was found from scanning electron microscope (SEM) and optical microscope images that with increasing B additions in the composites, the average size of primary Mg2Si particles was reduced, and that the amount of alpha phase surrounding the Mg2Si particles was increased. Meanwhile with the addition of B the pseudo-eutectic Al-Mg2Si was formed in a regular morphology 140th Annual Meeting & Exhibition

in cells separated with the alpha phase. Moreover, a small amount of B-containing compounds were formed as a result of B additions .

10:10 AM Break

10:30 AM

The Influence of Li on the Microstructure and Mechanical Properties of Hot Extruded Al-Mg2Si Metal Matrix Composite: Amin Bahrami¹; *Masoud Emamy*²; Ahmad Razaghian¹; Hamid Reza Jafari Nodooshan³; Ashkan Zolriasatein⁴; ¹Imam Khomeini International University; ²University of Tehran; ³Islamic Azad University; ⁴K. N. Toosi University of Technology

This article investigates the effect of Li as modifier on microstructure and mechanical properties of hot extruded the In-situ Al-15wt%Mg2Si composite. This composite have already been introduced as a new class of light materials but the brittle structure of the primary Mg2Si which is formed during solidification of these composites limits its application. Modified composite was directly extruded as rod by using three different dies with diameters 20, 10 and 5 mm and various temperature. Microstructures after this type of extrusion was studied by optical microscopy. Mechanical properties of the composite after various extrusions were tested by hardness and tensile tests. The results showed that Li addition were highly effective in reducing Mg2Si particle size from 30µm to about7µm and affects to the flow of material during the extrusion process and mechanical properties of extruded samples.

10:50 AM

Characterization of Composite Materials Interface Aimed to Suppress Vibration in Cast Parts: *M. David Hanna*¹; Shung Sung¹; ¹General Motors

Damping performance of inserted castings is critically dependent on the nature of the interface between the insert and the casting. This investigation involved an attempt to analyze sound data over a wide frequency range and assess the damping performance with different insert coating properties for a grey cast iron component. Based on the measured frequency response function, characteristic damping behavior of different coatings has been identified. The graphite base coating material showed enhanced sound damping properties compared to another refractory type material when applied to a steel insert. The parts with the graphite-based coated inserts have shown significant improvements in: (a) modal frequency reduction, (b) sound pressure level (SPL) reduction at the most dominant circumferential modes, (c) 1/3 octave band SPL reduction over wide frequency bands and finally (d) a modal damping ratio increase.

11:10 AM

In-Situ Synthesis of AlN/Mg Matrix Composites: *Xiao Ma*¹; Salin Kuplin¹; David Johnson¹; Kevin Trumble¹; ¹Purdue University

Magnesium matrix composites with AlN reinforcements are potential engineering materials for automobile and aerospace applications. Attractive properties of AlN include high thermal conductivity and hardness. AlN-reinforced Mg composites have been synthesized by in-situ reaction using pure Al and AZ31B and Si3N4 powder as raw materials. Microstructures containing 15 vol.% AlN were obtained by heating the raw materials at 770°C for one hour under argon atmosphere. Composite microstructures were characterized by X-ray diffraction, optical microscopy, scanning electron microscopy. Final microstructures consisted of AlN particles 1-5 \Box m in size distributed within the Mg alloy matrix.

11:30 AM

Performance Evaluation of Particulate Reinforced Al-SiC Bolted Joints:

Gergis William¹; Samir Shoukry¹; Jacky Prucz¹; ¹West Virginia University The increasing requirements of weight savings and extended durability motivated the potential application of metal matrix composite technology into the heavy vehicle market. However, significant technical barriers such as joining are likely to hinder the broad applications of MMC materials in heavy vehicles. This paper examines the feasibility of manufacturing and the behavior of bolted joint connections made from aluminum reinforced with silicon carbide particles. Initially, the study concentrates on experimental evaluation of bolted joints of 20% and 45% MMC material. The behavior of joints is studied as a function of various design parameters. Then, a finite element model is generated to predict the behavior of a double–lap joint of the same material. It is seen that experimental and numerical results agree well with each other. The results indicate that MMC joints are likely to fail early in the bearing mode, because of the brittle behavior of MMC materials.

11:50 AM

Synthesis and Mechanical Behavior of Ultrafine-Grained Al-B4C Composites: *Zhihui Zhang*¹; Ying Li¹; Troy Topping¹; Rustin Vogt¹; Yizhang Zhou¹; Julie Schoenung¹; Enrique Lavernia¹; ¹University of California Davis

The study of Al based ultrafine-grained (UFG) composites is prompted by the objective to develop ultrahigh strength (>1000 MPa), low density materials that also posses attractive high strain rate behavior. In this study, UFG Al/B4C composites with a B4C reinforcement size of ~1 μ m and ~50 nm, respectively, were produced via cryomilling followed by consolidating via HIP and extrusion. The results showed that the mechanical milling process led to a homogeneous distribution of the micro- and nano-particles in the matrix and the matrix had an average grain size of ~300 nm after consolidation. HRTEM revealed a clean Al/B4C interface and no detrimental interfacial phase or defects such as voids were observed. The mechanical behavior of the UFG composites were studied and the strengthening mechanisms were discussed in the frame work of load transfer, Hall-Petch strengthening, geometry necessary dislocation strengthening and dispersion strengthening.

Shape Casting IV: Light Metals Division Symposium in Honor of Prof. John T. Berry: Modeling

Sponsored by: The Minerals, Metals and Materials Society, TMS Light Metals Division, TMS: Aluminum Processing Committee, TMS: Solidification Committee

Program Organizers: Murat Tiryakioglu, University of North Florida; Paul Crepeau, General Motors Corporation; John Campbell, University of Birmingham

| Tuesday AM | Room: 15B |
|---------------|-------------------------------|
| March 1, 2011 | Location: San Diego Conv. Ctr |

Session Chairs: Mark Jolly, Univ of Birmingham; Daan Maijer, Univ of British Columbia

8:30 AM Introductory Comments

8:40 AM

The History of Casting Process Simulation: Christof Heisser¹; ¹MAGMA Foundry Technologies, Inc.

An overview of significant steps in the development of casting process simulation will depict its development from simple "solidification-only" tools to comprehensive casting process simulation tools, which are irreplaceably integrated in the current product development process. The presentation will include topics like autonomous optimization and transfer of simulation results to FEA and lifetime prediction tools.

9:05 AM

State of the Art Review of Modelling Entrainment Defects in the Shape Casting Process: Carl Reilly¹; Nick Green²; *Mark Jolly*²; ¹University of British Columbia; ²University of Birmingham

Entrainment of oxide films into liquid metals has been shown to be detrimental to casting integrity. A number of mechanisms have been shown to initiate the entrainment of oxide films including returning waves, plunging jets, bubble trails and fountains. Computational fluid dynamics (CFD) software packages allow foundry staff to improve casting systems using qualitative parameters. Optimization software is now a viable option for foundries. It does, however, require a measurable parameter which allows the quantification of defects. This is becoming an important research area to allow the optimization software manufacturers to meet the needs of industry. The current methods of modeling surface film and bubble generated casting defects have been described and critically reviewed shedding light on the qualities and issues currently associated with the present available methods. However, it is clear that further investigations and developments are still required to allow the accurate and efficient modeling of casting defects.

9:30 AM

Physical and Computational Models of Free Surface Related Defects in Low-Pressure Die-Cast Aluminum Alloy Wheels: *Jianglan Duan*¹; Daan Maijer¹; Steve Cockcroft¹; Carl Reilly¹; Ken Nguyen²; Dominic Au²; ¹University of British Columbia; ²Canadian Autoparts Toyota, Inc.

A water analogue model has been used to simulate the free surface behavior during mould filling of a low-pressure die-cast (LPDC) wheel. The water analogue has been used to validate a mathematical model of the filling process. A transparent die was manufactured with a 2D profile extracted from a typical production die, and the experimental parameters used were based upon the production process. The flow occurring in the model was recorded with camera. A mathematical model of the filling process was developed to reproduce the behavior observed in the water model. Both the experimental and modeled results have shown a relative tranquil fill of the sprue and the rim, while persistent returning waves were developed in the spoke. The results highlight the significant effects of venting, both in the water model and computational model. Future work is required to improve the accuracy of venting modeling of the mould cavity.

9:55 AM

Solidification Model Coupling Lattice Boltzmann Method with Cellular Automaton Technique: Hebi Yin¹; Liang Wang²; Sergio Felicelli¹; ¹Mississippi State University; ²Mississippi State University

A two dimensional model combining the lattice Boltzmann method (LB) and the cellular automaton technique (CA) was developed to simulate dendrite growth during solidification. The LB method was used for the coupled-calculation of temperature, composition, and velocity fields while the liquid/solid interface was tracked by the CA method. The LB-CA model was validated by comparing tip velocity and equilibrium composition with analytical solutions. Single and multi- dendrite growth was simulated with energy and solute transport not only by diffusion but also by convection. In addition, the simulation morphology and computational time obtained with the LB-CA model was compared to that of a finite element – CA model.

10:20 AM Break

10:40 AM

Physical Characterization of the Permeability of Equiaxed Eutectic Structures in Hypoeutectic Aluminum Alloys: *Ehsan Khajeh*¹; Daan Maijer¹; ¹University of British Columbia

The permeability of hypoeutectic aluminum alloys during equiaxed eutectic solidification has been determined through physical modeling. The 3D geometries of primary phase obtained from X-ray microtomography (XMT) scans of solidified aluminum alloys have been used to generate computational domains for use in simulating the eutectic transformation. By applying the Cellular Automaton technique to simulate the growth of eutectic colonies, the evolution of the liquid channels has been modeled. Large-scale analogues of the simulated structures were produced by rapid prototyping for use as physical models. A glycerin-based solution was passed through the physical models and the permeability was calculated from measurements of the discharge flow rate and pressure drop. This work presents an alternative technique to determine permeability compared to conventional permeameters and shows a deviation from the conventional Carman-Kozeny expression at high eutectic grain density.

11:05 AM

Foam Filters Used in Gravity Casting: *Fu-Yuan Hsu*¹; Huey-Jiuan Lin¹; ¹National United University

Ceramic foam filters are normally used for reducing the velocity of liquid metal in the design of runner system. In this study four designs of runner systems with various orientations of foam filters were explored and their apparent velocities were estimated by casting experiment and computational modeling. In the casting experiment, trajectory and metal weighing methods were employed for measuring apparent velocity and flow rate, respectively. Using Forchheimer's equation, a porous material such as a foam filter could be simulated in the modeling. The modeling result was validated by the casting experiment. For high efficient usage of a foam filter, through which liquid metal with high flow rate and low velocity was transformed, the optimized design is recommended in all of runner systems.

11:30 AM

Simulation of Macrosegregation during Directional Solidification Using Mesh Adaptation: Udaya Sajja¹; Sergio Felicelli¹; ¹Mississippi State University

Modeling of the formation of macroscopic segregation channels during directional solidification processes has important applications in the casting industry. Computations that consider thermosolutal convection involve different length scales ranging from the small solute boundary layer at the dendrite tips to the characteristic size of the casting. In general, numerical models of solidification in the presence of a developing mushy zone are computationally inefficient due to nonlinear transport in an anisotropic porous medium. In the present work, mesh adaptation with triangular finite elements is used in conjunction with an efficient fractional-step solver of the momentum equations to predict the occurrence of channel-type segregation defects or freckles. The triangulations are created dynamically using an unstructured grid generator and a refinement criterion that tracks the position of the channel segregates. The efficiency of mesh adaptation is illustrated with simulations showing channel formation and macrosegregation in directional solidification of a Pb-Sn alloy.

11:55 AM

A Mathematical Model for Simulating the Microporosity of Squeeze Casting of Aluminum Alloy: *Zhiqiang Han*¹; Jinxi Li¹; Wen Yang¹; Baicheng Liu¹; ¹Tsinghua University

A mathematical model for simulating the microporosity of squeeze casting of aluminum alloy has been developed, in which the heat transfer, solidification shrinkage, feeding flow, pressure transfer, and hydrogen conservation were taken into account. The shrinkage induced flow and the pressure drop in the mushy zone were calculated by solving continuity and momentum equations. A mechanical model was solved for obtaining the pressure transferred into the liquid core of the casting. By coupling the pressure drop and the pressure transferred into the liquid core, the pressure in the mushy zone was calculated. Based on the hydrogen conservation equation, the microporosity volume fraction was estimated by referring to the pressure in the mushy zone. The squeeze casting processes of aluminum alloy under different process conditions were simulated and the simulation results were compared with experimental results for assessment of the developed model.

Size Effects in Mechanical Behavior: In Situ Characterization to Understand Mechanically Driven Size Effects

Sponsored by: The Minerals, Metals and Materials Society, Not Applicable, TMS: Nanomechanical Materials Behavior Committee *Program Organizers:* Erica Lilleodden, GKSS Research Center; Amit Misra, Los Alamos National Laboratory; Thomas Buchheit, Sandia National Laboratories; Andrew Minor, UC Berkeley & LBL

| Tuesday AM | Room: 2 |
|---------------|-------------------------------|
| March 1, 2011 | Location: San Diego Conv. Ctr |

Session Chairs: Andrew Minor, UC Berkeley; Jun Lou, Rice University

8:30 AM Invited

Quantitative *In-situ* **TEM** to Investigate Defect – Strength Relations: *Daniel Kiener*¹; ¹Austrian Academy of Science & University of Leoben

While reports consistently find that 'smaller is stronger', the governing mechanisms remain elusive due to lack of direct observations. *In-situ*



TEM testing is ideally suited to provide this missing information, as the governing dislocation processes can be directly monitored. Experiments on FIB prepared samples depict that deformation is source controlled for compression samples, leading to single-slip deformation of small specimens oriented for multi-slip. With a novel tensile approach, we exclude effects from specimen taper and other compression boundary conditions and observe defect exhaustion with ongoing straining, resulting in strengths reported for whiskers. Significant changes in the 'mechanical annealing' behavior were observed for pre-deformed or proton irradiated samples. The proton irradiated material changes from a source controlled size-dependent strength at small dimensions to a size-independent strength governed by dislocation-defect interactions. Using *in situ* annealing, we achieved defect-free samples, which deformed at stresses near the theoretical strength of the material.

9:00 AM

Insights into Mg Plasticity From In Situ Nanomechanical Testing in the TEM: *Qian Yu*¹; Raj Mishra²; Andrew Minor³; ¹University of California Berkeley; ²General Motors Corporation; ³University of California Berkeley & Lawrence Berkeley National Laboratory

Magnesium is a lightweight metal that would be much more useful for structural applications than it currently is if not for its complicated and anisotropic plastic deformation behavior. The HCP structure of Mg has limited dislocation slip systems and, thus, twinning generally accompanies dislocation plasticity. Recently, we have run a series of in situ mechanical tests in a TEM on pure Mg where we have quantitatively measured and characterized the deformation behavior in both compression and in tension, and in both basal slip and non-basal slip orientations. By comparing the quantitative deformation behavior in these experiments we are able to provide significant insights into the twinning mechanisms and the origins of the compression-tension asymmetry in Mg.

9:20 AM Invited

In Situ TEM Studies of Plastic Deformation in Small-Volume Samples near Room Temperature: Evan Ma¹; ¹Johns Hopkins University

This talk reports on in situ TEM investigations of size effects in mechanical behavior carried out at our new research center, Center for Advancing Materials Performance from the Nanoscale (CAMP-Nano), founded in 2009 at XJTU. Recent projects at CAMP-Nano, led by Prof. Z. W. Shan, Prof. Ju Li and the speaker, have yielded interesting results. In this short talk, we will briefly describe two representative ongoing studies. For crystalline materials, an example will be given regarding the strong sample size effect on deformation twinning in a Ti alloy (Q. Yu et al., Nature 2010), illustrating a Hall-Petch type of dependence of deformation twinning on crystal size. For glassy materials, amorphous silica will be discussed as an example, demonstrating superplastic flow of nano-sized silica glass wires and particles near room temperature inside a TEM (in collaboration with K. Zheng, X.D. Han, Z. Zhang et al. at BJUT, Nature Communications, 2010).

9:50 AM

Dislocation Nucleation in Confined Crystalline Volumes: In-Situ TEM Observations and Micro-Mechanical Tests on Submicron Al Fibers: *Frederic Mompiou*¹; Marc Legros¹; Daniel Caillard¹; Daniel Gianola²; Andreas Sedlmayr³; Oliver Kraft³; ¹CEMES-CNRS; ²University of Pennsylvania; ³Karlsruher Institut für Technologie

Small crystals have an initial resistance to deformation much larger than their bulk counterpart, but the physical explanations for this multiplied yield stress are still highly debated. One critical step seems to be the nucleation of fresh dislocations and the nature of the sources. In the present work we present an extensive in situ TEM study of dislocation multiplication and shearing processes in sub-micrometer Al fibers that were kept free of FIB preparation. The size of operating sources and their production mode has been systematically analyzed and compared to the crystal dimensions and initial microstructure. In addition to the source operating regime, a very low ductility plastic regime has been observed in fibers containing no preexisting dislocations. These plastic behaviors have been correlated to stress and strain measurements obtained by micro-mechanical testing. Possible strengthening mechanisms and size effect on the mechanical properties will be discussed.

10:10 AM Break

10:40 AM

Mechanical Annealing in Submicro-sized Molybdenum Crystals: Ling Huang¹; *Zhiwei Shan*¹; Ju Li²; Jun Sun¹; Evan Ma³; ¹Xi'an Jiaotong University; ²University of Pennsylvania; ³Johns Hopkins University

In situ TEM compression tests were carried out to investigate the mechanical behavior of single crystal molybdenum pillars with diameters ranging from 75 nm to 300 nm. Despite the high density initial defects, the flow stress of those focused ion beam (FIB) fabricated pillars increased monotonously as the size decreased, with the maximum value up to 8.5 GPa for pillars with a diameter of 75 nm. The power-law exponent of strength vs. pillar diameter is -0.92, about 2 times higher than that reported in previous works for larger pillars. More surprisingly, contrary to that predicated by computer simulation, significant mechanical annealing phenomena, followed by catastrophic failure, is observed during the compression test of these body centered cubic (BCC) metal pillars when their size is less than 200 nm. These striking findings shed new light on revealing the underlying physical mechanisms that are responsible for the plasticity of small scaled BCC crystals.

11:00 AM

A Length Scale Dependent Phase Transformation in Si: *Aaron Beaber*¹; Steven Girshick¹; William Gerberich¹; ¹University of Minnesota

The phase transformation of silicon during indentation has been widely studied over the past thirty years. The use of in situ indentation, particularly Raman microscopy and electrical characterization, has greatly clarified the transformation process. In the current work, TEM in situ indentation of Si nanospheres and ex situ indentation of confined nanotowers are used to propose a length scale dependent phase transformation. Below a critical dimension of approximately 100 nm, deformation of Si is dominated by dislocation plasticity rather than a phase transformation. This is shown to be consistent with multiple geometries, including spheres, towers, and wedges. Furthermore, the reverse transformation upon unloading is shown to occur at decreasing stresses for smaller geometries. These findings reinforce the importance of shear stresses during anistropic loading and confirm the notion of enhanced ductility in Si at small scales.

11:20 AM Invited

Probing Size Dependent Mechanical Properties of Metallic Nanowires in Tension: Yang Lu¹; Cheng Peng¹; Yogi Ganesan¹; Hao Lu¹; Jianyu Huang²; *Jun Lou*¹; ¹Rice University; ²Sandia National Laboratories

This talk presents some of our recent efforts to study the size dependent mechanical behaviors of metallic nanowires. We have developed a simple micro-device that allows in situ quantitative mechanical characterization of metallic nanowires, in SEM or TEM chamber equipped with a quantitative nanoindenter. The unique design of this device makes it possible to convert compression from nanoindentation to uni-axial tension at the sample stages. By utilizing this device, in situ results on deformation and fracture behavior of Ni and Au nanowires will be discussed. Also in this work, we performed in situ quantitative tensile tests on individual <111> single crystalline ultrathin gold nanowires (diameter ~7-15 nanometers) inside TEM. Significant load drop observed in stress-strain curve suggests the occurrences of dislocation nucleation. Corresponding high resolution TEM (HRTEM) imaging demonstrated that plastic deformation was indeed initiated and dominated by surface dislocation nucleation, mediating ultrahigh yield and fracture strength in gold nanowires.

11:50 AM

Micro-Cantilever Testing of Ti Alloys: Jicheng Gong¹; *Angus Wilkinson*¹; ¹University of Oxford

Micro-cantilevers were machined using a focused ion beam from pure Ti(945), Ti-6Al (945) and Ti-6Al-4V (945+946) and tested in bending using a nano-indenter. The cantilevers had triangular cross-sections with widths varied across the range 10 μ m to 1 μ m. EBSD mapping of large areas allowed suitably oriented grains to be indentified and the cantilevers cut so as to select specific slip systems. Strain-bursts and/or load-drops are much less

severe for the load-displacement curves for the cantilevers than for similarly sized compression pillars. Critical resolved shear stresses were extracted from the bend tests by fitting load-displacement data with crystal plasticity finite element simulations. All three systems exhibit a size effect consistent with a back stress from pile-up of dislocations against the low stress region at the neutral axis.

Surfaces and Heterostructures at Nano- or Micro-Scale and Their Characterization, Properties, and Applications: Coatings, Surfaces, and Interfaces II - and - Magnetic Heterostructures I

Sponsored by: TMS Electronic, Magnetic, and Photonic Materials Division, TMS Materials Processing and Manufacturing Division, TMS: Nanomaterials Committee, TMS: Surface Engineering Committee

Program Organizers: Nitin Chopra, The University of Alabama; Ramana Reddy, The University of Alabama; Jiyoung Kim, Univ of Texas; Arvind Agarwal, Florida International Univ; Sandip Harimkar, Oklahoma State University

| Tuesday AM | Room: 31B |
|---------------|-------------------------------|
| March 1, 2011 | Location: San Diego Conv. Ctr |

Session Chairs: Arvind Agarwal, Florida International University; Sandip Harimkar, Oklahoma State University; Nitin Chopra, The University of Alabama; Ramana Reddy, The University of Alabama

8:30 AM Invited

Thermal Annealing of ZnO Films Using High-Density Plasma Arc Lamps: *Adrian Sabau*¹; Ralph Dinwiddie¹; Jun Xu¹; Joseph Angelini¹; David Harper¹; ¹Oak Ridge National Laboratory

Nanostructured materials are rarely synthesized with appropriate phase and/or morphology. In this study, critical additional of as-synthesized nanostructured materials, such as annealing and/or activation of dopants, are addressed using infrared plasma arc lamps (PAL) over areas as large as 1,000 cm2. The broad spectral range of the PAL and the spectral variation of light absorption in nanostructured materials make the selection of processing parameters extremely difficult, posing a major technological barrier. In this study, the measurement of the surface temperature using various techniques for ZnO films on crystalline silicon wafers is discussed. An energy transport model for the simulation of rapid thermal processing using PAL is presented. The experimental and computational results show that the surface temperature cannot be measured directly and that computer simulation results are an effective tool for obtaining accurate data on processing temperatures.

9:00 AM

Glass Transition at a Polymer Surface Monitored by Localized Surface Plasmon Resonance: *Kaan Kalkan*¹; Ratan Putla¹; ¹Oklahoma State University

We investigate glass transition on a polymer surface by embedding gold nanoparticles (AuNP). The impregnation of AuNP into the polymer causes a spectral shift in the LSPR due to the changing dielectric environment. AuNP, at an average size of 8 nm, were synthesized on poly isobutyl methacrylate (PiBMA) films on glass by thermal evaporation. Subsequently, time series LSPR spectra of AuNP on PiBMA were acquired in a temperature controlled optical cell. The effective dielectric constant surrounding the AuNP was calculated from LSPR optical extinction peak. Depth and velocity of penetration were derived from the measured dielectric constant on the basis of dielectric mixing. The onset of AuNP penetration was found to be at 45 C, which is 10 C below the reported glass transition of "bulk" PiBMA. The penetration velocity was found to be fairly constant in time until complete embedding while temperature activated at 0.05 eV.

9:20 AM

Oxidation and Interfacial Structure of Ti₃Al: *Muralidharan Ramachandran*¹; Ramana Reddy¹; ¹The University of Alabama

The isothermal oxidation of binary Ti_3Al was studied as function of temperature in pure oxygen atmosphere. Weight gain data were acquired using thermo-gravimetric analyzer (TGA). The phase analysis of the base metal and the oxide layer were performed using x-ray diffraction, while the morphology and elemental composition were determined using scanning electron microscopy (SEM) and Transmission Electron Microscopy (TEM). The rate constant of the oxidation process increases from 9.75 X 10^4 mg²/ cm⁴/min at 1023K to 5.05 X 10^2 mg²/cm⁴/min at 1223K. The activation energy for the oxidation process was determined to be 240.5 kJ/mol. The particle size in the oxide scale increased with the increase in temperature. At higher temperatures formation of layered structures was observed. The composition and structure of the metal/oxide interface was analyzed.

9:35 AM Break

9:45 AM

Fabrication and Characterization of MWCNT Reinforced Aluminum Using Spark Plasma Sintering

: Vineet Yadav1; Sandip Harimkar1; 1Oklahoma State University

Spark plasma sintering (SPS) technique was used to fabricate aluminumbased metal matrix composites reinforced with MWCNT. The developments of composites properties such as hardness, strength, wear resistance, and corrosion resistance with reinforcement content and composite microstructure was investigated. In this presentation, the influence of CNT dispersing agents and SPS processing parameters on microstructure and properties of the Al-MWCNT composite will also be discussed.

10:00 AM

Microstructure and Wear Behavior of Pulse Electrodeposited Nickel-Carbon Nanotube (Ni-CNT) Composite Coatings: *Tushar Borkar*¹; Sandip Harimkar¹; ¹Oklahoma State University

Due to excellent mechanical properties such as high strength, high elastic modulus and large elastic, as well as fracture strain, carbon nanotubes (CNTs) are attracting significant interest as reinforcements in metallic coatings. In the present investigation, carbon nanotube (CNT) reinforced nickel composite coatings were deposited on a stainless steel substrate using pulse electrodeposition process employing a nickel Watts bath. The presence of CNTs in the composite coating prohibited the columnar growth of the nickel grains resulting in random/weak texture and smaller thickness of the composite coatings. The Ni-CNT composite coatings exhibited significantly improved microhardness (580±15 HV) compared to pure nickel coatings (320±15 HV). The pin-on-disc wear testing data indicated that the reinforcement of CNTs significantly improved wear resistance of the composite coatings compared to pure nickel coatings.

10:15 AM

Synthesis and Characterization of Graphene after Ion Implantation: *Tomeka Colon*¹; Cydale Smith¹; Mohamed Seif¹; Satilmis Budak¹; Claudiu Muntele¹; Lawrence Holland¹; Robert Zimmerman¹; Daryush Ila¹; ¹Alabama A&M University

Graphene is a flat monolayer of carbon atoms tightly packed into a two-dimensional (2D) honeycomb lattice and is a basic building block for graphitic materials of all other dimensionalities. It can be wrapped up into 0D fullerenes, rolled into 1D nanotubes, or stacked into 3D graphite. Graphene nanoribbons (GNRs) are essentially single layers of graphene that are cut in a particular pattern to give it certain electrical properties. Graphene's high electrical conductivity and high optical transparency make it a candidate for transparent conducting electrodes, required for such applications as touchscreens, liquid crystal displays, organic photovoltaic cells, and organic light-emitting diodes. In this study, we have synthesized graphene on silicon dioxide, used accelerated ion beams to induce defects, and then studied the effects those defects have on the properties of epitaxial graphene.



10:30 AM

A Facile Route to Synthesis and Characterisation of Hydrophobic Titania Nanofibres: *T. Sundararajan*¹; S. Abirami¹; P. Manohar¹; ¹Anna University

Polymer based hydrophobic titania nano fibers were fabricated using a simple Low Volume Medium Pressure(LVMP) spray gun. The FE-SEM studies showed that it resembled the nanofibers produced by electro spinning method. Spraying parallel to the length of the glass slide gave better contact angle values and the fibers were more entangled. The hydrophobicity was developed in the coating immediately after spraying. The contact angle measurements were done using Goniometer. Curing the fibers in hot air oven at 80°C reduced the contact angles. Three different sources of titania were experimented. Powder characterization was done by XRD, Raman spectroscope. A set of nine experiments based on Taguchi's Method were also conducted for contact angle optimization. Even a small amount (0.03g) of hydrothermal titania with 0.7g of polystyrene gave a contact angle as high as 149.77°, which is close to super hydrophobic range.

10:45 AM

Application of the Strong Contrast Technique to Thermoelastic Characterization of Nanocomposites: *Majid Baniassadi*¹; Akbar Ghazavizadeh¹; David Ruch¹; Yves Rémond¹; Said Ahzi¹; Hamid Garmestani¹; ¹CRP Henri Tudor

The effective thermoelastic properties of composites filled with cylindrical nanofillers are evaluated using the statistical continuum theory of strong contrast. In terms of aspect ratio, the inclusions vary across a wide range from nanoplatelets to nanowires. As nanostructure descriptors, the statistical two-point correlation functions are calculated using the Monte Carlo method. Then the three-point correlation functions are estimated via an innovative technique. The resulting quadruple and sextuple integrals are calculated using the Monte Carlo integration. The final complex tensorial equations of the elastic part are solved by trial and error. Finally, to verify our proposed approach, it is implemented on a computer generated nanocomposite and the thermoelastic properties are compared with other results..

11:00 AM Break

11:10 AM Introductory Comments for Magnetic Heterostructures

11:15 AM Invited

Multifunctional Plasmonic-Ferromagnetic Surface Nanocomposites Synthesized by Bilayer Liquid Self-Organization: Hare Krishna¹; Ritesh Sachan²; Nozomi Shirato²; Jeremy Strader²; Hernando Garcia³; Anup Gangopadhyay¹; *Ramki Kalyanaraman*²; ¹Washington University in St. Louis; ²University of Tennessee; ³Southern Illinois University

Tunable ferromagnetic and resonant plasmon optical behavior in nanostructures provides opportunity to realize multifunctional materials. Here we will review the robust synthesis of such multifunctional surface nanostructures by self-organization via dewetting of bilayer films. Experimentally, such nanomaterials can be synthesized by nanosecond pulsed laser melting of ultrathin metallic films. We found that nanoscale bilayer _films of immiscible metallic liquids show different self-organized patterning characteristics based on their arrangement on a substrate. The different bilayer arrangements change the signs of intermolecular interactions, which changes the mode of coupled deformations and the patterning characteristics. We will also discuss the physical properties of the Ag-Co nanocomposite particles created by this process which show tunable concentration dependent ferromagnetism and localized surface plasmon resonances. * This work has been supported by NSF grants CAREER DMI-0449258, CMMI-0757589, and DMR-0805258 and by grants from CMI at Washington University and SEERC at the University of Tennessee.

11:45 AM Invited

Nanocomposite Magnetic Materials: Improved Performance by Nanostructuring: *Matthew Willard*¹; Maria Daniil¹; Keith Knipling¹; Ramasis Goswami¹; Ashish Baraskar²; Soack Yoon²; Vincent Harris²; ¹Naval Research Laboratory; ²Northeastern University

Development of new magnetic materials, capable of providing higher energy products for permanent magnets and lower core losses for soft magnets, enables smaller, lighter, and more efficient devices. Over the past two decades, a major focus of research has been microstructure refinement to the nanoscale, which has advantages for each class of magnetic material, allowing permanent magnets to store more energy and soft magnets to dissipate less energy than alternative materials. These advantages originate in the exchange correlation length, a fundamental magnetic length scale determined by the strength of coupling between magnetic moments causing them to align, which has typical values with nanoscale dimensions. This presentation will highlight recent work on nanocomposite soft and hard magnetic materials produced by pulsed laser deposition and rapid solidification processing. The effect of nanostructure on the magnetic material performance will be shown experimentally and discussed from a theoretical perspective.

Thermally Activated Processes in Plastic Deformation: Dislocation Ensemble Evolution Sponsored by: The Minerals, Metals and Materials Society, TMS Materials Processing and Manufacturing Division, TMS/ASM: Computational Materials Science and Engineering Committee Program Organizer: Christopher Woodward, Air Force Research Laboratory

| Tuesday AM | Room: 1B |
|---------------|-------------------------------|
| March 1, 2011 | Location: San Diego Conv. Ctr |

Session Chairs: Christopher Woodward, Air Force Research Laboratory; Ladislas Kubin, CNRS-ONERA

8:30 AM Invited

On the Cross Slip of Dislocations in the Face-Centered Cubic Metals: Joël Bonneville¹; ¹University of Poitiers

Cross slip is the mechanism by which a screw dislocation changes from its primary glide plane to move on a locally more favourable stressed glide plane. Cross slip has been recognised to significantly contribute to plastic deformation by creating dislocation microstructure and causing dislocation annihilation, dynamic recovery, obstacle bypass, strain softening as well as strain hardening, etc. There has been in the recent years a renewed interest for studying the cross-slip of screw dislocations in the face-centered cubic structure. The main reasons originate from the development in computational power and algorithms allowing for realistic atomistic simulations and the need in integrated computational materials engineering for precise quantitative and predictive models. Our purpose is to present relevant models used for describing cross-slip processes from historical approaches up to the more recent theoretical developments. A particular emphasis will be placed to extract the significant characteristics deduced by the different approaches.

9:00 AM

Measurement of Cross-Slip Activation Parameters in Pure Ni via Bonneville-Escaig Experiments: *Jaafar El-Awady*¹; Michael Uchic²; Sang-Lan Kim³; Paul Shade⁴; Satish Rao³; Dennis Dimiduk²; Christopher Woodward²; ¹Johns Hopkins University; ²Air Force Research Laboratory; ³UES, Inc.; ⁴Universal Technology Corporation

To accurately incorporate the thermally-activated process of dislocation cross-slip into mobility laws of dislocation dynamics simulations, it is necessary to experimentally determine the activation volume and energy barrier for dislocation cross-slip. To achieve this we revisit the Bonneville-Escaig experiments to characterize cross-slip activation in pure-nickel single crystals. In this study, large Ni-single crystals were pre-strained in



compression to strains that correspond to the transition between stage-II and stage-III deformation. Meso-scale (5-80 micrometeter diameter) and macro-scale (mm size) crystals were prepared from the pre-strained crystals, to explore whether modern microtesting methods can eliminate the need for 'large' single crystals in these experiments. The orientation of the compression axis of the children crystals is such that an avalanche of cross-slip events is produced at the yield stress. The results are interpreted in terms of the Escaig cross-slip model, and the recent molecular-statics simulations of cross-slip nucleation at screw-dislocation intersections with forest dislocations.

9:20 AM Invited

Atomistic Simulations of Cross-Slip Nucleation at Screw Dislocation Intersections in Face-Centered Cubic Nickel and Copper and L12 Ni3Al: *Satish Rao*¹; Dennis Dimiduk²; Jaafar El-Awady³; Triplicane Parthasarathy¹; Michael Uchic²; Christopher Woodward²; ¹UES Inc.; ²Air Force Research Laboratory; ³Johns Hopkins University

We describe molecular-statics simulations of screw character dislocation intersections with forest dislocations, in FCC Ni and Cu and L12 Ni3Al, to illustrate a mechanism for cross-slip nucleation. The simulations show how such intersections readily produce cross-slip nuclei. There exists a finite activation barrier for the screw dislocation to transfer from the fully glide plane or the fully cross-slip plane state to the partially cross-slipped state at these intersections, which is a factor of 2 - 5 lower than without the presence of an intersection. The activation barrier for cross-slip at these intersections is shown to be linearly proportional to (d/b)ln(1.732d/b)0.5, as with the case of no intersections, where 'd' is the Shockley partial spacing of the partial dislocations and 'b' is the Burger's vector of the screw dislocation. These results suggest that cross-slip should be preferentially observed at selected screw dislocation intersections in FCC materials as well as L12 Ni3Al.

9:50 AM

Dislocation Kinetics in Fe and Fe Alloys Investigated by In Situ TEM Straining Experiments: Daniel Caillard¹; ¹CNRS

Microsamples of pure Fe have been strained in a JEOL 2010HC transmission microscope, between 100K and 473K. At room temperature, dislocation loops exhibit straight screw portions moving slowly and steadily, and curved non-screw ones with a much higher mobility. The velocity of screw parts is proportional to their length, in agreement with the kink-pair model. The velocity-stress dependence of a single dislocation has been deduced from an in situ relaxation experiment. At low temperatures, the motion of screw dislocations becomes jerky. This change of kinetics has been interpreted by a change in the mechanism of motion of screw dislocations across the Peierls potential, and correlated to the change in the corresponding macroscopic activation parameters. The softening effect of carbon, and the hardening effect of silicon and chromium, are shown to result from the shift of the transition between the two mechanisms to respectively lower and higher temperatures.

10:10 AM Break

10:30 AM Invited

Discrete Dislocation Dynamics: Principle and Recent Applications: *Marc Fivel*¹; ¹SIMaP-GPM2

The concept of three-dimensional discrete dislocation (DD) simulations has been imagined by L. Kubin, Y. Bréchet and G. Canova in the early 1990s. The first code MICROMÉGAS was a simple model for which dislocation lines of a f.c.c. single crystal are discretized in sets of edge and screw dislocation segments embedded in a continuum media. Typical output of DD simulations are obviously the dislocation microstructure but also many statistical data such as the dislocation densities, the cumulated shear strain, the stored energy, the local stresses and also the actual shape of any part of the crystal deformed by the dislocations. From some points of view, DD simulations can be seen as an ideal tool to fill the gap between atomic simulations (MD) and continuum modelling (FEM). This talk presents recent simulations performed at Grenoble using the edge-screw code Tridis derived from Canova's initial model.

11:00 AM

Forest Hardening in Materials with High Lattice Friction: *Benoit Devincre*¹; Ghiath Monnet²; Jonathan Amodeo³; ¹CNRS; ²EDF; ³Lille 1 University

In materials with high lattice friction like body centred cubic (bcc) crystals at low temperatures, the thermally activated motion of screw dislocations by the kink-pair mechanism governs the yield properties and also affects strain hardening. In this work, the problem of forest hardening at low temperature is revisited with DD simulations. Results are presented in the case of two illustrative materials, i.e. Iron and MgO. Unlike the classical picture of forest hardening in fcc crystal, calculations show that the strength of forest interaction is temperature and strain rate dependant. Hence, simplistic models based on the Taylor equation do not apply and alternative approaches must be considered. The results of massive simulations are compared with existing models. Finally, a new model accounting in a quantitative manner for the effects of temperature and dislocation density is proposed.

11:20 AM

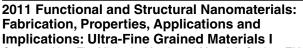
Simulating the Evolution of the Dislocation Network under Irradiation: Dan Mordehai¹; Georges Martin²; ¹Technion; ²CEA-Siège

The dislocation network evolution in metals under irradiation is a complex process, which is still a matter of controversy. While crystalline plasticity involves conservative motion of dislocations, the large concentration of point defects produced under irradiation contributes to plastic deformation either by eliminating at sinks (like climb of the existing dislocation network) or agglomerate into new defects. In this work, we propose a method to include dislocation climb in Dislocation Dynamics simulations, based upon the diffusion theory of point defects. In particular, we present an analytical model to calculate the climb rate of dislocations due to interstitial flux, in coordination with the dislocation network. We employ this model to demonstrate that when accounting for the dislocation network, the annihilation of dislocation pairs with opposite signs and the annihilation of low-angle tilt grain boundaries is accelerated under irradiation.

11:40 AM

Mobility of Dislocation Populations as a Thermally Activated Process: Craig Hartley¹; ¹El Arroyo Enterprises LLC

Dislocation Dynamics (DD) simulations offer an attractive means of providing basic input to Crystal Plasticity (CP) calculations by permitting micro-scale virtual experiments using models for dislocation behavior based on the physics of individual dislocations. While some of this information can be supplied by atomic models of lattice defects, modifications that employ the principles of stress-assisted, thermally activated motion of dislocations can expand the predictive power of such simulations. Deformation of an element is expressed as an appropriate average of unit processes over the volume of a representative element. To inform CP models, results of these virtual experiments must be expressed in terms of constitutive equations having parameters demonstrably related to the properties and behavior of the dislocation ensemble. This work describes a simple mathematical model for a constitutive relationship in terms of the motion of an ensemble of dislocations where individual dislocation behavior occurs by a thermally activated unit process.



Sponsored by: The Minerals, Metals and Materials Society, TMS Electronic, Magnetic, and Photonic Materials Division, TMS: Nanomaterials Committee

Program Organizers: Jiyoung Kim, Univ of Texas; David Stollberg, Georgia Tech Research Institute; Seong Jin Koh, University of Texas at Arlington; Nitin Chopra, The University of Alabama; Suveen Mathaudhu, U.S. Army Research Office

| Tuesday PM | Room: 8 |
|---------------|-------------------------------|
| March 1, 2011 | Location: San Diego Conv. Ctr |

Session Chair: Suveen Mathaudhu, US Army Research Lab

2:00 PM Introductory Comments

2:05 PM

Deformation Twinning in Nanocrystalline HCP Mg Alloys: *Yuntian Zhu*¹; X.L. Wu²; K.M. Youssef¹; C.C. Koch¹; S.N. Mathaudhu³; L.J. Kecskes³; ¹North Carolina State Univ; ²Institute of Mechanics; ³U.S. Army Research Laboratory

Nanocrystalline (nc) hexagonal close-packed (hcp) metals are rarely observed to deform by twinning, although twinning is a major deformation mechanism in their coarse-grained counterparts. This behavior is contrary to what is observed in face-centered cubic metals. Here we report that by alloying Mg with other elements, deformation twins are observed in the nc Mg alloy processed by severe plastic deformation. The formation of deformation twins is attributed to the alloying effect, which may change the energy path for twinning. These results point to a promising approach to design nc hcp alloys for superior mechanical properties.

2:35 PM

Deformation Twins in Nanocrystalline Magnesium-Based Alloy: *Marta Pozuelo*¹; Wei Kao¹; Jenn-Ming Yang¹; ¹UCLA

Deformation twins are rarely observed in nanocrystalline hexagonal closepacked Mg mainly due to its high stacking fault energy. Here, we report transmission electron microscopy observations that provide evidence of deformation twins in a nanocrystalline magnesium-based alloy processed by cryomilling and spark-plasma-sintering. The cryomilled powders result in an average grain size of 25 nm. After spark-plasma-sintering, we found a bimodal grain size distribution with coarse-grains around 500 nm and finegrains of 52 nm. Deformation twins have been observed in nanocrystalline grains smaller than 25 nm in the cryomilled Mg-based powders as well as in the spark plasma sintered sample. However, no evidence of twinning is observed in coarse-grains. These results indicate that the deformation twinning is directly related to the nanocrystalline structure. Deformation twins in nanocrystalline grains along with the reduced grain size presented in this work could lead to unique mechanical properties of nanocrystalline Mg-based alloys.

2:50 PM

Nanotechnology and the Army Research Laboratory: Suveen Mathaudhu¹; ¹U.S. Army Research Laboratory

U.S. Army Research Laboratory (ARL) programs on nanomaterials, nanoelectronics, nanophotonics and nanomagnetics have served as building blocks to innovative solutions for the future Army. Presented in this talk will be an overview of ARL research programs with key examples of successful applications of nanomaterials and nanotechnology, such as bulk nanostructured metals, nano-engineered additives for self-detoxifying surfaces, nano-porous glass-polymer composites and bio-inspired nanostructures.

3:05 PM

140th Annual Meeting & Exhibition

Solid Solutions in Ultra-Fine-Grained Al-Mg Alloys: Richard Karnesky¹; Nancy Yang¹; Chris San Marchi¹; Troy Topping²; Zhihui Zhang²; Ying Li²; Enrique Lavernia²; ¹Sandia National Laboratories; ²University of California, Davis

The microstructure and mechanical properties of various binary ultra-finegrained (d²200 nm) Al–Mg alloys is reported. The composition of alloys spans 0 wt.% Mg (pure Al) to 10.5 wt.% Mg (exceeding significantly the solubility limit). Powders are blended and mechanically alloyed during cryogenic milling in liquid nitrogen to obtain nanocrystalline structures. After cryomilling, powders are hot vacuum degassed and consolidated via hot isostatic pressing and extrusion. Local-electrode atom-probe tomography, X-ray diffraction, and electron microscopy are used with the goals of understanding microstructural evolution as a consequence of the various processing stages and Mg content. Alloys with the highest amounts of Mg exhibit strong Mg segregation to grain boundaries. The impact of this heterogeneous Mg distribution on microstructure and mechanical behaviors is discussed in the context of measured tensile and microhardness properties as a function of thermal exposure.

3:20 PM

Fabrication and Deformation of Bulk Lamellar Nanocomposites under Extreme Rolling Strains: *Nathan Mara*¹; Thomas Wynn¹; Jonathan Ledonne²; Dhriti Bhattacharyya¹; Duncan Hammon¹; Anthony Rollett²; Irene Beyerlein¹; ¹Los Alamos National Laboratory; ²Carnegie Mellon University

In this work, we study composite systems consisting of two immiscible metals, Ag-Cu and Cu-Nb, wherein the individual phases are submicron to nanometer in scale, and the interfacial content is high. The bulk nanocomposites have been produced via severe plastic deformation techniques following three different processes: 1) Casting of nanolamellar eutectic and subsequent rolling (Ag-Cu), 2) Physical Vapor Deposition and subsequent rolling (Cu-Nb), and 3) Accumulative Roll-Bonding (Cu-Nb). We have found that changes in the texture and interface crystallography after SPD can be explained based on predominance of slip in the case of Cu-Nb or predominant twinning in the case of Cu-Ag, as described theoretically by Beyerlein et al. (in this symposium). Interfacial evolution in terms of layer morphology, chemical intermixing, crystallography, and interface plane normal is determined as a function of rolling strain, and then discussed in terms of dislocation/interface interactions.

3:35 PM

Thermal Stability of Nanocrystalline Cu 10at% Nb: *Kris Darling*¹; Suveen Mathaudhu¹; Laszlo Kecskes¹; ¹ARL

Interfacial energy reduction has been suggested to be a superior method to prevent grain growth in nanocrystalline materials. Recently, examples of thermally stabilized nanocrystalline alloys have emerged showing dramatic high temperature stability owing to grain boundary segregation of solutes and the associated interfacial energy reduction. Such samples are typically synthesized through high energy non equilibrium processes and therefore limited to small product geometries such as particles. Furthermore, the very same mechanism responsible for the high thermal stability can often lead to frustrated atomic diffusion and hinder the densification required for production of bulk samples. The primary objective of this study was to delineate the grain growth kinetics of thermally stabilized nanocrystalline Cu 10at% Nb by use of differential scanning calorimetry and micro structural analysis. Knowledge of such grain growth kinetics will establish the appropriate consolidation parameters for successful densification in the future.

3:50 PM Break

4:05 PM Invited

Embedded Binary Eutectic Alloy Nanostructures: *Daryl Chrzan*¹; Swanee Shin¹; Julian Guzman¹; C.-W. Yuan²; Christopher Liao¹; Cosima Boswell-Koller¹; Peter Stone¹; Oscar Dubon¹; Andrew Minor¹; Masashi Watanabe³; Jeffrey Beeman⁴; Kin Man Yu⁴; Joel Ager⁴; Eugene Haller¹; ¹University of California, Berkeley; ²Ludwig-Maximilians Universitat; ³Lehigh University; ⁴Lawrence Berkeley National Laboratory

Ion beam synthesis (IBS) is a powerful method for fabricating a wide variety of nanoparticles embedded within a matrix. Here we use IBS to fabricate GeSn and GeAu nanoclusters within amorphous SiO_2 . The asformed nanocrystals assume a bi-lobed structure with one lobe nearly pure Ge, and the other nearly pure Sn or Au. Pulsed laser melting converts the bi-lobed nanoclusters into a nearly compositionally homogeneous amorphous alloyed state. Subsequent annealing recrystallizes the nanoclusters, and returns them to their initial bi-lobed state. The recrystallization temperature can be tuned by varying the net composition of the nanoclusters. It is suggested that embedded binary eutectic alloy nanostructures might form a basis for a new class of phase change materials with applications in optical storage and static RAM technologies. This research is funded primarily by the U. S. Department of Energy.

4:35 PM

Molecular Dynamics of Fatigue Crack Growth in Nanocrystalline Aluminium: Y. Purohit¹; Ram Mohan¹; ¹NCA&T State University

Comprehensive knowledge of fracture and fatigue of nano-crystalline metals and alloys is essential for their nano-structural applications. Limited experimental and computational studies have been conducted on fatigue damage of metals at nano-scale. Experimental techniques are prohibitive due to limitations of nano samples and advanced microscopic manipulators. In this study, crack propagation under cyclic loading in nano-crystalline Al is investigated via molecular dynamics (MD) simulations. The initial atomic configurations are generated using a Voronoi construction with the dynamic crack growth investigated via MD simulations using embedded atom method. Fatigue loading in a strain-controlled manner with a maximum strain (emax) of 0.035 and a load ratio (emin / emax) of 0.8 are considered. The plastic deformation mechanisms governing fatigue crack advancement such as the emission of dislocations from the crack tip and dislocation sub-structuring, as well as crack growth rates as a function of the stress intensity factor are analyzed and discussed.

4:50 PM

Atomic-Scale Simulations of Straining of Nanocrystalline Palladium along Different Loading Paths: *Dmitry Bachurin*¹; Peter Gumbsch¹; ¹Institut für Zuverlässigkeit von Bauteilen und Systemen (IZBS), Karlsruher Institut für Technology (KIT)

We present the results of molecular dynamics investigations of stress release and repeated straining of fully 3D nanocrystalline palladium structures with mean grain size of 10 nm at room temperature. Previously the sample was uniaxially deformed by compression (up to 6%) at a constant strain rate. Thereafter stress was released at different stages of elastic and plastic deformation. It was found that the sample has an irreversible strain even after unloading from a region corresponding to the elastic stage. Following the stress release, repeated straining was performed in two different mutually perpendicular directions. Simulations revealed very significant differencies in Youngs modulus (up to 25%) for all predeformed samples. Mechanical behavior of computer simulated nanocrystalline palladium during repeated straining will be discussed in details.

5:05 PM

Nanostructured Ti-alloys with Superior Fatigue Properties: *Vladimir Zhernakov*¹; Irina Semenova¹; Salavat Kusimov¹; ¹Ufa State Aviation Technical University

This report is related to the enhancement of the fatigue properties in ultrafine-grained Ti alloys produced by severe plastic deformation (SPD) techniques. To process the Ti alloys, combined SPD techniques that include equal channel angular pressing and thermo-mechanical treatments were used. As a result, the ultrafine-grained Ti materials with a similar grain size of about 300 nm but different in their shape and grain boundary structure (both low- and high-angle, equilibrium and non-equilibrium grain boundaries) were produced. It is shown that tailoring grain boundaries by SPD techniques makes it possible to considerably enhance the strength of Ti materials while preserving high ductility. In turn, ultrafine-grained materials with enhanced strength and ductility demonstrate superior fatigue endurance and life. High innovative potential of nanostructured Ti alloys is also considered and discussed.

5:20 PM

Principles of Control over Fatigue Properties in Ultrafine Grain Ti Materials: *Irina Semenova*¹; A. Yu. Vinogradov²; V.V. Polyakova¹; R.Z. Valiev¹; ¹Ufa State Aviation Technical University; ²Osaka City University

The purpose of this work is to understand the basic principles governing the fatigue behavior of ultrafine grain (UFG) materials manufactured by severe plastic deformation and to formulate the microstructure-based approaches towards controlling the fatigue life and achieving the enhanced durability under low and high cycle deformation. CP Ti Grade 4 was produced using equal channel angular pressing followed by thermal mechanical treatment and annealing. As a result, UFG Ti samples with grain sizes of 120 nm and 1 and 5μ m were produced. In discussion we argue that tailoring grain boundaries by severe plastic deformation techniques makes it possible to considerably enhance the strength of UFG Ti while preserving high ductility. In turn, UFG materials with enhanced strength and ductility demonstrate superior fatigue properties. Finally a simplified modeling framework is proposed to rationalize the experimental findings on the grounds of a dislocation kinetics approach adapted for cyclic deformation.

5:35 PM Concluding Comments

2nd International Symposium on High-Temperature Metallurgical Processing: Ferrous and Nonferrous Metals

Sponsored by: The Minerals, Metals and Materials Society, TMS Extraction and Processing Division, TMS: Pyrometallurgy Committee, TMS: Energy Committee Program Organizers: Jiann-Yang Hwang, Michigan Technological

University; Jerome Downey, Montana Tech; Jaroslaw Drelich, Michigan Technological University; Tao Jiang, Central South University; Mark Cooksey, CSIRO

| Tuesday PM | Room: 18 |
|---------------|-------------------------------|
| March 1, 2011 | Location: San Diego Conv. Ctr |

Session Chairs: Mark Cooksey, CSIRO; Tao Jiang, Central South Univ

2:30 PM

Enhancing the Pelletization of Brazilian Hematite by Adding Boron Bearing Additives: Wei Yu¹; *Deqing Zhu*¹; Tiejun Chun¹; Jian Pan¹; ¹Central South University

One kind of Brazilian hematite is characterized by refractory balling and firing performance, such as poor ballability, higher firing temperatures and lower compressive strength of fired pellets. In this paper, improving the pelletization of Brazilian hematite by adding a boron bearing additive was carried out, and the pelletization parameters was also optimized. In the meantime, the mechanism of boron bearing additive was revealed in the kinetics of crystal grain growth by using LEICA microscopy and its software to measure hematite grain growth. Good qualities of green balls are manufactured with drop numbers above 5.7 times/0.5m, compressive strength higher than 13 Newton per pellet and thermal shock temperature over 620° under the following conditions: 1.2% bentonite, 0.4% boron bearing additive, 7% moisture and pelletizing in disc for 15min. When the green balls were preheated at 1000° for 8min and fired at 1280° for 15min, the



compressive strength of the fired pellets containing boron bearing additive is about 3096 Newton per pellet, which is far beyond the standard requirement for good quality pellets. Compared to the fired pellets without adding any boron bearing additives, the compressive strength of fired pellets containing boron bearing additive is increased by 1225N per pellet. It is revealed that adding boron additive into the hematite pellets help to form more liquid phases, lower the activation energy of the hematite grain growth by 135.24 kJ/mol and augment grain growth rate by 33.60%, leading to higher strength of fired pellets due to forming more coarse and dense recrystallized hematite and energy saving by firing at lower temperatures for shorten time.

2:50 PM

Study on Improving the Quality of Pellet Made from Vale Hematite Pellet Feed: *Vinicius Mendes*¹; Deqing Zhu¹; Marcus Emrich²; Jian Pan¹; Tiejun Chun¹; ¹Central South University; ²CVRD

Some joint projects of studies of hematite acid pellet have been implemented to develop technological solutions for using CVRD hematite pellet feed in Chinese palletizing plant. Beneficial improvements on the pellets quality were achieved by adjusting the blends composition and using new technology of pre-treating the blended pellet feed with High Pressure Grinding Rolls(HPGR) on rotary kiln pellet technology. The drop strength of green balls increased from 3.4 to 6.0 times from 0.5m height, at the same time, the bentonite dosage decreased from 1.5% to 0.7%. The compressive strength of roasted pellets reaches 2500N/pellet. The reduction swelling index of roasted pellets is below 15%. The Reducibility of roasted pellets is also improved markedly.

3:10 PM

Decomposition and Oxidation of Bismuthinite in Nitrogen–Oxygen Atmospheres: *Rafael Padilla*¹; Ricardo Villa¹; Maria Ruiz¹; ¹University of Concepcion

Bismuth is an impurity in copper minerals where it occurs mainly as the mineral bismuthinite (Bi_2S_3). In smelting of copper minerals, most of the bismuth reports to the white metal, as a result, a substantial amount of bismuth accompanies the copper to the electrorefined cathodes. Thus understanding the behavior of Bi_2S_3 at high temperatures is crucial to eliminate bismuth before electrorefining. In this paper, some experimental data on the decomposition/volatilization of bismuthinite in nitrogen- oxygen atmospheres is discussed. The results indicated that in nitrogen atmosphere, bismuth volatilization occurs through a fast decomposition of bismuthinite to metallic bismuth and sulfur with subsequent volatilization of bismuthinit the range 850-1100 °C. Similarly, in the presence of oxygen, bismuthinite decomposes to bismuth too, followed by oxidation to the non-volatile bismuth trioxide at temperatures higher than 750 °C. Both, temperature and partial pressure of oxygen affect significantly the bismuth volatilization and oxidation rates.

3:30 PM

Kinetic Study on Vanadium Oxidation in Low Vanadium Bearing Hot Metal during BOF Process: *Qingyun Huang*¹; Bing Xie¹; Xiaopeng Zhen¹; ¹Chongqing University

Extraction of vanadium from low V-bearing hot metal to slag by BOF process is a successful approach mainly used in China. In order to make oxidation of vanadium as more as possible, the kinetic behavior of vanadium oxidation was investigated under the laboratory condition. Firstly the paper summarized the oxidation mechanism of vanadium recovery from hot metal, then experiments were carried out in induction furnace to understand the oxidation behavior of vanadium. Also, the influence of the composition of final slag on oxidation rate of vanadium was researched. The restrictive step of vanadium oxidation and the expression of reaction rate were obtained. And reasonable temperature system and composition of vanadium slag at the end point were proposed.

3:50 PM

Production of Srontium Metal from Strontium Oxide Using Vacuum Aluminothermic Reduction: *Yeliz Demiray*¹; Onuralp Yücel¹; ¹Istanbul Technical University

In this present study production of strontium metal from its oxide was studied under the pressure of 1 mbar. In the experiments 99 % SrO was used. Effects of Al powder addition (100-200 % of stoichiometric ratio) and time were investigated on recovering of metallic strontium from SrO. Effects of BaO addition and additive concentrations were also investigated. The final residues were examined for their chemical composition. XRD, AAS and Flame Photometer devices were used for chemical analysis. More than 90 % of strontium metal recovery was observed.

4:10 PM Break

4:20 PM

Pyrometallurgical Controls of Silver-residue Smelting in a Short Rotary Furnace: *Atsuhiro Nabei*¹; Ken-ichi Yamaguchi¹; ¹Mitsubishi Materials Corp. Central Research Institute

Wet chlorination process of de-copperized anode slimes is followed by de-chlorination stage in which lead sulphate and metallic silver form silver residue. The silver residue is subsequently reduced to Ag2Se matte and PbO-SiO2 slag to remove lead to the slag in a short rotary furnace. Although this smelting process is proven well in actual operations, few papers have investigated its metallurgical aspect. This paper will describe the effectiveness of controlling parameters adopted at the Naoshima smelter and discuss decisive factors influencing silver loss to PbO-SiO2 slag.

4:40 PM

A Study of Pelletization of Manganese Ore Fines: *Deqing Zhu*¹; Vinicius Mendes¹; Tiejun Chun¹; Jian Pan¹; ¹Central South University

Comparing with the lump manganese ores, fine manganese fines are characterized by large amount and low price. However, they must be agglomerated as EAF (electric arc furnace) feed. In this paper, high quality fired pellets were produced by simulating grate-kiln process to supply the feed for EAF from some imported manganese ore fines containing high combined water, which was pretreated by high press roll grinding. Manganese ore fines assaying 44.47%Mn, 5.89%Fe, 12.09%LOI and with 72.67% ranging between 0.5mm and 8mm, are pretreated up to the specific surface areas of 2764 cm2/g and 84.74% passing 0.074mm by passing the fines through HPGR (high press grinding roller) twice in open circuit. The finely ground manganese fines were mixed with 1.2% bentonite, balled at 15% moisture for 7min in disc pelletizer, the drop numbers, compressive strength and thermal shock temperature of green balls reach 11 times/0.5m, 11 Newton per pellet and 360°, respectively. After the green balls drying in the oven, the dry pellets were preheated at 1050° for 12min and then fired at 1300° for 12min in electric tube furnace, and the compressive strength of fired pellets reaches 2621 Newton per pellet. Therefore, these pellets are high quality burden for blast furnace or electric furnace due to high mechanical strength and high Mn grade of 49.11% and low detrimental elements.

5:00 PM

Microwave Induced Arcing of Metallic Sulfide Bearing Ore Particles: Matthew Andriese'; ¹Michigan Technological University

It has been observed that ore particles of a metallic sulfide bearing ore are readily able to heat by microwave irradiation. Upon heating, an electric arc is often produced between particle interfaces containing chalcopyrite (Ccp), nickel-rich pyrrhotite (Ni-Po), and pyrrhotite (Po) minerals resulting in liquid formation and subsequent fusion of particles. Upon cooling, SEM imaging in back scatter mode shows new phases have formed within the melt. EDS examination of the new phases reveals incongruent melting (Solid1 Solid2 + Liquid) of the peridotite host rock with the liquid containing some amounts of dissolved sulfur. Also formed is a solid solution of the sulfide-bearing minerals (Ccp + Ni-Po) dispersed within the liquid. The newly formed solid solution (or matte) has implication of yielding higher nickel recovery during hydro/pyro metallurgical processes as it may prove difficult or not feasible to separate Ni-Po from Po by conventional methods.

5:20 PM

Reduction of Carbon-burdened Chromite Pellets in the Presence of Additives: *Guanghui Li*¹; Jianchen Li¹; Mingjun Rao¹; Guohua Bai¹; Tao Jiang¹; ¹Central South University

By using thermogravimetry, optical microscope and chemical phase analysis, the solid-state reduction of carbon-burdened chromite pellets in the absence and presence of additives were investigated in this paper. The effects of reduction temperature, reduction time and additives on the metallization of chromite pellet were studied. The results indicate that the pre-reduction ratio of carbon-burdened chromite pellets is improved with the increase of reduction temperature and the presence of additives. The metallization of chromium is increased from 63.9% to 92.8% reducing at 1300 oC for 4h with the addition of 2 wt.% of sodium borate. The reduction of carbon-burdened chromite pellets is diffusion controlled. The apparent activation energy of the reaction without sodium borate is 192.053kJ/mol, while that of the reaction with sodium borate decreases to 170.437kJ/mol.

5:40 PM

Purification of Boron Trichloride by Decomposition of Phosgene in Co. Laser System: *Duygu Agaogullari*¹; Ismail Duman¹; ¹Istanbul Technical University

In this study, COCl_2 was removed from the gas mixture by excitation and molecular level thermal decomposition with 250 W IR CO₂ laser beams. Different ratios of gas mixtures were provided from pure gases stored in steel cylinders. The effects of COCl_2 amount, flow rates of the gas mixtures and exposure time on the COCl_2 decomposition efficiencies were investigated. The decomposition was carried out in a glass reactor which was originally designed and equipped with gas inlet and outlet pipes on its barrel and NaCl windows on each end. Unattacked BCl₃ molecules in the gas mixture absorbed energy from CO₂ laser radiation that is followed by an intermolecular energy transfer to COCl_2 molecules. So, it results in decomposition and CO+Cl_2 formation. Decomposition products were separated by distillation in two different columns externally cooled by ethanol. The COCl_2 decompositions were interpreted with FTIR analysis.

Alumina and Bauxite: Red Mud

Sponsored by: The Minerals, Metals and Materials Society, TMS Light Metals Division, TMS: Aluminum Committee, TMS: Aluminum Processing Committee

Program Organizers: James Metson, University of Auckland; Carlos Suarez, Hatch Associates Consultants Inc

Tuesday PMRoom: 17AMarch 1, 2011Location: San Diego Conv. Ctr

Session Chair: To Be Announced

2:00 PM

Application of Nanofiltration Technology to Improve Sea Water Neutralisation of Bayer Process Residue: *Kelvin Taylor*¹; Mark Mullett¹; Lee Fergusson²; Helen Adamson¹; Juerg Wehrli¹; ¹Hatch & Associates; ²Virotec Global Solutions

Sea Water Neutralization of alkaline Bayer Process Residue is a sustainable solution to turn a hazardous waste material into a benign, non-hazardous material that can be re-used in many applications. The concentrations of the active neutralizing agents in seawater, calcium and magnesium, are low and large volumes of sea water are required to neutralize the alkaline residue. Nanofiltration of seawater can produce a concentrate containing up to four times the calcium and magnesium levels in seawater, while the mono-valent ions, like sodium and chloride, are only marginally concentrated. This significantly reduces the volume of seawater required for the neutralization process and hence the size of neutralization equipment. Other advantages include improved reaction kinetics and reduced salinity of the neutralized residue, making it more suitable for certain applications. The nanofiltration permeate, with lower scaling potential, is also an improved feed for sea water RO plants to produce potable water.

2:25 PM

Caustic and Alumina Recovery from Bayer Residue: Songqing Gu¹; ¹Chalco

Bayer process is not suitable for alumina production from high silica bauxite due to too much caustic and alumina loss in the Bayer residue. The caustic and alumina recovery from the Bayer residue by various processes, such as sintering, lime treatment and hydration process etc, is analyzed and compared theoretically. The most important target to treat Bayer residue for the recovery is to find an efficient DSP containing less alumina and caustic soda by some suitable and less consumption processes.

2:50 PM

Investigation on Alumina Discharge into Red Mud Pond at Nalco's Alumina Refinery, Damanjodi, Orissa, India: Birendra Kumar Mohapatra¹; Barada Kanta Mishra¹; Chitta Ranjan Mishra²; ¹Institute of Minerals & Materials Technology(IMMT); ²National Aluminium Company Limited(NALCO)

Around 14% of alumina gets discharged in to red mud pond from Nalco's alumina refinery, Damanjodi, Orissa. The minerals hosting alumina in red mud have been investigated using Scanning Electron Microscope (SEM) and Electron Probe Micro Analyzer (EPMA). The minerals identified are: gibbsite, goethite, sillimanite, muscovite and kaolinite. The average particle size of red mud is ~8 μ except isolated grains of gibbsite, goethite and rutile which are > 20 μ in size. The gibbsite invariably contains up to 60 mole % of boehmite. The nodular goethite contains over 30-mol % of 'Al' in its lattice and termed as alumo-goethite. Around 34% of Al2O3 are present in muscovite/sillimanite. Studies reveal that most of the minerals in red mud have either alumina in their lattices or are undigested aluminium silicates that do not get dissolved during alumina refining, thus a considerable amount of alumina gets discharged through these phases into the red mud.

3:15 PM Break

3:25 PM

Production of Ordinary Portland Cement(OPC) from NALCO Red Mud: *Chitta Mishra*¹; Devendra Yadav²; M Alli²; P Sharma²; ¹National Aluminium Company Limited; ²National Council for Cement & Building Materials(NCB)

A unique process for production of Ordinary Portland Cement(OPC) from NALCO Red Mud has been successfully developed from a raw mix containing limestone, red mud,shale and fine coal. The raw materials are ground to the required fineness and then blended to prepare the raw mix. The raw mix is fed in to a kiln and fired to a temperature of 1400-1450 degree centigrade to obtain clinker. Clinker was cooled and gypsum was added in to it to obtain OPC. 3-4.5% of NALCO red mud was used for production of OPC. OPC prepared from this clinker confirmed to the requirements of three Indian Standard Specifications for 33, 43 & 53 grade of OPC. The process is most efficient, cost-economic and effectively addresses the environmental problems associated with the waste material red mud generated during the refining of bauxite for manufacture of alumina employing Bayer process.

3:50 PM

Recovery of Metal Values from Red Mud: *Puliyur Krishnaswamy Narasimha Raghavan*¹; Nand Kumar Kshatriya¹; ¹Bharat Aluminium Co. Ltd., (A Unit of Vedanta Resources Plc.,), BALCO Nagar, Korba

In processing bauxite for production of alumina by Bayer's process, huge quantities of red mud is generated which are disposed of as a waste product. The red mud is normally disposed contains caustic soda and therefore poses pollution hazardous and requires storage in specially made large size ponds. This waste material at present does not find any use, hence, in addition to pollution hazardous, considerable expenditure and wastage of land is involved in disposal of this waste material. Hence, it is desirable to recover the oxides of iron, titanium and aluminium from red mud. The process applies to the recovery of alumina,titania and ferric oxide from red mud in Four Steps. Balco's red mud contains 45-47% Fe2O3 and 16-25%



of undigested alumina. The present papers provide an alternative and more environmentally acceptable process for the recovery of iron, titanium and aluminum from Balco's red mud.

4:15 PM

Red Mud Flocculants Used in The Bayer Process: *Scott Moffatt*¹; Frank Ballentine¹; Morris Lewellyn¹; ¹Cytec Industries

Flocculation and separation of red mud is an integral part of the Bayer process. Over the latter half of the 20th century, flocculant technology changed dramatically from natural starches to use of "rationally designed" synthetic polymers. Many of these advancements were due to the introduction of liquid or emulsion based flocculants which enabled elaborate post-reaction chemistry to be done on the polymer backbone. This paper presents a historical overview of milestones of flocculant technology used in the Bayer Process up to the present day. Discussion of flocculants is based on inventions in the published literature that have gained widespread use throughout the industry and will include the benefits/advantages of different flocculant technology for settling red mud.

4:40 PM

Reductive Smelting of Greek Bauxite Residues for Iron Production: *Anthimos Xenidis*¹; C. Zografidis¹; I. Kotsis¹; D. Boufounos²; ¹National Technical University of Athens; ²Aluminium of Greece, SA

The reductive smelting of Greek bauxite residues was investigated for the production of an iron product that meets the minimum industrial requirements as a blast furnace feed. Fine-grained Greek bauxite residues -either as is or in the form of pellets- and solid fuel reducing agents –lignite and coke-, were used as raw materials. The effect of parameters such as the smelting temperature, the amount of the reducing agent in the mixture, the retention time and the addition of fluxes on the quality of the metallic product, as well as the basicity and the desufulfurization capability of the slag, was investigated. The obtained results regarding the chemical properties of the metallic product were very promising, providing input for further research on the optimization of the proposed pyrometallurgical method for the production of an attractive ferrous raw material for the iron ore industry.

Aluminum Alloys: Fabrication, Characterization and Applications: Thermal Mechanical Processing Sponsored by: The Minerals, Metals and Materials Society, TMS

Light Metals Division, TMS: Aluminum Processing Committee Program Organizers: Subodh Das, Phinix LLC; Zhengdong Long, Kaiser Aluminum; Tongguang Zhai, University of Kentucky

| Tuesday PM | Room: 14A |
|---------------|-------------------------------|
| March 1, 2011 | Location: San Diego Conv. Ctr |

Session Chair: Xiyu Wen, University of Kentucky

2:00 PM

Study of the Artificial Aging Kinetics of Different AA6013-T4 Heat Treatment Conditions: *Josef Berneder*¹; Ramona Prillhofer¹; Josef Enser¹; Peter Schulz¹; Carsten Melzer¹; ¹AMAG rolling

Aluminium alloy AA6013 was developed for aircraft fuselage applications and the transportation industry and its attractive combination of mechanical properties, formability, corrosion resistance and weldability makes it ideal for automotive sheet applications. Due to the high strength level of AA6013 in temper T6 it can be considered as a replacement option for commercial steel grades allowing maximum weight savings without losses in strength. In the present work an (i) improved heat treatment cycle for industrial production of alloy AA6013 in temper T4 is presented with the objective to reduce the subsequent time consuming and costly artificial aging. The hereby produced T4 temper sheet material is (ii) analyzed in comparison to standard T4 in terms of artificial aging kinetics and (iii) the process of formation and dissolution of precipitates is studied by using differential scanning calorimeter (DSC).

2:20 PM

Textures and Particle Structures of a Continuous Cast AA3004 Aluminum Alloy after Cold Rolling and Annealing: *Xiyu Wen*¹; Yansheng Liu²; Jingwu Zhang³; Shridas Ningileri¹; Tongguang Zhai¹; Zhong Li⁴; ¹University of KY; ²Secat Inc.; ³State Key Lab of Matastable Materials Science and Technology; ⁴Aleris International Inc.

Measurements of textures of an AA3004 aluminum alloy sheets made from twin belt casting after cold rolling and annealing are carried out by use of the orientation distribution function (ODF) method. The particle structures of the sheet samples are observed and analyzed by use of scanning electronic microscopy (SEM) and Transmission electron microscopy (TEM) as well as X-ray diffractionmeter (XRD). The textures and particle structures resulting from the thermo-mechanical processing are studied and presented.

2:40 PM

Mechanical Properties of Bulk Nanostructured 7075 Al Alloy Prepared by Severe Plastic Deformation: *Yonghao Zhao*¹; Tory Topping¹; Xiaozhou Liao²; Yuntian Zhu³; Enrique Lavernia¹; ¹University of California, Davis; ²The University of Sydney; ³North Carolina State University, Raleigh

Age-hardened 7000 series Al alloys exhibit the highest strength amongst Al alloys and therefore are of interest in the aerospace, transportation, and sports industries. Grain refinement down to the nanometer region by severe plastic deformation is a promising technique for further enhancing the strength of Al alloys. However, precisely how to optimize the mechanical properties of nanostructured aged hardened Al alloys remains a challenge. In this study, the as-received 7075 Al alloys were first homogenized at 500 C for 5 h to form super saturated solid solution, then processed by equal-channel-angular pressing (ECAP), cryo-rolling and high pressure torsion (HPT) techniques, respectively, to form microstructures with different grain sizes ranging from nanometer to micrometer. Post-deformation aging treatments were then performed to introduce GP zones, metastable/stable phases. Precipitation kinetics and responding mechanical properties were finally measured and analyzed. Our work provides basic guidance for optimizing mechanical properties of the age-hardened nanostructured alloys.

3:00 PM

Investigation of High Strain Rate Flow of Aluminum Alloys: Yansheng Liu¹; Xiyu Wen²; Shridas Ningileri²; ¹SECAT Inc; ²University of Kentucky

Industrial produced aluminum panels and parts are stamped or punched at a speed far beyond quasi-static state. Understand the deformation behavior of aluminum alloys at high strain rate is critical to determine the process parameters for a successful production. Both regular hydro-servo tensile test machine and foil tester were applied in the test. The dynamic properties of aluminum alloy sheets and foil were investigated at different strain rate from 0.01/s to 2.5/s. Filtration of wave signal is discussed. The results were used to derive the equations governing the strain-stress relationship at different strain rate. A combined exponent formula gives a good description from low to high strain rate. The test can provide important data for industrial simulation and production design.

3:20 PM

Estimating Response to Hot Rolling of Al-Mn-Mg Alloys from Hot Torsion Testing: Hugh McQueen¹; ¹Concordia University

Enhanced hot rolling and properties for additional forming can be designed from understanding the dependencies of flow stress, malleability, textures and microstructural evolution on temperature, strain rate, pass strains with related intervals and final cooling schedules. Recent hot torsion tests on Al-Mn-Mg at 250-550°C, 0.1-10 /s are made more applicable by comparison to a range of compositions, pretreatments and characterization methods. As in most Al alloys, dynamic recovery enhances the hot workability and subgrain size to such a degree that subsequent static recrystallization (SRX) requires long maintenance at or even above the finishing temperature. With variations dependent on slab thickness, segregation and homogenization, Al6Mn as fine dispersoid raises strength and retards SRX but when large stimulates nucleation; in contrast, Mg is a potent solute hardener reducing subgrain size and promoting SRX.

3:40 PM Break

3:55 PM

A Study on Solute Redistribution during Solution Treatment and Aging Bahavior in a Bi-Layer AA6xxx-AA3xxx Alloy System: *Shahrzad Esmaeili*¹; Ehsan Foroozmehr¹; Lihua Liao¹; Samuel Huberman¹; David Lloyd²; Mark Gallerneault²; ¹University of Waterloo; ²Novelis Global Technology Centre

AA6xxx alloy sheets are used for automotive skin panel applications for their light weight and high strength. The recent invention of Novelis FusionTM technology has allowed the development of novel laminated alloy systems with AA6xxx alloys as the core layers and ductile alloys with superior surface properties as the clad layers. The resulting bi-layer alloy systems can be thermomechanically processed and/or strengthened through conventional thermal treatments. However, the microstructural changes during their processing constitute complex phenomena due to the inherent compositional gradients. The present work examines the effect of solution heat treatment on solute redistribution across the core-clad interfaces in an AA6xxx-AA3xxx system. The solute redistribution is modeled using a finite element analysis combined with physically-based descriptions for the precipitate dissolution and diffusion processes in the bi-layer system. The aging behavior across the interface and within the core layer is also examined using a combination of experimental and modeling approaches.

4:15 PM

Interactive Processes during Non-Isothermal Annealing of an AA6xxx Alloy: *Panthea Sepehrband*¹; Xiang Wang²; Haiou Jin³; Shahrzad Esmaeili¹; ¹University of Waterloo; ²McMaster University; ³Novelis Global Technology Centre

Annealing of precipitation hardening alloys involve interactions between precipitation and recovery-recrystallization processes. A broad range of such interactions in an AA6xxx alloy has been investigated through employing a non-isothermal annealing process during which precipitates nucleate, grow and coarsen. The interactive phenomena and microstructural evolution have been analysed using transmission electron microscopy (TEM), differential scanning calorimetry (DSC), microhardness measurements, and Electron backscatter diffraction (EBSD) analysis. A new computational method to quantify the EBSD results has also been developed. The method enables analysing the early stages of recrystallization, the spatial distribution of recrystallized grains and the evolution of grain size during recrystallization. The combined experimental and computational study has provided new knowledge on the strong effects of precipitate evolution on early stages of annealing processes.

4:35 PM

Microstructural Characterization and Heat Treatments of Different Al-Zn-Mg/Zr Alloys: *Paola Leo*¹; Emanuela Cerri¹; Hugh McQueen²; ¹Università del Salento; ²Concordia University

Two Al-Zn-Mg alloys (Zr modified and not) were investigated by optical microscopy, hardness and tensile tests. The alloys were solutionized (2h at 490°C) and artificially aged at 130,160, 190 and 210°C. Tensile tests were performed at room temperature on as-cast, solutionized and peak aged and the deformed samples annealed at 500°C. For both the alloys at room temperature, the solutionized samples exhibited the best ductility, the peak aged the highest strength and the as-cast alloy the highest strain-hardening rate. The higher average grain size of the Zr alloy does not lead to lower hardness and peak stresses during room temperature (RT) tensile tests. Recrystallization of Zr-modified alloy.

4:55 PM

Effect of Die Entry Angle on Extrusion Responses of Aluminum 6063 Alloy: *Samson Adeosun*¹; Sanmbo Balogun¹; Olatunde Sekunowo¹; Wasiu Ayoola¹; Oluwashina Gbenebor¹; ¹University of Lagos, Akoka

The effect of die entry angles on the mechanical properties of extruded 6063 aluminum alloy at 32°C has been investigated. Mild steel and tool steel dies with entry angles of 15, 30, 45, 60, 75 and 90° were used for the extrusion

and the extruded samples were subjected to mechanical and microstructural tests. The results show that peak extrusion pressure and hardness of extrudes increase with increasing die entry angle which is in agreement with the literature. Good extrusion response by samples was observed in mild steel dies over that of tool steel at entry angles of 45,75 and 90°. Extrusion ratio for the die materials are practically the same except at 450 die entry angle where mild steel die exhibited superior extrusion ratio of 2.1 to that of tool steel of 1.8.

5:15 PM

Hot Deformation Behaviour of 7075 Al Alloy: Hossein Mohammadi¹; *Mostafa Ketabchi*¹; ¹Amirkabir University

7075 Al alloy is one of the most used high-strength materials for aircraft structural components. In the present work, the effect of hot deformation parameters such as temperature and strain rate on the dynamic restoration processes of a 7075 Al alloy was studied. Hot compression tests were performed in the temperature range of 300-500°C and the strain rate range of 0.001-0.1 s⁻¹. The results show that the true stress–true strain curves exhibit a peak stress at a critical strain, after which the flow stresses decrease monotonically until high strains, showing a dynamic flow softening. The peak stress level decreases with increasing deformation temperature and decreasing strain rate, which can be represented by a Zener–Hollomon parameter in the hyperbolic-sine equation with the hot deformation activation energy of 125 kJ/mol.

5:35 PM

Development of Microstructures and Mechanical Properties Aluminum Alloy after Equal Channel Angular Pressing: Miroslav Greger¹; *Ladislav Kander*²; ¹VSB-Technical University Ostrava; ²Material & Metallurgical Research Ltd,

Microstructure and texture development of an aluminum alloy during equal channel angular pressing (ECAP) was investigated and correlated with the mechanical properties. The microstructure was effectively refined by ECAP, and the original fiber texture of the extruded aluminum alloy was disintegrated and a new texture was gradually developed by repetitive ECAP pressing. After 6 ECAP passes following route Bc, the yield stress is lower than for the as-extruded aluminum alloy, indicating that the texture softening is dominant over the strengthening due to grain refinement. Cross-section of original samples was 10 x 10 mm and their length was 45 mm. Deformation forces were measured during extrusion, resistance to deformation was calculated and deformation speed was determined approximately. Analysis of structure was made with use of light microscopy and SEM. Mechanical properties of samples after extrusion were determined by tensile test and by so called penetration test.

Aluminum Reduction Technology: Cells Thermal Balance

Sponsored by: The Minerals, Metals and Materials Society, TMS Light Metals Division, TMS: Aluminum Committee, TMS: Aluminum Processing Committee

Program Organizers: Mohd Mahmood, Aluminium Bahrain; Abdulla Ahmed, Aluminium Bahrain (Alba); Charles Mark Read, Bechtel Corporation; Stephen Lindsay, Alcoa, Inc.

| Tuesday PM | Room: 17B |
|---------------|-------------------------------|
| March 1, 2011 | Location: San Diego Conv. Ctr |

Session Chair: Bernard Allais, Rio Tinto Alcan

2:00 PM

Increasing the Power Modulation Window of Aluminium Smelter Pots with Shell Heat Exchanger Technology: Pascal Lavoie¹; Sankar Namboothiri¹; *Mark Dorreen*¹; John Chen¹; Donald Zeigler²; Mark Taylor¹; ¹Light Metals Research Centre, The University of Auckland; ²Alcoa Primary Metals, Aluminerie Deschambault

With power prices constantly rising, and varying aluminium prices requiring operating flexibility, the financial incentive for smelters to adopt a power modulation strategy is becoming larger. However, the power modulation window, in which a smelter can safely operate its reduction cells, is limited. The Light Metals Research Centre has developed the Shell Heat Exchanger (SHE) technology for controlling the heat dissipation from aluminium smelting potshells. By varying the air flow through the SHE, the heat removal from the potshell can be increased or decreased as desired, allowing for an increased power modulation window with minimal disturbance to the pot thermal balance. This paper presents experimental results from LMRC's test facility, which show the shell temperature response when the SHE is operated in cooling or insulating mode. Steady state thermo-electric model results for these operating scenarios are also presented, outlining the impact on ledge thickness and other pot operating conditions.

2:20 PM

New Approachs to Power Modulation at Trimet Hamburg: *Till Reek*¹; ¹Trimet Aluminium AG

Trimet Aluminium AG acquired the Reynolds technology smelter in Hamburg in 2006 after shut down. The 135 ktpa smelter was restarted successfully in 2007 and is in continuous operation since. The increasing spread of the energy price during night and day time, as well as long term price difference have lead to novel approaches to decrease the average energy price by operating the smelter with non linear energy input. Theoretical calculations were done to estimate the maximum energy difference of cell states. Experiences were gained of the impact on performance vs. modulation range. This paper will present theoretical background as well as practical data of a smelter operating with power modulation.

2:40 PM

Some Aspects of Heat Transfer between Bath and Sideledge in Aluminium Reduction Cells: Asbjorn Solheim¹; ¹SINTEF

A literature review concerning the heat transfer coefficient between bath and sideledge (h) is given. Normally, the heat transfer is controlled mainly by the circulating bath motion due to gas drainage into the peripheral channel. After the introduction of slotted anodes that direct the gas towards the centre channel, it is likely that h will be determined by natural convection in some cases, and an equation is suggested to take this into account. The coupling between heat and mass transfer during melting and freezing of sideledge was studied in a numerical model involving multicomponent diffusion. During freezing, the concentration of bath components other than cryolite is higher at the ledge surface than in the bulk of the bath. The surface temperature of the ledge varies with the rate of freezing and melting in such a way that the variation of the ledge thickness is slower than thought earlier.

3:00 PM

Heat Recovery from Aluminium Reduction Cells: Yves Ladam¹; *Asbjorn Solheim*¹; Martin Segatz²; Odd-Arne Lorentsen²; ¹SINTEF; ²Hydro PMT

About half of the energy spent in aluminium electrolysis is lost as heat. A preliminary study concerning the possibilities of recovering part of that heat was carried out, primarily focusing on electrical power production. The three main heat sources (cathode sides, anode yokes, and gas) were combined in different ways, using different types of power cycles. The potential for electric power production is significant (up to 9 percent of the total consumption). The two most promising families of power cycles appear to be 1) distributed open Brayton cycle based on a turbo charger and 2) centralised power production with a Rankine cycle. The temperature and amount of heat available in the anode match well with the heat from the sides, while the potential of integrating the flue gas is limited. The main aims in energy recovery may be increased productivity or reduced energy consumption, which gives different strategies for heat collection.

3:20 PM Break

3:30 PM

Effects of Composition and Granulometry on Thermal Conductivity of Anode Cover Materials: *Hasini Wijayaratne*¹; Margaret Hyland¹; Mark Taylor¹; Ionela Grama²; Tania Groutso¹; ¹Light Metals Research Centre; ²University of Auckland

Thermal conductivity of anode cover material is critical in determining cell top heat loss. It has been observed that thermal conductivity of cover material is strongly dependent on packing and particle size distribution. Granular material that is densely packed (lower voidage) has higher thermal conductivity. When two sizes of spherical particles are mixed at various size ratios, the theoretical voidage can be reduced from 0.4 to 0.2-0.3. This can be applied to a particle system of crushed bath and alumina that constitute cover material. Currently, many smelters produce cover material that is too fine with high voidages. This has the effect of lowering the thermal conductivity which can cause unnecessary operational problems within the cell. Additionally, the effect of cover composition on thermal conductivity is not obvious. This paper describes studies conducted in the laboratory to understand the effects of composition and voidage on thermal conductivity of cover material.

3:50 PM

Multiblock Monitoring of Aluminum Reduction Cells Performance: *Jayson Tessier*¹; Carl Duchesne²; Gary Tarcy³; ¹STAS; ²Aluminium Research Centre-REGAL; ³Alcoa

Aluminum reduction cell performance are affected by many factors. In order to efficiently understand possible causes of performance upsets, all major sources of variations have to be monitored. This implies monitoring all anode and alumina properties, as well as pot state and manipulated variables, while also taking into account pot design or integrity after startup. Considering the high number of variables involved in such a task, this is practically impossible using typical statistical process control tools. The problem is worst when applied on a pot basis. This paper proposes the use of multiblock PLS (MBPLS) to build a monitoring scheme on a pot basis, simultaneously taking into account the influence of alumina and anode properties, of pot state and manipulated variables, as well as the pot state following its start-up. Derived from a regression model, the monitoring policy ensures that only variations relevant to pot performance variations are highlighted.

4:10 PM

Towards a Design Tool for Self-Heated Cells Producing Liquid Metal by Electrolysis: *Sophie Poizeau*¹; Donald Sadoway¹; ¹Massachusetts Institute of Technology

As part of an effort to assess the technical feasibility of producing metals by molten salt electrolysis, a design tool is under development for the purposes of estimating the threshold cell size and current for self-heating operation. To make the model broadly applicable to the production of different metals, two major issues must be addressed. First, accurate values of the heat transfer coefficient are required in order to model the position of the ledge. In the Hall-Héroult cell, the heat transfer coefficient is determined experimentally from industrial operation, an approach that is not possible for a cell that has never been built. Second, thorough treatment of transport phenomena in the cell involves solving the equations for liquid and gas flows simultaneously; however, the methods used to model the turbulent flows in the Hall-Héroult cell are usually not well coupled.

4:30 PM

Restart of 300kA Potlines after 5 Hours Power Failure: Xinliang Zhao¹; Bingliang Gao²; Hua Han¹; Jie Liu¹; Jiuyi Xiao¹; Jianxun Qian¹; ¹Keao Aluminium Company; ²Northeastern University, China

A Chinese reduction plant has an installed capacity of 140 kt of metal per year and employs 180 pots with line current of 300kA. In May, 2008, power failure happened. The situation lasted 5 hours. The bath temperatures fell to 900°C below. Power was switched on after recovering the power system. At the initial stage of restart the anode effect frequency was high. The voltage and amperage of lines fluctuated severely, which caused higher anode effects. The situations may cause rectiformer failure. We finally solved the problems and led the lines to the normal status. The paper discusses the strategies adopted; restart operations and the technological parameter normalization during restart.

Approaches for Investigating Phase Transformations at the Atomic Scale: Other Systems and Transformations

Sponsored by: The Minerals, Metals and Materials Society, ASM International, TMS Materials Processing and Manufacturing Division, TMS/ASM: Computational Materials Science and Engineering Committee, TMS/ASM: Phase Transformations Committee *Program Organizers:* Neal Evans, Oak Ridge National Laboratory; Francisca Caballero, Spanish National Research Center for Metallurgy (CENIM-CSIC); Chris Wolverton, Northwestern University; David Seidman, Northwestern University; Rajarshi Banerjee, University of North Texas

| Tuesday PM | Room: 32B |
|---------------|-------------------------------|
| March 1, 2011 | Location: San Diego Conv. Ctr |

Session Chairs: Mark Asta, University of California - Berkeley; Jeffery Hoyt, McMaster University

2:00 PM Invited

A Molecular Dynamics Study of the Cavitation Pressure in Liquid Al: Jeffrey Hoyt¹; Alice Potter¹; ¹McMaster University

During the casting of alloys density differences between the liquid and solid and/or thermal stresses establish a flow of liquid from the dendrite tips to the dendrite roots. If the pressure drop which drives the liquid filling is sufficiently large, voids can nucleate in the liquid, leading to a deleterious casting defect known as hot tearing. The critical pressure at which cavities can nucleate is an important parameter in models of hot tearing and in this study we have employed molecular dynamics simulations and an embedded atom description of Al to derive the cavitation pressure in the liquid. The cavitation pressure as a function of system size has been computed and the results are compared to classical nucleation theory. In addition, the cavitation pressure has been studied for heterogeneous void nucleation at the solid-liquid interface and with the addition of trace amounts of solute (Mg).

2:25 PM

Defect Structure at Rocksalt/Tetradymite-Telluride Interfaces: *Douglas Medlin*¹; J. Sugar¹; N. Heinz²; T Ikeda²; G. Snyder²; ¹Sandia National Labs; ²California Institute of Technology

Chalcogenide compounds based on the rocksalt and tetradymite structures possess good thermoelectric properties and are of emerging interest in thermoelectric nanocomposites, where the aim is to improve thermoelectric energy conversion efficiency by harnessing phonon scattering processes at embedded heterophase interfaces. Here, we discuss our work on the interfacial structure of tetradymite precipitates in rocksalt-structured tellurides, focusing on Sb₂Te₃ precipitates in PbTe and AgSbTe₂. We discuss the particular aspects of interfacial coherency at rocksalt/tetradymite interfaces, laying out the formal crystallographic description of interfacial defects in these systems, and using this description to interpret transmission electron microscopy observations of the interfaces obtained through both HRTEM and weak-beam dark-field methods. From these results, we identify a defect that can accomplish the rocksalt-to-tetradymite phase transformation through diffusive-glide motion along the interface and we clarify the mechanisms of interfacial strain accommodation and the relationship of the step and dislocation structure to the tetradymite precipitate morphology.

2:40 PM

Phase Transformation Identification in Beta Titanium Alloys Using ETMT, Gleeble and SSDTA: *Yufeng Zheng*¹; Robert Williams¹; Boian Alexandrov¹; John Lippold¹; Hamish Fraser¹; ¹The Ohio State University

Beta titanium alloys are promising candidates for future biomedical implants as well as high temperature aerospace applications. Developing an understanding for the microstructural evolution in beta titanium alloys is critical for tailoring mechanical properties. Omega phase and b' phase are widely believed to be precursors of alpha precipitates during an intermediate temperature aging process. Using state of the art equipment, the onset of alpha precipitates formation in beta titanium alloys can be identified precisely using electrical resistivity measurement by the Electro-Thermo-Mechanical Tester (ETMT). Therefore, the ETMT has provided the ability for a detailed study of the microstructure and composition evolution during the initial stage of alpha precipitation formation with transmission electron microscopy (TEM). The phase transformation sequence is also compared with the result of the single sensor differential thermal analysis (SSDTA). The microstructure evolution in Ti- Xwt%Mo binary alloy will be introduced to illustrate the power of the method above.

2:55 PM

Investigating Omega Precipitation in Titanium Alloys at the Atomic Scale: Arun Devaraj¹; *Soumya Nag*¹; Robert Williams²; Srinivasan Rajagopalan³; Srinivasan Srivilliputhur¹; Hamish Fraser²; Rajarshi Banerjee¹; ¹University of North Texas; ²The Ohio State University; ³Exxon Mobil Corporation

The omega phase is commonly observed in beta or near-beta titanium alloys on quenching from above the beta-solutionizing temperature. These omega precipitates are highly refined (nanometer scale), homogeneously distributed, and can potentially act as heterogeneous nucleation sites for the precipitation of the equilibrium alpha phase. The present study primarily focuses on omega precipitation within the beta (body-centered cubic or bcc) matrix of simple model binary titanium-molybdenum (Ti-Mo) alloys. Direct atomic scale observation of pre-transition omega-like embryos in quenched alloys, using aberration-corrected high-resolution scanning transmission electron microscopy coupled with 3D atom probe tomography will be presented. First-principles computations have been performed using the Vienna ab initio simulation package (VASP) to determine the minimum energy path for the beta to omega transformation in Ti-Mo alloys with upto 20wt%Mo and the results of these computations will be compared and contrasted with the results from the HAADF-HRSTEM and 3DAP characterization studies.

3:10 PM Break

3:25 PM Invited

Computational and Experimental Investigations of Core-Shell Precipitates in Al-Sc-Li Alloys: *Mark Asta*¹; Colin Ophus²; Abhay Raj Singh Gautam²; Marta Rossell²; Emmanuelle Marquis³; Velimir Radmilovic²; Uli Dahmen²; ¹University of California, Berkeley; ²Lawrence Berkeley National Laboratory; ³University of Michigan

Two-step aging treatments in ternary Al-Sc-Li alloys have been shown to lead to the formation of highly monodisperse coherent core-shell precipitates with Al3Sc-based cores and Al3Li-based shells. In this talk we will discuss insights into the thermodynamic driving forces and kinetic pathways leading



to the formation of these precipitates, gained through a combination of advanced electron-microscopy techniques, small-angle X-Ray scattering, atom-probe tomography and first-principles computational modeling. Detailed measurements of compositional distributions within the precipitate establish the presence of appreciable levels of Li in the core phase, which is present even after very long annealing times. The origins of the observed Li partitioning and its effect on nucleation kinetics is analyzed with the aid of first-principles based Monte-Carlo simulations.

3:50 PM

Remarkable Microstructural Stability of Cu-Based Ternary Alloys during High Temperature Annealing: *Xuan Zhang*¹; Nhon Vo¹; Pascal Bellon¹; Robert Averback¹; ¹UIUC

The microstructural evolution of dilute Cu-based ternary Cu-W-Nb alloys under high temperature annealing was investigated by both experiments and Kinetic Monte Carlo simulations. Experiments using TEM/STEM and x-ray diffraction show that while annealing of Cu90Nb10 at 600C leads to extensive coarsening, with precipitate sizes greater than 40nm, the addition of only 1.5 at% of W dramatically suppresses this precipitate growth. The average precipitate size in the ternary alloy reaches only ~ 18nm at 700C, and then, surprisingly, decreases on annealing at higher temperatures. The precipitate size distribution, moreover, is bimodal. Kinetic Monte Carlo simulations provide insight for understanding these observations. Using kinetic and thermodynamic parameters representative of the experimental Cu-W-Nb system, we find that a subtle combination of the very low mobility of one of the solute components (W), and of its very low solubility, can explain the experimental results. Extension to other systems with refractory precipitates is discussed.

4:05 PM

Ab-Initio Calculation of the Phase Stability of Mechanically Unstable High-Temperature Phases: Nikolas Antolin¹; Oscar Restrepo¹; *Wolfgang Windl*¹; ¹Ohio State University

Ab-initio calculations have been hugely successful in the past decade to provide the necessary free energies to predict phase transformations and phase stability for elemental and alloyed materials. The application of abinitio methods, however, is problematic when it comes to model metals and their alloys with mechanically unstable high-temperature phases, such as the bcc high-temperature phases of Ti, Zr, Hf, or U. In this study, we propose an approximate first principles approach, considerably simpler and more efficient than previous methods, to calculate free energies of elemental and alloy phases, materials constants, and defect energies while addressing the problems of phase instability. We show examples for phase stability and transformations, defect energies and mechanical properties for systems with unstable high-temperature phases, including Ti alloys, metallic uranium, and NiTi shape memory alloys.

4:20 PM

Effect of Dilute H on Phase Transformations near Hcp Zr Crack Tip: Margarita Ruda¹; Graciela Bertolino²; *Diana Farkas*³; Peter Evans³; ¹CAB-CNEA; ²CONICET; ³Virginia Tech

We present atomistic studies of the deformation mechanisms occurring in the crack tip region during low temperature fracture of hcp Zr. Several competing processes are involved, including the phase transformation to the bcc structure. Other major mechanisms which are responsible for ductility are twinning and dislocation emission. For the cases in which a phase transformation to bcc is observed, it results in a considerable improvement in ductility. A dilute amount of H impurities placed at different distances from the crack tip significantly affects the competition between crack propagation, twin generation and phase transformations in the crack tip region. In particular, the presence of H can modify the size of the transformation region and can lead to an increase in ductility.

4:35 PM

Precipitation of Prismatic Plates in Mg-0.3Ca-(0.3-1)in (at%) Alloys: *Chamini Mendis*¹; Keiichiro Oh-ishi¹; Tadakatsu Ohkubo¹; Kazuhiro Hono¹; ¹National Institute for Materials Science

Addition of over sized elements like RE and Ca in Mg alloys with a small amount of undersized elements like Zn and Al often cause the precipitation of basal plates, e.g., internally ordered GP zones in Mg-RE-Zn, Mg-Ca-Zn, and Mg-Ca-Al alloys. However, for effective age hardening response, precipitation of prismatic plates is proposed to be more effective. In this study, we report the precipitation of a high number density of thin prismatic plates in Mg-0.3Ca-In alloys. Optimized In additions led to the enhancement of age hardening response 3 times higher than that for the binary Mg-0.3Ca alloy. The peak aged Mg-0.3Ca-1.0In alloys consisted of uniformly dispersed prismatic plates with three atomic layers. The morphology, size and composition of the precipitates in the Mg-0.3Ca-1.0In alloys were characterized by TEM, HAADF and 3DAP, and the mechanism of the formation of the precipitates on the prismatic planes will be discussed.

4:50 PM

Strengthening Precipitate Phases in the WE43 Alloy at Peak Hardness: Shengjun Zhang¹; Gregory Olson¹; ¹Northwestern University

The precipitates in the WE43 alloy aged to peak hardness at 250°C have been characterized by local-electrode atom-probe (LEAP) tomography. The accurate chemical compositions of the matrix and the precipitates were determined and compared with the results calculated using the Mg-Nd-Y thermodynamic database. In parallel, the theoretical strengths of pure Mg and the Mg with yttrium along the prismatic and basal directions have been investigated by means of first-principles calculations with the highly-precise full-potential linearized augmented plane-wave (FLAPW) method within the method of ab initio tensile test. Both experimental and theoretical investigations show that the majority of yttrium and neodymium goes to the strengthening precipitates, and the remains in the hcp Mg-rich matrix contribute to the good toughness and ductility. This work provides an important calibration point for quantitative modeling of precipitation strengthening for high performance Mg alloys design. Work supported by U.S. Army Research Laboratory.

Biological Materials Science: Biomedical Materials, Implants and Devices

Sponsored by: The Minerals, Metals and Materials Society, TMS Electronic, Magnetic, and Photonic Materials Division, TMS Structural Materials Division, TMS: Biomaterials Committee *Program Organizers:* Jamie Kruzic, Oregon State University; Nima Rahbar, University of Massachusetts, Dartmouth; Po-Yu Chen, University of California, San Diego; Candan Tamerler, University of Washington

| Tuesday PM | Room: 15A |
|---------------|-------------------------------|
| March 1, 2011 | Location: San Diego Conv. Ctr |

Session Chairs: Marian Kennedy, Clemson University; John Nychka, University of Alberta

2:00 PM Invited

Biomaterial Advances and Failure in Total Joint Replacement: Roy Bloebaum¹; ¹University of Utah/ VA Medical Center

A historical review of the use and the application of biomaterials for cementless fixation and bearing surfaces in total joint replacement will be presented. An argument will be made that the history of what made the materials work is often ignored to the detriment of the patients and industry. Also experimental flaws that continue to be made when developing or selecting a material for cementless fixation or a load bearing surface in total joint replacement will be presented. The goal is that by understanding the history, success and failures of new and proven biomaterials that patient care will no longer be compromised thereby preventing industry medical legal complications as well.

2:30 PM

Can Mechanical Properties of Bioactive Glass-Ceramics be Improved Without Sacrificing Their Bioactivity?: *John Nychka*¹; Satadru Kashyap¹; Hamidreza Pirayesh¹; ¹University of Alberta

Whilst bioactive glasses have been used as implant materials for many years they lack sufficient mechanical properties for a wide range of applications. This presentation will discuss different strategies for processing fixed compositions of bioactive glasses in order to change their properties via phase transformations. For example, crack deflection and thermal shock resistance can be substantially increased. Analysis of the effects of phase transformations on bioactivity is presented along with characterization of the glass-ceramics.

2:50 PM

Mechanical and In-Vitro Behaviour of Alumina and Zirconia Based Bioceramics: Ajoy Pandey¹; Usha Jena¹; Debika Mandal¹; *Koushik Biswas*¹; ¹Indian Institute of Technology Kharagpur

Yttria/ceria stabilized zirconia (Y/C-SZ) and yttria/ceria stabilized zirconia toughened alumina (Y/C-SZTA) powders were synthesized by coprecipitation technique and conventionally sintered to full density. Polished (Ra=0.03\956m) samples were subjected to fretting (ball on disc) and sliding (pin on disc) wear at different loads for 10⁵ cycles taking (WC)/UHMWPE as counter body. The surface roughness, wear depths and wear volumes were estimated by surface profilometer from the surface scan of the worn profile. From the measured wear volume, specific wear rates were calculated. Hydrothermally treated (for 20-100 h in presence of simulated body fluid at 134°C/ 0.2 MPa) specimens were subjected to wear and found that the wear rates were different for different compositions and are influenced by the extent of phase transformation (tetragonal to monoclinic) during ageing. Biocompatibility (Osteoconduction) test of the developed materials were for various ageing times (1-4 weeks) by subjecting the specimens in SBF solution at 37°C.

3:10 PM

Effects of Nanocrystalline Calcium Deficient Hydroxyapatite on the Resorption of Conventional Glass Ionomer Cements (GIC): Sumit Goenka¹; Rajkamal Balu²; T. S. Sampath Kumar²; ¹Visveswaraya National Institute of Technology (VNIT), Nagpur, India; ²Indian Institute of Technology Madras (IITM), Chennai, India

The study focuses on developing a GIC-Calcium deficient hydroxyapatite (CDHA) composite with improved resorption properties of the cement. Nano-crystalline CDHA was synthesized via accelerated microwave synthesis and characterized using X-Ray Diffraction (XRD) and Fourier Transform Infrared Spectroscopy (FTIR). CDHA was mixed in 5%, 10%, and 15% with GIC as substitution, maintaining powder to liquid ratio and capsules of dimensions 8mm x 4mm diameter were made. XRD and FTIR of capsules showed increased crystallinity and characteristic apatite bands with increased CDHA content Scanning Electron Microscopy (SEM) showed the surface morphology. The capsules were kept at 37° C in deionized water (pH=7) to check for ionic release via Inductive Coupled Plasma Spectroscopy (ICP) and demineralized solution (pH=5) for weekly weight loss study of 4 weeks. The ionic release and %weight loss were found to increase with increasing CDHA, whereas micro-hardness was found to decrease with CDHA substitution using Vickers micro hardness test.

3:30 PM

Spark Plasma Sintering of Complex Shape HAP-CNT Composites: Yen-Shan Lin¹; Marc.A Meyers¹; Eugene.A Olevsky²; ¹UCSD; ²SDSU

Hydroxyapatite (Ca10(PO4)6(OH)2 - HAP) is an attractive biocompatible material which can be utilized for implant fabrication. However, its insufficient mechanical strength limits its implementation in major load bearing components. In this study, carbon nanotubes were employed to enhance the mechanical properties of hydroxyapatite due to their unique mechanical properties. An HAP powder and carbon nanotubes were mixed through ultrasonication and freeze drying; the produced composite powder mixtures were consolidated by spark plasma sintering (SPS) process. 2vol%CNT-HAP,0.5vol%CNT-HAP and pure HAP powders were sintered at 900C with dwelling time of 5 min. It is shown that the CNT-HAP composites exhibit higher nano-hardness values and elastic modulus in comparison with pure HAP-based components. The retention of the carbon nanotubes in the HAP matrix during SPS was confirmed by SEM analyses. Furthermore, the feasibility of the fabrication of complex shape CNT-HAP components via SPS is demonstrated as a possible venue for dental implant applications

3:50 PM Break

4:00 PM

Nanopillared Metal Stent for Superior Endothelialization and Controlled Drug Release: Karla Brammer¹; Mariana Loya¹; Sungho Jin¹; ¹UC San Diego

Due to the late-stent-thrombosis concerns and limited endothelialization associated with drug-eluting stents, bare metal stents are receiving much attention in recent years. We have created radially emanating high aspect ratio metallic nanopillar structures on the surface of MP35N (Co-Ni-Cr-Mo) stent alloy wires using an argon RF plasma processing technique. It is shown that superior endothelial cell growth is also combined with a well organized monolayer formation and improved endothelialization on the nanopillar structure. Additionally, the nanopillar structure with deep grooves in between offers a much increased surface area and adds an important capability for trapping drugs and controlled release for therapeutics. We believe that these optimistic findings are likely to contribute to new surface design concepts for bare metal stents, eventually lead to medical advances toward mitigating stent thrombosis and restenosis, and eliminate the need for polymer modified stent surfaces.

4:20 PM

Corrosion Products of Iron Wire Arterial Implants from In Vivo and In Vitro Studies: Daniel Pierson¹; *Jacob Edick*²; Justine Farina¹; Jonathan Zuidema¹; Donisha Das¹; Nikki Long¹; Jon Stinson²; Heather Getty²; Jaroslaw Drelich¹; Jeremy Goldman¹; ¹Michigan Technological University; ²Boston Scientific

Pure iron has been proposed as a bioabsorbable stent material due to its biocompatibility and mechanical strength. Presently, the degradation products and mechanisms of iron corrosion in an artery are largely unknown. In the present study, iron wire was implanted into either the abdominal rat aortic wall or lumen to simulate the implantation of an iron stent. In both implantation environments, the corrosion product hematite was produced on the surface of the implanted iron wire. In vitro studies revealed that iron plates submerged under culture medium or first encapsulated in fibrin exhibited similar corrosion product as the implant. The formation of the hematite corrosion product on the aortic wire implant, the submerged iron plate, and the iron plate encapsulated in fibrin suggests that cell culture medium may act as a realistic bio-simulating solution for investigating iron corrosion in vitro and that encapsulation within a networked extracellular matrix may promote bio-corrosion.

4:40 PM

Surface Patterning Effects on Wear and Friction in Metal-Polymer and Metal-Metal Contact: Caleb Eljach¹; Marian Kennedy¹; John DesJardins¹; *Nathan Mitchell*¹; ¹Clemson University

Interest in the friction and wear properties of joint materials has resulted in some studies on the effect of micropatterned surfaces on the frictional coefficient during sliding contact while under lubricated conditions. Our study focuses on the effect of pattern geometry and feature size using 316 steel. We will present data on the affect of the pattern geometry (holes, pillars and ovals) and surface feature size (10, 50 and 100 um) of 316 stainless steel on its frictional when in contact with either a stainless steel or polyethylene. All samples were fabricated by a proprietary process by Hoowaki Inc and initial results will include characterized for surface uniformity and pattern aspect ratio. The coefficient of friction was measured for each surface (smooth, 10um round holes, 50um round holes, and 100um round holes) using a CETR system. All testing was done using both a stainless steel pin and a polyethylene pin.

5:00 PM

Bi-functional Chimeric Peptide Coatings for Improved Osteointegration of Titanium Implants: Hilal Yazici¹; *Mustafa Gungormus*²; Mehmet Sarikaya²; Candan Tamerler²; ¹Istanbul Technical University; ²University of Washington

The problems associated with osteointegration remains to be the main cause of failure of titanium implants into bone and dental tissues. To date, many of the surface modification techniques to improve integration of bone into implants rely on the chemical and physical tailoring of the substrates which otherwise contain biologically undesirable hostile surfaces leading to undesirable reactions. We demonstrate the use of chimeric peptide motifs as surface coatings towards improving osteointegration. The genetically designed, robust bi-functional peptide coatings require no specially prepared biological environment in binding to implant surfaces and could be linked to bioactive entities. The bi-functional peptides consist of both titaniumbinding and mineralization-directing components. Solution and cell-based in vitro mineralization assays show that the peptides significantly increase the mineral formation on the implant creating an osteoconductive surface for cell attachment and proliferation. Research is supported byNSF-MRSEC, NSF-BIOMAT, TUBITAK-NSF IRES Joint Projects, and TR-SPO.

5:20 PM

Mechanical Behavior of a Biological Beta-Ti Alloy: *Sudhakar Vadiraja*¹; ¹Montana Tech

β-titanium alloys are developed as high-efficient biomedical alloys because of their high strength, high fracture toughness, good workability, low elastic modulus, and excellent corrosion resistance as opposed to commonly used a+β type titanium alloys. The presently investigated β-titanium alloy (Ti-15V-3Al-3Cr-3Sn) was subjected to annealing treatment to maximize its forming characteristics. The mechanical properties; yield strength, tensile strength, %elongation in addition to hardness and impact strength were evaluated. The microstructural constituents were examined using HiRox digital microscope. The fracture morphology was also investigated using SEM to characterize the mode of fracture. The biological beta-Ti alloy exhibited a good combination of tensile and impact properties. The microstructure revealed the presence of stabilized beta phase with alpha particles. The fractography revealed a typical ductile fracture demonstrating its good level of toughness.

5:40 PM

Effects of Extrusion and Heat Treatment on the Mechanical Properties and Bio-Corrosion Behaviors of Mg-Nd-Zn-Zr Alloy for Biomedical Applications: Xiaobo Zhang¹; Guangyin Yuan¹; Lin Mao¹; *Guohua Wu*¹; Wenjiang Ding¹; ¹Shanghai Jiaotong University

Room temperature mechanical properties and biocorrosion behaviors of Mg-3Nd-0.2Zn-0.4Zr (NZK) alloy prepared at different extrusion temperatures, as well as heat treatment, were studied. The mechanical properties of magnesium alloy at room temperature improve significantly after extrusion and heat treatment compared to as-cast alloy. The results of mechanical properties show that the yield strength (YS) decreases apparently with increasing extrusion temperature. The tensile elongation decreases a little while the ultimate tensile strength (UTS) has no obviously difference. The yield strength and ultimate tensile strength improve clearly after heat treatment at 200°C for 10 hours compared with that at extrusion state, which can be mainly contributed to the precipitation strengthening. The biocorrosion behaviors of the NZK alloy were studied using immersion tests and electrochemical tests. The results reveal that the extruded NZK alloy and the aging treatment on the extruded alloy show much better biocorrosion resistance than that at solid solution state (T4 treatment). The corrosion mechanism is regarded as uniform corrosion.

Bulk Metallic Glasses VIII: Structures and Mechanical Properties II

Sponsored by: The Minerals, Metals and Materials Society, TMS Structural Materials Division, TMS/ASM: Mechanical Behavior of Materials Committee

Program Organizers: Gongyao Wang, University of Tennessee; Peter Liaw, Univ of Tennessee; Hahn Choo, Univ of Tennessee; Yanfei Gao, Univ of Tennessee

| Tuesday PM | Room: 6D |
|---------------|-------------------------------|
| March 1, 2011 | Location: San Diego Conv. Ctr |

Session Chairs: Katharine Flores, The Ohio State University; Michael Atzmon, University of Michigan

2:00 PM Invited

High Heating Rate Crystallization Behavior of a Zr-Based Metallic Glass: Insights into Glass Structure: *Katharine Flores*¹; Hongqing Sun¹; ¹The Ohio State University

Metallic glasses exhibit a pronounced asymmetry in their critical cooling and heating rates required to prevent crystallization. This has been attributed to the presence of pre-existing phase separation or quench-in nuclei that accelerate the crystallization process upon heating. The crystallization temperature increases with heating rate, suggesting that critical steps in the crystallization process may be bypassed at high heating rates. The present study examines the crystallization mechanisms for a Zr-based bulk metallic glass heated at 0.167 K/s–50 K/s. Crystallization at low heating rates results in nanocrystallization, while micro-scale spherulites form at high heating rates. The activation energy required for spherulite formation is markedly lower than that for nanocrystallization, contributing to the asymmetry in critical heating and cooling rates. TEM analysis reveals no compositional difference at the interface between the crystallized spherulite and amorphous parent material, suggesting that the structure of the spherulites may provide insight into the glass structure.

2:20 PM

Investigation of Elevated Temperature Effect on the Mechanical Behaviors of a Thin Film Metallic Glass Cu52Zr48: *Jianjun Pang*¹; Yuchan Liu²; Ming-Jen Tan¹; ¹Nanyang Technological University; ²Singapore Institute of Manufacturing Technology

An amorphous thin film Cu52Zr48 was grown on a Si substrate. The mechanical properties at the elevated temperatures were characterized through the instrumented nanoindentation. It was found that the displacement bursts in the loading process are facilitated as the temperature increases, i.e., very few burst events occur at the room temperature while they do more commonly at higher temperatures. Additionally, the indentation size effect (ISE) was probed. Interestingly, the reduced modulus shows more significant ISE rather than the hardness especially at higher temperatures. In other words, the modulus decreases with increasing indentation depth while the hardness holds almost constant throughout the range of test depths.

2:30 PM Invited

Nanoscale Mechanics and Medium Range Order in Bulk Metallic Glasses: *Don Stone*¹; Zenon Melgarejo¹; Jinwoo Hwang¹; Jon Puthoff¹; Joseph Jakes²; Hongbo Cao¹; Chuan Zhang¹; Eren Kalay³; Matthew Kramer³; Paul Voyles¹; ¹University of Wisconsin; ²USDA Forest Products Laboratory; ³Iowa State University/Ames Laboratory

Broadband nanoindentation creep (BNC) measures hardness of Cu-Zr and Cu-Zr-Al metallic glasses across 5-6 decades in deformation rate. The experiments generate activation volume data across a wide enough range of flow stress to test atomistic theories of plastic deformation and to detect subtle differences in behavior depending on composition and annealing. For instance, BNC-based estimates place the shear transformation zone (STZ) size at between about 150 and 600 atoms, depending on composition, which falls in the regime of medium range order (MRO). Additional information about MRO is gained from fluctuation electron microscopy (FEM), which reveals the "graininess" of the structure at nanometer length scales. FEM experiments demonstrate an ordering length scale of 1.7-2.5 nm in Zr-Cu metallic glass. Annealing experiments demonstrate quantitatively the structural relaxation of our metallic glass samples including an increase in STZ size.

2:50 PM

Mechanical Polarization of Cu50Hf41.5Al8.5 Bulk Metallic Glass: *Rainer Hebert*¹; Arif Mubarok¹; ¹University of Connecticut

Structurally relaxed Cu50Hf41.5Al8.5 bulk glasses were elastically compressed for up to 50 hours at loads of approximately 70 % of the yield strength. The effect of the static elastic compression on the bulk glass was examined with temperature-modulated thermomechanical analysis (MTMA) in directions parallel and perpendicular to the compression direction. The MTMA studies reveal anisotropy in the non-reversible length changes. Non-reversible length reductions with heating are more pronounced parallel to the loading direction and less pronounced perpendicular to the loading direction compared to structurally relaxed samples that were not elastically loaded. The MTMA results are compared with results of X-ray studies and are furthermore analyzed with an activation energy spectrum approach. It is proposed that the static elastic compression induces a re-orientation of atomic bond orientations and that the MTMA results reflect the tendency of the glass to regain an isotropic atomic bond distribution upon heating.

3:00 PM Invited

Multiscale Mechanical Studies for Investigating the Role of the Metallurgical Structure on the Mechanical Properties of Metallic Glasses: *Jian Lu*¹; Y. Yang²; C.T. Liu²; Q. Wang²; J.C. Ye²; P. Liaw³; ¹City University of Hong Kong; ²The Hong Kong Polytechnic University; ³University of Tennessee

In this presentation, we summarize our recent works in the field of the mechanical behaviors of metallic glasses. The mechanisms of brittle and ductile transition as a function of the sample size will be studied using the multiscale mechanical testing techniques: compression test, micropillar compression test, nano-indentation and micro-bending tests. The newly developed high frequency dynamic micro-pillar tests have been used to probe both atomic clusters and flow defects in metallic-glasses. It is clearly revealed that atomistic free-volume zones are composed by two phases with distinguished characteristic dynamics signatures. The significant enhancement of ductility of Zr based; Cu based; Ti based; and Al based metallic glasses using the SMAT (Surface Mechanical Attrition Treatment) will be presented. The results show clearly the metallurgical structures play a key role for generating different toughening mechanisms.

3:20 PM

Measurement of Viscosity of a Metallic Glass in the Inaccessible Temperature Region Using Rapid Joule Heating: Georg Kaltenboeck¹; Joseph Schramm¹; Marios Demetriou¹; William Johnson¹; ¹California Institute of Technology

The lifetime of metallic glasses in the temperature region of the crystallization nose is so short that conventional heating techniques are far too slow to allow for the measurement of liquid properties. Therefore, a lack of physical data exists for metallic glasses in this temperature region. For example, a wide gap in the temperature-dependent viscosity exists around the crystallization nose even for the most robust glass formers. Recently, a novel joule heating method was developed that utilizes the unique electrical properties of the metallic glass to rapidly and uniformly heat to any temperature within the undercooled liquid region. Heating rates as high as 10⁶ K/s were achieved, which enable the complete bypass of crystallization during the heating phase. Using parallel plate rheometry in combination with this heating technique, the viscosity of $Zr_{41,25}Ti_{13,75}Cu_{12,5}Ni_{10}Be_{22,5}$ was measured around the crystallization nose over a range inaccessible with conventional heating methods due to crystallization.

3:30 PM Break

3:40 PM Invited

Properties of Shear Transformation Zones: Michael Atzmon¹; Jong Du Joo¹; Dongchan Jang²; Amadi Nwankpa¹; ¹University of Michigan; ²Caltech

The different modes of time-dependent deformation of metallic glasses are believed to involve activation of shear transformation zones (STZs). Most studies of the subject focus on large local strains, with cross-interactions among STZs. In order to determine fundamental properties of STZ, it is advantageous to study them at low densities, when the probability of interactions among them is low. At low densities, STZs can be reversed by the elastically-deformed matrix upon release of external strain, resulting in macroscopic anelasticity. Therefore, we have measured anelastic relaxation in amorphous Al86.8Ni3.7Y9.5, using a combination of nanoindenter cantilever, and bend relaxation, measurements, spanning over 7 orders of magnitude in time. The resulting relaxation-time spectra indicate at least seven distinct processes. Using Argon's theory,* we estimate the respective density of potential and active STZs, as well as their size. *A. Argon, Acta Metall. 27, 47 (1979).

4:00 PM

Microscale Characterization of Amorphous-Crystalline Metallic Composites: J. Sosa¹; K. Flores¹; *Nicholas Hutchinson*¹; ¹The Ohio State University

Bulk metallic glasses (BMG) are limited in application by their propensity for highly localized deformation that occurs with little to no ductile deformation when loaded in tension. To improve the toughness of these alloys, a number of Ti-Zr BMG composites have been created by a semi-solid processing technique that results in a two phase microstructure. The effectiveness of the reinforcement phase on improving toughness and ductility depends on both alloy composition and the microstructure. In the present work, we characterize two related composite compositions which exhibit vastly different mechanical properties. Microstructural variations are characterized 3-dimensionally using focused ion beam serial sectioning and a unique image processing technique. The effectiveness of the reinforcement phase is related to the ability to transfer deformation across the crystallineamorphous interface, TEM characterization of the interface structure is also examined. Finally, the mechanical properties of the individual composite phases are characterized using a micro-compression technique.

4:10 PM Invited

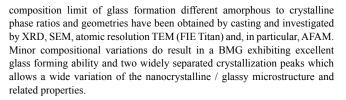
Understanding Roles of Secondary Amorphous Phases in Glassy Matrix: *Eun Soo Park*¹; ¹Seoul National University

Previous research on phase separating metallic glasses (PSMGs) suggests that exploring these paradigm shifting materials would be very fruitful for design of new types of composite structure. Thus, PSMGs have been actively studied not only to understand conditions for separation but also to investigate their unique properties. However, there has been no systematic approach to understand the role of secondary amorphous phase (SAP) in these PSMGs. In this study, we examine the effect of SAPs on their properties in various metallic glasses. We can fabricate SAP with different sizes in glassy matrix by controlling the kinds and amount of additional elements. Firstly, we will provide systematic discussion of the relationship between atomic scale SAPs and shear band formation. Secondly, we will discuss how nanometer scale SAP containing magnetic elements influences magnetic properties in PSMGs. Our results would contribute to a deeper understanding of various roles SAPs play in glassy matrix.

4:30 PM Invited

Nanocrystallization of a Bulk Metallic Glass in the Zr-Al-CuNiCo System – Structure and Mechanical Properties: Arnaud Caron¹; Rainer Wunderlich²; *Hans Fecht*²; ¹Tohoku University; ²Ulm University

A controlled two-phase mixture in terms of volume fraction and morphology of nanocrystalline and amorphous components offers the possibility of tailoring the ductility and mechanical strength of BMG forming complex alloys. This has been investigated in the Zr-Al-CuNiCo alloy system as a sole function of the Al-concentration varied between 7 and 20 at%. At the



4:50 PM

On Interfacial Bonding in Mg-Cu-Gd Metallic Glass via High Pressure Torsion (HPT): *Baolong Zheng*¹; Yizhang Zhou¹; Chi Y.A. Tsao²; Ruslan Valiev³; Enrique Lavernia¹; ¹University of California, Davis; ²National Cheng Kung University; ³Ufa State Aviation Technical University

The nature of the interface between particles critically influences the mechanical properties of bulk Metallic glasses (MGs) consolidated from powder. However, the low atomic diffusion ability and low thermal stability under a favorable consolidation temperature window (Tg to Tx), might hinder a good diffusion bonding. In this work, high pressure torsion (HPT) technique was applied to consolidate Mg-Cu-Gd amorphous powder via introduction of high pressure and severe plastic deformation, and to study fundamental phenomena associated with atomic diffusion and interfacial bonding during HPT consolidation of MG powder. The microstructural evolution at/near the interfaces of HPT'ed Mg-Cu-Gd BMG samples was characterized using SEM and TEM, and the phase transformation and thermal stability were analyzed with XRD and DSC. The influence of severe plastic deformation via HPT on interfacial bonding in bulk Mg-Cu-Gd and resultant mechanical response are discussed in an effort to provide insight into fundamental phenomena in MGs with HPT.

5:00 PM Invited

Ni-Free Zr-Ti-Cu-Al Bulk Metallic Glasses: Tensile Property and Fracture Toughness: *Jian Xu*¹; Qiang He¹; Evan Ma²; ¹Institute of Metal Research, Chinese Academy of Sciences; ²Johns Hopkins University

In this work, we report an effort to simultaneously follow the three considerations/leads above, to reach a Ni-free, Zr-rich, high-toughness BMG with higher GFA. Specifically, concentrating on the Zr-rich compositions, we investigated the GFA of quaternary Zr(Ti)-Cu-Al alloys using the "3D pinpointing approach". A new Zr-Ti-Cu-Al BMG (denoted as ZT1) was discovered to have a good GFA to yield as-cast glassy rods of 10 mm in diameter, permitting the measurement of fracture toughness in accordance with ASTM standard E399. For this Ni-free BMG, yield strength (sy) in tension at the strain rates of 1×10 -4/s and 2×10 -1/s was determined to be ~1590 MPa and ~1400 MPa, respectively. Furthermore, this Ni-free BMG exhibits a fracture toughness of ~100 MPa \sqrt{m} , together with a small variation. Summarizing the available toughness data for Zr-based BMGs, the previously suggested correlations between the fracture toughness and Poisson's ratio and shear modulus are discussed.

5:20 PM

Mg-Cu/Ni-Nd Bulk Metallic Glasses: Glass Transition Temperature and Elastic Properties Versus Toughness: *Ling Shi*¹; Jian Xu¹; ¹Institute of Metal Research, Chinese Academy of Sciences

Intrinsic brittleness of Mg-based BMGs correlates with lower Poisson's ratio (υ -0.31). Meanwhile, the elastic constants of BMGs can be roughly estimated based on the weight-averaged elastic constants of the constituent elements. It is helpful for the alloy design to use the elastic constants as the indicators of ductility of BMGs. Among RE elements, Nd possesses the highest υ . Thus, the Mg-Cu/Ni-Nd ternary BMGs are of interest for searching tough BMGs by tuning υ . In this work, the optimized BMG-forming formers are located at the Mg57Cu34Nd9 and Mg64Ni21Nd15, with shear modulus μ and υ determined to be 20.5 GPa and 0.322, and 17.9 GPa and 0.324, respectively. In addition, the Mg64Ni21Nd15 BMG exhibits Tg around 37 K higher than that of the Mg57Cu34Nd9 BMG which led to the increased the room temperature structural relaxation resistance. The low μ and high Tg of Mg64Ni21Nd15 BMG contribute to its higher notch toughness.

5:30 PM Invited

140th Annual Meeting & Exhibition

Topological and Chemical Order in Liquids and Glasses – Influence on Phase Transitions: *Ken Kelton*¹; ¹Washington University

Recent studies have demonstrated significant short- and mediumrange chemical and topological order in liquid alloys; some examples are discussed. Quantitative measurements of the time-dependent nucleation rate in a metallic glass (Zr59Ti3Cu20Ni8Al10) and associated structural studies of the supercooled liquid show that icosahedral short-range order grows significantly on supercooling and likely contributes to the glass transition. Recent studies of liquid Zr80Pt20 demonstrate medium-range order at temperatures even above the melting temperature, suggesting that it is important in liquid solidification and glass formation in this alloy. Abrupt chemical ordering is observed in supercooled liquid Cu46Zr54 near 850oC; it is correlated with a specific heat maximum, which yields information about the change in energy of the liquid with ordering. Nanoscale phase separation in Al88Y7Fe5 glass explains the poor glass stability and the high crystal nucleation rates.

5:50 PM Invited

Inhomogeneous Flow and Fracture of Glassy Materials: *Akira Furukawa*¹; Hajime Tanaka¹; ¹University of Tokyo

Understanding the mechanism of the non-Newtonian rheological response in inhomogeneous flow of glassy materials, which eventually develops into macroscopic shear-band, fracture, and so on, has been a long-standing unresolved fundamental problem of science despite intensive efforts so far. On the basis of a novel rheological model of fracture, we demonstrate that nonlinear behavior associated with fracture is a consequence of the coupling between density fluctuations and deformation fields: shear-induced enhancement of density fluctuations is self-amplified by the resulting enhancement of dynamic and elastic asymmetry between denser and lessdense regions. This positive feedback may be the origin of fracture. We propose novel criteria for the onset of mechanical instability. The criteria enable us to predict and design fracture behavior of materials from the pressure or density dependence of their viscoelastic properties of glass formers.

Cast Shop for Aluminum Production: Dross Formation, Control and Handling

Sponsored by: The Minerals, Metals and Materials Society, TMS Light Metals Division, TMS: Aluminum Committee, TMS: Aluminum Processing Committee

Program Örganizers: Geoffrey Brooks, Swinburne University of Technology; John Grandfield, Grandfield Technology Pty Ltd

| Tuesday PM | Room: 16A |
|---------------|-------------------------------|
| March 1, 2011 | Location: San Diego Conv. Ctr |

Session Chair: Pierre Le Brun, Alcan CRV

2:00 PM Introductory Comments

2:05 PM

Oxidation of AlMg in Simulated Dry and Humid Atmospheres: *Anne Kvithyld*¹; Darcy Stevens¹; Shawn Wilson¹; Thorvald Engh²; ¹SINTEF; ²NTNU

The loss of aluminium is expected to be higher in cast houses that are hot and humid, due to increased oxidation. Al-Mg alloys are known to oxidise easily, and are investigated in our new thermo-gravimetric furnace with humidity control with possibility to measure evolved gases simultaneously. The effects of dry and humid atmospheres on aluminium oxidation are studied. Oxidation is compared for the given conditions and alloy composition as a function of time. Using the data from both the thermo-gravimetric furnace and mass spectrometer, the mechanisms of oxide formation can be described and modelled.

2:30 PM

Study of Early Stage Interaction of Oxygen with Al; Methods, Challenges and Difficulties: *Behrooz Fateh*¹; Geoff Brooks¹; M. Akbar Rhamdhani¹; John Taylor²; Jeff. Davis³; Martin Lowe³; ¹Swinburne University of Technology; ²CAST CRC; ³The Centre for Atom Optics and Ultrafast Spectroscopy (CAOUS), Swinburne University of Technology

Aluminium is one of the metals with the greatest affinity for oxygen. Kinetics of early-stage oxidation are believed to have an important influence on the later steady-state oxide growth. Furthermore, there are many aspects of aluminium melt handling and casting processes that result in oxidation and dross formation. Sophisticated experimental studies such as scanning tunneling microscopy (STM), combined ellipsometry-auger electron microscopy and etc have clarified some aspects of the initial stage oxidation. However, most of the experimental data are not consistent and reproducible. Furthermore, the dynamics of absorption and oxidation processes are much less understood. This paper reviews the methods, techniques and the challenges of measuring and quantifying the oxidation of Al during its initial stages and also introduces a new method for studying the formation of an oxide layer upon solid aluminum, following ablation of the surface with an ultra-fast laser beam and a fast imaging techniques.

2:55 PM

Quality Assessment of Recycled Aluminum: *Derya Dispinar*¹; Anne Kvithyld¹; Arne Nordmark¹; ¹SINTEF Materials and Chemistry

One of the significant aspects during remelting of aluminum is surface oxide also with contaminations such as coatings. In this work, a wrought and a cast alloy were selected and subjected to remelting experiments. Bifilm index was measured as a measure of metal quality; 3-point bending and tensile testing samples were collected for mechanical testing. 3105 wrought alloy sheets were collected from before anodising, between anodising and painting and after painting. It was found that the surface of all the charges were accumulated over the surface and skimmed off. Therefore, the quality of all three charges was same and the mechanical properties were also the same. For the cast alloy, A356 alloy was subjected to remelting with decreased mechanical properties. Overall, a good correlation between the mechanical properties and the bifilm index were found.

3:20 PM

Preserving Metal Units Utilizing the Latest Generation of Aluminum Dross Press: James Herbert¹; Alan Peel²; ¹Altek LLC; ²Altek Europe Ltd.

The proper handling and processing of dross at the generation site is critical to reclaiming maximum metal units from this valuable by-product. A widely used technology designed to cool dross and maximize metal recoveries is the dross press. Since its introduction to the industry in the early 1990's this technology has been significantly improved to meet the demands of the modern cast house and increasingly stringent environmental legislation. This paper describes developments that address the weaknesses and limitations of early systems and enhancements that have enabled the cooling of a wide variety of dross types including salt slag from rotary furnaces. Areas addressed include mechanical design/reliability, extended capacity, automation, safety and environmental compliance, and metal recovery. Data from recent installations will be discussed along with economic models showing the positive effect small improvements in dross recoveries can have on the bottom line.

Characterization of Minerals, Metals and Materials: Characterization of Non-Ferrous Alloys

Sponsored by: The Minerals, Metals and Materials Society, TMS Extraction and Processing Division, TMS/ASM: Composite Materials Committee, TMS: Materials Characterization Committee *Program Organizer:* Sergio Monteiro, State University of the Northern Rio de Janeiro - UENF

| Tuesday PM | Room: 14B |
|---------------|-------------------------------|
| March 1, 2011 | Location: San Diego Conv. Ctr |

Session Chairs: Shadia Ikhmayies, Al Isra University; Augusta Isaac, Laboratório Nacional de Luz Síncrotron

2:30 PM

Evolution of Crystallographic Texture of Cold Roll Bonding and Annealing Ti-Al-Nb Multilayer Sheets: *Peng Qu*¹; Liming Zhou¹; Viola Acoff¹; ¹the University of Alabama

Usually, the mechanical properties of sheet materials strongly rely on the crystallographic texture. Also, it is commonly known that cold rolling will affect the texture of a material extensively. A ternary Ti-46Al-9Nb intermetallic alloy (at. %) was produced by accumulative cold roll bonding (ARB) followed by reaction annealing in our previous research. In this paper, Electron Backscattered Diffraction (EBSD) was employed to explore the influence of deformation conditions on microstructure and texture evolution of Ti-Al-Nb multilayer sheets made by the ARB process. As the reduction amount increased, the textures of Al and Nb changed significantly. The texture of Ti became more random due to the increase in defects as a result of ARB. The rolling texture of thin sheet materials was found to be different from that of rolled bulk materials. The texture evolution of the sheet materials after annealing was also investigated.

2:45 PM

Capillarity-Driven Migration of a Thin Ge Wedge on a Bicrystalline Au Substrate: *Tamara Radetic*¹; Andrew Minor¹; Ulrich Dahmen¹; ¹NCEM, Lawrence Berkeley National Lab

This work reports on the retraction of an anisotropic, solid thin Ge wedge in epitaxial contact with a bicrystalline Au film. Using TEM, we have observed striking crystallographic and morphological effects at the junction of the Ge-wedge with the Au substrate. In-situ microscopy and FIB-prepared cross-sectional samples allowed a 3D characterization of the observed morphological changes and enabled us to elucidate the mechanism of the transformation. We found that capillary forces at the Au/Ge interface result in ridge formation during wedge retraction. The bicrystalline Au substrate was not inert, but underwent abnormal grain growth in the area swept by the receding Ge-wedge. The morphological evolution of a solid wedge on a deformable substrate is of particular interest as a simple model system to investigate the stability of non-equilibrium configurations and its evolution under the influence of capillary forces and crystallographic anisotropy. This work is supported by DOE/BES/MSD under Contract No.DE-AC02— 05CH11231.

3:00 PM

Characterization of Laser Shock Peened IN718 SPF: Amrinder Gill¹; Vijay Vasudevan¹; S.R. Mannava¹; ¹University of Cincinnati

Laser shock peening improves service lifetimes of critical aero engine components.LSP introduces deep compressive residual stresses which improves fatigue strength, life and crack propagation resistance. This study aims to understand effects of LSP parameters on residual stress distributions and microstructural changes in an important aero-engine material, IN718 SPF. Coupons of alloy with and without sacrificial layer were peened with varying energy densities. Depth-resolved characterization of macro residual strains and stresses was achieved using high-energy synchrotron x-ray diffraction and conventional XRD. Near surface and through the depth changes in strain, texture and microstructure were also studied using EBSD in SEM and TEM. Local property changes were examined using micro and nano-indentation measurements. Studies were also done on thermal stability of residual stresses and microstructure

3:15 PM

Classification of Precipitation Shapes in Nickel Base Gamma-Gamma Prime Alloys: Jason Van Sluytman¹; Tresa Pollock²; ¹University of Michigan; ²University of California - Santa Barbara

Changes to the nominal compositions of nickel (Ni)-base superalloys provides a wide array of gamma prime (γ') morphology that has not typically been quantified. Two-dimensional moment invariants are implemented to classify morphologies and provide quantitative values for particle shapes. An experimental set of platinum group metal containing Ni-base superalloys, which contain variations in γ' morphology, has been examined using 2D moment invariants. Using the shape parameter ratio, η , it is demonstrated that Al, Cr, and Ta change η to a greater extent over Re and Ir. Plotting η as a function of lattice misfit magnitude results in a peak maximum at η approximately equal to 1 - indicative of a cuboidal morphology - when the misfit magnitude is 0.3%. This peak coincides with the misfit possessed by many highly creep resistant commercial superalloys. Thus, tailoring nominal compositions to provide η equal to 1 may be desirable in designing future superalloys.

3:30 PM

Dynamic-Tensile-Extrusion of Zirconium: The Role of Texture: *Carl Trujillo*¹; George Gray III¹; Ellen Cerreta¹; Daniel Martinez¹; ⁻¹Los Alamos National Laboratory

The effect of high strain-rate and high strains on mechanical behavior has been observed primarily in isotropic, cubic materials. The behavior of low-symmetry, textured, materials is not as well understood. To examine the high strain and high strain rate response of structural metals a dynamic extrusion technique has been developed at Los Alamos National Laboratory. In this study, high-purity zirconium bullets were accelerated up to velocities of 615m/s and extruded through a high-strength steel die. A combination of in-situ and ex-situ characterization techniques has been used to study the response of Zr under this dynamic loading condition. For the first time, PDV (Photonic Doppler Velocimetry) has been employed to capture the time and velocity of the evolved deformation through the die. Quantitative examination of the influence of texture and extrusion velocity will be presented.

3:45 PM

TUESDAY PM

Effect of Ti Addition on Microstructure and Tensile Property of Aged Cu-Ni-Si Alloy: *Eungyeong Lee*¹; Sangshik Kim¹; Kwangjun Euh²; Seungzeon Han²; ¹Gyeongsang National University; ²Korea Institute of Materials Science

Age-hardenable Cu-Ni-Si alloy is categorized as a high-electrical conductivity, high-strength copper alloy for the application of lead-frame and connector in the electronic devices, and the addition of trace amount of Ti, such as 0.09 wt.% and 0.18 wt.%, may improve both electrical conductivity and strength by increasing the driving force of δ -Ni₂Si precipitation during aging. In this study, the effect of trace amount of Ti addition on microstructure and tensile property of aged Cu-4.4Ni-1.0Si alloys at 450°C with varying time ranging from 10 to 360 minutes were examined. The tensile property of aged Cu-Ni-Si alloys was substantially influenced by small amount of Ti addition, as associated with a considerable microstructural evolution. The tensile behavior of Cu-4.4Ni-1.0Si-xTi alloys with different aging condition is discussed based on the detailed micrographic and fractographic observations.

4:00 PM Break

4:15 PM Invited

Comparison of Ni-Cr and Co-Based Alloys for Fuel Injectors: Giorgio Scavino¹; Paolo Matteis¹; Giovanni Mortarino¹; *Donato Firrao*¹; ¹Politecnico di Torino

A sintered Nickel-Chromium alloy (wt.% composition: Ni 50, Cr 48) is compared with cast or sintered Cobalt-based alloys (wt.% composition: Cr 25, W 5, C 1.2) for fuel injectors production. Each alloy underwent structural and microstructural examinations and tensile as well as fatigue tests at the maximum service temperature (500 °C). The 2 million cycles fatigue limit was estimated by the staircase method. Microscopic mechanisms for fatigue crack nucleation and growth and for overload fracture were also investigated. The Ni-Cr alloy is isotropous and homogeneous; it is biphasic, constituted by a Ni-rich FCC phase (about 70 vol.%) and a Cr-rich BCC one (30 vol.%), both with 2 μ m grain size. Its 500 °C tensile strength is intermediate between those of the sintered and cast Cobalt alloys, whereas its fatigue limit is somewhat lower than that of the sintered Cobalt alloy, but much higher than that of the cast Cobalt one.

4:45 PM

Microstructural Characterization of 70Cu-30Ni Alloy Formed by Direct Metal Deposition (DMD®) Process: Sudip Bhattacharya¹; *Jyotirmoy Mazumder*¹; Guru Prasad Dinda²; Ashish Dasgupta²; Bhaskar Dutta³; ¹University of Michigan, Ann Arbor; ²Focus:HOPE; ³POM

Direct Metal Deposition (DMD®) is a rapid prototyping technique used to generate near-net shape components from their computer aided design (CAD) files with very fine and controlled microstructures, and properties In this investigation a 70Cu-30Ni alloy was deposited on a rolled C71500 alloy substrate using a CO2 laser. The optical and scanning electron microscopy were used for microstructural investigation, the x-ray diffraction (XRD) technique was used for phase analysis, and the transmission electron microscopy (TEM) was used for crystal structure analysis. The microstructure consists of columnar dendrites. XRD analysis identified a CuNi solid solution phase in the sample. TEM selected area diffraction (SAD) patterns corroborated the phase analysis but the calculated lattice parameters were approximately 0.18% longer than the lattice parameters of the corresponding phase identified from XRD powder diffraction data file. This is caused by high residual stresses generated due to extremely high cooling rates during DMD®.

5:00 PM

Characterization of the Manganese Oxide Scales Formed on a Grooved Cast Pb-Ag Anode from a Zinc Electrowinning Operation: *Tzong Chen*¹; John Dutrizac¹; ¹CANMET-MMSL

Grooved cast Pb-Ag anodes are used by some zinc refineries to improve current efficiency. The manganese oxide scale formed on a grooved Pb-0.75% Ag anode consists mainly of MnO2, which occurs characteristically in rhythmically banded colloform structures. These adhere to a layer of "PbO2+PbSO4" that oxidized from the anode. The relatively homogeneous and nearly fracture-free morphology of the "PbO2+PbSO4" layer suggests the relatively uniform corrosion of the anode. Deposition of Mn oxide initially follows the contours of the anode surface, but the grooves eventually become filled with Mn oxide and gypsum. Hydrous Mn oxides and amorphous Mn oxides are believed to be also present in the manganese oxide scale. Tiny particles of PbSO4 and SrSO4, together with gypsum, other impurities and micro-pores, tend to concentrate in the grooves.

5:15 PM

Microstructure Evolution in Ultrafine-Grained CuZr Polycrystals Processed by High Pressure Torsion: Miloš Janecek¹; *Ondrej Srba*¹; Petr Harcuba¹; Milan Dopita¹; Jakub Cížek¹; Radomír Kužel¹; Hyoung Seop Kim¹; ¹Charles University

Coarse grained CuZr polycrystals were processed by high pressure torsion (HPT) at room temperature with different number of rotations (N=1-15). The microstructure evolution and grain fragmentation as a function of strain induced by HPT was investigated by different experimental techniques, in particular electron backscatter diffraction (EBSD), transmission electron microscopy (TEM), positron annihilation spectroscopy (PAS) and X-ray diffraction (XRD). The evolution of microstructure with strain due to HPT was correlated with mechanical properties characterized by detail 2D-microhardness profile analysis throughout round disc specimens of 20mm in diameter.

5:30 PM

The Effect of Rolling Mill Geometrical Parameters in Bulk Texture Analysis of Processed TiAl Based Multi-Layered Sheet Material: *Liming Zhou*¹; Peng Qu¹; Viola Acoff¹; ¹The University of Alabama

Multi-layered sheet materials processed by accumulative roll bonding technique are used to process lightweight materials such as TiAl-based alloy. Characteristics of cold roll bonded sheet materials using stacked Ti, Al, and Nb foils were studied by pervious researchers, however, the texture evolution analysis of the cold rolled condition of the sheet materials is still unclear. Few studies reported the bulk texture changes and anisotropic characteristics that exist for the rolling direction and transverse direction as a function of layers along normal direction of multi-layered sheet materials. In this study, the bulk texture analysis will be investigated by both X-ray diffraction and electron back scattered diffraction techniques. Rolling mill geometrical parameters are treated as variables to impact anisotropic characteristics, like textures and disorientation distribution. The geometrical parameters influence on texture in ARB sheet materials consist of rolling speed, speed gear ratio, mean width, thickness of multi-layered specimens, reduction, and reduction ratio.

5:45 PM

Thermophysical Properties of Platinum-Copper System: *Shahid Mehmood*¹; Ulrich E. Klotz²; Gernot Pottlacher¹; ¹Institute of Experimental Physics TU Graz; ²Fem Research Institute Precious Metals and Metals Chemistry

Platinum alloys are frequently used in technical applications and in jewellery. Their thermophysical properties such as density, heat capacity, thermal conductivity and surface tension play an important role in casting processes and are required as input data for casting simulation. Scope of this work was to investigate these properties by different methods. Platinum and four alloys namely, Pt-4Cu, Pt-32Cu, Pt-50Cu and Pt-75Cu were investigated. Thermal expansion was measured by dilatometry at fem, as well as surface tension by a sessile drop method. At TU Graz, wire shaped samples were investigated by an ohmic pulse heating technique. This technique allows the calculation of specific heat capacity and the temperature dependencies of electrical resistivity, enthalpy, and density of these alloys in the solid and liquid phase. Experimental results were compared with available literature and data from thermodynamic calculation using the SNOB1 database and ThermoCalc.

6:00 PM

Processing and Characterization of Ultra-Fine Grain Structure in Al Alloy by Equal Channel Angular Pressing: *Prasad Shanmugasandaram*¹; Narayani Narasimhan²; Balasivanadha Prabhu³; ¹State University of New York, Stony Brook; ²Stanford University; ³Anna University

The grain refinement and mechanical properties of 6061 aluminium alloy produced by equal channel angular pressing (ECAP) have been analyzed in this present study. A innovative triple shear ECAP die was developed for the processing. It was observed that the grain refinement takes place for greater number of passes. It was also found that reducing the process temperature gives fine grain and high microhardness and hence improved properties.

6:15 PM

Advances in Elemental Analysis, Characterization of Minerals and Ores, and Identification of Metal Alloys Using Handheld X-ray Fluorescence Technology: *Jeff Walker*¹; Chris Smith¹; ¹Thermo Fisher Scientific

In recent years, elemental analysis using handheld x-ray fluorescence (XRF) has enjoyed significant growth in mineral analysis for mining and exploration, as well as for metal alloy characterization and identification. The introduction of large area silicon drift detectors (SDD) into handheld XRF instruments has produced significant performance improvements over traditional XRF capabilities, especially in the area of light element analysis such as Mg, Al, Si, P and S. Coupled with a high output, 50kV, miniaturized x-ray tube, the new systems can also perform light element analysis work without vacuum or helium purge. This paper will offer an explanation of the XRF technique and the evolution of handheld XRF systems. Performance considerations and specific applications will be explored.

Computational Plasticity: Atomistic Modeling in Plasticity

Sponsored by: The Minerals, Metals and Materials Society, TMS Materials Processing and Manufacturing Division, TMS Structural Materials Division, TMS/ASM: Computational Materials Science and Engineering Committee, TMS: High Temperature Alloys Committee *Program Organizers:* Remi Dingreville, Polytechnic Institute of NYU; Koen Janssens, Paul Scherrer Institute

| Tuesday PM | Room: 1A |
|---------------|-------------------------------|
| March 1, 2011 | Location: San Diego Conv. Ctr |

Session Chair: To Be Announced

2:00 PM Invited

Deformation Mechanism in Nanocrystalline Metals: Experiments and Atomistic Simulations: *Helena Van Swygenhoven*¹; Mario Velasco¹; Christian Brandl²; Andreas Elsener³; Steven Van Petegem¹; Michael Weisser¹; ¹Paul Scherrer Institut; ²Los Alamos National Laboratory; ³University of Zurich

Molecular dynamics deformation studies of nanocrystalline metals suggest a dislocation mechanism where dislocations travel through the grain, to be absorbed in the surrounding GBs. Cross-slip (PRL 100(2008)235501, Phil. Mag 2010-in press) is observed as a mechanism to avoid stress intensities in grain boundaries. On the other hand, many experimental observations often demonstrate grain coarsening during deformation, often referred as coupled grain boundary motion. This talk discusses the latest simulation results in terms of dislocation mediated mechanisms and coupled grain boundary motion. The influence of dilute oxygen in grain boundaries is addressed using a local chemical potential approach that optimizes the charge on only those atoms expected to be ionic (Acta Mat 57(2009)1988). Furthermore the simulation results are assessed in terms of experiments performed on nc Ni involving strain rate sensitivity measurements (APL 89(2006)73102), stress dip and in-situ tensile tests during X-ray diffraction (Scripta Mat 60(2009)297, Scripta Mat 58(2008)61).

2:30 PM

Grain Boundary Migration as a Deformation Mechanism in Nanocrystalline Materials: Diana Farkas¹; ¹Virginia Tech

This talk will present results of atomistic simulation showing grain boundary motion in nanocrystalline materials as an important deformation mechanism. The simulations constitute virtual tensile tests of model nanocrystalline fcc materials described by empirical potentials. Grain boundary motion occurs as a response to applied stress, but not always coupled with grain boundary sliding. The atomistic mechanisms of the observed migration will be discussed. The simulation results also show that the presence of impurities in the grain boundaries can inhibit this process.

2:50 PM

Extracting Dislocations and other Defects from Atomistic Simulations: *Alexander Stukowski*¹; Karsten Albe¹; ¹Darmstadt University of Technology, Germany

We present a novel method for extracting dislocation lines from atomistic simulation data in a fully-automated way. Our algorithm delivers a geometric description of all dislocation lines contained in arbitrary crystalline model structures in a matter of seconds. Burgers vectors are determined reliably, and the extracted dislocation network fulfills the Burgers vector conservation rule at each node. All remaining crystal defects (grain boundaries, surfaces, etc.) are output as triangulated surfaces. In contrast to the recently proposed on-the-fly dislocation detection algorithm [Modelling Simul. Mater. Sci. Eng. 18 (2010), 015012], the new method is extremely robust, easy to use, and enables a detailed analysis of complex dislocation processes even in highly distorted crystal regions, as they occur, for instance, close to grain boundaries or in dense dislocation networks. We present applications of the

new method to simulations of nanostructured metals and discuss prospects of a fully-automated analysis of secondary grain boundary dislocations.

3:10 PM

Grain Boundary Kinetics in Molecular Dynamics: The Effect of the Driving Force on Mobility and Migration Mechanisms: *Christopher Race*¹; Johann von Pezold¹; Joerg Neugebauer¹; ¹Max-Plank-Institute for Iron Research

Molecular dynamics (MD) simulations of grain boundaries often employ some form of external driving force on the atoms to promote grain boundary motion. To obtain measurable motion of a boundary on the timescales accessible to MD, these forces must be much greater in magnitude than those responsible for real processes of microstructural evolution. Given this fact, we must take care that our externally imposed force, be it in the form of an elastic deformation or an artificial potential, does not fundamentally alter the atomic scale processes that give rise to the motion of the grain boundary. In this study we systematically investigate the effect of the strength and nature of the driving force on the mobility and migration mechanisms of representative tilt boundaries in Al. Based on an in-depth analysis of these results, we discuss possible schemes that guarantee the correct limit at zero driving force.

3:30 PM Break

3:45 PM Invited

Slip Coupling in Crystal Plasticity: *Vasily Bulatov*¹; ¹Lawrence Livermore National Laboratory

The traditional computational crystal plasticity equates the plastic strain rate at a material point with the sum of component rates associated with the individual slip systems. However, experimental evidence and theoretical considerations suggest a stronger coupling between slip systems in BCC metals under certain straining conditions. When a BCC single crystal is deformed at a sufficiently low temperature and/or at a high straining rate, the fraction of screw dislocations in the total dislocation population is known to rapidly increase. Should the fraction of screws grow to become a majority, formation of (twist) dislocation networks can become the dominant mechanism by which the screw dislocations reduce their elastic energy. Such twist networks are indeed observed in BCC metals deformed at low temperatures. Each twist network ties together screw dislocations with two different 1/2<111> Burgers vectors for the total of six distinct Burgers vector pairs. In addition to a significant energy reduction through elastic screening, such tightly coupled dislocation networks can glide very easily along the {110} planes common to the two Burgers vectors of each couple. Careful analysis of atomic mechanisms and associated stress yield contours suggests that such cooperative network glide must be highly anisotropic in the {110} network planes and that the net effect of each network glide mode must be roughly equivalent to slip on a <110>{110} pseudo-system. In BCC crystals, only three of such strongly coupled pseudo-systems are linearly independent. These observations suggest a novel interpretation of some of the known slip anomalies in BCC deformation and lead us to predict unusual new effects in crystal plasticity that can be verified by straining experiments.

4:15 PM

Partial Dislocation Nucleation and Twinning in Aluminum: Nitin Daphalapurkar¹; *K.T. Ramesh*¹; ¹The Johns Hopkins University

Recently, wide stacking fault (SF) ribbons with average widths as large as 3.5 nm have been reported in nanocrystalline Al. We use molecular dynamics (MD) simulations to investigate the widths of extended dislocations in aluminum, and demonstrate that the SF widths in aluminum are strongly dependent on the orientation of the applied stress and presence of stress-gradients. The results demonstrate a reasonable agreement between simulations, theoretical predictions, and experimental observations, and help explain recent observations of SFs in nanocrystalline-aluminum. Further, information on the Generalized Planar Fault Energy associated with Al (obtained from MD simulations) is used to arrive at orientation and temperature dependent stress required for nucleation of partial dislocations under initially homogeneous shear stress conditions, and equivalent values for heterogeneous nucleation are derived. The qualitative and quantitative results will be useful in developing discrete models for incorporating nucleation of partial dislocation in a crystal plasticity framework.

4:35 PM

Atomistic Simulations of Cu/Cu-Oxide Planar Interface Properties: *Abdelmalek Hallil*¹; Remi Dingreville²; Stéphane Berbenni¹; Mohammed Cherkaoui¹; ¹Georgia Tech - CNRS; ²NYU-Poly

Preliminary work has been already carried-out for homogeneous interfaces by characterizing the general formula of Gibbs' interfacial excess energy (IEE) as a function of the interfacial excess stress. In the case of heterogeneous interfaces, the key issue is the matching of lattice vectors in the interface plane of each material, so that the overall strain is small when the interface is formed. Here, we focus on the extension of the global expression of the IEE by including the role of interfacial mismatch on the strained interfaces. Molecular Dynamics (MD) calculations are used to evaluate the role of this mismatch for a given heterogeneous interface. The Cu/Cu-oxide interface model is stretched along the interface plane regarding the length and angle of the surface-cell vectors. For each deformation process, Molecular Statics and MD simulations (NPT, NVT) are performed to compute the interfacial excess energy at the equilibrium state of the system.

4:55 PM

Plastic Deformation of Au Nanoparticles and Thin-Films: A Comparative Experimental and Simulation Study: *Dan Mordehai*¹; Eugen Rabkin¹; David Srolovitz²; ¹Technion; ²Institute of High Performance Computing

We report a combined experimental/molecular dynamics study of the indentation of faceted Au nanoparticles and thin-films of similar dimensions on a sapphire surface. The particles were created via the dewetting of a polycrystalline Au film on sapphire substrate. Experiments show that the larger nanoparticles are softer, i.e. the strength is size dependent. The Molecular Dynamics simulations supply us with insights of the dislocation mechanisms within the nanoparticles during deformation and aide in rationalizing the size effect observed experimentally. The atomistic simulations show that deformation is controlled by dislocation nucleation near the tip. In nanoparticles, nucleation is followed by fast dislocation glide toward the lateral surfaces, leading to defect-free particles during indentation (dislocation starvation), while in thin films and elongated particles dislocations accumulated around and beneath the indenter. We conclude that the back-stress of the accumulated dislocations made the nucleation of new dislocations more difficult, which elucidates the experimentally-observed size effect.

5:15 PM

Molecular Dynamics Analysis of Edge Dislocation Walls: Sebastian Echeverri Restrepo¹; Barend Thijsse¹; ¹TUDelft

One of the simplest types of symmetrical tilt grain boundaries (GBs) can be described as a wall of equally spaced edge dislocations lying on the same plane and whose Burgers vectors are parallel to each other and perpendicular to the common plane. There exist analytical models, based mainly on the elastic isotropic theory of dislocations, to describe their structure, stress distribution and energy. We present an alternative approach to model this type of GB using molecular dynamics (MD). A new method of generating infinite dislocation walls is introduced. Edge dislocations are inserted into single aluminum crystals by selectively removing half-planes and applying the displacement field predicted by the elastic isotropic theory of dislocations. The system is subsequently relaxed to a temperature of 0K and a pressure of 0Pa using MD. The stress fields, energies and mechanical properties of the different configurations are calculated, analyzed and compared to the available models. Sponsored by: The Minerals, Metals and Materials Society, ASM International, TMS Electronic, Magnetic, and Photonic Materials Division, TMS Materials Processing and Manufacturing Division, TMS: Alloy Phases Committee, TMS: Chemistry and Physics of Materials Committee, TMS/ASM: Computational Materials Science and Engineering Committee, ASM: Alloy Phase Diagrams Committee *Program Organizers*: Raymundo Arroyave, Texas A & M University; James Morris, Oak Ridge National Laboratory; Mikko Haataja, Princeton University; Jeff Hoyt, McMaster University; Vidvuds Ozolins, University of California, Los Angeles; Xun-Li Wang, Oak Ridge National Laboratory

| Tuesday PM | Room: 9 |
|---------------|-------------------------------|
| March 1, 2011 | Location: San Diego Conv. Ctr |

Session Chairs: Vidvuds Ozolins, UCLA; Stefano Curtarolo, Duke University

2:00 PM Invited

First-Principles Approaches to Li-Air Batteries: *Donald Siegel*¹; Max Radin¹; ¹University of Michigan

Of the many possible battery chemistries, the so-called "Li-air" system is noteworthy in that its theoretical capacity (~5 kWh/kg, including mass of O2) exceeds that of any electrochemical system. Perhaps more importantly, the simplified composition of its air cathode – involving only the inlet of oxygen from the atmosphere – has the potential to provide cost benefits in comparison to the Li-ion systems of today. Although the first rechargeable Li-air battery was demonstrated by Abraham and Jiang 13 years ago, performance in many dimensions remains poor, and relatively little work has been done to elucidate performance-limiting phenomena. This talk will introduce the basic properties and main performance issues associated with Li-air batteries. Opportunities for first-principlessimulations to assist in overcoming these obstacles will be highlighted.

2:30 PM

The Li-Graphite System and Surface Reactions from First-Principles: *Kristin Persson*¹; ¹LBNL

Graphitic carbon is the most commonly used anode in rechargeable Li batteries. We recently showed by kinetic Monte Carlo simulations that intralayer Li motion in bulk graphite is intrinsically very fast, even at high Li concentrations. However, carbonaceous anodes show relatively low rates, especially at low temperature. This indicates that transport through the graphite surfaces could be the slow step in the process. Furthermore, there are indications that water contamination of Li electrodes can cause damage to capacity retention [1]. In this context, we examine from first principles the graphite surfaces, and how different absorbing species and contaminants affect the Li potential at the surface, relevant for rechargeable Li batteries. [1] M. Kerlau, and R. Kostecki, J Elec. Soc. 153 (9). A1644-A1648, (2006).

2:45 PM

A First Principles Study of Nanostructured Thermoelectric Materials: *Philippe Jund*¹; Romain Viennois¹; Jean Claude Tédenac¹; Mathieu Fèvre²; ¹Université Montpellier 2 - ICGM; ²LEM - ONERA

We present DFT based simulations of magnesium silicide composites. After the determination of the energy of formation of the different structural defects, we compute the physical properties and in particular the phonon dispersion curves of Mg2Si containing various transition metal silicide nanoclusters with the aim of improving the thermoelectric properties of magnesium silicide.

3:00 PM

Defects in Perovskites for Solid Oxide Fuel Cell Cathodes: Surface and Strain Effects: *Yueh-Lin Lee*¹; Milind Gadre¹; Dane Morgan¹; ¹University of Wisconsin-Madison

Understanding how interfaces, surfaces, and strain effects can alter defect and ionic transport properties of oxides is an area of increasing research interest in solid state ionics. In this talk we discuss *ab initio* modeling of how surfaces and strain can alter defect chemistry and kinetics in perovskites of interest as solid oxide fuel cell cathodes, such as $(La,Sr)MnO_3$ and (La,Sr) Co_{03} . We demonstrate that defect energy changes near surfaces are very large but can be understood in terms of a simple model based on defect charge and local oxidation level. We also show how strain can alter defect formation energies and integrate these results into a strain dependent thermodynamic defect model for $(La,Sr)CoO_3$ thin films.

3:15 PM Invited

Data, Methods and Search Strategies for Metal Catalysts: *Stefano Curtarolo*¹; Gus Hart²; Ohad Levy³; Wahyu Setyawan¹; ¹Duke University; ²BYU; ³NRCN

With a combination of "data-mining-high-throughput" and "cluster expansion" methods, we have parameterized the whole set of transition-metal binary intermetallics (435 alloys). In this talk, we introduce the method/tools [1], and we present examples for Rh-M [2], Hf-M [3] alloys, in addition to the automatic generation of ab-initio structure maps for hexagonal systems [4]. Furthermore, by tackling two test cases, we show the importance of the complete knowledge of the stable and metastable phases to understand deactivation in catalytic particles [5] and the solubility of species inside systems [6] leading to search strategies for novel catalytic materials with concurrent optimization of electronic [7] and thermodynamical properties [8]. [1] JACS 132, 4830 (2010)[2] JACS 132, 833 (2010)[3] Acta Mat. 58, 2887 (2010)[4] PRB 81 174106 2010[5] PRL 100, 195502 (2008)[6] Acta Mat. 57, 5314 (2009)[7] http://dx.doi.org/10.1016/j.commatsci.2010.05.010[8] JACS 132, 6851 2010

3:45 PM Break

3:55 PM Invited

Self-Assembly of Stable Ti, Y, and O-Enriched Nanoclusters in Fe: H. Zhao¹; M. Krcmar²; C. L. Fu¹; M. K. Miller¹; ¹Oak Ridge National Laboratory; ²Grand Valley State University

Stable nanoclusters (2-4 nm in diameter) in Fe-based alloys fabricated by mechanical alloying (MA) have been observed after isothermal aging up to 1400 C. Nanophase materials are known to be metastable in nature, because of coarsening processes that occur rapidly at elevated temperatures. These stable nanoclusters are an exception to this norm. First-principles theory has been used to investigate the defect mechanism and their formation and stability. The presence of preexisting vacancies (created during MA) is necessary for achieving high oxygen solubility and preventing the precipitation of FeO. This O-vacancy mechanism enables the nucleation of O-enriched nanoclusters with structures coherent with the underlying Fe lattice in the presence of solutes with high O affinities. An essential condition for stabilizing these nanoclusters is their exceptionally low interfacial energy in the Fe matrix. This research was sponsored by the U.S. Department of Energy, Office of Basic Energy Sciences, Materials Sciences and Engineering Division.

4:25 PM

First-Principles Study of the Structure of RuO₂*****x**H**₂**O**: *Fei Zhou*¹; Yongduo Liu¹; Mark Asta²; Vidvuds Ozolins¹; ¹UCLA; ²UC Berkeley

Hydrous ruthenia, $\text{RuO}_2 * x \text{H}_2\text{O}$, is a high-performance electrode material for electrochemical supercapacitors. Two different structural models for thermodynamically stable hydrous ruthenia have been proposed, differing in whether hydrogen is located inside or outside the bulk oxide. We present a theoretical examination of the validity of the bulk model using a combination of a systematic search algorithm based on electrostatics, database searching and density-functional theory calculations. We find that all the considered bulk model structures are unstable by ~0.3 - 0.4 eV per H2O molecule with



respect to phase separation into anhydrous RuO2 and water. Structures with hydroxyl groups or aggregate H2O are significantly lower in energy, demonstrating that the water prefers to agglomerate outside RuO2. This trend is shown to be present in other metal hydroxides with high valence and can be explained by qualitatively examining the water-metal oxide mixing energy. Our results strongly support the core+grain-boundary model of hydrous ruthenia.

4:40 PM

Reaction Pathways of Methane Decomposition on Cu Surface from Ab Initio Calculations: Grzegorz Gajewski¹; Chun-Wei Pao¹; ¹Research Center for Applied Sciences, Academia Sinica

Growth of large-area single- or few-layer graphene films has been reported recently by catalytic decomposition of methane on Cu surface at high temperature. However, the surface reaction pathways toward graphene formation have not been studied in detail. In this work, the minimum energy reaction pathways for successive dehydrogenation reactions of methane on Cu (111) surface have been investigated theoretically. Climbing image nudged elastic band method with spin-polarized DFT and periodic slab model have been used to identify geometries, energies of all reaction intermediates and transition states as well as activation barriers. The complete decomposition of isolated methane molecules on Cu surface is found endothermic. We also found activation barriers for methane decomposition on Cu surface are much lower than those in gas phase, which demonstrates the role of Cu as a catalytic material for large-area graphene film fabrication.

5:00 PM Invited

Water Splitting on Reduced CeO2(111): Heine Hansen¹; *Chris Wolverton*¹; ¹Northwestern University

Solar thermochemical cycles have the potential to convert solar energy into chemical fuels at high thermodynamic efficiency. This could for example be done by thermal reduction of CeO2 to CeO2-x at high temperature followed by oxidation of CeO2-x in H2O at a lower temperature to produce H2. In this work we use density functional theory to identify the most stable surface structures on CeO2(111) containing surface or subsurface oxygen vacancies, H2O or H. We find the positions of Ce3+ ions in the reduced surface affect the stability of vacancies and adsorbed hydrogen, but has only little effect on the adsorption of water. We calculate barriers for diffusion of oxygen vacancies, and for desorption of hydrogen from the surface. We use this information to derive a kinetic model of H2 production from this reduced surface.

5:30 PM

Thermodynamic Analysis of Phase Transformations in La_eSr_{1-c}MnO₃ **Perovskite Solid Solutions**: Royi Glass¹; *David Fuks*¹; Eugene Kotomin²; Joachim Maier²; ¹Ben Gurion University of the Negev; ²Max Planck Institut für Festkörperforschung

Peroviskite solid solutions La_cSr_{1-c}MnO₃ of different compositions are widely used as cathodes for solid oxide fuel cells (SOFC). The phase diagram for the La Sr MnO₃ quasi-binary system is calculated combining the statistical thermodynamic approach with ab initio calculations. The temperature and concentration dependences of the long-range order parameters are calculated and used in constructing the phase diagram. The analysis of the competition between ordered structures (with the different states of order) and with the disordered state with different compositions, c and temperatures is carried out. Two-phase regions on the phase diagram are calculated. The critical temperatures for the order-disorder phase transformations are found and the type of the order-disorder phase transitions is determined. The particular La_{0.125}Sr_{0.875}MnO₃ and La_{0.25}Sr_{0.75}MnO₃ phases show extremely narrow homogeneity region and first-order type orderdisorder transformation, in contrast to La_{0.5}Sr_{0.5}MnO₃ which reveals a rather extended homogeneity region and is characterized by the second-order type transformation.

5:45 PM

Calculation of the Thermoelectric Power of Titanium, Zirconium, and Hafnium: Zhongliang Xiao¹; Hanli Yang¹; Zhichao Ma¹; Horst Brodowsky²; Qiyuan Chen³; ¹Changsha University of Science and Technology; ²Christian-Albrechts-Universität zu Kiel; ³Central South University

The thermoelectric power of titanium, zirconium, and hafnium has been calculated on the assumption, that number of electrons per atom as well as the pressure are constant in a temperature gradient and the electrochemical potential of the electrons is a unique function of the temperature in pure metals, and the local thermal equilibrium between electrons and metal ion cores is established. The diffusional thermopower is approximately equal to the gradient of the electrochemical potential of the electrons (calculated from the density of states), divided by the electronic charge. The calculated results agree with experimental results well.

David Pope Honorary Symposium on Fundamentals of Deformation and Fracture of Advanced Metallic Materials: Deformation, Fracture, and Hydrogen Effects

Sponsored by: The Minerals, Metals and Materials Society, TMS Materials Processing and Manufacturing Division, TMS Structural Materials Division, TMS: High Temperature Alloys Committee, TMS/ASM: Mechanical Behavior of Materials Committee, TMS: Nanomechanical Materials Behavior Committee

Program Organizers: E. P. George, Oak Ridge National Laboratory; Haruyuki Inui, Kyoto University; C. T. Liu, The Hong Kong Polytechnic University

| Tuesday PM | Room: 32A |
|---------------|-------------------------------|
| March 1, 2011 | Location: San Diego Conv. Ctr |

Session Chairs: Dennis Dimiduk, Air Force Research Laboratory; Dilip Shah, Pratt & Whitney

2:00 PM Invited

Non-Associated Flow of Crystalline Solids: John Bassant¹; ¹University of Pennsylavnia

The structure of classical plasticity theory for crystalline materials is generally assumed to be associative in the sense that the flow potential is taken to be the yield function. Ample experimental evidence now exists that non-associated flow more appropriately characterizes dislocation glide. Indeed, in 1985, A. Cottrell remarked: "... for too long we have taken the FCC dislocation as the paradigm of all dislocation behaviour; but, as the studies of BCC screw dislocations have shown, the FCC structures and properties are the exception rather than the norm." Intermetallic compounds, in particular L12 alloys which were extensively studied by D. P. Pope, are another prominent example. Multislip models for single crystals are developed from atomistic simulations, and polycrystal behavior is estimated using simple homogenization techniques. At all levels, non-associated flow persists, and this is shown to significantly affect macroscopic deformations and failure mechanisms.

2:30 PM Invited

The Ice-Structure Interaction Problem: Creep, Fracture and the Ductile-Brittle Transition of Ice: Erland Schulson¹; ¹Dartmouth College

Engineered structures situated within ice-infested waters must withstand loads that can exceed 100-year wave forces. The loads are induced through wind-and current-driven movement of floating ice sheets and icebergs, and, for a given feature, reach a maximum when the velocity of impact is great enough to activate a transition from ductile to brittle behavior of the ice. At still higher velocities where fracture dominates, structures can vibrate. This talk will review the problem, and then focus on ice and on the physical processes underlying its mechanical behavior. On scales both large and small, deformation mechanisms include dislocation climb, dynamic recrystallization, frictional sliding and crack initiation and propagation — processes common to all crystalline materials.

3:00 PM Invited

Micro-Scale Investigations of Interfacial Delamination in Thermal Protection Systems: Kevin Hemker¹; ¹Johns Hopkins University

Modern thermal protection systems have multiple layers and functionalities; important phenomena governing the life of these systems occur in each layer and especially at the interfaces between disparate layers. Mechanical characterization of these systems is complicated by their reduced dimensionality. Micro-scale tensile and bending experiments provide direct routes for characterizing the constitutive properties of individual layers and for experimentally quantifying interfacial delamination. Results involving both commercial thermal barrier coatings for aircraft engines and developmental coatings for a solar probe satellite designed to fly within nine solar radii of the sun will be presented. The experimental insight gained in these experiments will be interpreted and used to facilitate hierarchical modeling of layered thermal protections systems.

3:30 PM Break

3:45 PM

A TEM Study of the Micromechanisms Associated with Hydrogen Embrittlement in Steels: Srinivasan Rajagopalan¹; Neeraj Thirumalai¹; Ning Ma¹; Dakshina Valiveti¹; Sanket Desai¹; ¹ExxonMobil Research and Engineering

The study of hydrogen embrittlement of steels remains a focus area in the oil and gas industry. Several mechanisms, such as Hydrogen Enhanced Localized Plasticity (HELP) and Hydrogen Enhanced Decohesion (HEDE) have been proposed to explain the embrittling effect of hydrogen at the atomic level. Recently, another model, based upon the stabilization of vacancies in the presence of hydrogen, has also been proposed to explain this effect. However, a clear understanding of the effect of hydrogen on deformation mechanisms is still lacking. This study attempts to examine the micromechanisms associated with deformation in specific hydrogencharged steels. Transmission Electron Microscopy (TEM) observations of deformation substructures from fracture surfaces of tensile and fracture toughness samples will be discussed. By coupling the understanding generated from these studies with observations of dislocation activity in controlled-strain tensile tests, an attempt is made to understand the effect of hydrogen on deformation and failure in specific steels.

4:00 PM

Strain-Induced Metal-Hydrogen Interactions Across the First Transition Series – An Ab Initio Study of Hydrogen Embrittlement: Johann von Pezold¹; Ugur Aydin¹; Tilmann Hickel¹; Joerg Neugebauer¹; ¹Max-Planck-Institut für Eisenforschung GmbH

The susceptibility of modern, high strength steels to H-embrittlement has spawned renewed interest in this long-standing, unresolved challenge in Materials Science. A key mechanism underlying all the currently discussed mechanisms of hydrogen-induced embrittlement of metals, such as hydrogen enhanced local plasticity (HELP), hydrogen enhanced decohesion (HEDE) and stress-induced hydride formation is the attractive interaction between hydrogen and distorted regions of the host matrix. In this study we systematically investigate these interactions by determining heat of solutions, H-H binding energies within the metal matrix, as well as phase diagrams as a function of the lattice strain and the H chemical potential across the first transition series (3d elements) using density functional theory (DFT) calculations. A careful analysis of the resulting extensive data sets provides direct insight into chemical trends and allows an identification whether the metal is susceptible to H-embrittlement and of the relevant embrittlement mechanism.

4:15 PM

Influence of Hydrogen Loading on the Tensile Behavior of Fe-Ga Alloys: *Meenakshisundaram Ramanathan*¹; Biswadeep Saha¹; Chai Ren¹; Gavin Garside¹; Sivaraman Guruswamy¹; ¹University of Utah

Fe-Ga and other ferrous alloys exhibit large magnetostrictive behavior and are candidates for use in sensing, actuation and energy harvesting applications. Exposure to aqueous electrochemical environments is anticipated in some of these applications. This could potentially introduce hydrogen in to the alloy and cause severe ductility reduction due to hydrogen embrittlement effect. The present study examined the influence of electrochemical hydrogen loading on tensile behavior of FeGa alloys. Hydrogen was charged electrochemically prior-to and during the tensile test. The results show a dramatic reduction in the ductility with hydrogen charging. The fracture surfaces were examined using scanning electron microscope, to confirm the brittle failure in the presence of hydrogen. Influence of simultaneous presence of magnetic field during testing was also examined. *Support of this work by NSF through the award DMR-0854166 is gratefully acknowledged.

4:30 PM

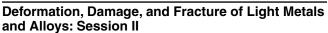
Prismatic Cross-Slip in Mg from First Principles: *Joseph Yasi*¹; Louis Hector²; Dallas Trinkle¹; ¹University of Illinois at Urbana-Champaign; ²General Motors R&D Center

New ductile Mg alloys with high specific strength are of great interest to the transportation industry. At room temperature, forming is difficult due to the low ductility of Mg. Prismatic dislocations are two orders of magnitude stronger than basal dislocations at room temperature, but nonbasal dislocation mobility is necessary to achieve the five independent slip systems required to handle an arbitrary deformation. Efficient, accurate computational models of dislocation/solute interactions provide insight into new Mg alloy development. We employ a first principles flexible boundary condition method to compute *a*-type basal and constricted prismatic screw and prismatic edge dislocation geometries in Mg. For these dislocations, we calculate solute binding energies for Al, Li, Y and Zn in the optimized dislocation cores. We predict changes in prismatic critical resolved shear stress with temperature and solute concentration from the differences in core energies on the basal and prismatic planes in the presence of solutes.

4:45 PM

Substructure Evolution during Creep in Zirconium Alloys: *Benjamin Morrow*¹; Robert Kozar²; Kenneth Anderson²; Michael Mills¹; ¹The Ohio State University; ²Bechtel Bettis, Inc.

Zirconium alloys are commonly used for applications in nuclear reactors. Accurately predicting creep deformation of zirconium alloys throughout the lifecycle of a reactor depends on reliable deformation models. The Modified Jogged-Screw Model (MJSM) asserts that the motion of tall jogs in screw dislocations act as the rate controlling mechanism during creep in certain regimes. Previous studies have demonstrated the applicability of the MJSM to the thermal creep behavior of hcp metals, but effects of accumulated strain have never been fully explored. Scanning transmission electron microscopy (STEM) was used to directly observe and characterize the dislocation structure of creep tested Zircaloy-4 as a function of accumulated strain, and quantify pertinent model parameters such as jog height, jog spacing, and dislocation density. Thorough characterization will provide a better understanding of material behaviors in both primary and secondary creep regimes, which will ultimately result in more robust creep deformation predictions.



Sponsored by: The Minerals, Metals and Materials Society, MS&T Organization, TMS Light Metals Division, TMS: Chemistry and Physics of Materials Committee, TMS/ASM: Mechanical Behavior of Materials Committee

Program Organizers: Qizhen Li, University of Nevada, Reno; Xun-Li Wang, Oak Ridge National Laboratory; Yanyao Jiang, University of Nevada, Reno

| Tuesday PM | Room: 13 |
|---------------|-------------------------------|
| March 1, 2011 | Location: San Diego Conv. Ctr |

Session Chair: Qizhen Li, University of Nevada, Reno

2:00 PM Invited

Visualizing the 3D Microstructure Evolution during Deformation: Henning Poulsen¹; Masakazu Kobyashi²; Jette Oddershede¹; Christian Wejdemann¹; Ulrich Lienert³; Soeren Schmidt¹; Ulrik Olsen¹; Bettina Camin⁴; Grethe Winther¹; Dorte Juul Jensen¹; Hiroyuki Toda²; Walter Reimers⁴; ¹Risoe DTU; ²Toyohashi University of Technology; ³Argonne National Lab.; ⁴TU Berlin

We present methodologies, limitations and examples of results for a coherent set of synchrotron based methods, primarily for in-situ studies of mm-sized samples during tension: • Grain mapping and grain-by-grain stresses: 3D maps with 1000+ grains have been made and compared to crack propagation as determined simultaneously by tomography. Likewise grain rotation studies of 1000+ bulk grains will be presented. • Plastic strain tomography: The strain field of an Al alloy was mapped in 3D to 10% strain and compared to the 3D grain structure and local rotations. •

Orientation Imaging Microscopy. A non-destructive and 3D equivalent of the familiar EBSD technique has been established. • Formation and evolution of dislocation structures: Using a reciprocal-space approach focus will be on recent results for strain path changes. The methodologies can all be combined. The possible impact for plasticity modeling is outlined. (Experiments were performed at ESRF, APS and Spring-8.)

2:30 PM

Development of <111> Fiber Texture and {111}<112> Shear Bands in Pure Al Metal by Wire Drawing: Mohammad Shamsuzzoha¹; ¹University of Alabama

Conventional transmission electron microscopy and x-ray diffraction techniques have been applied to study the microstructure of heavily wire drawn samples of pure Al metal. Samples thus drawn (~40% of the original value) have been found to be comprised of columnar grains with no evidence of any recrytallization and to exhibit a strong <111> texture. The microstructure of thus drawn samples contain deformation bands that are made of closely spaced parallel slip bands, which lie on {111} and extends along a <112> . Electron diffraction patterns taken from these slip bands in the microstructure are probably produced by coalescences of a group of parallel {111}<112> stacking faults. Most of the materials de-cohesions present in the deformed samples were found propagating along directions that are normal rather than parallel to the deformation bands.

2:45 PM

Effects of Spatial Locations of Nucleation Sites on Incipient Damage in High Purity Aluminum: *Matthew Tucker*¹; John Bingert¹; Timothy Ulrich¹; Cheng Liu¹; Ching-Fong Chen¹; George Gray¹; ¹Los Alamos National Lab

To accurately predict the failure of components, the mechanisms driving incipient damage nucleation must be more fully understood. This study aims to quantify the effect of the spatial location of nucleation sites on the earliest stages of damage evolution. A large-grained, high-purity aluminum provides a matrix with no significant level of homogeneous damage nucleation sites. OIM analysis will be employed to determine optimal sample extraction location with respect to grain orientation, shape, boundary inclusion, etc. Once a suitable location is determined, a section will be extracted and prepared for the placement of designed damage nucleation sites and smaller tracer particles. The mating surfaces will then be diffusion bonded and a tensile specimen will subsequently be fabricated. The embedded nucleation and tracer particles will be monitored via XCMT and coupled with digital image correlation between interrupted tensile tests to capture the evolution of localized strain fields and damage nucleation.

3:00 PM

140th Annual Meeting & Exhibition

Fracture Behavior of Short Carbon Fiber Reinforced Aluminium Matrix Composite: Pengfei Yan¹; Guangchun Yao¹; Jianchao Shi¹; Xiaolan Sun¹; *Hongjie Luo*¹; ¹School of Materials & Metallurgy, Northeastern University

The microstructure and fracture behavior of aluminum matrix composites reinforced with copper coated short carbon fiber were investigated. 4% carbon fibers were added to aluminium matrix through the stir casting method. The microstructure of composites showed that there was a uniform distribution of carbon fibers and good interfacial bonding with the matrix. The tensile test was carried out to evaluate the tensile strength of the composites. The microstructure of the fracture surface were observed by using scanning electron microscopy (SEM), and the facture mechanism of the composites was discussed.

3:15 PM Break

3:30 PM

Microscale Discontinuous Displacement Measurement Techniques: Helena Jin¹; Sandip Haldar²; Hugh Bruck²; Wei-Yang Lu¹; ¹Sandia National Labs; ²University of Maryland

This research is to develop a feasible technique to measure the discontinuous deformations at the microscale, such as those associated with crack tips. Both grid method and digital image correlation (DIC) technique were explored to measure the microscale and discontinuous displacements at the crack tip during the fracture test of aluminum specimens. Three point bending test of aluminum specimens were conducted inside a Scanning Electron Microscopy (SEM). A unique pattern which can be applied for both techniques was generated by sputtering gold films onto the specimen surface through copper mesh. The displacement fields calculated from both techniques are compared with each other to identify the strengths and weaknesses of each technique for the microscale and discontinuous displacement measurements.

3:45 PM

Microstructural Influence on the Mechanical Behaviour of Ti-5Al-5Mo-5V-3Cr: *Nicholas Jones*¹; David Dye¹; Trevor Lindley¹; ¹Imperial College London

High strength titanium alloys, e.g. Ti-5Al-5Mo-5V-3Cr (Ti-5-5-5-3), are currently used in large components such as the truck beam in landing gear assemblies. Unlike other classes of titanium alloys, metastable beta alloys can be processed to develop a wide range of microstructures, all of which can influence the mechanical properties of the final component, e.g. strength, fatigue and fracture toughness. This ability to tailor the microstructure has resulted in significant interest into possible applications of these alloys into areas of the airframe traditionally dominated by other alloy classes. Thus, properties previously thought to be second order, such as high cycle fatigue (HCF) life have become important. Limited research concerning the fatigue behaviour of Ti-5-5-5-3 has been available in the public domain, with little or no consideration of the relationship between microstructure and micro-mechanisms of cracking. Here we consider the effect of different microstructures on the HCF properties of Ti-5-5-5-3.

4:00 PM

Effects of Rolling Induced Anisotropy on Fatigue Crack Initiation and Short Crack Propagation in Al 2024-T351 under Uniaxial and Biaxial States of Stress: *Admir Makas*¹; Ikshwaku Atodaria¹; Ross MacKinnon¹; Pedro Peralta¹; ¹ASU

The influence of rolling-induced anisotropy on fatigue properties is important for the prediction of useful life of aerospace structures via computational modeling. In this work, fatigue behavior is studied using notched uniaxial samples with load axes along either the longitudinal or transverse direction, and biaxial samples (cruciforms), where local composition and crystallography are quantified using Energy Dispersive Spectroscopy and Electron Backscattering Diffraction. Subsequently, interrupted fatigue testing at stresses close to yielding is performed on the samples to nucleate and propagate short fatigue cracks and nucleation sites are located and characterized using standard optical and Scanning Electron Microscopy. Results indicate that scatter is higher for loading along the transverse direction. The 3-D geometry of the critical precipitates, obtained using ion beam machining, is correlated to local crystallography to understand the effects these variables have on cracking behavior. Work funded by Department of Defense, AFOSR Grant FA95550-06-1-0309, David Stargel program manager.

4:15 PM

Damage Evolution in Ultrasonic Welded Aluminum/Fiber-Reinforced Polymer Joints with Different Welding Geometries: *Natalia Konchakova*¹; Ralf Mueller¹; Franz Josef Barth¹; Frank Balle¹; Dietmar Eifler¹; ¹University of Kaiserslautern

This research aims at the investigation of damage evolution in light weight engineering structures, like aluminum/fiber-reinforced polymer welding joints. The finite element method is used for a numerical analysis of mechanical behavior of a single overlap tensile specimen, which is produced by ultrasonic welding. The influence of the welding geometry on the joint's damage is consider. An elastoplastic model with Lemaitretype-damage is applied. The present work contains results for three different welding geometries: square, circle and moon. It is shown that the damage is lower in the specimen with circle welding zone as compared to square interface. The damage progress in the joint with moon welding domain takes place later than in the other specimens. The specimen with moon welding geometry has the highest point of maximal load. The simulated results show agreement with the experimental data for the ultrasonic welded joint with square welding area.

4:30 PM

Role of Austenite Plasticity in the Deformation of Superelastic Nitinol: *David Xu*¹; Robert Ritchie¹; ¹UC Berkeley

Nitinol is an important biomedical shape memory alloy that can behave superelastically. It derives its superelasticity from transformation between austenite and martensite phases. The transformation occurs when local strain on the austenite phase exceeds 1.2%. Traditionally, the martensitic transformation is assumed to be the major source of strain. We loaded Nitinol tensile dogbone samples under X-ray microdiffraction to study the phase transformation and texture. It was found that numerous austenite grains went untransformed over 1.2% local strain. Beyond the orientation effects of transformation, it was found that martensite transformation is not the only contributing factor for strain. There are evidence of that some of the austenite phases. The austenite plastically deformed instead of transformed into the martensite phase. The austenite plasticity can provide an explanation for the limits to the reversibility of transformation in cyclic loading of Nitinol.

4:45 PM

Deformation in Two-Phase Titanium Alloys Studied by Surface Strain Mapping Techniques: *Rebecca Sandala*¹; João Fonseca¹; Michael Preuss¹; ¹University of Manchester

The purpose of this study is to investigate the slip character at the a/β interface in two phase titanium alloys. Detailed in situ deformation studies have been carried out on lamellar and bilamellar microstructures of Ti-6246. Digital Image Correlation was used to obtain the strain maps from optical images taken during loading where high localised strain was mainly observed close to grain boundary a and in favourable a orientations. It was found on further loading that high strain areas also coincided with slip traces. Several of these slip traces transferred across grain boundary a regardless of the difference in neighbouring orientations. For further clarification CPFEM was used to predict the deformation by creating a virtual microstructure from the EBSD data. Furthermore studies of the a_1 , a_2 , and a_3 slip were carried

out using EBSD and TEM to clarify why slip occurs in some regions of favourable orientations more than others.

5:00 PM

Vanadium Effects on a BCC Iron Sigma 3 Grain Boundary Strength: Sungho Kim¹; Seong-Gon Kim¹; Mark Horstemeyer¹; ¹Center for Advanced Vehicular Systems

The effects of micro-alloying element, vanadium, on a BCC Fe sigma 3 (111)[1-10] symmetric tilt grain boundary strength are studied using Density Functional Theory calculations. The lowest energy configuration of the grain boundary structure are obtained from the first-principles calculations. The substitutional and interstitial point defect formation energies of vanadium in the grain boundary are compared. The substitutional defect is prefered to interstitial one. The segregation energies of vanadium onto the grain boundary and its fractured surfaces are computed. The cohesive energy calculation of the grain boundary with and without vanadium show that vanadium strengthen the BCC iron grain boundary. The tensile and shear tests on the grain boundary with and without vanadium segregation are carried out to study the vanadium effecton the grain boundary.

Dynamic Behavior of Materials V: Shock Compression

Sponsored by: The Minerals, Metals and Materials Society, TMS Structural Materials Division, TMS/ASM: Mechanical Behavior of Materials Committee

Program Organizers: Marc Meyers, UCSD; Naresh Thadhani, Georgia Institute of Technology; George Gray, Los Alamos National Laboratory

| Tuesday PM | Room: 5A |
|---------------|-------------------------------|
| March 1, 2011 | Location: San Diego Conv. Ctr |

Session Chair: Jerry La Salvia, US Army Research Lab

2:00 PM Invited

Material Deformation Dynamics at Ultrahigh Pressures and Strain Rates: Bruce Remington¹; ¹Lawrence Livermore National Laboratory

Solid state dynamics experiments at extreme pressures, P > 1000 GPa (10 Mbar), and strain rates (1.e6 -1.e8 1/s) are being developed for the NIF laser. The experimental methods are being developed on the Omega laser facility. VISAR measurements establish the ramped, high pressure conditions. Recovery experiments offer a look at the residual microstructure. Dynamic diffraction measurements allow phase, shear stress (strength), and possibly twin volume fraction and dislocation density to be inferred with < 1 ns time resolution. Constitutive models for material strength are currently being tested at ~Mbar pressures by comparing 2D simulations with experiments measuring the Rayleigh–Taylor instability evolution in solid state samples of vanadium and tantalum. We suggest that the material deformation at these conditions falls into the phonon drag regime, and make an estimate of the (microscopic) phonon drag coefficient, by relating to the (macroscopic) effective lattice viscosity.

2:30 PM

Length- and Timescales for Dynamic Deformation in Materials: Neil Bourne¹; ¹AWE Aldermaston

Materials respond to dynamic loading with a variety of mechanisms. Each has it's own mechanical threshold for operation including discrete stress levels. However it also responds with a defined kinetics to the impulse applied. When a crystalline material is exposed to extremes of pressure such mechanisms include martensitic phase transformation, dislocation nucleation and propigation, twinning and potentially melting. The mechanical environment and the thermodynamics of the mechanisms determine the kinetics and the effect upon the microstructure. Energy considerations define timescales and thus lengthscales over which such mechanisms are operate. Thus lengthscale regimes exist within which certain mechanisms are confined. Examples are drawn from a variety of metallic responses showing the suite of available mechanisms and the range of observables that result.

2:45 PM

Extracting Plastic Flow Properties from Shock Velocimetry: *Bryan Reed*¹; James Stolken¹; Roger Minich¹; Mukul Kumar¹; ¹Lawrence Livermore National Laboratory

We present a coherent set of analysis methods designed to deduce the evolution of plasticity inside a shocked material from measurements of free surface velocities. While the problem is inherently underconstrained, much information may still be deduced with these methods, provided one may apply a few fairly modest assumptions about the wave propagation (a statement we support in part through analysis of simulated data sets in which the correct answers are known). This is particularly challenging when one is concerned with rate-dependent effects in nonsteady waves, which invalidates many assumptions commonly made in such analysis. Instead, we derive an estimate of the full deviatoric-stress/plastic-strain-rate relation for every point in the material. Viewing the data in this way provides insights into the coupling among elastic precursor decay, post-shock relaxation, and the speed of the plastic wave.

3:00 PM

High Strain Rate and Pressure Induced Twinning in Tantalum: *Jeffrey Florando*¹; James McNaney¹; Luke Hsiung¹; Nathan Barton¹; Mukul Kumar¹; ¹Lawrence Livermore National Laboratory

Experiments on both single crystal and polycrystalline Ta deformed under various high rate loading conditions were performed to help determine the twinning threshold. For the single crystal samples, recovery experiments under gas gun plate impact loading conditions were conducted at two shock pressures, 25 and 55 GPa, and for four orientations $\{(100), (110), (111), (123)\}$. For the polycrystalline Ta samples, compression experiments were conducted at liquid nitrogen temperatures at stain rates ranging from 10⁻⁴ to 10⁻³ s⁻¹. In addition, samples were cold-rolled and then tested at liquid nitrogen temperatures to determine the effect of dislocation density on the overall twin fraction. Recovered samples were characterized using EBSD orientation mapping along with a limited amount of transmission electron microscopy to assess the occurrence of twinning under each test condition.

3:15 PM

Isomorphic Phase Transformation of Cerium under Shock Loading Using Molecular Dynamics: *Virginie Dupont*¹; Timothy Germann¹; Shao-Ping Chen¹; ¹Los Alamos National Laboratory

Cerium (Ce) has an atypical phase diagram with an isomorphic phase transition between two FCC structures that induces a volume collapse of \sim 16%. We present an Embedded Atom Method (EAM) potential for Ce and its use in shock loading via MD simulations. The samples studied are single crystalline and defect-free. The velocity profiles of the shocked samples show a split wave structure typical of a phase transition. Two waves are observed, an elastic precursor followed by a plastic wave. The plastic wave causes the expected phase transition. Comparisons to experiments on Ce and MD simulations on Cesium (Cs) indicate that three waves could be observed, one elastic precursor, a first shock compression wave in the gamma phase, and finally the phase transition wave from gamma to alpha. The construction of the potential is believed to be responsible for the two-wave structure.

3:30 PM

Laser Compression of Monocrystalline Tantalum: *Chia-Hui Lu*¹; Bruce Remington²; Brian Maddox²; Bimal Kad¹; Fabienne Gregori³; Hye-Sook Park²; Marc Meyers¹; ¹University of California, San Diego; ²Lawrence Livermore National Laboratory; ³Université Paris Nord

Monocrystalline tantalum with orientations [100] and [111] was subjected to laser compression at energies of 350 to 685 J, generating shock amplitudes varying from 15 to 100 GPa. The laser beam, with a diameter slightly higher than 1 mm, created a crater of significant depth, on the surface of which traces of twins were visible by back-scattered SEM. The decay of the pulse through the specimens was accompanied by an attendant decrease in the density of shock-generated dislocations. Microhardness measurements paralleled this decay. TEM revealed profuse mechanical twinning within a distance from the energy deposition surface of \sim 1.5 mm at 684 J compression power, corresponding to an approximate pressure of 40 GPa. The experimentally measured dislocation densities and threshold stress for twinning are compared with predictions using an analysis based on the constitutive response and the similarities and differences are discussed in terms of the mechanisms of defect generation.

3:45 PM Break

3:55 PM Invited

Shock Response and Recovery of Cu-Nb Nanolayer Composites: *Timothy Germann*¹; ¹Los Alamos National Laboratory

Large-scale classical molecular dynamics (MD) simulations and laserlaunched flyer plate experiments have been used to study the shock response of Cu-Nb nanolayered composites. At a layer thickness of 5 nm, the hardness of such metallic multilayers (as measured by quasistatic indentation or compression tests) reaches a maximum due to the difficulty of dislocation transmission across the interfaces. We observe a similar strengthening effect under dynamic shock loading, both in the MD simulations and in post mortem examinations of shock-recovered samples subjected to 10-20 GPa shock loading. The MD simulations provide insight into the dislocation nucleation and transmission processes that occur under compression, as well as the subsequent annihilation upon release. The Cu-Nb interfaces serve both as dislocation sources during shock compression, and dislocation sinks upon release, and thus lead to a greater degree of recovery as compared to either constituent Cu or Nb single crystal.

4:25 PM

Mode Transitions in Shocked Single-Crystal Tantalum: *Luke Hsiung*¹; Brian Maddox¹; Bruce Remington¹; ¹Lawrence Livermore National Laboratory

TEM studies of shocked single-crystal tantalum recovered from gasgun impact and laser-shock experiments are presented to reveal the transitions of deformation mode from dislocation glide to twinning and shear transformation. The transitions take place to accommodate insufficient dislocation flow resulting from the exhaustion of dislocation sources when dynamic-recovery reactions for dislocation annihilation and cell formation are largely suppressed under dynamic pressure conditions. The exhaustion of dislocation sources is proposed to occur when the stress for dislocation multiplication exceeds the threshold stresses for twinning and shear transformation. This work was performed under the auspices of the U.S. Department of Energy by Lawrence Livermore National Laboratory under Contract DE-AC52-07NA27344.

4:40 PM

Analytical Models for Predicting Pressure-Volume Compressibility of Low-Density Compacts of Iron Nano-Particles: Chengda Dai¹; Daniel Eakins²; *Naresh Thadhani*³; ¹Southwest Institute of Fluid Physics; ²Imperial College ; ³Georgia Institute of Technology

The shock compression behavior of nano-sized powders is investigated to determine the applicability of analytical models for predicting the pressure-volume compressibility of nano-particles of iron, pre-pressed to \sim 35% and \sim 45% TMD compacts. Time-resolved experiments were performed to measure the pressure-volume Hugoniot using piezoelectric stress gauges which monitored the input and propagating stress profiles and the shock velocity. The results show a densification-distension transition at \sim 2 GPa for the \sim 35% TMD, and \sim 6 GPa for the \sim 45% TMD compacts. Correlations of the model calculations with the measured data indicate that the shock Hugoniot of pre-pressed nano-iron powder compacts cannot be correctly described by the analytical models, which are otherwise capable of predicting the Hugoniot of highly porous materials (pre-pressed compacts) of micronsized powders of similar density. The principal cause for the ineffectiveness is the lack of incorporating the difference in internal energy between the powder compact and the solid.

4:55 PM

Simultaneous Contour Forming and Shock Hardening in Planar Impact Forming: *Huimin Wang*¹; Yuan Zhang¹; Geoff Taber¹; Glenn Daehn¹; ¹Ohio State University

Nominally flat components with a number of features are desired for a range of components ranging from heat exchangers, to bipolar plates, to micro-reactors to micro-fluidics. To fabricate such components in standard presses, the forming pressure must often exceed the flow stress of the workpiece by a factor of 2 to 3, requiring very large presses. In contrast, impact velocities beyond 100 m/s collisions can provide impact pressures large enough to cause the workpeice to fully conform. Such a manufacturing process, driven by electromagnetic discharge is very viable and has two very interesting advantages: 1) dimensional reproduction is exceptional and 2) rates of hardening at the strain rates seen at surface impact (often in excess of $10^{\circ}6$ s-1 cause much greater rates of strain hardening than press forming. Detailed experiments with copper will show variations in material microstructure and properties that result from this high strain rate impact forming process.

5:10 PM

Spatial Distribution of Damage after Shock Loading: *Veronica Livescu*¹; John Bingert¹; Davis Tonks¹; ¹Los Alamos National Laboratory

The quantification of shock damage in polycrystalline materials is critical for the understanding of mechanisms controlling failure under dynamic conditions. Ductile fracture in metals occurs by the nucleation, growth, and coalescence of voids. Most damage models characterize the distribution of the voids by volume fraction and assume uniform porosity, but voids in a real material are neither uniform in size nor spatial distribution, and vary with experimental parameters. Physically-based damage models must statistically reproduce this heterogeneity of void damage to accurately model ductile failure of materials under shock loading. This work investigates void damage distributions and clustering of void damage by using a correlation function-based approach to produce quantitative descriptors of microstructural damage. Damage statistics were obtained from threedimensional reconstructions of experimentally shock-induced damage in plate impact and high-explosive driven specimens. Discussion will include evolution of damage statistics with experimental parameters, and plastic flow localization due to non-uniform void distribution.

5:25 PM

The Effect of Cold Work on the Shock Response of Tantalum: *Jeremy Millett*¹; Glenn Whiteman¹; Neil Bourne¹; Nigel Park¹; ¹AWE

The response of the body centred cubic metal tantalum to shock loading has been studied for several decades, due to its use by the military in explosively formed projectiles. Previous studies on well controlled, annealed specimens has shown that deformation is controlled by the motion of rather than the generation of $a/2 <111 > \{110\}$ screw dislocations in straight segments, which result in little if any post shock hardening. In situ-shear strength measurements have also shown a significant strength reduction behind the shock front, suggesting that the motion of these dislocations acts as a stress relief mechanism. Similar effects have also been noted in tungsten and its alloys. In this presentation, we return to tantalum, investigating the differences in shock response between a low dislocation density (annealed) and high dislocation density (cold rolled) material. Results are discussed in terms of the shear strength and its variation with time behind the shock front.

5:40 PM

The Role of the Structure of Grain Boundary Interfaces during Shock Loading: *Alejandro Perez-Bergquisi*¹; Juan Escobedo¹; Carl Trujillo¹; Ellen Cerreta¹; George Gray¹; Saryu Fensin¹; Timothy Germann¹; ¹Los Alamos National Laboratory

In order to understand the role of interfaces in the shock tolerance of metals, three specific copper bi-crystal boundaries have been studied under shock loading and incipient spall conditions. These boundaries, two 001/111 boundaries and a 001/001 tilt boundary and their structures have been characterized prior to deformation using both electron back scattered diffraction (EBSD) and transmission electron microscopy (TEM) to obtain

their axis/angle pair relationship and the structure at the boundary. This characterization has been utilized as input for MD simulations to examine in-situ dislocation/grain boundary interactions. These boundaries were then shocked at 2.5 and 10GPa in an 80mm gas gun and soft recovered. Post-mortem characterization, EBSD and TEM, has revealed that typical grain boundaries readily form damage during shock loading but the special boundaries (S3) are resistant to failure. This is linked to differences in slip transmissibility across these types of boundaries.

5:55 PM

Role of Twinning in Shock Related Deformation: Veronica Livescu¹; John Bingert¹; Thomas Mason¹; George Gray III¹; ¹Los Alamos National Laboratory

Twinning is observed under shock loading conditions in metals that do not twin under conventional loading conditions. The occurrence of twinning depends on both material properties and experimental parameters. However, real time diagnostics used currently in shock experiments are insufficient to identify and characterize specific deformation and damage processes and their precise sequence in time. The post-mortem microstructure characterization presented here provides insight on the progression of deformation in high-explosive driven Tantalum and validates deformation and damage mechanisms under shock loading. Crystallographic aspects that contribute the most to the twinning behavior will be presented, as well as effects of shock obliquity on the twinning behavior. Spatial distribution and morphology of twins found in high-explosive driven Tantalum show that twinning is a critical deformation mechanism and must be incorporated into dynamic deformation models for an accurate description of shock damage.

Electrode Technology for Aluminium Production: Petroleum Coke VBD

Sponsored by: The Minerals, Metals and Materials Society, TMS Light Metals Division, TMS: Aluminum Committee Program Organizers: Alan Tomsett, Rio Tinto Alcan; Ketil Rye, Alcoa Mosjøen; Barry Sadler, Net Carbon Consulting Pty Ltd

| Tuesday PM | Room: 16B |
|---------------|-------------------------------|
| March 1, 2011 | Location: San Diego Conv. Ctr |

Session Chair: Angelique Adams, Alcoa

2:00 PM Introductory Comments

2:10 PM Invited

Historical and Future Challenges with the Vibrated Bulk Density Test Methods for Determining Porosity of Calcined Petroleum Coke: *Jignesh Panchal*¹; Mark Wyborney¹; Jeffrey Rolle¹; ¹A.J.Edmond Company

Over several decades, calcined petroleum coke producers and the aluminum industry have been using various techniques such as Vibrated Bulk Density (VBD), Mercury Intrusion Porosimetry (MIP), and Mercury Apparent Density to predict the porosity of calcined petroleum coke. Better knowledge of the coke porosity allows a more accurate estimation of coke quality and pitch demand for fabricating anode of optimum performance. Industry has had limited success in accurately predicting porosity using the existing VBD methods. Direct measurement of porosity by MIP is an alternative way to measure porosity accurately. Currently there is limited correlation between VBD and MIP. Any improvements to the VBD test method should demonstrate improved correlation to the results obtained from MIP. This paper covers the historical and traditional approach to predict calcined coke porosity, correlation study of VBD test method and porosity by MIP, and input to the development of superior test methods to meet Industry requirements.



2:35 PM Invited

Prediction of Calcined Coke Bulk Density: *Marie-Josée Dion*¹; Hans Darmstadt¹; Nigel Backhouse¹; Frank Cannova²; Mike Canada²; ¹Rio Tinto Alcan; ²BP

The vibrated bulk density (VBD) is an important calcined coke property. Due to changing green coke quality, a reliable forecast of the calcined coke VBD from small green coke samples is required. The VBD can be predicted from green coke properties, like the Hardgrove Grindability Index (HGI) and volatiles content but the precision of this forecast is often not sufficient for procurement decisions. Several laboratory calcination techniques were studied including the use of two different laboratory rotary kilns at BP Coke and a contractual facility. When compared to RTA's Arvida calciner it was determined certain methods could achieve good agreement for VBD and coke calcination level (Lc)and it was also possible to replicate phenomena that cause problems at an industrial scale such as coke ring formation. The methods will be used in the future to support the RTA calcining operations.

3:00 PM Invited

Calcined Coke Particle Size and Crushing Steps Affect Its VBD Result: Frank Cannova¹; *Mike Canada*¹; Bernie Vitchus¹; ¹BP Coke

The size of a calcined coke particle used in the Vibrated Bulk Density (VBD) test and the size of the particle before crushing affects its VBD analysis. That is, naturally occurring particles usually have a higher packing density and VBD compared with particles that are crushed to the same size. Consequently, calcined coke preparation crushing steps can dramatically affect the VBD result. Data, showing how calcined coke particle size and crushing steps affect the VBD result will be presented. These data help explain why the roll crushing steps need to be controlled to improve VBD repeatability and reproducibility. In addition, data will be presented showing how the roll crusher operation and maintenance affects the VBD result.

3:25 PM Invited

Bulk Density - Overview of ASTM and ISO Methods with Examples of between Laboratory Comparisons: Lorentz Petter Lossius¹; Bill Spencer²; Harald A. Øye³; ¹Hydro Aluminium AS; ²Oxbow Calcining; ³Norwegian University of Science and Technology

The bulk density of petroleum coke is recognized as a key coke property for the density of anodes in primary aluminum electrolysis, and this makes the bulk density important in petroleum coke trade. ASTM and ISO have standards for testing; ASTM with the two VBD methods D4292 and D7454, and ISO with the TBD method, ISO 10236. There is a concern in anode production that it is difficult to obtain good between-laboratory comparisons. The paper will compare the methods, give results from several interlaboratory studies and discuss the observed within- and between-laboratory results.

3:50 PM Break

4:00 PM Invited

Improving the Repeatability of Coke Bulk Density Testing: Les Edwards¹; Marvin Lubin¹; James Marino¹; ¹Rain CII Carbon

The "Pechiney" mercury apparent density test was used by the aluminium industry for many years to measure the density/porosity of calcined petroleum coke. Over the last 5 years, the industry has moved away from this test for occupational health and safety reasons. The current alternative tests are based on vibrated or tapped bulk density methods. The value of measuring bulk density is reduced due to poor reproducibility caused by differences in equipment and sample preparation. This paper reviews different bulk density test methods and presents repeatability data on a new method for measuring coke bulk density. The method is based on automated equipment which uses transverse axial pressure to measure bulk volume and hence bulk density, of calcined coke samples. The new equipment shows improved repeatability compared to existing equipment.

4:25 PM Invited

ASTM D7454 Vibrated Bulk Density Method – Principles and Limitations: Francois Laplante¹; Luc Duchesneau¹; ¹RioTinto Alcan

This method proposed by Rio Tinto Alcan and approved by ASTM in 2008, differs from method D4292 by the introduction of a semiautomated

equipment and also by referring to a tighter sample preparation procedure. The performance expressed in terms of repeatability is = 0.008 g/mL when the preparation variance is not included and 0.01 g/mL when the preparation variance is included. The intralaboratory reproducibility over a two-year period came out to 0.02 g/mL. The interlaboratory reproducibility has not yet been systematically determined but appears to be high considering the large punctual differences observed between coke providers and coke purchasers. The underlying principles of D7454 will be presented, the factors causing differences between laboratories will be discussed and a mitigation strategy will be proposed.

4:50 PM Invited

Vibrated Bulk Density (VBD) of Calcined Petroleum Coke and Implications of Changes in the ASTM Method D4292: *Bill Spencer*¹; Laura Johnsen¹; David Kirkpatrick¹; Desiree Clark¹; Miguel Baudino¹; ¹Oxbow Calcining LLC

Vibrated bulk density (VBD) is a quantitative measurement used in the aluminum industry to evaluate the density of calcined petroleum coke. In the calcining industry, the reproducibility and ambiguity of the current ASTM International (ASTM) method D4292 generates a wide range of VBD data. Therefore, Oxbow Calcining LLC (Oxbow) made an investigation into the VBD procedure - D4292. Issues with D4292 include the use of the appropriate crushing equipment, crushing of the gross sample, sieving of the prepared sample, determination of the sample volume using appropriate graduated cylinder vibration time, and apparatus setup. This investigation led to a revision in the ASTM D4292 method to remove the ambiguities.

5:15 PM Panel Discussion

Fatigue and Corrosion Damage in Metallic Materials: Fundamentals, Modeling and Prevention: Fatigue and Corrosion Interaction and Materials Corrosion

Sponsored by: The Minerals, Metals and Materials Society, TMS Structural Materials Division

Program Organizers: Tongguang Zhai, University of Kentucky; Zhengdong Long, Kaiser Aluminum; Peter Liaw, University of Tennessee

| Tuesday PM | Room: 31C |
|---------------|-------------------------------|
| March 1, 2011 | Location: San Diego Conv. Ctr |

Session Chairs: Chengjia Shang, University of Science and Technology Beijing; Soo Yeol Lee, The University of British Columbia

2:00 PM Invited

Effect of Sensitized Microstructure on Corrosion Fatigue Crack Growth in Al 5083: *Peter Pao*¹; Ramasis Goswami²; Robert Bayles¹; Ronald Holtz¹; ¹Naval Research Laboratory; ²SAIC

The influence of β phase (Al3Mg2) at the grain boundaries on the corrosion fatigue crack growth of sensitized (175 °C/1 – 1000 hrs) and as-received (H131) Al 5083 was investigated. TEM investigations reveal, while β is absent at the grain boundaries of as-received Al 5083, small and discontinuous β precipitates at the grain boundaries after few hours at 175 °C. On prolonged aging at 175 °C, β grows and coalesces and most grain boundaries are covered with continuous β . The presence of β at the grain boundaries significantly reduces the high stress ratio corrosion fatigue crack threshold and increases the crack growth rates in saltwater. Such corrosion fatigue degradation is proportional to the amount of β present at the grain boundaries. The observed fatigue crack growth responses are discussed in terms of differences in microstructure and the interplay between stress-corrosion and corrosion fatigue cracking thresholds.

2:20 PM

The Effect of Hot Corrosion Pits on Fatigue Crack Initiation and Fatigue Life of a Disk Superalloy: *Yoshiki Yamada*¹; Ignacy Telesman²; Timothy Gabb²; Louis Ghosn²; ¹Ohio Aerospace Institute; ²NASA GRC

Type II Hot Corrosion pitting can occur for disk superalloys having salt deposits and exposures near 700oC. These pits act as stress concentrators and thus can significantly reduce low cycle fatigue life at both low and high temperatures. In this study, the effect of hot corrosion pits on fatigue crack initiation and low cycle fatigue life was investigated. In order to understand a mechanism of crack initiation around corrosion pits, FEA model was used to estimate the localized elevation in stress concentrations. The FEA models were based on SEM observations of the type and size of the corrosion pits initiating cracks. In addition, fatigue life prediction based on equivalent initial flow size was attempted and compared with test results.

2:40 PM

Effect of Proximity and Dimension of Two Artificial Pitting Holes on the Fatigue Endurance of Aluminum Alloy 6061-T6 under Rotating Bending Fatigue Tests: *Gonzalo Dominguez Almaraz*¹; Victor Hugo Mercado¹; J. Jesus Villalon¹; ¹University of Michocan

This work is oriented to study the effect of two artificial pitting holes, its dimensions and proximity, on the fatigue endurance of aluminum alloy 6061-T6 under rotating bending fatigue tests. Stresses concentration induced by artificial pitting holes is analyzed and correlated with the experimental fatigue life. It is found that the stresses concentration increases exponentially when the two pitting holes approaching and this induces an important reduction on the fatigue life. Concerning the dimensions variation of one pitting in regard the second, no important influence was observed on fatigue life for a given separation between them; this implies that separation between the two artificial pitting holes and the associated stress concentration is the principal parameter on the fatigue life under these conditions. The results are discussed and conclusions are presented involving the fatigue life, proximity and dimension of pitting holes, stress concentration and the fracture surfaces related to failure origin.

3:00 PM

Microstructural and Environmental Effects on Fatigue Crack Growth in 7075 Aluminum Alloy: *Amir Bonakdar*¹; Fengjiang Wang¹; Jason Williams¹; Nikhilesh Chawla¹; ¹Arizona State University, School of Mechanical, Aerospace, Chemical, and Materials Engineering

The fatigue behavior of aluminum alloys is greatly influenced by environment and precipitate structure. In this talk, the role of moisture on fatigue crack growth behavior of 7075 Al alloy was investigated. In particular, the role of crystallographic slip, as dictated by precipitate structure, was studied. Rolled 7075 Al alloy was heat-treated to underaged, peak-aged, and overaged conditions. Fatigue crack growth rates were measured under various partial pressures of water vapor. Standard compact tension specimens along the S-T orientation were used, and testing was performed under load ratios of R = 0.1 and R = 0.8. The experimental results were analyzed by the two parameter approach (\Box K-Kmax). The microstructure and morphology of the fracture surfaces were examined by scanning electron microscopy (SEM) and correlated with thecrack growth behavior.

3:20 PM Invited

A Study of Corrosion of Pure Aluminum and AA2037 Al Alloy in a NaOH Solution by Positron Annihilation: Yichu Wu¹; *Tongguang Zhai*²; ¹University of Wuhan; ²University of Kentucky

Pure Al and a continuous cast AA 2037 Al alloy were analyzed with positron beam-based Doppler broadening spectroscopy after corrosion in Imol/L NaOH for various periods of time. By varying the incident positron energy, corrosion-induced defects in different depth from the surface could be detected by measuring the S parameter in these samples. It was found that the S parameter near the surface was significantly increased in pure Al after corrosion. This was likely to be due to the interaction between positrons and the nanometer-sized voids formed in the Al surface during corrosion. AFM examination indicated that many cavities were formed on the Al surface after corrosion. A significant decrease in S parameter was observed in the AA

2037 Al alloy, which was cold-rolled, solid solution heat-treated and waterquenched, after corrosion. This could be caused by Cu enrichment occurred at the metal-oxide interface during corrosion in this alloy.

3:40 PM Break

3:50 PM Invited

Constituent Particle Clustering and Pitting Corrosion: *D Gary Harlow*¹; ¹Lehigh University

Corrosion in aluminum alloys results from local galvanic coupling between constituent particles and the metal matrix; it is a complex stochastic process. Severe pitting is caused by particle clusters, of which are dependent on the spatial statistics of particles. Critical statistics include location, size, density and chemical composition. The localized corrosion growth rate is primarily dependent on the galvanic process perpetuated by particle-toparticle interactions and electrochemical potentials. Frequently, severe pits are millimeters in length, and these pits have the dominant impact on structural prognosis. To accommodate large sizes, a model for threedimensional constituent particle microstructure is proposed. The model employs a fusion of classic stereological techniques, spatial point pattern analyses, and qualitative observations to describe the constituent particle microstructure in three-dimensions. The methodology can be carried out using standard optical microscopy and image analysis techniques.

4:10 PM Invited

Life Prediction of a New Developed Ferrite Stainless Steel for Automobile Muffler: Chengjia Shang¹; ¹University of Science and Technology Beijing

The ferrite stainless steel has been used in automobile exhaust system for many years. However, the damage of muffler is severely by using low Cr content stainless steel, especially serving in poor oil quality district. The corrosion mechanism of the condensate water in muffler shows that pin corrosion by chloride and sulfur are the main reasons, and with Cr content increasing the pin corrosion resistance can be improved dramatically. In this paper, the life prediction of different Cr content ferrite stainless steels were invested by simulating tests. The life prediction shows that as the Cr content reached about 17%, the life of muffler can be increased about 50% comparing with 409L type ferrite stainless steel (11%Cr content). The newly developed 439M was used in passenger car in Chinese automobile work. The road testing result of muffler life show that it can be more than 100,000km, which satisfy specified requirements.

4:30 PM

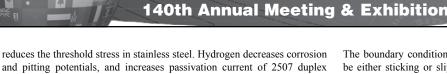
A Versatile Component Testing Method for the Life Time Determination of Automotive Exhaust Mufflers: *Muhammad Yasir*¹; Gregor Mori¹; Helmut Wieser²; Martin Schattenkirchner²; Manuel Hogl²; ¹Christian Doppler Laboratory of Localized Corrosion, University of Leoben, Austria; ²Faurecia Emissions Control Technologies, Germany

The problem originates in the automotive exhaust industry where a manufacturer has to perform number of tests on different types of samples before selection of a right material. Correlations of these testing methods often lead to a disagreement. All these tests provide information about relative ranking of different grades under different conditions. To predict the life time of a complete system under real conditions is always a difficult task and sometimes also uncertain. There is no test available in which simulation of external and internal corrosion can be performed simultaneously. The objective of this study was to develop a type of testing procedure that can determine the combined effect of salt corrosion, condensate corrosion and high temperature corrosion. Corrosion resistance of different materials and designs are studied in this research. A comparative study was performed between field systems and test systems to establish a relation for the life time calculation.

4:50 PM Invited

Effect of Hydrogen on the Localized Corrosion of Steels: *Lijie Qiao*¹; ¹University of Science and Technology Beijing

This paper presents our recent work on the effects of hydrogen on the properties of steels. The results show that hydrogen enhances nucleation of micro-cracks, increases propagation rates of stress-corrosion cracks, and



stainless steels in 0.5mol/LH2SO4+3%NaCl solution. Hydrogen promotes pitting initiation in ferrite phase in duplex stainless steel in which increase in hydrogen density decreases the time for pitting initiation and growth rate. Both hydrogen and Cl- decrease linearly corrosion and pitting potentials, and increase the passivation current of carbon steel in boric acid buffer solution.

5:10 PM

Studying Properties of Zn-Coated Carbon Steel: *Ruqaya Khammas*¹; ¹Technical College

This study includes coating low carbon steel, with pure Zn, Zn-0.2Al for one coat layer and two coat layer using batch hot dip galvanizing method and studying the coating properties, to protect the base metal from corrosion in several medias. Microstructure shows series of Fe-Zn alloy layer with a surface of free Zn, and the effect of adding (0.2%Al) is to suppressing the alloying layers and increase the bath fluidity. The coating phases presents, gamma γ (Fe3Zn10), delta δ (FeZn7), zeta ζ (FeZn13) and eta η (Zn). Coating thickness Zn one coat layer is (55µm), Zn two coat layer is (180µm), that's mean when we doubled the immerging time the coating thickness is almost trebled. For Zn-0.2Al one coat layer the thickness mean was about (45µm), the double coat of Zn-0.2Al was failed. Corrosion test done by potentiostat system with two different medias, tap water and sea water.

Friction Stir Welding and Processing VI: Aluminum and Magnesium Alloys II

Sponsored by: The Minerals, Metals and Materials Society, TMS Materials Processing and Manufacturing Division, TMS: Shaping and Forming Committee

Program Organizers: Rajiv Mishra, Missouri University of Science and Technology; Murray Mahoney, Retired from Rockwell Scientific; Yutaka Sato, Tohoku University; Yuri Hovanski, Pacific Northwest National Laboratory; Ravi Verma, General Motors

| Tuesday PM | Room: 5B |
|---------------|-------------------------------|
| March 1, 2011 | Location: San Diego Conv. Ctr |

Session Chair: Murray Mahoney, Retired from Rockwell Scientific

2:00 PM Invited

Novel Techniques for Corner Joints Using Friction Stir Welding: Jonathan Martin¹; Chris Stanhope¹; Sam Gascoyne²; ¹TWI; ²Centre for Doctoral Training in Advanced Metallic Systems

Most commercial FSW applications use simple butt joint configurations and alternative designs such as T-sections and corner welds are very rarely considered. This paper presents the development of novel techniques which have demonstrated the ability to produce high quality internal and external corner welds using an adaption of Stationary Shoulder Friction Stir Welding. Further enhancements using a shaped shoulder have also allowed fillet radii to be added to internal corners and a consumable filler wire to provide the material for the fillet. The principles of these techniques are explained including the results of process development trials on a range of aluminium alloys including metallurgical examinations, mechanical property evaluations and how they are related to the thermal weld cycles. The development of these techniques has the potential to be applied to a range of new joint geometries and extend the product design possibilities.

2:25 PM

Investigation of the Material Shear Layer in Bobbin Tool Friction Stir Welding: Jakob Hilgert¹; Jorge dos Santos¹; Norbert Huber¹; ¹GKSS Forschungszentrum GmbH

In bobbin tool FSW the material flow around the tool is of great importance for the process stability and weld seam quality. This study presents a CFD model of the shear layer implemented in Comsol-Multiphysics. The material used is AA2024-T3. The metal is treated as a highly viscous shear thinning liquid governed by an inverse hyperbolic sine relationship for the viscosity. The boundary condition at the interface between tool and work piece can be either sticking or slipping in any ratio. This information is part of the output of the model. The temperature information as well as the applied machine torque are taken from previous numerical and experimental work. The predicted shear layer shape and velocity profile are experimentally validated. The shear rate distribution and contact state predicted by the model for parameter sets that result in sound welds are compared to those that result in defective or instable welds.

2:45 PM

Effect of Tool Geometry and Process Condition on Static Strength of Magnesium Friction Stir Lap Linear Weld: *Qi Yang*¹; Xiang Li¹; Ke Chen¹; Yijing Shi¹; ¹Hitachi America, Ltd.

Friction stir lap linear welding is conducted on overlapped AZ31 Mg plates with different welding tools. Welds are made mainly with the orientation such that the weld retreating side on the upper plate is to be placed under load. Welding tools consist of a concave shoulder and a pin having a cylindrical, or triangular, or pie shape. This work addresses the effects of tool geometry and process condition on lap shear strength of welds. The shape of hook formed due to upward bending of the plate interface is examined. Compared to the cylindrical tool, the triangular tool effectively suppresses the hook on the retreating side due to an enhanced horizontal material flow, and this primarily leads to a 78% increase in optimized weld strength. A 'pure' shear surface present on the tool pin significantly reduces weld strength.

3:05 PM

Effect of Tool Feature on the Joint Strength of Dissimilar Friction Stir Lap Welds: Saumyadeep Jana¹; Yuri Hovanski¹; Glenn Grant¹; Karl Mattlin¹; ¹PNNL

Several variations of friction stir tools were used to investigate the effects on the joint strengths of dissimilar friction stir lap welds. In the present lap weld configuration the top sheet was 2.32 mm thick AZ 31 alloy. The bottom sheet consisted of two different steels, a (i) 0.8 mm thick electrogalvanized (EG) mild steel, or a (ii) 1.5 mm thick hot dip galvanized (HDG) high strength low alloy (HSLA) steel. Initially the tool shape was modified to accommodate the material, at which point the tool geometry was fixed. With a fixed tool geometry an additional feature was added to the pin bottom on one of the tools by incorporating a short hard insert, which would act as a stronger bottom sheet cutter. The effects of such modification on the unguided lap shear strength, and associated microstructural changes are discussed in this study.

3:25 PM

Friction Stir Fabrication of Spar T-Joints Made from 7075 Aluminum: Jeremy Brown¹; Dwight Burford¹; ¹Wichita State University

Corrosion or mechanical damage may result in the removal of an aircraft from service. The grounded aircraft must wait until replacement parts can be located and delivered or fabricated. Since many aircraft are out of production, the replacement parts may be difficult and costly to procure. Friction Stir Welding presents a cost-effective and timely alternative to create one-off structures from plate material. An evaluation was undertaken on the feasibility of joining plates of AA7075 aluminum into T-beams with friction stir welding. The fabrication approach involves lap welding through a top horizontal plate into a bottom vertical plate. Different forms of cooling to control heat input were also evaluated. Mechanical and metallurgical properties for these joints show the viability of using friction stir welding to create structures for aircraft.

3:45 PM

A Study Of a Versatile Method To Attach a Portable FSW System To an Aluminum Structure Using Adhesives: *Jordan Walser*¹; Tracy Nelson¹; Carl Sorensen¹; Murray Mahoney¹; ¹Brigham Young University

This study demonstrates a versatile method to attach a portable FSW system to an aluminum structure using adhesives. After preliminary tests of a number of adhesive candidates, Acrylic DP 820 epoxy was chosen because of its high strength, ease of application, and repeatability. Tests were developed to determine adhesive characteristics for all stages of friction stir welding

associated with repair of an aluminum structure. Tests included tensile strengths over a range of temperatures, peel strength, and dynamic loading that simulates a friction stir loading environment. Further, practical issues such as the effects of non parallel attachment and gaps between the fixture and the structure on adhesive performance were examined. Procedures for proper application and removal of the adhesive were developed. The results demonstrate that an adhesive approach meets the requirements to attach a portable FSW system to aluminum structures.

4:05 PM

Microstructural and Mechanical Properties of Friction Stir Welding Joints of 6082-T6 with 6063-T6: *Farzad Baratzadeh*¹; Alan Handyside¹; Enkhsaikhan Boldsaikhan¹; Hamid Lankarani²; Blair Carlson³; Dwight Burford¹; ¹National Institute for Aviation Research; ²Wichita State University; ³General Motors Corporation

Friction stir welding (FSW) offers a "green" alternative to fusion welding automotive bumpers. Therefore, a case study was initiated to compare a friction stir welded bumper design to a conventional fusion welded bumper design. To that point, a unique set of FSW tools were designed, fabricated and coupons were prepared for developing the process parameters through a Design of Experiment (DOE). Once the coupons were completed, a mechanical and metallurgical characterization study of the friction stir welded butt joints of aluminum alloy 6082-T6 with 6063-T6 was carried out. Sheets of 3.5 mm (0.138 inch) thick were friction stir welded with a set of optimized welding parameters. The work included microstructural examination and tensile testing of 1) as-welded coupons, 2) naturally aged coupons, and 3) post-weld heat treated coupons. In addition, the feedback signals gathered during the welding process were analyzed by e-NDE method that is used for detecting weld anomalies

4:10 PM Break

4:20 PM Invited

Microstructure and Corrosion Behavior of Friction Stir Welded Mg/ Al- and Mg/Mg-Joints: *Guntram Wagner*¹; Otmar Klag¹; Dietmar Eifler¹; ¹University of Kaiserslautern

Friction stir welding (FSW) is a well suited solid state welding process to produce high-quality light weight metal joints. In the present work the developing microstructure and the monotonic stress-strain behavior of dissimilar joints between AZ91-Mg-alloy and AA5454-Al-alloy are presented. SEM investigations, EDX element mappings and electron probe microanalysis (EPMA) as well as temperature measurements during the welding process have been carried out to describe the welding zone in detail and to develop a phase-diagram which indicates the possible fracture of the different phases. Microstructural investigations showed that under load the cracks are predominantly initiated at the intermetallic phases precipitated as interlayers in the contact areas between of the two alloys. Furthermore the corrosion behavior of the friction stir welding zone of the hybrid joints and of die casted Mg/Mg-joints (AZ91D, MRI 153M and MRI 230D) will be discussed.

4:45 PM

Corrosion and Mechanical Behavior of Friction Stir Processed Mg-CeO2 Surface Composite: *Kumar Kandasamy*¹; Gourav Argade¹; Sushanta Panigrahi¹; Rajiv Mishra¹; ¹Missouri University of Science and Technology

Rare-earth conversion coatings are proven to improve corrosion properties of magnesium alloys. The mechanism behind the improvement is precipitation of oxides and hydroxides of rare-earth elements. In this study, friction stir processing was used to add 50-80 nm size cerium oxide particles at the magnesium alloy plate surface. The improvement in corrosion property has been attributed to the presence of cerium oxide, and as well as the formation of fresh cerium oxide/hydroxide which forms from the reduced cerium from cerium oxide during friction stir processing. The advantages of this approach include flexibility of second phase volume fraction and the depth of surface layer. In addition, the refined microstructure and the nano sized cerium oxide particles in the matrix enhance the compressive strength of the material from 210 MPa to 380 MPa, and the hardness from 74 VHN to 160 VHN.

5:05 PM

Mechanical Properties of Al and Mg Alloy Welds Made by Friction Stir Lap Welding: *Shamzin Yazdanian*¹; Zhan Chen¹; Guy Littlefair¹; ¹AUT university

The unfavourable effect of hooking or softening, respectively, on fracture strength of joints made using friction stir lap welding (FSLW) is known but the combined effect on the magnitude of strength reduction is not clear. In this study, FSLW experiments using AA6060-T5 and AZ31B-H24 alloys were conducted. For both alloys, rotation speed has a dominant effect on increasing the hook size due to increasing the stir flow volume thus lifting more the original lapping surfaces. In AA6060 welds, FS softening has limited the strength, when hook size approaches zero. Meanwhile hook starts to reduce the strength significantly, when its size reaches a critical value. The maximum strength of AA6060 FSL welds reaches \sim 70% of the base metal UTS when hook size approaches zero. This is in contract to \sim 30% for AZ31B FSL welds. This can be explained by the local plastic deformation behaviour during lap tensile testing.

5:25 PM

Microstructure and Tensile Fracture Characteristic of 7005 Aluminum Alloys with Friction Stir Processes: *Ming-Hsiang Ku*¹; Fei-Yi Hung¹; Truan-Sheng Lui¹; Li-Hui Chen¹; ¹National Cheng Kung University

In this study, the structures and the tensile properties of 7005 aluminum alloys containing lower Mg content after friction stir process (FSP) were investigated. After aging treatments, the friction stir process induced behaviors in the mechanical properties were compared. The ZM35 alloy (Zn/Mg ratio was 3.5) and the ZM57 alloy had different fracture characteristics. After FSP and then natural aging for 12 days, the experiment results showed that the strengths of ZM35 and ZM57 were lower than that of the base metal (extruded material with T6, no FSP). Notably, the strength of as-FSP specimen was promoted after aging treatments. The one-step (80 \square /16hr+T6) treatments exhibited the similar results for ZM35 and ZM57 alloys. However, the three-step (T4+80 \square /16hr+T6) treatments, the strength and the ductility of the ZM57 alloy had reduced, and the deterioration rate of the ductility reached 65%. The ZM35 alloy possessed a better ductility.

5:45 PM

Evaluation of Microstructure and Mechanical Properties of Aluminum / Copper Friction Stir Butt Welds: *Rouzbeh Sarrafi*¹; Amir Hossein Kokabi¹; Majid Abbasi Gharacheh¹; Babak Shalchi¹; ¹Department of Materials Science and Engineering, Sharif University of Technology

In this research, the friction stir welding of aluminum to copper is studied. A sound Al/Cu butt joint was achieved with a relatively high strength in uniaxial tensile tests. Mechanical properties (tensile strength and microhardness) and microstructure of the obtained sound FSW welds were examined. The ultimate tensile strength of the joints reached about 75 percent of that of the aluminum base metal, with the fracture occurring at aluminum side. The metallurgical study of the welds showed that the heat affected zone of aluminum controls the strength of the joints in tensile loading. Microscopy of the stir zone (SZ) showed the relatively small volume fraction of intermetallic compounds and their discreteness. The presence of these phases did not to have a considerable harmful effect on the tensile properties of the welds. The formation of the observed microstructure in the SZ is discussed in the paper. Sponsored by: The Minerals, Metals and Materials Society, TMS Electronic, Magnetic, and Photonic Materials Division, TMS: Chemistry and Physics of Materials Committee, TMS: Solidification Committee

Program Organizers: Jeffrey Hoyt, McMaster University; Daniel Lewis, Rensselaer Polytechnic Institute

| Tuesday PM | Room: 6E |
|---------------|-------------------------------|
| March 1, 2011 | Location: San Diego Conv. Ctr |

Session Chair: To Be Announced

2:00 PM Invited

Phase Field Crystal Modelling of Solidification: *Ken Elder*¹; ¹Oakland University

In this talk I would like to discuss methods for modelling solidification on atomic length scales and diffusive time scales. The main advantage of such an approach is that elasticity, dislocations and multiple crystal orientations are naturally incorporated. This allows modelling of elastically strained solids, such as occurs in liquid phase epitaxially growth or the creation of grain boundaries when grains of different orientation collide during solidification. Additionally the method can be used to evaluate the mechanical properties of the final solidified product. Connection of this approach with others will also be discussed.

2:30 PM Invited

Phase-Field Crystal Modeling of Homogeneous and Heterogeneous Crystal Nucleation: Laszlo Granasy¹; Gyorgy Tegze¹; Gyula Toth¹; Gergely Toth²; Tamas Pusztai¹; ¹Research Institute for Solid State Physics and Optics; ²Eotvos University

We address crystal nucleation in non-equilibrium fluids using atomistic phase-field crystal (PFC) methods (original PFC and eight-order-fitting version by Jaatinen et al.) via solving (i) the equation of motion supplemented with Langevin noise to model thermal fluctuations and (ii) the Euler-Lagrange equation. Relying on approach (i), it will be shown that in these PFC models crystal nucleation at high supersaturations happens via an amorphous precursor. Remarkably, the effective pair potentials corresponding to these PFC models, evaluated from structural data for the glassy state (obtained by deep quenching the liquid), differ significantly. These findings support the view that the two-stage nucleation process observed here might be fairly general. Next we apply approach (ii) to explore the microscopic aspects of Greer's free growth model of liquid inoculation by solid particles, and study the role played by the structure and shape of the foreign particles, and the effect of lattice mismatch.

3:00 PM Invited

Spacing Characterization in Al-Cu Alloys Directionally Solidified under Transient Growth Conditions: Morteza Amoorezaei¹; Sebastian Gurevich¹; *Nikolas Provatas*¹; ¹McMaster University

We examine primary spacing in Al-Cu alloys grown under transient conditions. The mean value of the primary spacing is shown, both experimentally and numerically, to evolve between characteristic incubationlike periods during which the array configuration is statistically stable. Our results display a rapid, but continuous, transition period from one spacing range to another, consistent with the fact that the sharp doubling of spacing predicted by the transient theory of Warren and Langer affects different wavelengths of a distribution at different times. This transition is shown to depend on the rate of change in growth speed using phase field simulations of directional solidification where the pulling speed is ramped at different rates. For high rates of change of the pulling speed we observe temporary marginally stable array configuration separated by relatively short-lived transitions, while for lower rates of change of the pulling speed, the distinction between incubation and transition periods disappears.

3:30 PM Break

140th Annual Meeting & Exhibition

3:45 PM Invited

Thermodynamic and Mechanical Properties of Hot Grain Polycrystalline Evolution during Late-Stage Solidification: *Alain Karma*¹; Ari Adland¹; 'Northeastern University

This talk will discuss recent progress made using phase-field-crystal and amplitude-equation based simulation methods to characterize the interaction between solid-liquid interfaces that come into close contact during the late stages of solidification. When interfaces belong to different crystal grains, this interaction can be either attractive or repulsive depending on the relative orientation of the two grains. For strong repulsion, crystal cohesion is retarded and interface bridging only occurs substantially below the liquidus temperature. The thin liquid films that persist in between the liquidus and bridging temperatures are believed to promote strain localization and hot cracking through a reduction of shear resistance of wet grain boundaries. Results will be presented that shed light on complex factors that control interface bridging as well as grain boundary shearing as a function of temperature and grain boundary bicrystallography.

4:15 PM Invited

Unified Derivation of Phase-Field Models for Alloy Solidification: *Mathis Plapp*¹; ¹CNRS/Ecole Polytechnique

In the literature, two quite different phase-field formulations for the problem of alloy solidification can be found. In the first, the material in the diffuse interfaces is assumed to be in an intermediate state between solid and liquid, with a unique local composition. In the second, the interface is seen as a mixture of two phases that retain their macroscopic properties, and a separate concentration field for each phase is introduced. It is shown that both types of models can be obtained by the standard variational procedure if a grand potential functional is used as a starting point instead of a free energy functional. The dynamical variable is then the chemical potential instead of the composition. In this framework, a complete analogy with phase-field models for the solidification of a pure substance can be established. This analogy is exploited to formulate quantitative phase-field models for alloys with arbitrary phase diagrams.

4:45 PM Invited

Phase-Field Model for Strong Non Equilibrium Solidification: Ingo Steinbach¹; ¹Ruhr-University

A multi-phase-field model is developed where the interface condition between the different phases is treated out of chemical equilibrium. This results in a finite interface dissipation rate dependent on the deviation from equilibrium. The model is based in the standard multi-phase-field model with separate phase concentration fields in solid and liquid. These concentration fields are coupled via a dynamic equation accounting for finite interface dissipation. The model is shown to converge towards the standard model with equal diffusion potentials in the interface for infinitely fast relaxation. It can be applied to investigate the initial state of contact of a solid with a melt in an arbitrary off equilibrium state. Applications are melt coating of sheet products of soldering. The model is also shown to be applicable to rapid solidification.

5:15 PM

Phase-Field Simulations of Stress-Induced Twin Formation during Solidification: *Shenyang Hu*¹; Chuck Henager Jr.¹; ¹Pacific Northwest National Laboratory

Twin formation during crystal growth from the melt due to crucible contact stresses or growth stresses can be problematic for processing of single crystals, such as the case of CZT growth via the vertical gradient freeze method. In this talk, we present a phase-field model to describe twin evolution in an FCC polycrystalline material. The model assumes that twin nucleation and growth is a process of partial dislocation nucleation and slip on successive habit planes. Stacking fault energies, energy pathways, critical stresses for the formation of stacking faults, and dislocation core energies are used to construct the thermodynamic model. With the model, twin formation and evolution during crystal growth from the melt is simulated. The effect of grain orientation and cooling rate on the twin structure is systematically studied. The potential application of the model in studying the deformation twinning in polycrystalline materials will also be discussed.

Hume-Rothery Symposium Thermodynamics and Diffusion Coupling in Alloys - Application Driven Science: Diffusion Theory and Diffusion in Grain Boundary

Sponsored by: The Minerals, Metals and Materials Society, TMS Electronic, Magnetic, and Photonic Materials Division, TMS: Alloy Phases Committee

Program Organizers: Zi-Kui Liu, The Pennsylvania State University; Larry Kaufman, CALPHAD, Inc.; Annika Borgenstam, Royal Institute of Technology; Carelyn Campbell, NIST

| Tuesday PM | Room: 31A |
|---------------|-------------------------------|
| March 1, 2011 | Location: San Diego Conv. Ctr |

Session Chairs: Jian Luo, Clemson University; Sybrand van der Zwaag, Technical University Delft

2:00 PM Invited

Development of a Theory of Solute Diffusion Enhancement for Analyzing Interdiffusion Experiments: *Irina Belova*¹; Alan Allnatt²; Yongho Sohn³; Nagraj Kulkarni⁴; Sarah Brennan³; Graeme Murch¹; ¹The University of Newcastle; ²University of Western Ontario; ³University of Central Florida; ⁴Oak Ridge National Laboratory

Recently, the accuracy of interdiffusion measurements has increased greatly. The SIMS technique allows for very precise determination of interdiffusion concentration profiles down into the ppm range. At such small concentrations of solute, an interdiffusion enhancement theory becomes relevant. However, previous development of a diffusion enhancement theory has focused exclusively on tracer solute diffusion and not interdiffusion. Here, we consider the steps for undertaking the development of an interdiffusion enhancement theory applicable to interdiffusion data. These include: the 5-frequency vacancy mechanism in fcc (or related mechanisms for other lattices) with expansion of this model to higher order vacancy-solute atoms clusters, asymptotic analysis of the phenomenological coefficients, vacancy concentration and thermodynamic factor. It is shown that a correct diffusion enhancement theory for the interdiffusion coefficient must involve consideration of clusters of vacancy and two solute atoms (triplets) in order to assess the contribution of off-diagonal phenomenological coefficients.

2:30 PM Invited

The 17 Diffusion Path Theorems by Kirkaldy and Brown Revisited: *John Morral*¹; ¹Ohio State University

In a 1963 review paper by Kirkaldy and Brown a list of 17 theorems were given for diffusion paths in multicomponent diffusion couples. These same theorems were repeated in the 1987 text entitled Diffusion in the Condensed State by Kirkaldy and Young. In the nearly 50 years since they were first published, these theorems have withstood the test of time. However now it is possible to formulate additional theorems that are more specific about what happens to diffusion paths in multiphase regions. The theorems are based on theoretical work that was developed to explain features seen in DICTRA simulations and experimental work. Examples are theorems about how boundaries in diffusion couples can be classified and identified on diffusion paths and also when zigzag features and horns occur on diffusion paths. Both the original and new theorems will be discussed in this work

3:00 PM Invited

Determination of the Intrinsic Interface Mobility in Binary Ferrous Alloys Using Reversible Partial Transformation Experiments: Sybrand van der Zwaag¹; Hao Chen¹; ¹Technical University Delft

The kinetics of the principal austenite to ferrite phase transformation is determined both by the kinetics of the diffusional solute partioning and the intrinsic interface mobility. However, the determination of the interfacial mobility is not straightforward due to the fact that the usual transformation kinetics are determined by nucleation and growth kinetics simulaneously and can not be separated. In this work we will present the transformation kinetics for incomplete phase transformation in the two phase region which do allow a far more accurate determination of the interface mobility as nucleation effects can be excluded. The data are interpreted in the context of both the TU Delft mixed mode model and the diffusional tranformation model developed at KTH by Agren and colleagues.

3:30 PM Break

3:50 PM

Diffusion Coefficients in Liquid and Grain Boundary Predicted by Ab Initio Molecular Dynamics: Zi-Kui Liu¹; Huazhi Fang¹; Bill Wang¹; ¹The Pennsylvania State University

Molecular dynamics (MD) is a powerful tool to probe the thermodynamic and kinetic properties of solid, glass and liquid phases. In classical molecular dynamics (CMD), empirical models are used to describe the force by considering bond, bend and dihedral angle contributions with parameters fitted to experimental data or first-principles calculations of small clusters. In the ab initio molecular dynamics (AIMD), the forces are calculated on the fly using the first-principles density functional theory as discussed above. In the present work, we use AIMD simulations to follow the random walk of atoms in the liquid state. Based on the mean square displacements (MSD), the diffusion coefficients are calculated from the Einstein equation. Furthermore, we extend this approach to understand the diffusion in grain boundaries.

4:20 PM

Grain Boundary "Phase" Diagrams and Their Applications in Predicting Activated Sintering and Microstructure Development: Jian Luo¹; ¹Clemson University

Our recent HRTEM studies revealed that impurity-based, nanometer-thick, quasi-liquid, intergranular films can be thermodynamically stabilized well below the bulk solidus lines at grain boundaries in W and Mo based alloys [Acta Mater. 55:3131 (2007); APL 94:251908 (2009)]. Enhanced diffusion in such liquid-like grain boundaries explained a long-standing mystery regarding the mechanism of "solid-state activated sintering". Similar impurity-based interfacial films have been widely observed in other materials (especially ceramic materials), where they often control the microstructural evolution as well as mechanical and electronic properties [Crit. Rev. Solid State Mater. Sci. 32:67 (2007)]. We propose a long-range scientific goal of developing grain boundary "phase" diagrams as a new materials science tool [APL 92:101902 (2008); Curr. Opin. Solid State Mater. Sci. 12:81 (2008); APL 95: 071911 (2009)]. Most recent results on Mo-Ni and Mo-Si-B based alloys will be presented, with an emphasis on the correlation among grain boundary disordering, diffusion and sintering.

4:50 PM

Finding Critical Nucleus Configuration and Activation Energy for Heterogeneous Nucleation at Grain Boundaries: *Ning Zhou*¹; Yipeng Gao¹; Yunzhi Wang¹; ¹The Ohio State University

A free-end nudged elastic band(NEB) algorithm is used to explore the free-energy landscape of phase field models of Ni4Ti3 precipitation in a polycrystal Ni-Ti shape memory alloy. The saddle-point configuration and energy for heterogeneous nucleation of a coherent Ni4Ti3 precipitate on large angle B2 grain boundaries are determined. Thermodynamic inputs such as the Gibbs free energy of the B2 phase are obtained from databases developed using the CALPHAD method. The elastic strain energy contribution from the coherency stress due to the lattice mismatch is calculated using experimentally measured lattice constants and lattice correspondence. The influences of grain boundary segregation on nucleation barrier and critical nucleus configuration are investigated. The simulation results could provide insights on how to control Ni4Ti3 precipitation to tailor the property of NiTi-based shape memory alloys. The work is supported by NASA under grant NNX08AB49A.



5:20 PM

Influence of Porosity on Grain Boundary Diffusion of Fe in Ultrafine-Grained 14YWT Steel Produced by Mechanical Alloying: *Reeti Singh*¹; Sergiy Divinski¹; Joachim Schneibel²; Gerhard Wilde¹; ¹Institute of Material Physics, Westfälische Wihelms-University Münster, Germany; ²Institute for Materials and Joining Technology, University of Magdeburg

The diffusion of Fe in nanocluster-strengthened ferritic 14YWT steel has been investigated. The grain boundary penetration at lower temperatures was found to reveal a specific time dependence, which indicates the existence of interconnected porosity in the ferritic steel. The solid state diffusion along boundaries and the penetration along interconnected cavities were verified by ⁵⁹Fe diffusion measurements as well as by room temperature penetration of the liquid ^{110m}Ag tracer. The presence of porosity in the given material affected the diffusion kinetics introducing a hierarchy of short-circuit diffusion paths. The grain boundary diffusion coefficient and the diffusivity along internal surfaces were determined in the so-called type C C, C-B and B-B kinetic regimes of interface diffusion in the hierarchical microstructure, according to the Divinski's classification. The results of the diffusion analyses are discussed with respect to the high creep strength of the material at high temperatures.

Magnesium Technology 2011: High-Temperature Alloys; High-Strength Alloys; Precipitation

Sponsored by: The Minerals, Metals and Materials Society, TMS Light Metals Division, TMS: Magnesium Committee Program Organizers: Wim Sillekens, TNO Science and Industry; Sean Agnew, University of Virginia; Suveen Mathaudhu, US Army Research Laboratory; Neale Neelameggham, US Magnesium LLC

| Tuesday PM | Room: 6F |
|---------------|-------------------------------|
| March 1, 2011 | Location: San Diego Conv. Ctr |

Session Chairs: Alan Luo, General Motors; Alok Singh, National Institute for Materials Science

2:00 PM

Creep and Elemental Partitioning Behavior of Mg-Al-Ca-Sn Alloys with the Addition of Sr: *Jessica TerBush*¹; Olivia Chen¹; J.Wayne Jones¹; Tresa Pollock²; ¹University of Michigan; ²University of California

The partitioning of elements during solidification can strongly affect precipitation and solute strengthening during creep, especially in alloys where creep is controlled by viscous glide of dislocations. Elemental partitioning during solidification and its influence on creep behavior has been examined for Mg-6.5Al-2.25Ca-0.8Sn with and without 0.25wt% Sr additions. The alloy containing Sr experienced increased partitioning of Al and Ca to the α -Mg phase. However, the creep behavior in compression at 110 MPa and 180°C was not significantly different from that of the alloy without Sr. In addition, it was determined that the elemental partitioning profiles of permanent mold cast specimens were representative of the grain interiors of die-cast specimens, although greater disagreement was observed for interdendritic regions of the microstructure. These observations are discussed in terms of current models for solid solution and precipitation strengthening.

2:20 PM

Effect of Mn Addition on Creep Property in Mg-Al-Ca Systems: *Tomoyuki Homma*¹; S. Nakawaki¹; K. Oh-ishi²; Kazuhiro Hono²; Shigeharu Kamado¹; ¹Nagaoka University of Technology; ²National Institute for Materials Science

The effect of Mn addition on creep property in Mg-2Al-2Ca (mass%) alloys has been investigated by analytical transmission microscopy and atom probe tomography. The Mn addition can reduce the minimum creep rate of the Mg alloys so that fine and dense precipitates are dispersed during the creep deformation at 175-225 °C. The fine precipitates are Al2Ca phases and G.P. zones. Nevertheless, while the creep temperatures are high, these

precipitates are stable at the high temperature. Mn tends to be involved in the fine precipitates, leading to the dense distribution of the precipitates. The measured number density of the fine precipitates is one order of magnitude higher than that in Mn-free alloy.

2:40 PM

The Effect of Precipitate State on the Creep Performance of Mg-Sn Alloys: Mark Gibson¹; Xi-ya Fang²; Colleen Bettles³; *Christopher Hutchinson*⁴; ¹CSIRO Manufacturing and Infrastructure Technology; ²Monash Centre for Electron Microscopy; ³ARC Centre of Excellence for Design in Light Metals; ⁴Monash University

The Mg-Sn system has recently received attention as a potential base for the development of creep resistant alloys. In this work we report our efforts at using alloying additions to modify both the shape and the number density of the Mg2Sn precipitates and our measurements of the resulting effects on the creep behaviour. Under a load of 60MPa, it is shown that the secondary creep rates can be improved by at least five orders of magnitude compared to the binary alloy. Transmission electron microscopy observations show that the origin of the excellent creep properties is a remarkable thermal stability of the precipitate structure. The possible origins of the stability are discussed.

3:00 PM

Microstructure and Mechanical Properties of Mg-Zn-Y-M (M: Mixed RE) Alloys with LPSO Phase: *Jonghyun Kim*¹; Yoshihito Kawamura²; ¹Kumamoto Technology & Industrial Foundation; ²Kumamoto University

Magnesium alloys are emerging as potentially good candidates for numerous applications, especially in automotive, aerospace and electronic industry. Their advantages, such as low density and high specific strength, make them promising structural materials for applications. Among the various alloy systems developed, the commonly used magnesium alloys, such as AZ91 and AM60, are based on Mg-Al system. However, the use of these Mg alloys has been limited to temperatures below 120° because of their poor heat resistance, especially creep property at elevated temperatures. Therefore, it is necessary to develop some heat-resistant magnesium alloys for elevated temperature applications. Recently, Kawamura et al. have developed the Mg-Zn-Y alloys with the LPSO phase. These alloys have the excellent mechanical properties. The investigation reported here focused on the influence of mixed RE, which was also effective in strengthening Mg-Zn-Y alloys at elevated temperature, on the microstructure and mechanical properties of the Mg-Zn-Y-M (M: Mixed RE) alloys.

3:20 PM

Analysis of Texture Evolution during High-Temperature Creep in Magnesium Alloys with Application of Neutron Diffraction: *Dimitry Sediako*¹; Scott Shook²; Sven Vogel³; Anton Sediako⁴; ¹National Research Council Canada; ²Applied Magnesium International; ³Los Alamos Neutron Science Center; ⁴McGill University

Although a large share of the material used in industry is in the form of castings, the use of wrought products in automotive applications is on the rise. Extrudability and high temperature performance of wrought material became critical factors in developing new wrought alloys and processing technologies. This paper shows some results received in creep testing and studies of in-creep texture evolution for several wrought magnesium alloys developed for use in elevated-temperature applications. These studies were performed using E3 neutron spectrometer of the Canadian Neutron Beam Centre in Chalk River, Ontario, and HIPPO time-of-flight spectrometer at Los Alamos Neutron Science Center, NM. It was confirmed that there is a notable difference in the strength of extrusion-type texture for the extruded samples of studied alloys, that represent four alloying systems; namely, Mg-Al-RE, Mg-Al-Ca, Mg-Al-Sr, and Mg-Zn-RE. This difference in texture likely affected material performance in high-temperature creep tests.

3:40 PM

Improved Processing of Mg-Zn-Y Alloys Containing Quasicrystal Phase for Isotropic High Strength and Ductility: *Alok Singh*¹; Yoshiaki Osawa¹; Hidetoshi Somekawa¹; Toshiji Mukai¹; ¹National Institute for Materials Science

The stable quasicrystal phase in Mg-Zn-Y alloys has been proved to be beneficial for strength and ductility and has also been shown to be impart high fracture toughness. However, the strength of these alloys has been limited by effective dispersion of the quasicrystal phase by wrought processing. Yield strengths have been limited to 300MPa with a grain size of 1 µm. We show a simple procedure in which a Mg₉₃Zn₆ Y alloy was chilled cast and then extruded. Yield strengths of up to 400 MPa in tension and compression, accompanied by ductility of ≈14% were obtained with grain of size of about 1 µm. Compression to tension yield anisotropy ratios were in the narrow range of 0.95 to 1.03. These alloys also showed ageing response with two peaks. The effect of ageing on mechanical properties has been studied. Precipitation effects slip more than twinning, decreasing the yield asymmetry ratio.

4:00 PM Break

4:20 PM

Precipitation Hardenable Mg-Ca-Al Alloys: *J. Jayaraj*¹; C.L. Mendis¹; T. Ohkubo¹; K. Oh-ishi¹; K. Hono¹; ¹National Institute for Materials Science

The combinations of oversized element like RE and Ca and undersized element like Zn in Mg causes the formation of plate like precipitates on the basal plane. Both Mg-RE-Zn and Mg-Ca-Zn alloys exhibit age hardening response and good creep properties, which are attributed to the formation of plate like GP zones. It is intriguing to see whether or not other undersized elements like Al exhibit the similar effect. Thus, the effect of Al additions in a Mg-0.5Ca(wt.%) alloy on age hardening responses have been investigated. The Mg-0.5Ca-0.3Al alloy showed peak hardness (72 HV) higher than that for the Mg-1Ca-1Zn alloy. TEM and 3DAP analyses confirmed the dense distribution of ordered G.P. zones on the basal planes and the subsequent formation of Al₂Ca causes the over-aging. Since only a trace addition of inexpensive alloying elements contribute to the age hardening, this alloy may be suitable for wrought applications.

4:40 PM

Microstructure, Phase Evolution and Precipitation Strengthening of Mg-3.1Nd-0.45Zr-0.25Zn Alloy: Galit Atiya¹; Menachem Bamberger¹; *Alexander Katsman*¹; ¹Technion - Israel Institute of Technology

The microstructure of the Mg-3.1%Nd-0.45%Zr-0.27%Zn (%wt) alloy has been investigated after solution treatment at 540°C for 24hr followed by isothermal aging at 175°C up to 32 days. After solution treatment the bct (Mg,Zn)₁₂Nd phase dissolved and small tetragonal Zn₂Zr₃ rod-like particles precipitated at α -Mg grain interiors. Precipitation during isothermal aging involves the formation of metastable phases β " (Mg₃Nd)_{hep} (DO₁₉ structure) and β ' (Mg₃Nd)_{fee} (DO₃ structure). The β " precipitates formed during the first 8 days of aging have a platelet shape and are fully coherent with Mg matrix. During 16-32 days of aging, the β " precipitates transform to β ' precipitates with an FCC structure. The β ' precipitates are semi-coherent with the Mg matrix and have the following orientation relationship: $[0001]_{Mg}$: $[101]_{\beta}$. and $[-1100]_{Mg}$: $[-112]_{\beta}$. After prolonged aging of 32 days, the β ' precipitates transform to the stable incoherent β (Mg,Zn)₁₂Nd phase. The growth, coarsening and phase transformations were followed by microhardness tests.

5:00 PM

Precipitation Process in Mg-Nd-Zn-Zr-Gd/Y Alloy: *Jiehua Li*¹; Gang Sha²; Peter Schumacher¹; Simon Ringer²; ¹Chair of Casting Research, Department of Metallurgy, the University of Leoben; ²Australian Centre for Microscopy and Microanalysis, The University of Sydney

Transmission electron microscopy (TEM) and atom probe tomography (APT) were employed to investigate the solute cluster and precipitates formed in different Mg-Nd-Zn-Zr-Gd/Y alloys aged at 200°C up to 100h. TEM characterizations confirmed the precipitation microstructure evolution and the precipitation sequence in these alloys, which involved the formation

of phase such as β ", β ', β 1 and β . These precipitates had ideal-shaped and distribution, with the plate lying on (01-10) a-Mg and very thin plate lying on (0001) a-Mg. APT analyses, for the first time, revealed that the precipitates were enriched with Nd, Zn and Gd. Moreover, Nd partitioned more strongly into the precipitates than Gd and Zn. In contrast, Y was less prone to partition into precipitates than any other alloying element in these alloys. These careful TEM characterizations and quantitative atom probe data analyses elucidated the precipitation behavior of Mg-Nd-Zn-Zr-Gd/Y alloys.

5:20 PM

Mechanical Properties and Microstructures of Twin-Roll Cast Mg-2.4Zn-0.1Ag-0.1Ca-0.16Zr Alloy: *Chamini Mendis*¹; Jun Ho Bae²; Nack Kim²; Kazuhiro Hono¹; ¹National Institute for Materials Science; ²Pohang University of Science and Technology

In our previous study, we reported that the additions of 0.1 at.% Ag and 0.1 at.% Ca to Mg-2.4Zn-0.16Zr (at.%) alloy enhanced the age hardening response, and extruded alloy showed tensile yield strength of 325 MPa with the T6 heat treatment. Considering its excellent age hardenability, we attempted to develop high strength sheets from the alloy by twin-roll casting (TRC). TRC sheet of 2 mm in thickness were hot rolled to ~1.2 mm. The TRC Mg-2.4Zn-0.1Ag-0.1Ca-0.16Zr alloy sheet showed tensile yield strength of ~320MPa and an elongation to failure of 17% after T6 heat treatment. EBSD study indicated the average grain size is ~18±2.5\956m and the grains have a weak basal texture. TEM, showed a uniform distribution of ~5 nm diameter MgZn₂ phase. The dispersion of rod-like precipitates was attributed to the high yield strength observed.

5:40 PM

The Solidification Microstructure and Precipitation Investigation of Magnesium-Rich Alloys Containing Zn and Ce: *Chuan Zhang*¹; Alan A. Luo²; Y. Austin Chang¹; ¹UW-Madison; ²General Motors Research & Development Center

Solidification microstructure and precipitation of Mg-Zn-Ce alloys were investigated to develop high-strength and high-ductility lightweight magnesium alloys for structural applications. The characterized microstructures of four directionally solidified Mg-Zn-Ce alloys agree well with the calculated solidification paths using computational thermodynamics coupled with the Scheil model. Equilibrium calculations were also performed on these Mg-Zn-Ce alloys. The precipitation of Mg12Ce intermetallic phase was predicated thermodynamically, and characterized using high-resolution transmission electron microcopy (HRTEM).

Magnetic Materials for Energy Applications: Soft Magnetic Materials

Sponsored by: TMS Electronic, Magnetic, and Photonic Materials Division, TMS: Energy Conversion and Storage Committee, TMS: Magnetic Materials Committee; JSPS 147th Committee on Amorphous and Nanocrystalline Materials; Lake Shore Cyrotronics, Inc.; AMT&C

Program Organizers: Victorino Franco, Sevilla University; Oliver Gutfleisch, IFW Dresden; Kazuhiro Hono, National Institute for Materials Science; Paul Ohodnicki, National Energy Technology Laboratory

| Tuesday PM | Room: 11A |
|---------------|-------------------------------|
| March 1, 2011 | Location: San Diego Conv. Ctr |

Session Chair: Paul Ohodnicki, National Energy Technology Laboratory

2:00 PM Keynote

Soft Magnetic Materials Fabricated by Rapid Quenching Technique for Energy Applications: *Motoki Ohta*¹; Yoshihito Yoshizawa¹; ¹Hitachi Metals Ltd.

Recently, the Fe-based amorphous alloys have been coming into use for iron core materials because of their low iron loss. However, since there is problem of noise due to their large saturation magnetostriction, the magnetic

2:40 PM Invited

Recent Advances in Non-oriented Electrical Steel for EV/HEV Traction Motor: *Ichiro Tanaka*¹; Hiroyoshi Yashiki¹; ¹Sumitomo Metal Industries, Ltd

To improve efficiency of traction motors for environmentally friendly vehicles, we have developed two kinds of non-oriented electrical steels: low core loss and high magnetic induction grades for stator core and highstrength grades highly suitable for rotor core of IPM motors. Excellent magnetic properties of the developed steel for stator core were ascribed to recrystallization texture control by phosphorus addition. Phosphorus segregation at initial grain boundaries enhances beneficial texture evolution. High-strength of the developed steel for rotor core of IPM motors was achieved by dislocation strengthening through niobium addition. Solute niobium moderately retards recrystallization kinetics; then the retardation leads to specific microstructure favorable for great strength. The newly developed electrical steels of notable characteristics will significantly contribute to an improvement in performance of traction motors for electric vehicles and hybrid electric vehicles, and furthermore, motors for appliances, particularly compressor motors for air conditioners.

3:05 PM Invited

The Requirements of Soft Magnetic Materials for Industrial Applications: *Francis Johnson*¹; Satish Prabhakaran¹; Ayman El-Refaie¹; ¹GE Global Research

Advanced magnetic materials are required to enhance the performance of electrical power generation, distribution, and conversion systems. The complementary needs of high power density and high system efficiency demand components that exhibit low power loss at high frequencies. The trend in power conversion technology is to move away from all-passive low frequency transformers to modular power electronic systems with high frequency transformers. New magnetic materials operable from the MW-level-20 kHz range up to the kW-level -MHz range with operating temperatures up to 300 °C will be required. Advanced electric machines and drives, often with permanent magnet architectures, are being developed to operate at continually higher speeds and temperatures. In addition to excellent magnetic properties, these rotating machines place demands on the mechanical and thermal properties of the material. Strategies for improved material performance include nanoscale structure control, novel device geometries, and improved processing methods to maintain a sustainable value chain.

3:30 PM Invited

Soft Magnetic Materials for Improved Energy Performance: *Matthew Willard*¹; Maria Daniil¹; Keith Knipling¹; Ramasis Goswami¹; ¹Naval Research Laboratory

Recent activity to improve the sustainability of our energy use has resulted in increased awareness of the impact of energy efficiency on the performance of devices. Magnetic materials play an important role in improving the efficiency due to their widespread use in electric power generation, conditioning, conversion, transportation, and other technology-based sectors of the economy. This presentation will focus on state-of-the-art amorphous and nanocrystalline soft magnetic alloys optimized for energy applications, including electricity generation, conditioning, conversion, refrigeration, and transportation applications. Our recent work on Fe-based nanocrystalline alloys for high temperature applications and (Fe,Si,Al)-based nanocrystalline alloys for cryogenic applications will be highlighted.

3:55 PM Break

4:25 PM Invited

FeCo and FeNi-based Nanocomposite Magnets for Energy Applications. *Michael McHenry*¹; ¹Carnegie Mellon University

Magnetic nanocomposites and derived magnetic properties impact energy applications: (1) FeCo nanocomposites for power conversion applications. (2) High Co-containing alloys for magnetic sensors for deep well oil exploration. (3) Ni- and FeCoCr-based alloys for magnetocaloric cooling. FeCo-based nanocomposites have large saturation inductions and Curie temperatures. Field crystallization impacts high frequency core losses. AC power conversion applications in hybrid vehicles will be discussed. In Co-rich nanocomposites 2- and 3-phase nanocrystallization impacts induced magnetic anisotropy. Low loss, linear B(H) and and corrosion resistance of makes these alloys candidates for high temperature fluxgate and giant magnetoimpedance magnetometers for oil and strategic mineral exploration and well-leak remediation. FeCoCr-based alloys have sizeable magnetocaloric effects near room temperature. The synthesis of low T_c Fe-Ni nanocomposites require stabilization of the metastable \947-phase at Fe-rich compositions discussed in light of the T₀ construction in the Fe-Ni eutectoid phase diagram.

4:50 PM Invited

140th Annual Meeting & Exhibition

Field-Annealed FeCo-Based Amorphous and Nanocrystalline Alloys with Improved Magnetic Softness: *Ivan Skorvanek*¹; Jozef Marcin¹; Peter Svec²; ¹Institute of Experimental Physics; ²Institute of Physics

The continuing interest in the development of FeCo-based amorphous and nanocrystalline alloys is mainly due to their ability to combine a high saturation magnetic flux density with relatively good magnetic softness. In this work, a controllable field annealing induced magnetic anisotropy is produced in series of Fe-Co-Nb-B and Fe-Co-B-Cu amorphous and (nano) crystalline alloys. We show that the specimens annealed without the presence of external magnetic field show an appreciable increase of the coercivity with crystallization. A heat treatment under the presence of longitudinal magnetic field results for the Fe-Co-Nb-B alloy in squared hysteresis loops characterized by very low coercive field values in the range of 2 - 8 A/m. The saturation magnetic flux density for the optimum field annealed amorphous Fe₆₃Co₂₁B₁₅Cu alloy reaches 1.83 T and the value of coercive field is 1.7 A/m. Such low Hc values are superior to those previously reported for FeCo-based amorphous and nanocrystalline alloys.

5:15 PM

Effect of Different Annealing Methods on Structure and Texture of Primary Recrystallization of Grain-oriented Silicon Steel: *Lijuan Li*¹; Li-hua Liu¹; Xue-liang Wu¹; Wen Shi¹; Qi-jie Zhai¹; ¹Shanghai University

The effects of different annealing methods which include pulse current annealing, salt bath annealing and conventional furnace annealing on microstructure and texture of primary recrystallization of grain-oriented silicon steel were studied. Comparing with the sample treated by conventional furnace annealing, pulse current annealing and salt bath annealing increase the intensity of (110), which may means more Goss grains(secondary nucleus) forming and will be good for the development of structure and texture of secondary recrystallization. Pulse current annealing can obviously decrease the proportion of $\Sigma 1$ grain boundary which is harm for secondary recrystallization, however, salt bath annealing increases $\Sigma 1$ grain boundary. There are strong {111}<12> texture in the samples of pulse current annealing, salt bath annealing and conventional furnace annealing. The results show that by pulse current annealing we can obtain better structure and texture of primary recrystallization of grain-oriented silicon steel.

5:30 PM

Solute Effects on Magnetic Properties and Thermal Stability in Fe-Mo-B-P-Si Metallic Glasses: *Gary Shiflet*¹; S. Bhattacharya¹; S. Joseph Poon¹; ¹University of Virginia

The role of gallium, copper and cobalt on the size and morphology of BCC iron crystals forming from an amorphous matrix will be discussed in this presentation. Among the metallic glasses, the Fe-based systems with high glass formability (GFA) are of significant interest for their possible excellent soft magnetic properties. This talk will focus on the above listed element's effects, as well as the role of metalloids on the thermal stability and magnetic properties of Fe-X–B–C–P–Si metallic glasses (X=Ga, Cu, Co, or Mo). The beneficial effect of controlling the BCC nanocrystalline iron phase (ca. 10 nm) will also be shown and discussed. Time-temperature–transformation (TTT) studies and investigation of nano-crystallization properties will be

presented based on results using transmission electron microscopy and magnetic measurements.

5:45 PM

Fabrication of High Performance Fe-Si-Al Soft Magnetic Composites: Junhua You'; 'Shenyang University of Technology

The Fe-Si-Al soft magnetic composites were produced by cold pressing of water-atomized Fe-Si-Al powder using organic binder. The effect of shaping pressure, annealing tempreture, magnetic annealing and dielectric content on properties of Fe-Si-Al soft magnetic composites was investigated. The results showed that increasing shaping pressure increases density and radial crushing strength of Fe-Si-Al soft magentic cores, and decreases coercivity and total loss. Increasing annealing temperature can increase effective permeability and decrease total loss owing to decreasing hysteresis loss, and overannealing (>660°) can deteriorate magnetic properties. The magnetic annealing can decrease total loss of Fe-Si-Al magnetic powder core. Increasing dielectric content can reduce the eddy current loss of Fe-Si-Al magnetic powder core and decrease the real part of permeability. Fe-Si-Al magnetic powder core with shaping pressure of 1800 MPa, annnealing temperature of 660° and dielelctic content of 0.7% presented the optimum magnetic properties with an effective permeability of 127, a total loss of 78 mW/cm3 and a radial crushing strength of 18MPa.

Materials for the Nuclear Renaissance II: Zirconium and Fuel

Sponsored by: The Minerals, Metals and Materials Society, TMS Structural Materials Division, TMS/ASM: Corrosion and Environmental Effects Committee, TMS/ASM: Nuclear Materials Committee

Program Organizers: Raul Rebak, GE Global Research; Brian Cockeram, Bechtel-Bettis; Peter Chou, Electric Power Research Institute; Micah Hackett, TerraPower, LLC

| Tuesday PM | Room: 4 |
|---------------|-------------------------------|
| March 1, 2011 | Location: San Diego Conv. Ctr |

Session Chair: Peter Chou, EPRI

2:00 PM Introductory Comments

2:05 PM

Determination of Zircaloy Liquidus and Solidus with an Instrumented Transvarestraint Test: Micah Hackett¹; George Young¹; ¹KAPL

Zirconium alloys are commonly welded for nuclear and chemical process applications, but they can be susceptible to solidification cracking during fusion welding. Determining the liquidus and solidus temperatures is of fundamental importance to an alloy's weldability since the extent of the twophase 'mushy' zone defines the region susceptible to solidification cracking. However, the high melting temperature and reactivity of molten zirconium makes conventional methods (e.g. differential thermal analysis) to determine the liquidus and solidus impractical. An instrumented transvarestaint test was developed to determine the liquidus and solidus via a series of thermocouples attached to zircaloy test plates outside of the weld fusion zone. At high applied strains, solidification cracks span the length of the mushy zone and can be used in conjunction with temperature measurements and finite element modeling to estimate the solidus and liquidus temperatures. Details of the experimental setup and results for industrial alloys will be discussed.

2:25 PM

Development of Microstructure and Irradiation Hardening of Zircaloy during Low Dose Neutron Irradiation at Nominally 300C: Brian Cockeram¹; Lance Snead²; Richard Smith¹; ¹Bechtel-Bettis; ²ORNL

Wrought Zircaloy-2 and Zircaloy-4 were neutron irradiated at nominally 300C in the High Flux Isotope Reactor (HFIR) at relatively low neutron fluences between 1X10^23 and 6X10^25 n/m2 (E>0.1 MeV). The irradiation hardening and change in microstructure were characterized following

irradiation using tensile testing, hardness and examination of microstructure using Analytical Electron Microscopy. Small increments of dose were used in the range where the saturation of irradiation hardening is typically observed so that the role of microstructure evolution, <a>loop formation, and change in precipitate structure on irradiation hardening may be understood. An incubation dose between 1X10^23 and 2X10^24 n/m2 was needed for loop nucleation to occur that resulted in irradiation hardening, but saturation of the <a>loop number density to values within the range of those reported in literature was observed to occur over the fluence range in this work.

2:45 PM

Fabrication and Irradiation of LWR Hydride Mini-Fuel Rods: Kurt Terrani¹; Mehdi Balooch¹; Donald Olander¹; ¹University of California, Berkeley

Benefits of incorporation of hydride fuels into the current fleet of light water reactors (LWRs) have been previously investigated by the means of calculations and laboratory-scale experiments. Recognizing the necessary shift from laboratory scale experiments to more relevant environments, an irradiation experiment is underway to evaluate the feasibility of LWR hydride fuel concept. The irradiation experiment is supported by US DOE's Advanced Test Reactor National Scientific User Facility program. The present work focuses on demonstrating the viability of the combination of hydride fuel (U(30wt%)-ZrH1.6), liquid metal bond, and Zircaloy cladding by long-term irradiation of multiple mini-fuel elements in the MIT reactor. The fuel-cladding gap that is conventionally filled with helium, is replaced with liquid metal of eutectic lead-bismuth alloy. Each mini-fuel is instrumented with thermocouples at fuel- centerline and cladding surface. Rods are kept inside the core at various times in order to generate burnup dependent information upon post-irradiation investigation.

3:05 PM

Vanadium and Zirconium Interaction with HT-9 Stainless Steel: Randall Fielding¹; James Cole¹; ¹Idaho National Laboratory

Metallic nuclear fuel is a candidate fuel form for advanced high burnup fuel cycles. To achieve high burnups metallic fuel will require an advanced cladding resistant to fuel cladding chemical interaction. Zirconium/HT-9 stainless steel and vanadium/HT-9 stainless steel diffusion couples were fabricated and heated to the tempering temperature of 704°C for 50, 100, and 200 hours. Diffusion couples were also heated to 815°C for 100 hours. After heating the samples were microstructurally examined to determine the amount of interaction. The main interaction seen was decarburization of the HT-9 by the vanadium. Zirconium diffusion couples showed some iron/zirconium interactions, but to a much lower extent than the vanadium decarburization. Based on these results although vanadium has been shown to be a better diffusion barrier zirconium has much less interaction with the cladding material.

3:25 PM Break

3:35 PM

Fuel-Cladding Development for Sodium Fast Reactor Metallic Transmutation Fuels: *James Cole*¹; Randall Fielding¹; Jian Gan¹; Haiyan Wang²; Todd Allen³; Kumar Sridharan³; ¹Idaho National Laboratory; ²Texas A&M University; ³University of Wisconsin

As part of the US Department of Energy's Fuel Cycle R&D (FCRD) program, metallic transmutation fuels have been extensively studied. One issue that remains to be fully resolved in metallic fuel is fuel-cladding chemical interaction. Past studies have shown that as fission product content increases due to carry over from separation processes and build up due to higher burn-up of the fuel, fuel constituents will diffuse into the cladding and cladding constituents will diffuse into the fuel alloy. Of particular concern is cladding wastage when brittle phases form in the cladding, which reduces the maximum allowable stress that can build up in the fuel element. To overcome these issues, liner and coating materials have been examined which will act as diffusion barriers, effectively stopping or greatly slowing FCCI. An overview of efforts to identify, test and fabricate liner and coating options for fuel cladding tubes will be provided.



3:55 PM

Rapid Synthesis of Nuclear Nitride Fuels at Low Temperatures: *Brian Jaques*¹; Daniel Osterberg¹; Cole Smith¹; Mike Hurley¹; Darryl Butt¹; ¹Boise State University

According to the advanced fuel cycle, energy must be harvested from spent fuel and future fuels must reach higher burn-ups. Accordingly, complex fuels comprised of fissile materials must be developed. Although disadvantages exist, nitride fuels have advantages such as: high actinide loadings, high thermal conductivities, and compatibility with candidate inert matrices. Phase pure nitrides were formed from their elements in one hour by milling at ambient temperatures, as confirmed with XRD, EDS, and elemental combustion analysis. The kinetics of nitride synthesis (UN and surrogates for AmN, PuN) through high energy reaction milling in nitrogen was quantified. The extent of the reaction was monitored using in-situ pressure and temperature measurements and the Benedict-Webb-Rubin equation of state. An actinide recycling facility designed around pyro-processing, reactive milling, and SPS would be a relatively closed, proliferation resistant facility with a small footprint. Such a facility would enable simple, quick, and inexpensive partitioning and transmutation.

4:15 PM

Statistics of Grain Boundary Crystallography in Surrogates for Oxide Nuclear Fuels and its Effects on Mass Transport: Comparison between 2-D and 3-D Measurements and Models: *Karin Rudman*¹; Kapil Krishnan¹; Pedro Peralta¹; Chris Stanek²; Kenneth J. McClellan²; ¹Arizona State University; ²Los Alamos National Laboratory

Mass transport in oxide nuclear fuels can be strongly influenced by grain boundary (GB) crystallography. In particular, diffusion of fission products can be enhanced or suppressed depending on the GB misorientation and character (tilt, twist, mixed). However, experimental data are scarce on full GB crystallography of oxide fuels and their surrogates. This study aims to characterize the full GB crystallography in Yttria stabilized Zirconia and depleted Urania using Electron Backscattering Diffraction (EBSD) and serial sectioning. For each section, three parameters for the GB misorientation were collected using EBSD. These EBSD maps were used to create 3D reconstructions and obtain the GB normal. Then, 2-D and 3-D finite element models were created with these data to account for actual microstructure and model local and global diffusion of chosen fission products. The 2-D and 3-D results are compared and contrasted to elucidate role of GB crystallography on mass transport in oxide fuels.

4:35 PM

The Development of Crystalline Ceramic Wasteforms for an Advanced Nuclear Fuel Cycle: *Kyle Brinkman*¹; Amanda Billings¹; Kevin Fox¹; James Marra¹; Ming Tang²; Kurt Sickafus²; ¹Savannah River National Laboratory (SRNL); ²Los Alamos National Laboratory (LANL)

Crystalline materials with potentially enhanced thermodynamic stability as compared to glass wasteforms are currently being developed and evaluated for the encapsulation of species for repository disposal. Ceramic waste forms based on titanate and alumina were investigated for cesium and lanthanide (CS/LN) waste streams; titanate, alumina and calcium based oxides were targeted for cesium and lanthanide streams with transition metal additions (CS/LN/TM). Wasteform processing involved a melting and solidification approach as well as conventional ceramic sintering and sparks plasma sintering. This approach allows for a comparison of amorphous to crystalline phase formation that occurs via the melt versus solid state reactions encountered in conventional sintering and spark plasma sintering. Conclusions to date include i) identification of crystalline phase assemblage in ceramics by XRD and SEM/EDS as a function of composition, waste loading, and processing conditions ii) initial product consistency "dissolution" tests for crystalline ceramics and iii) room temperature irradiation studies.

4:55 PM

Alloy Optimization for Metallic Inert Matrix Nuclear Fuels: Vincenzo Lordi¹; James Belak¹; Patrice Turchi¹; ¹Lawrence Livermore National Lab Inert matrix nuclear fuels (IMF) are promising advanced fuel forms exhibiting high tolerance for fission gases (FG) and irradiation dose, while maintaining high fuel density and thermal conductivity. IMF in a dispersed metallic matrix form, fabricated by impregnation with molten matrix metal as suggested by Savchenko *et al.*, may meet these requirements by providing space for FG and a direct metallurgical bond between fuel and cladding. Impregnation must occur below 950°C to maintain the integrity of the fuel meat. Computational optimization based on coupling between thermodynamic software and a global constrained search engine was performed for a series of Zr-based metal matrix alloys to achieve low melting temperatures, while incorporating constraints on phases formed during solidification to ensure strength and reliability. Optimized alloys were identified, including an example that promotes formation of precipitates in a ductile matrix, providing both strength and FG gettering. Prepared by LLNL under Contract DE-AC52-07NA27344.

5:15 PM

Initial Microstructure Formation and Evolution in U-Pu-Zr Alloys: *Dawn Janney*¹; Rory Kennedy¹; ¹Idaho National Laboratory

The United States Department of Energy (DOE) is developing actinide alloys (primarily U, Pu, and Zr, with lower concentrations of Np, Am and lanthanides) as metal fuels for transmuting minor actinides as part of a closed nuclear fuel cycle. Previous research suggests that U-Pu-Zr alloys form a continuous solid solution at the solidus, and that this solid solution may include Np. This paper reports results of scanning electron microscope (SEM) examinations in several actinide alloys. Microstructures in rapidly cooled 4-mm cylinders demonstrate phase segregation on a sub-micron scale; those in a more slowly cooled sample are coarser. Although the mechanism of unmixing is not yet understood in detail, some geometrical relationships appear consistent with heterogeneous nucleation. This presentation will discuss results from ongoing studies of early nucleation and phase-segregation mechanisms and processes in these important materials.

5:35 PM

Modeling of Molten Salt Mixtures: Thermodynamic Assessment of CeBr3 and MBr-CeBr3 Systems (M=Li, Na, K, Rb): Yue Wu¹; Weiping Gong²; Leszek Rycerz³; Ewa Ingier-Stocka³; Ida Chojnacka³; Jan Kapala³; Slobodan Gadzuric⁴; *Marcelle Gaune-Escard*⁵; ¹Central South University; ²a)State Key Laboratory of Powder Metallurgy, Central South University and b) Huizhou University; ³Wroclaw University of Technology; ⁴University of Novi Sad; ⁵Polytech

Lanthanide halides and their mixtures with alkali metal halides play a significant role in a number of industrial applications largely based on molten salt technologies, many still under development. Their thermodynamic and transport properties can provide basic information for process development and optimization. However these data are scarce and not easily accessible in literature. Accordingly, intensive efforts are being made at an international level both in R&D aspects and also in database development. The thermodynamic properties (temperature and enthalpy of phase transition, heat capacity of solid and liquid phases) of CeBr3 and MBr-CeBr3 mixtures as the phase diagrams were experimentally investigated by Differential Scanning Calorimetry (DSC). Assessment and optimization were performed over the whole temperature/composition range. Two different models and two optimization procedures were used for the thermodynamic description of the liquid phase. A critical discussion is given.

Materials in Clean Power Systems VI: Clean Coal-, Hydrogen Based-Technologies, and Fuel Cells: SOFC I - Interconnects

Sponsored by: The Minerals, Metals and Materials Society, TMS Electronic, Magnetic, and Photonic Materials Division, TMS Structural Materials Division, TMS/ASM: Corrosion and Environmental Effects Committee, TMS: Energy Conversion and Storage Committee, TMS: High Temperature Alloys Committee *Program Organizers:* Xingbo Liu, West Virginia University; Zhenguo "Gary" Yang, Pacific Northwest National Laboratory; Jeffrey Hawk, U.S. Department of Energy, National Energy Technology Laboratory; Teruhisa Horita, AIST; Zi-Kui Liu, The Pennsylvania State University

| Tuesday PM | Room: 33C |
|---------------|-------------------------------|
| March 1, 2011 | Location: San Diego Conv. Ctr |

Session Chairs: Paul Jablonski, US Department of Energy; Jeffrey Fergus, Auburn University

2:00 PM Invited

On the State of the Art of Metal Interconnects for SOFC Application: *Paul Jablonski*¹; ¹US Department of Energy

One of the recent developments for Solid Oxide Fuel Cells (SOFC) is oxide component materials capable of operating at lower temperatures such as 700-800C. This lower temperature range has provided for the consideration of metallic interconnects which have several advantages over ceramic interconnects: low cost, ease in manufacturing, and high conductivity. Most metals and alloys will oxidize under both the anode and cathode conditions within an SOFC, thus a chief requirement is that the base metal oxide scale must be electrically conductive since this constitutes the majority of the electrical resistance in a metallic interconnect. Common high temperature alloys form scales that contain chrome, silicon and aluminum oxides among others. Under SOFC operating conditions chrome oxide is a semi-conductor while silicon and aluminum oxides are insulators. In this talk we will review the evolution in candidate alloys and surface modifications which constitute an engineered solution for SOFC interconnect applications.

2:25 PM Invited

Development of a New Alloy for SOFC Interconnects: *Nobutaka Yasuda*¹; Toshihiro Uehara²; Shigenori Tanaka¹; Kazuhiro Yamamura¹; ¹Hitachi metals, Ltd.; ²Hitachi Metals, Ltd.

Recently, metallic materials, especially Fe-Cr ferritic alloys (ex. ZMG \Box 232L, our current alloy), are promising as interconnect materials of solid oxide fuel cells (SOFCs) operated at around medium temperatures such as 700 – 850°C. These metallic materials are usually machined or pressed into various shapes of interconnect parts, and thickness of these parts is often thin. As for these alloys, good oxidation resistance and good electrical conductivity in very thin sheets are required. Moreover, it is needed to reduce Cr evaporation from Cr2O3 layer of alloy surface, because Cr evaporation causes the degradation of the cell. In this study, the effect of chemical compositions on required properties at elevated temperature was investigated on the basis of our previously developed alloy, and a new alloy with excellent oxidation resistance and reduced Cr-evaporation was developed. This study was supported by New Energy and Industrial Technology Research Development Organization (NEDO).

2:50 PM

Chromium Poisoning and Degradation of Cathodes for Solid Oxide Fuel Cells: *Teruhisa Horita*¹; DoHyong Cho¹; Taro Shimonosono¹; Haruo Kishimoto¹; Katsuhiko Yamaji¹; Manuel Brito¹; Harumi Yokokawa²; ¹AIST; ²Tokyo City University

Chromium poisoning is one of the major degradation factors in Solid Oxide Fuel Cells (SOFCs). The vaporization of chromium can occur from the metallic components surface with very low Cr-vapor pressures (less than 10-8 atm at 1073 K). To correlate the Cr poisoning and electrochemical degradation at cathodes, we have analyzed the Cr concentration in cathodes

by using Secondary Ion Mass Spectrometry (SIMS). This technique enabled us to determine the distribution of Cr and its concentration lower than 1 ppm. We examined the degradation tests of cathodes under Cr vapor supply; (La,Sr)MnO3 and (La,Sr)FerO3 on Gd0.2Ce0.8O2. It was found that the location of Cr-deposition and the degradation of cathodes are different due to the difference of electrochemical reaction and chemical reactivity. We will show the relationship between the Cr-concentration levels and the performance of LSM cathode. The effects of Cr poisoning and estimation of long-term degradation will be also discussed.

3:10 PM Break

3:25 PM Invited

Degradation of Manganese Cobalt Spinel SOFC Interconnect Coatings: *Jeffrey Fergus*¹; Yingjia Liu¹; Yu Zhao¹; ¹Auburn University

The reduced operating temperatures of intermediate temperature solid oxide fuel cells allows for the use of metallic alloys as interconnects. Although most materials degradation processes become significantly less severe with decreasing temperature, the formation of chromium oxyhydroxide gases remains significant even at relatively low operating temperatures. To reduce this volatilization and the associated cathode poisoning ceramic coatings are applied to the metal interconnects. The interaction of these coatings with the alloy over long periods of time can lead to the formation of reaction layers, which can affect the coating performance. This paper will focus on the degradation of coatings based on the manganese cobalt spinel. The reaction mechanism and the effect of the reaction on relevant properties, such as electrical conductivity and coefficient of thermal expansion, will be presented.

3:50 PM Invited

Development of Protective Coating on Alloy Interconnect for SOFCs: *Yoshitaka Baba*¹; Harukuni Kameda¹; Yoshio Matsuzaki¹; Satoshi Yamashita¹; Nobutaka Yasuda²; Toshihiro Uehara²; Katsuhiko Yamaji³; Teruhisa Horita³; Harumi Yokokawa³; ¹TOKYO GAS CO., LTD.; ²Hitachi Metals, Ltd.; ³National Institute of Advanced Industrial Science and Technology (AIST)

In intermediate temperature operation SOFCs, metallic interconnects are often used in order to increase in strength of the stack and to reduce material cost. However, there are many problems remaining such as a cathode degradation by Cr-poisoning from the alloy and an increase of the electrical resistance by growth of oxide scale. Therefore, in the SOFCs using metallic interconnects the stability of the alloy at the operation temperature is the greatest technical challenge. We have examined manganese-cobalt spinel coating on metallic interconnects for improvement of the stability of the alloy and reported the manufacture methods of the spinel coating made a difference to the oxide scale growth rate. In this study, we investigate the cause of the difference to the oxide scale growth rate by focusing on the oxide scale, and improve the more protective coating in order to reduce further not only the oxide scale growth but Cr evaporation.

4:15 PM

Electrophoretic Deposition of (Mn,Co)3O4 Spinel for SOFC Interconnects Application: *Hui Zhang*¹; Zhaolin Zhan²; Xingbo Liu¹; ¹West Virginia University; ²Kunming University of Science and Technology

(Mn,Co)3O4 spinel is a promising coating for SOFC interconnect application due to its high conductivity and capability of blocking Cr evaporation, as well as good CTE match with stainless steel and YSZ electrolyte. Slurry coating, PVD, and electroplating have been reported to apply the (Mn,Co)3O4 spinel for SOFC interconnect application. Electrophoretic Deposition (EPD) offers another fast and cost-effective coating method. In this research, we investigated the effects of deposition parameters and sintering environments on the morphology, microstructure, and area specific resistance (ASR) of Mn-Co spinel coatings by EPD. By varying the deposition voltage, time, and sintering atmosphere, the dense spinel coating was successfully deposited onto stainless steel, whose surface and cross section was characterized by SEM/EDX and XRD. ASR of coatings are about 45–90 mO cm2 at 800 °C after more than 10,000 minutes, indicating the long-term stability of spinel layer.



4:35 PM

Electrodeposited Mn-Co Alloy Coating For SOFC Interconnects: *Heather McCrabb*¹; Tim Hall¹; Junwei Wu²; Hui Zhang²; Xingbo Liu²; EJ Taylor¹; ¹Faraday Technology; ²West Virginia University

The decrease in the SOFC operating temperatures from 1000°C to 850 °C has enabled the use of ferritic stainless steels as interconnects instead of ceramics. However, even newly developed ferritic alloys such as SS441, cannot completely eliminate the chromia scale growth and chromium evaporation into cells that can cause degradation in the SOFC electrochemical performance. One attractive method to resolve the scale growth and diffusion issues is to coat the interconnect surface. Faraday Technology and WVU are developing an electrodeposition process that can produce uniform dense, crack-free, well-adhered Mn-Co alloy coatings of various alloy compositions and thickness onto a SS441 interconnect surface. A post-deposition thermal treatment converts the alloy coating to (Mn,Co)₃ O)₄ spinels. The electrodeposited spinel coatings have demonstrated a low ASR after 500 hours of thermal treatment and EDX analysis suggests the coating has the potential to prevent chrome diffusion to the interconnect surface.

4:55 PM

Electrodeposited Metal Ni Coating on Ferritic Stainless Steel for Intermediate Temperature SOFC Interconnect Application: *Shujiang Geng*¹; Fuhui Wang²; ¹Northeastern University; ²Institute of Metal Research, Chinese Academy of Sciences

Ferritic stainless steels (FSS) have been widely employed as solid oxide fuel cell (SOFC) interconnects. However, the evaporation of chromia scale might migrate to and poison the cathode. In this study, Ni, Ni-Fe and Ni-Fe-Co coatings were deposited on FSS by means of a cost-effective technique of electroplating method. They were evaluated at 800°C in air corresponding to the cathode environment of SOFC. The surface and cross-sectional morphologies of the steel with these coatings after thermal exposure were observed using scanning electron microscopy (SEM) with an energy dispersive X-ray spectroscopy (EDX). The phase structures of oxide scale formed on them were identified by X-ray diffraction (XRD). NiO/ (Ni,Fe)3O4, (Ni,Fe)3O4 and (Ni,Fe,Co)3O4 outer layer with chromia inner layer were developed on the steel with Ni, Ni-Fe and Ni-Fe-Co coatings, respectively. Long-term area specific resistance (ASR) of oxide scales was measured. The promising electrodeposited metal/alloy coatings as SOFC interconnect application was discussed.

Materials Processing Fundamentals: Smelting, Refining, and Liquid Processing

Sponsored by: The Minerals, Metals and Materials Society, TMS Extraction and Processing Division, TMS: Process Technology and Modeling Committee

Program Organizers: Prince Anyalebechi, Grand Valley State University; Srikanth Bontha, Temple University

| Tuesday PM | Room: 12 |
|---------------|-------------------------------|
| March 1, 2011 | Location: San Diego Conv. Ctr |

Session Chair: Prince Anyalebechi, Grand Valley State University

2:30 PM

Removal of Textile Dye using Electrocoagulation: *Jewel Gomes*¹; Sadia Jame¹; Daniel Chen¹; Venkata Palla¹; Paul Bernazzani¹; David Cocke¹; ¹Lamar University

Textile industries use various kinds of chemicals including dyestuffs and pigments during dyeing and finishing processes. The effluent from these processes includes suspended particles, strong color, high pH and high chemical oxygen demand (COD) that are extremely toxic and make environmental hazard. Although physical, chemical, photochemical, and biological methods are available for treating such wastewater, the electrochemical technique, electrocoagulation (EC), has emerged as an efficient, simple, and cost-effective technology in the last few decades. In this study we present the applicability of EC technique for removing dye, such as direct red dye using iron electrodes, and the optimized conditions such as dye concentration, current density, conductivity, no. of cycles and pH. The degradation of dye molecules was investigated using HPLC and UV-visible spectroscopy. The EC-floc was also characterized using SEM/ EDS, XRD and FTIR.

2:45 PM

A Study On Ferromolybdenum Production By Metallothermic Reduction Process: *Güvenç Güven*¹; Murat Alkan¹; Bora Derin¹; Onuralp Yücel¹; ¹Istanbul Technical University

In this study, production conditions of ferromolybdenum alloys by metallothermic reduction process were investigated. Metallothermic reduction process was carried out producing ferromolybdenum alloys that suits for the standarts by using a mixture of technical grade molybdenum trioxide, Fe based components, aluminium, ferrosilicon (75 wt.% Si) and calcium oxide powders in open air. In the experimental studies, different ratios of Al/FeSi powder mixtures and different amounts of calcium oxide and steel scrap additions were used and the effects of these parameters on the molybdenum recovery efficiency and final chemical compositions were carried out. The obtained alloys and slags were characterized by wet chemical analysis (AAS), XRD and EPMA techniques and due to the molybdenum recovery and ferromolybdenum production efficiency, production parameters were also optimized.

3:00 PM

Development of a Surface Micro Texturing Process Based on the Ablation at Cathode Spots of Atmospheric Arc: *Rouzbeh Sarrafi*¹; Mehdi Asgharifar¹; Radovan Kovacevic¹; ¹Research Center for Advanced Manufacturing, Southern Methodist University

This paper investigates the application of atmospheric GTAW arc for surface texturing of aluminum alloy in micro scale. The evolution of cathode spots, which occur during electron emission from non-thermionic materials, is used for roughening the smooth surface of aluminum. Surface microscopy and real-time observation by high-speed camera are used to understand the process. SEM microscopy of arc-treated surfaces shows the evolution of a very dense texture with the micro-scale feature size on the aluminum surface under the effect of numerous cathode spots of the arc. The roughness is generated by the combined effect of material evaporation and melt ejection at cathode spots. By using variable-polarity GTAW arc and the adjustment of the duty cycle of polarities, the issue of damage to the tungsten electrode (which is observed in DC arc)is resolved, and the same equipment used for AC GTAW arc welding can be used for high-speed surface texturing.

3:15 PM

DRI Carburization in the Reduction and Transition Zones of a Shaft Furnace MIDREX Type: Ferry Benique¹; *Jose D'Abreu*¹; Hélio Kohler²; Mauricio Otaviano³; ¹Pontifical Catholic University; ²Independent Consultant; ³Samarco Mineração SA

Nowadays the MIDREX process is one of the most important iron ore direct reduction routes. Aiming to a better understanding of the carburization phenomenology of the DRI into the industrial reactor, the current work is a result of the cooperative program between SAMARCO Mining Company and the Pontifical Catholic University of Rio de Janeiro / PUC-Rio. It presents the methodology utilized for the laboratory scale tests and they were a simulation for the reactor seen as divided into three zones: Reduction, Transition and Cooling zones. For each of these ones, a set of experiments were designed in a way to permit kinetic measurements of the carburization. The experimental methodology, encompassing pellet reduction and carburization, employed gaseous mixtures similar to those present in the industrial process, obeying the scale fluidodynamic similarities.

3:30 PM

Low Grade Ore Leaching to Produce Cheap Dry Cell: Alphonse Djorgbenoo¹; ¹Mining

My work presents column leaching to the treatment of low grade rhodochrosite (MnCO3) ore using spent solution of sulfuric acid to establish on a preliminary basis essential design parameters for heap leaching plant, and using the leachate to produce dry cell (battery). The physical and chemical characteristics of the low grade (MnCO3) ore, the tonnage or volume to be handled, the economics and safety of operations were discussed. The porosity of the ore was found to be 5% indicating that the material has been sufficiently weathered for heaping leaching. Consequently, when it was leached with 1M H2SO4, about 20% of the total dissolved material (1000g) was found to be manganese after 12 hours of leaching and 30% was found after 15 days of leaching. It was found out that some of the material precipitated and the exact composition determined analytically. The leached solution was also used to produce dry cell.

3:45 PM

Preparation and Properties of CuInS2 Thin Films by Electrodeposition and Sulfurization: *Min Li*¹; Huimin Lu¹; Lisha Yang¹; ¹Beihang University

CuInS2 thin films solar cells have been drawn much attention due to their potential prospects for its low-cost, high conversion efficiency and high stability. The electrodeposition of Cu-In precursor films, as the first step in making CuInS2 solar cells electrochemically in the air-and water-stable ionic liquid based on choline chloride/urea eutectic mixture has been investigated at constant potential.Compared with aqueous electrolytes, the large electrochemical window as well as the high thermal stability of this ionic liquid allow the direct electrodeposition of Cu-In precursor films. Then the precursor films were sulfuretted in a tube furnace at different sulfurization temperatures to optimize the films properties. The films obtained were characterized by X-ray diffraction (XRD), scanning electron microscope (SEM), energy dispersive spectroscopy (EDS).

4:00 PM Break

4:15 PM

Effect of Technological Conditions on Enrichment of Phosphor during Melting Adjustment Process of Converter Slag: Min Chen¹; Hong-xu Cui¹; *Zhen Tian*¹; ¹Northeastern University

Many studies have focused on dephosphorization of the slag for its internal reuse inside metallurgical enterprises, but little has considered the phosphor resource in the slag. On the other hand, as one of the strategy resources, the mining and application of phosphate rock have been causing much attention. The present work investigated the effect of adjustment technologies on enrichment of phosphor using molten converter slag as starting material. The result showed that the grain size of 2CaO•SiO2 containing high-grade phosphor increased slightly with decrease the cooling rate, with the proper one around 1.0°C/min. In addition, the morphology of the phosphor-rich 2CaO•SiO2 phase changed from granular in high basicity slag to coexistence of granular and rod-like in in lower basicity of the adjusted slag. By melting adjustment treatment, phosphor was effectively enriched into 2CaO•SiO2 phase, with P2O5 content over 30%.

4:30 PM

Experimental Study on the Production of Nitrogen-bearing Stainless Steel by Injecting Nitrogen Gas: *Liyuan Sun*¹; Jingshe Li¹; Lifeng Zhang²; ¹University of Science and Technology Beijing; ²Missouri University of Science and Technology

Instead of nickel-based stainless steel, nitrogen-containing stainless steel was developed to reduce the production cost stemming from the shortage of nickel recourses. Thermodynamic model to calculate the saturation nitrogen content in the stainless steel were developed and the model was validated by experiments. In these experiments with a high temperature induction furnace, nitrogen gas under constant pressure was injected by which the nitrogen was transferred to the nitrogen-containing stainless steel. The effects of chemical compositions, temperature, superficial active elements and nitrogen-flow rate on transferring nitrogen to the steel were investigated and discussed.

A New Method of Synthesis of Rod-like Magnetite: Xiyun Yang¹; *Xichang Shi*¹; Hui Xu¹; Xiaofeng Zhang¹; Xiang Xiao¹; Liwen Ma¹; ¹Central South University

Rod-like magnetite particles were prepared by precipitation of iron salts with urea under the induction of magnetic field. Temperature and initial Fe3+/Fe2+ ratio have a significant effect on the composition of the product. Magnetite particles change from spherical into rod shape in the presence of 0.35T magnetic field. The addition of a small amount of spherical seeds increases the rod-like magnetite particles yield. The seeds are prepared by aging ferrous and ferric solution with sodium hydroxide as precipitator. The aspect ratio of the rod is controlled by varying the ratio of seed to iron salt.

5:00 PM

Preparation of Fibrous CoO Particles by Thermal Decomposition of a New Precursor: Jing Zhan¹; Difei Zhou¹; Chuanfu Zhang¹; *Jianfeng Yue*¹; ¹Central South University

A novel precursor of fibrous CoO powders has been synthesized by coordination-precipitation process using oxalic acid and cobalt chloride as starting materials, and ammonia as coordinator. The phase, composition and morphology of the novel precursor were characterized by XRD, IR, DTA/TGA and SEM analysis. The results show that the precursors obtained at pH=9.0 is different from that of β-CoC2O4•2H2O precipitated at pH=1.0, which indicates that the existance of ammonia in the precursor formed at pH=9.0 and the formula of the new precursors was inferred as [Co(NH3) x]C2O4•yH2O•nNH3 in reaction system Co(II)-C2O42-- NH3-NH4+-H2O. The fibrous CoO particles with about 0.3~0.5µm in diameter and 20~40 in aspect ratio were produced in the condition of 800°C for thermal decomposition and nitrogen atmosphere with sufficient oxygen.

5:15 PM

Direct Observation of Al Drop and Gas Bubbles in the Anode–Cathode Space during Aluminum Electrolysis: *Jilai Xue*¹; Yifang Zheng¹; Zhu Jun¹; Lin Li¹; ¹Unversity of Science and Technology Beijing

Al drops and gas bubbles in the anode-cathode space of aluminum electrolysis cell are of great importance for cell operation improvement in metal loss, current efficiency and energy consumption. A direct observation on the Al drop, gas bubble and ultrasound was carried out through a seethrough cell. The Al drop immersed into the cryolitic melt was found moving up and down irregularly in the anode-cathode space without electrolysis, which was then completely dissolved into the melt. During electrolysis, the Al drop came to the anode area and reacted with the gas bubbles generated on the anode. Under ultrasound, the gas bubbles were removed from the anode surface while the Al drop was kept on the side of anode. The observed phenomena were useful for reducing anode-cathode distance or lower the energy consumption.

5:30 PM

Extracting Al2O3 from Coal Gangue by Carbonthermal Reduction -Alkaline Leaching Process: Jun Zhu¹; Jilai Xue¹; Tao Li¹; ¹University of Science and Technology Beijing

Coal gangue is industrial waste containing Al2O3 and SiO2 with great recycling and reuse values. This work is aimed at extracting Al2O3 content in the coal gangue by a process of carbonthermal reduction - alkaline leaching. The Al2O3 and SiO2 contents first became a mixture of SiC and Al2O3 in the process of carbonthermal reduction, and then Al2O3 was separated by leaching in NaOH solution, thus producing the sodium aluminate solution for Al(OH)3 precipitation. The products generated at various stages in the process were inspected using XRD and chemical analysis. The effects of parameters such as reduction temperature, carbon ratio, NaOH concentration, leaching time, leaching temperature, stirring speed, etc will be presented in details.

TMS2011 140th Annual Meeting & Exhibition

5:45 PM

ESP Dust Recovery Process Test Works, Plant Trial, Commissioning, Operations and Metallurgical Performance: *Pengfu Tan*¹; ¹Xstrata Copper

Arsenic enters the Mount Isa copper circuit in the form of arsenic rich minerals in concentrates from both the Mount Isa and Ernest Henry copper mines. Arsenic is a volatile metal, and will partition in the copper smelter between smelter off gases, slag and anode. Most of the volatile arsenic will report to Isasmelt Electrostatic Precipitator (ESP) or Waste Heat Boiler dusts where it will form a re-circulating load within the smelter. ESP dust is produced at a rate of 15,000 – 20,000 t/y and is currently removed from the precipitator and leached in the new ESP Dust Recovery Plant to separate copper and arsenic from the ESP dust. This paper describes the lab test works of ESP dust leaching, neutralisation and cementation processes. The plant trial, commissioning and operation have been presented as well.

Microstructural Processes in Irradiated Materials: Phase Stability

Sponsored by: The Minerals, Metals and Materials Society, TMS Structural Materials Division, TMS/ASM: Nuclear Materials Committee

Program Organizers: Gary Was, University of Michigan; Thak Sang Byun, Oak Ridge National Laboratory; Shenyang Hu, Pacific Northwest National Laboratory; Dane Morgan, UW Madison; Yasuyoshi Nagai, Tohoku University

| Tuesday PM | Room: 3 |
|---------------|-------------------------------|
| March 1, 2011 | Location: San Diego Conv. Ctr |

Session Chairs: Emmanuelle Marquis, University of Michigan; Philippe Pareige, Universite et INSA de Rouen

2:00 PM Invited

Characterization of Solute Atom Distribution in Grain Interior of Neutron-Irradiated 304L and 304 Stainless Steels: *Naoki Soneda*¹; Kenji Nishida¹; Akiyoshi Nomoto¹; Kenji Dohi¹; Peter Chou²; ¹Central Research Institute of Electric Power Industry; ²Electric Power Research Institute

Solute atom distribution of 304L and 304 stainless steels irradiated by neutrons was investigated by means of atom probe tomography (APT). The materials were retrieved from control-rod blades or removed from the top guide of commercial boiling water reactors. The doses of materials range from 3.6 to 13 dpa. As the first step of the characterization of these materials, solute atom distribution in grain interior was investigated. Features enriched with Ni and Si atoms were clearly and commonly identified in all samples examined. Many of such Ni-Si features at low dose are not very well shaped like precipitates. Some Ni-Si features to dislocation loops segregated with Ni and Si atoms. In 304L materials, formation of Al clusters was also observed. The size and number density of such clusters are $2\sim3$ nm in diameter and $3\sim6x10^{23}$ m⁻³, respectively.

2:40 PM

Grain Boundary Chemistry in Irradiated Fe-Cr Alloys: Rong Hu¹; *Emmanuelle Marquis*²; ¹University of Oxford; ²University of Michigan

Ferritic Fe-Cr alloys are the base for structural steels currently considered for Gen IV nuclear plants and future fusion reactors. Among the outstanding issues related to the use of these alloys under irradiation are a' precipitation (and the uncertainty of the position of the solvus line at low temperatures) and radiation induced segregation (RIS) or depletion (RID) of grain boundaries. These phenomena could indeed significantly affect the properties of these alloys. Past observations reported grain boundary Cr depletion or segregation without any clear correlation to irradiation conditions (Lu et al. Scripta Mater. 2008). Moreover, common impurities such as carbon are expected to affect the integrity of grain boundaries and modify the extent of radiation induced segregation phenomena. The experimental approach using atomic scale characterization techniques as well as the role of carbon will be described and the effect of irradiation discussed as function of carbon content and grain boundary orientation.

3:00 PM

Precipitation and Grain Boundary Segregation under Neutron Irradiation in Fe-12at%Cr Based Alloy: *Philippe Pareige*¹; Viacheslav Kuksenko¹; Brigitte Décamps²; Pierre Desgardin³; Cristelle Pareige¹; ¹GPM - UMR 6634 CNRS, University and INSA of Roeun; ²CSNSM, UMR CNRS 8609, Université Paris-Sud; ³CEMHTI/CNRS site Cyclotron

High-chromium ferritic-martensitic steels are up to now candidates as structural materials in the next Generation IV power plants. For the first time, a nanoscale description of an industrial purity Fe-12at%Cr model alloy, neutron irradiated at 300°C, was performed using the 3D atom probe technique. This paper presents a quantitative description of intragranular α ' clusters and NiSi complexes formed under the neutron irradiation, as well as low-angle grain boundary segregations. These atomic scale results are compared to those obtained by complementary techniques such as SANS [1] and TEM [2] performed on the same model alloy. These results are important for the understanding of the basic mechanisms at the origin of the decomposition of these alloys under irradiation and for comparison or improvement of multi-scale modelling. [1] F.Bergner, A.Ulbricht and C.Heintze,Scripta mater.61 (2009) 1060. [2] M.Matijasevic, A.Almazouzi, J.Nucl.Mater.377 (2008) 147.

3:20 PM

Characterization of Radiation-induced Precipitation in Ferritic-Martensitic Alloys by Different Particle Types: *Zhijie Jiao*¹; Gary Was¹; ¹University of Michigan

Ferritic-martensitic (F-M) alloys are of great interest as cladding and structural materials in fast fission and fusion reactors. However, they are prone to hardening and embrittlement caused by radiation-induced precipitates. In this study, three F-M alloys, T91, HT-9 and HCM12A, were irradiated to 7 dpa at 400\176C using 2 MeV protons, to 100 dpa at 500\176C using heavy ions, and to 3 dpa at 500\176C using neutrons. Radiation-induced precipitates were characterized using atom probe tomography. Preliminary results have showed that Ni/Si/Mn-rich, Cu-rich and Cr-rich precipitates form under proton or heavy ion irradiations. This study will compare the types and nature of precipitates formed by different particle irradiations.

3:40 PM Break

4:00 PM

Effects of Helium on Cavity and Microstructural Evolution in Tempered Martensitic Steels and Nanostructured Ferritic Alloys – In Situ Helium Implantation Studies: *G. Robert Odette*¹; Danny Edwards²; Yuan Wu¹; Takuya Yamamoto¹; Richard J. Kurtz²; ¹University of California, Santa Batrbara; ²Pacific Northwest National Laboratory

Two-step thermal neutron $(n_{tb})^{58}$ Ni $(n_{tb},\gamma)^{59}$ Ni (n_{tb},α) reactions in micron scale NiAl layers injected high-energy α -particles to a depth of ~ 5 to 8 μ m into adjacent alloys simultaneously undergoing fast neutron induced displacement (dpa) damage in HFIR irradiations. The implantations were carried out for a large matrix of alloys over a wide range of temperatures and dpa at controlled He/dpa ratios from << 1 to 40 appm He/dpa. Earlier studies showed that 9Cr tempered martensitic steels contain a bimodal distribution of bubbles and voids for irradiations to 9 dpa and 380 appm He at 500°C. In contrast, the same irradiations Y-Ti-O nanofeatures in nanostructured ferritic alloys trap He in ultrafine scale interface bubbles. Building on the earlier studies, we compare the cavity structures in a 14Cr NFA, MA957, to those in an 8Cr TMS, F82H, following HFIR irradiations up to 25 dpa and 1200 appm He.

4:05 PM

Ni-Si Clusters in Neutron-irradiated 304 Stainless Steel Studied by Three-dimensional Atom Probe: *Takeshi Toyama*¹; Yoshitaka Matsukawa¹; Yasuko Nozawa¹; Masahiko Hatakeyama¹; Yasuyoshi Nagai¹; Wouter Van Renterghem²; Steven Van Dyck²; Abderrahim Al Mazouzi³; ¹Tohoku University; ²SCK•CEN; ³EDF R&D

Ni-Si clusters such as γ ' precipitate (Ni₃Si) are the typical irradiation-induced solute clusters in stainless steel (SS). They are considered to contribute to the changes of mechanical properties. In this study, the morphologies of Ni-Si clusters in neutron-irradiated 304 SS were characterized using laser-assisted local electrode-type three-dimensional atom probe. The studied sample was irradiated to a neutron fluence of $1.6E+22 \text{ n/cm}^2(E>1MeV)$: 24 dpa at ~300°C in the fuel wrapper plate of a commercial pressurized water reactor. A high number density (3E+17 /cm³) of Ni-Si enriched and Cr-Fe depleted clusters was observed. In some clusters, Mn enrichment and P segregation at the cluster-matrix interface were observed as well. The average chemical composition of the clusters was Ni: 55%, Si: 20%, Mn: 5%, Cr: 5%, Fe: 10% (at.%), close to that of a γ ' precipitate. Effects of these clusters on the irradiation-hardening will be presented.

4:25 PM

Microstructure Evolution in Irradiated Austenitic Stainless Steels: Gary Was¹; Zhijie Jiao¹; ¹University of Michigan

The evolution of radiation induced segregation and radiation induced precipitation in austenitic stainless steels is characterized using atom probe tomography (APT) and STEM-EDS. Types 304 and 316 stainless steels were irradiated with 2 MeV protons to a dose of 5 dpa at 360°C and with 5 MeV Ni++ to 100 dpa. Boron segregation to the grain boundary prior to irradiation is not affected by the irradiation while phosphorus segregation is enhanced by irradiation and carbon depletes. Segregation at dislocations mirrors that at the grain boundary plane and along the dislocation loop core. Ni/Si-rich clusters formed in irradiated commercial purity 304 were likely precursors of γ ' or other Si- and Ni-rich phases. Copper clusters were observed to form adjacent to Ni/Si-rich clusters and copper depletion was observed at both the grain boundary and at dislocation loops.

4:45 PM

Phase Stability of Solution Strengthened 316 Stainless Steel Under Fast Neutron Irradiation Using a Diffusion Couple Approach: *Luke Brewer*¹; Khalid Hattar²; Joseph Puskar²; Steven Goods²; Mark Reece²; ¹Naval Postgraduate School; ²Sandia National Laboratories

Austenitic stainless steels are critical materials for the structural components of fast neutron reactors and must be able to withstand prolonged exposure to fast neutrons at high temperatures. The phase stability of refractory element-based solution strengthened stainless steels under high dose irradiation (up to and greater than 100 dpa) is not known. This talk will discuss a diffusion couple approach that allows for the rapid assessment of many compositions and irradiation levels. 316L steel substrates were diffusion bonded with tantalum, tungsten, molybdenum, and niobium plates and then annealed at 1100°C for 400 hours. A suite of spatially-registered, microscale techniques such as x-ray microanalysis, electron backscatter diffraction, and nanoindentation was used to map out the phase stability, elastic modulus, hardness and other properties as a function of composition. This microscale, structure-property assessment will be discussed for several irradiation levels from 1 dpa to 100 dpa.

5:05 PM

Solute Rich Clusters Formation under Neutron Irradiation of Fe Dilute Alloys Representative of Model and RPV Steels by Atomic Kinetic Monte Carlo: *Christophe Domain*¹; Raoul Ngayam Happy¹; Charlotte Becquart²; ¹EDF R&D; ²UMET, UMR8207

The embrittlement and the hardening of pressure vessel steels under radiation has been correlated with the formation of more or less dilute clusters containing Cu, Ni, Mn and Si which are investigated in this work using a multiscale approach based on ab initio and atomistic kinetic Monte Carlo simulations. The parameterisation of the interactions is based on DFT calculations and some of the parameters have been adjusted on binary alloys isochronal annealing experiments. The model has been used to simulate the medium term evolution of different Fe dilute alloys under neutron irradiation. Alloys of growing complexity have been simulated allowing an investigation of the synergetic roles of the different solutes. The influence of dose and dose rate on the point defect clusters and solute clusters.

5:25 PM

The Role of Carbon in Copper Precipitation Process in Neutron Irradiated Fe-Cu Binary Alloys: *Milan Konstantinovic*¹; ¹SCK.CEN

In spite of general understanding of the copper precipitation in neutron irradiated Cu-rich alloys, the role of carbon in the precipitation process, and their overall effect to the dislocation dynamics, as well as to the hardening and embrittlement, are not yet fully elucidated. The ability of internal friction (IF) technique to detect both the carbon relaxation and dislocation-related relaxation processes makes the IF experiment as one of the most suitable techniques to study afore mentioned problems. The behaviour of the Snoek-Koster peak intensities in the temperature dependent IF spectra of neutron-irradiated Fe-Cu binary alloys indicate the existence of carbon redistribution as a function of dose. By correlating the IF and results of mechanical tests, we argue that carbon is not a passive observer of the copper precipitation process and estimate the contribution of the carbon redistribution to the hardening in these alloys.

Neutron and X-Ray Studies of Advanced Materials IV: Dislocations, Strains and Stresses I

Sponsored by: The Minerals, Metals and Materials Society, TMS Structural Materials Division, TMS/ASM: Mechanical Behavior of Materials Committee, TMS: Chemistry and Physics of Materials Committee

Program Organizers: Rozaliya Barabash, Oak Ridge National Laboratory; Xun-Li Wang, Oak Ridge National Laboratory; Jaimie Tiley, Air Force Research Laboratory; Peter Liaw, The University of Tennessee; Erica Lilleodden, GKSS Research Center; Brent Fultz, California Institute of Technology; Y-D Wang, Northeastern University

| Tuesday PM | Room: 10 |
|---------------|-------------------------------|
| March 1, 2011 | Location: San Diego Conv. Ctr |

Session Chairs: Klaus-Dieter Liss, The Bragg Institute; E-Wen Huang, National Central University of Taiwan

2:00 PM Keynote

Pursuing 3DXRD at the Sub-Micron Scale: *Henning Poulsen*¹; Erik Lauridsen¹; Wolfgang Ludwig²; Alexei Snigirev²; Ulrik Olsen¹; Soeren Schmidt¹; Haihua Liu¹; Xiaoxu Huang¹; Gavin Vaughan²; ¹Risoe DTU; ²ESRF

We present several approaches being explored at beamline ID11, ESRF, for generalising the 3DXRD & DCT grain and orientation mapping methodologies towards the sub-micron scale: • C o n v e n t i o n a 1 3DXRD. By going to the limit of the existing detector technology a resolution of 400 nm has been achieved. • Full field microscopy for tomography and DCT. Using compound refractive lenses as an objective, and placing the detector 52 m from the sample, this set-up comes with ~50cm of free space around the sample and a 100 nm spatial imaging resolution. • N e w detectors. A 3D detector has been commissioned, with enhanced possibilities for 3D orientation mapping of deformed specimens. At the time of writing a new detector principle with nominal 100 nm resolution is being tested. The latter is directly compatible with parallel beam tomography, holography and 3DXRD. • Stochastic type experiments on grains in the 20-100 nm range.



2:25 PM Invited

3D Orientation Imaging Microscopy Based on Monochromatic Beam Synchrotron X-Ray Diffraction and Imaging Techniques: *Wolfgang Ludwig*¹; Andrew King²; Peter Reischig³; Michael Herbig¹; Henry Proudhon⁴; ¹Université de Lyon; ²ESRF; ³Karlsruhe Institute of Technology; ⁴Mines Paristech

3D X-ray diffraction (3DXRD) is a methodology, which combines the principles of X-ray diffraction imaging (topography) and image reconstruction from projections (tomography) for investigation of polycrystalline materials. We present a new acquisition strategy aiming at the reconstruction of local orientation and elastic strain distribution via a combination of full-field imaging and micro-beam diffraction techniques. Associating this 3D orientation mapping with conventional attenuation and/or phase contrast tomography yields a non-destructive characterization technique, enabling time-lapse observation of crystal growth, deformation and damage mechanisms in the bulk of structural materials. The capabilities and limitations, as well as perspectives of this combined characterization approach will be discussed and illustrated on selected application examples.

2:45 PM Invited

Measuring Complete Strain Tensors from Individual Dislocation Cells in Deformed Cu: Lyle Levine¹; Peter Geantil²; Bennett Larson³; Jonathan Tischler³; Francesca Tavazza¹; Michael Kassner⁴; Wenjun Liu⁵; ¹National Institute of Standards and Technology; ²University of Southern California; ³Oak Ridge National Laboratory; ⁴Director of Research, Office of Naval Research; ⁵Argonne National Laboratory

The use of depth resolved, sub-micrometer X-ray beams for studying dislocation structures in plastically deformed metals has advanced considerably over the past five years. Thus, we previously measured elastic strains (and thus stresses) from individual cell interiors and cell walls in plastically deformed Cu specimens and compared these results with model calculations. However, these measurements included just a single component (e_{11}) of the elastic strain tensor, since only a single X-ray reflection could be examined with the necessary accuracy. Recently, additional detectors were installed to allow multiple reflections to be measured over a wide range of angles, enabling us to measure both the crystallographic orientation and the complete elastic strain tensor (and thus the stress tensor) from spatially resolved, sub-micrometer sample volumes within deformed metal specimens. The first results of these experiments will be presented along with model-based simulations of the stress tensor in cell walls and cell interiors.

3:05 PM Invited

Synchrotron X-Ray Laue Microdiffraction for the Study of Materials Micromechanics: *Nobumichi Tamura*¹; Martin Kunz¹; Kai Chen¹; ¹Lawrence Berkeley National Lab.

Laue X-ray microdiffraction is a powerful tool which allows mapping crystal orientation and elastic strains in 2D and 3D at the mesoscopic scale $(0.1 - 10 \ \mu\text{m})$. Small displacements of the reflection positions with respect to their calculated "unstrained" positions allows determining the deformation of the unit cell and thus the elastic strain (in effect the deviatoric component of the elastic strain). Plastic deformation on the other hand manifest itself as broadening of the Laue reflections. Symmetric broadening is linked to statistically stored dislocations (SSD) but asymetric broadening in the form of peak streaking can be explained in term of geometrically necessary dislocations (GND) causing local bending of the lattice. Examples of the application of x-ray microdiffraction to the study of deformation in polycrystalline thin films and single crystal nanopillars will be given.

3:25 PM

A Study of Casting Residual Stress: *Thomas Watkins*¹; Eric Johnson²; Camden Hubbard¹; Joshua Schmidlin¹; ¹ORNL; ²Deere and Company

Stringent regulatory requirements, such as Tier IV norms, have pushed the cast iron for automotive applications to its limit. As such, castings need to be designed with closer tolerances by incorporating hitherto unknowns, such as residual stresses. In the present work, a benchmark study was undertaken for casting residual stress measurements through neutron diffraction, which was subsequently used to validate the accuracy of a simulation prediction.

Castings of lattice specimen geometry were made such that adequate residual compressive and tensile stresses were generated during solidification, without any cracks. The residual stresses in the cast specimen were measured using neutron diffraction. Simulations were performed using the identical geometry and casting condition for predictions of residual stresses. The simulation predictions were found to agree well with the experimentally measured residual stresses.

3:40 PM

Laue Microdiffraction Measure of Crystal Distortion and Dislocation Density Profile in a Plastically Deformed Multi-Crystal: Gael Daveau¹; Benoit Devincre²; Thierry Hoc³; Odile Robach⁴; ¹LEM (CNRS-ONERA) / MSSMAT (ECP); ²LEM (CNRS-ONERA); ³LTDS (EC-Lyon); ⁴CEA-Grenoble DSM/INAC/SP2M/NRS

In this study, a dislocation density based model [1] initially developed for fcc single crystal is extended to strain hardening in polycrystal. For this reason, the early stages of plastic deformation in a Cu tri-crystal are investigated with Laue microdiffraction. Measures are made in the vicinity of a triple node after approximately 0.5% of compression. The existence of extended rotation and strain gradients at the grain boundaries (GBs) is shown. Peak broadening analysis provides qualitative and quantitative evolutions of the GNDs density distribution during deformation. The GB impact on strain hardening is thus clearly revealed. Those results are compared with simulations of dislocation dynamics that calculate the reduction of dislocation mean free path imposed by GBs. This information serves as an input to a crystal plasticity code reproducing the tri-crystal plastic deformation. [1] Devincre, Hoc, Kubin, Science, 320 (2008) p 1745–1748.

3:50 PM

Pair Distribution Function of a High Entropy Alloy: A Neutron Scattering Study: *Wei Guo*¹; Peter Liaw¹; Takeshi Egami¹; ¹university of tennessee, knoxville

A ZrNbHf high entropy alloy is prepared. Laboratory X-ray diffraction indicates the lattice structure is body center cubic. Since this material is composed of different elements with various dimensions and valances, it is compelling to study the local structure of the alloy to unveil how the atoms construct this structure. Samples deformed at different strains and as-cast samples with no deformation are investigated by neutron scattering with high-intensity powder diffractometer. Pair distribution functions of the samples are obtained and compared. The local structural features of the high entropy alloy are discussed, and the deformation mechanism is suggested.

4:00 PM Break

4:10 PM Invited

Cyclic-loading Effects on Lattice-Strain Asymmetry Behavior in Loading and Transverse Directions: *E-Wen Huang*¹; Kyle Woods²; Bjorn Clausen³; Rozaliya Barabash⁴; Peter Liaw²; ¹National Central University; ²Univ. of Tennessee; ³Los Alamos Neutron Science Center; ⁴Oak Ridge National Laboratory

Cyclic loading and the subsequent fatigue-induced structural transformations have been investigated using in-situ neutron-diffraction experiments at elevated temperatures. In-situ neutron-diffraction measurements identify the development of different fatigue stages in the cyclic-deformation-induced structural transformations, such as bulk hardening, softening, and eventual saturation. A transition is observed during the saturation cycles, which is characterized by the emergence of the lattice-strain asymmetry in the loading and transverse directions. An anomaly during saturation cycles is believed to arise from dislocation self-organization – possibly during the formation of microcracks. The single-phase, polycrystalline nickel-based alloy is selected for the present study of the loading and transverse asymmetry subjected to cyclic loading at both room and high temperatures. In this investigation, we compare the deformation at room and elevated temperatures. The identical loading and transverse -asymmetry feature is found to be valid at both room and high temperatures.

4:30 PM

Twin Boundaries and Dislocation Densities in <111>, <100> and <211> Textured Ni Thin Films Determined by X-Ray Line Profile Analysis: *Gábor Csiszár*¹; Karen Pantleon²; Hossein Alimadadi²; Tamás Ungár¹; ¹Eötvös University Budapest; ²Technical University of Denmark

Ni thin films were grown by electrochemical deposition resulting in <111>, <100> and <211> textures and about 15 μ m thickness. The X-ray diffraction measurements were carried out in a special high resolution diffractometer with a plane Ge (220) primary monochromator. The Co K α 1 beam of 0.1×2 mm size hit the specimen under different angles selected in order to obtain diffraction always from the same texture component. The dislocation density and the frequency of twin boundaries was determined by the extended Convolutional Multiple Whole Profile (eCMWP) line profile analysis procedure. The dislocation densities are found to be relatively high and the twin boundary densities are varying between zero and a few percent. The X-ray results are discussed in relation to electron microscopy investigations and the different growth conditions.

4:45 PM Invited

Grain Resolved Strain Evaluation Using Hard X-Rays: Marcin Moscicki¹; *Andras Borbely*²; Jonathan Wright³; Anke Pyzalla⁴; ¹Max-Planck Institut für Eisenforschung; ²Ecole des Mines de Saint-Etienne; ³ESRF; ⁴Helmholtz Zentrum für Materialien und Energie Berlin

In situ diffraction experiments during uniaxial straining of OFHC copper and stainless steel of grade 1.4301 were performed at beamline ID11 of the European Synchrotron Radiation Facility. The crystallographic orientation change, location of center of mass and the strain tensor of individual grains have been evaluated. The accuracy of strain tensor elements is discussed based on simulated and experimental 2D diffractograms. Issues related to the calibration of the 3DXRD setup are presented and a two-step calibration method based on the use of reference powder and single crystal specimens is presented. Problems concerning the stress free lattice parameter "a0" are highlighted and a solution based on the minimization of the elastic energy of the polycrystal aggregate is proposed. The experimentally obtained strain tensor elements characterizing single grains show a large scatter, but their average values are in good agreement with the macroscopically imposed strain state and known Poisson's ratio.

5:05 PM Invited

High Resolution Reciprocal Space Mapping of Individual Grains within Deformed Polycrystals: *Ulrich Lienert*¹; Matthew Brandes²; Joel Bernier³; Peter Kenesei¹; Michael Mills²; Matthew Miller⁴; ¹Argonne National Laboratory; ²Ohio State University; ³Lawrence Livermore National Laboratory; ⁴Cornell University

The High Energy Diffraction Microscopy program at the 1-ID beamline of the Advanced Photon Source employs high energy x-rays for the structural characterization of polycrystalline bulk materials on individual grain and subgrain scales during themomechanical loading. The status of distinct techniques that enable orientation mapping and the measurement of strain tensors and centroid positions of hundreds to thousands of individual grains will be summarized. Emphasis will be put on high resolution reciprocal space mapping which has been demonstrated to provide orientation and strain information on the subgrain scale. A case study of Ti-7Al after tensile deformation will be presented. The combination with electron microscopy investigations of the same grains will be discussed. Use of the Advanced Photon Source was supported by the U. S. Department of Energy, Office of Science, Office of Basic Energy Sciences, under Contract No. DE-AC02-06CH11357.

5:25 PM

Evolution of Internal Strain with Temperature in Depleted Uranium in the Presence of Hydrides: *Michael Hemphill*¹; Elena Garlea²; Jonathan Morrell²; Don Brown³; Thomas Sisneros³; Sven Vogel³; G Powell²; Peter Liaw¹; ¹University of Tennessee; ²Y-12 National Security Complex; ³Los Alamos National Laboratory

The effects of temperature and hydrogen corrosion on the mechanical behavior of depleted uranium (DU) were investigated by neutron diffraction to relate the grain-level behavior to the observed macroscopic behavior. Three cylindrical compression specimens of rolled depleted uranium were charged with 0 wppm, 0.3 wppm, and 1.8 wppm of hydrogen and compared to a reference specimen that remained in the as-rolled condition. Uniaxial compression was performed at room temperature, 100°C, and 150°C to measure the macroscopic stress versus strain. In-situ neutron diffraction was performed during the loading sequence to measure the internal strain evolution at the grain level. Additionally, a series of unloading sequences was used to measure the residual strain build-up. Texture measurements were performed before and after loading to describe texture changes due to temperature and loading. These micro- and macroscopic results provide insight into the effect temperature and hydrogen/hydrides has on the activation of deformation modes.

5:35 PM

Measuring Single Crystal Diffuse Neutron Scattering on the Wombat High Intensity Powder Diffractometer: *Ross Whitfield*¹; Darren Goossens¹; Andrew Studer²; Jennifer Forrester³; ¹Australian National University; ²Australian Nuclear Science and Technology Organisation; ³The University of Newcastle

Single crystal diffuse scattering was collected on the Wombat highintensity powder diffractometer at the OPAL reactor at the Bragg Institute. The difficulty in measuring diffuse scattering come from its relative low intensity compared to the Bragg peaks, some 10^3 - 10^4 factor smaller. Wombat allows collection of diffuse scattering due to its high intensity and large twodimensional detector. Diffuse scattering data from yttria-stabilised cubic zirconia and PZN (PbZn_{1/3}Nb_{2/3}O₃) have been successfully collected, the latter at a range of temperatures. The data have been processed, normalised and background subtracted to reconstruct flat reciprocal space sections with a minimum of artefacts. The strategies used to tackle the collection of neutron diffuse scattering and the way in which they are implemented will be discussed.

5:45 PM

Validation of Predicted Residual Stresses within DC Cast Magnesium Alloy WE43 Slab: *Mark Turski*¹; Anna Paradowska²; Shu Yan²; Dag Mortensen³; Hallvard Fjaer³; John Grandfield⁴; Tim Wilks¹; Bruce Davis⁵; Richard DeLorme⁵; ¹Magnesium Elektron; ²Rutherford Appleton Laboratory; ³Institute for Energy Technology; ⁴Grandfield Technology Pty Ltd, ; ⁵Magnesium Elektron North America

During direct chill (DC) casting of the high strength magnesium alloy Elektron WE43, a significant level of cold cracking has been observed. In order to ensure good slab yields for this alloy, the effect of casting parameters on the residual stress field within the cast material has been investigated. A finite element modeling (FEM) code, called ALSIM, has been used to determine the residual stress within DC cast slab. Validation of FEM simulations were carried out using neutron diffraction measurements of the residual stress field within a slab of cross section 870 x 315 mm. Given that measurements in such large scale components using diffraction measurements are particularly challenging and expensive, efficient use of neutron diffraction measurements is emphasized. These measurements allowed validation of the FEM code. The use of this validated model has allowed optimized casting parameters to be developed to produce crack-free Elektron WE43 slab via DC casting.



Sponsored by: The Minerals, Metals and Materials Society, TMS Electronic, Magnetic, and Photonic Materials Division, TMS: Electronic Packaging and Interconnection Materials Committee *Program Organizers*: Indranath Dutta, Washington State University; Darrel Frear, Freescale Semiconductor; Sung Kang, IBM; Eric Cotts, SUNY Binghamton; Laura Turbini, Research in Motion; Rajen Sidhu, Intel Corporation; John Osenbach, LSI Corporation; Albert Wu, National Central Univ, Taiwan; Tae-Kyu Lee, Cisco Systems

| Tuesday PM | Room: 7B |
|---------------|-------------------------------|
| March 1, 2011 | Location: San Diego Conv. Ctr |

Session Chairs: Tae-Kyu Lee, Cisco Systems; Hongtao Ma, Cisco Systems, Inc.

2:00 PM Invited

Comparison of Extensive Thermal Cycling Effects on Microstructure Development in Micro-Alloyed Sn-Ag-Cu Solder Joints: *Iver Anderson*¹; Adam Boesenberg²; Joel Harringa¹; David Riegner²; Andrew Steinmetz²; David Hillman³; Tim Pearson⁴; ¹Ames Laboratory; ²Iowa State University; ³Rockwell-Collins; ⁴Rockwell-Collins

Pb-free solder alloys based on the Sn-Ag-Cu (SAC) ternary eutectic have promise for widespread adoption across assembly conditions and operating environments, but enhanced microstructural control is needed. Micro-alloying with elements like Zn was demonstrated for promoting a preferred solidification path and joint microstructure both in simple (Cu/ Cu) solder joints studies for different cooling rates and in (reworked) ball grid array (BGA) joints, using dissimilar, Sn-3.5Ag-0.5Cu (SAC305), solder paste. In addition to this industrial assembly operation, the BGA joints made with a preferred Sn-3.5Ag-0.74Cu-0.21Zn (SAC3595+0.21Zn) solder were tested in thermal cycling (-55°C/+125°C) along with baseline SAC305 BGA joints, beyond 3000 cycles with continuous failure monitoring. A correlation of thermal cycle lifetime with initial as-solidified BGA joint microstructure features, i.e. large Ag3Sn "blades" and distributed pro-eutectic Cu6Sn5 phase, was attempted to compare these SAC305 and SAC3595+0.21Zn joints. Support from Iowa State University Research Foundation and Nihon-Superior through Ames Lab Contract No. DE-AC02-07CH11358

2:25 PM Invited

The Role of Elastic and Plastic Anisotropy on Microstructure Evolution and Strain History during Thermomechanical Cycling of Lead-Free Solder Joints: *Thomas Bieler*¹; Bite Zhou¹; Payam Darbandi¹; Farhang Pourboghrat¹; Guilin Wu²; Stefan Zaaefferer²; Tae-kyu Lee³; Kuo-Chuan Liu³; ¹Michigan State University; ²Max-Planck-Institut für Eisenforschung; ³Cisco Systems, Inc.

Because failures in lead-free solder joints occur in locations other than the most highly shear strained regions, reliability prediction is challenging, requiring physically based understanding of how the microstructure and properties evolve during thermomechanical cycling. Sn-Ag-Cu solder joints can be initially single, tri- or multi-crystals, depending on the composition of the solder and underbump metallurgy and melting history. The evolution of microstructures and properties are characterized using optical and orientation imaging microscopy and in-situ synchrotron x-ray measurements during thermal cycling. With time and thermal history, microstructural evolution unique to each joint occurs, due to the interaction between local boundary conditions and strong anisotropic elastic, plastic, expansion, and diffusional properties of Sn crystals. Initial efforts to simulate well-characterized joint microstructures and strain histories measured with synchrotron measurements with crystal plasticity finite element modeling will be compared to assess the effectiveness of constitutive models. Supported by NSF-GOALI contract with Cisco Systems, Inc.

2:50 PM Invited

140th Annual Meeting & Exhibition

Studies of Impact Fracture Modes on Pb-Free Solder Joint Reliability: T. Kobayashi¹; Andre Lee¹; K. Subramanian¹; ¹Michigan State University

Fracture modes encountered during impact can have important influences on the capabilities of as-reflowed, as well as reliability during service, of electronic solder joints. Such considerations arise due to damages resulting from field influences and their relative orientations of such damage with respect to the direction of impact loading. An analysis based on impact strength and energy indicates potential fracture modes that can improve the solder joints reliability, both for shipping and service scenarios. The fracture initiation plays important roles during early stages of services, while propagation plays important roles during the later stages. The interplay of these features in different alloy systems, as well as modes of impact fracture, affects the overall impact reliability during service. Findings of this study may provide significant insights into the interconnect design strategies for microelectronic applications.

3:15 PM Invited

Damage and Fracture in SnAgCu Solder Alloys: Dennis Chan¹; *Ganesh Subbarayan*¹; ¹Purdue University

Cyclic fatigue damage leading to crack initiation and propagation in solder joints is very challenging to model on account of extensive plasticity and large crack area relative to the size of the joint. We present in this talk a nonempirical approach to modeling damage accumulation and fracture based on two experimentally observed facts: (1) cracks result from irreversible, dissipative process, and (2) fracture has an inherent length-scale, time-scale, and/or spatial hierarchy influenced by the microstructural state. The proposed single-parameter, geometry-independent, failure model, the hierarchal fracture process model, is founded on the theoretical principles of Information Theory and Maximum Entropic dissipation. The model maximally accounts for microstructural uncertainty in relating entropic dissipation to material's loss of load bearing capacity. We present detailed experiments and finite element simulations of fracture initiation and propagation in Wafer-Level CSP (WLCSP) and Quad-Flat Nolead (QFN) packages with significantly different joint geometries to validate the failure model.

3:40 PM Break

3:50 PM Invited

Dynamic Recrystallization in Pb-Free Solder Joints during Fatigue Tests: *Liang Yin*¹; Luke Wentlent²; Linlin Yang²; Babak Arfaei²; Awni Oasaimeh²; Peter Borgesen²; ¹Universal Instruments Corp; ²Binghamton University

The dynamic recrystallization of beta-Sn profoundly affects deformation and failure of Pb-free, SnAgCu solder joints under cyclic stressing. The numerous grain boundaries of recrystallized beta-Sn enable grain boundary sliding. Strain localization is also augmented by the thermal mismatches due to the anisotropy of recrystallized grains. Fatigue cracks initiate at, and propagate along, recrystallized grain boundaries, eventually leading to intergranular fracture. A better understanding of these phenomena could help to develop more accurate constitutive relations for these materials. Thus the dynamic recrystallization behavior of SnAgCu solder joints was examined during thermo-mechanical fatigue and isothermal mechanical fatigue tests. The degree of recrystallization was observed to depend on fatigue loading conditions, alloy composition and the thermal history of joints. The results suggested a relation between recrystallization behavior and the morphology and distribution of secondary precipitates. Discussions are presented on microstructure evolution during the fatigue tests, including dynamic recovery and persistent slip bands.

4:15 PM

Creep of Bi-Containing Pb-Free Solders: *David Witkin*¹; ¹The Aerospace Corporation

SAC-Bi and Sn-Ag-Bi alloys have demonstrated superior performance in thermal cycling reliability tests of printed circuit boards, but due to their Bi content they have not been widely used in electronics manufacturing. Constant-stress creep tests were performed on bulk samples of these alloys at 25, 75, 100 and 125°C, with emphasis on comparison of properties in as-solidified and aged microstructures. The addition of Bi results in shear strain rates that are relatively unaffected by thermal aging, while creep rates of SAC305 and SAC-Sb increase by more than an order of magnitude after aging. At a given temperature, the applied shear stress at which the power law exponent changed was not altered by aging in Bi-containing alloys, while for SAC305 and SAC-Sb after aging the change in exponent was shifted to lower stress. These differences suggest that thermal fatigue reliability of solder joints may be enhanced by addition of Bi.

4:35 PM

Fracture Mechanics of Solder Joint under Mechanical Fatigue: Selection and Transition of Failure Location with Microstructure: *Woong Ho Bang*¹, Emil Zin¹; Huili Xu¹; Choong-Un Kim¹; Hong-Tao Ma²; Tae-Kyu Lee²; Kuo-Chuan Liu²; ¹University of Texas Arlington; ²Cisco Systems, Inc.

Mechanics of solder joint failure under various loading conditions has been investigated in numerous recent studies, yet these studies often show several inconsistencies especially on the location of failure site. While some report the solder/IMC to be predominant fracture site, the others identify IMC or solder matrix to be the crack growth path. Structural similarities in solder joint used in these studies yet varying locations of cracking site suggest that fracture in solder joint is affected greatly by a subtle change in microstructure and geometry of the solder. This paper reports experimental and theoretical findings that the weakest link of fracture in solder joint changes sensitively with local constraints resulted by inhomogeneous distribution of mechanical strength of solder. Specifically, transition in fracture site within an identical lead-free solder joint by a simple change in aging condition will be presented along with mechanistic analysis of fracture on each case.

4:55 PM

Impact of Isothermal Aging on Sn-Ag-Cu Solder Interconnect Board Level Mechanical Shock Performance: *Tae-Kyu Lee*¹; Weidong Xie¹; Kuo-Chuan Liu¹; ¹Cisco Systems, Inc.

The mechanical stability of solder joints with SnAgCu was an issue since the material was applied to the consumer electronic field. Various shock test methods were developed and standardized tests are used in the industry worldwide. Although it is applied for several years, the detailed mechanism of the shock induced failure mechanism is still under investigation. The work reported here concerns the impact of isothermal aging on board level shock performance. A test vehicle is developed to have various strain and shock level conditions. Along with no aged 17x17mm CABGA package samples, isothermal aging were applied to the samples to observe the impact of different microstructures. The result revealed a clear indication of the strain and shock correlation with a trend of isothermal aging induced degradation. A test condition by eliminating the strain and maintaining the shock level revealed interesting aspects which will be presented and discussed.

Phase Stability, Phase Transformations, and Reactive Phase Formation in Electronic Materials X: Solder-Related Reliability Issues

Sponsored by: The Minerals, Metals and Materials Society, TMS Electronic, Magnetic, and Photonic Materials Division, TMS: Alloy Phases Committee

Program Organizers: Chih-Ming Chen, National Chung Hsing University; Hans Flandorfer, University of Vienna; Sinn-Wen Chen, National Tsing Hua University; Jae-ho Lee, Hongik University; Yee-Wen Yen, National Taiwan Univ of Science & Tech; Clemens Schmetterer, TU Bergakademie Freiberg; Ikuo Ohnuma, Tohoku University; Chao-Hong Wang, National Chung Cheng University

| Tuesday PM | Room: 7A |
|---------------|-------------------------------|
| March 1, 2011 | Location: San Diego Conv. Ctr |

Session Chairs: Chih-Ming Chen, National Chung Hsing University; Ikuo Ohnuma, Tohoku University

2:00 PM Introductory Comments

2:05 PM Invited

Whisker Growth Behavior in a High Vacuum with Thermal Cycling: *Keun-Soo Kim*¹; Jung-Lae Jo¹; Ki-Ju Lee¹; Alongheng Baated¹; Katsuaki Suganuma¹; Norio Nemoto²; Tsuyoshi Nakagawa³; Toshiyuki Yamada³; ¹Osaka University; ²Japan Aerospace Exploration Agency; ³Nippon Avionics Co., Ltd.

Aerospace electronics are placed in a very special environment compared to consumer electronics used on the ground. They exposed severe thermal cycling and vacuum conditions. The temperature range between -30 °C and 125 °C, and the vacuum ranges from 10-2 Pa to 10-4 Pa. In this work, the influence of vacuum environment on tin whisker growth was examined by means of a specially designed vacuum thermal cycling chamber. 42 alloy lead-frames with matte tin plating were tested in a high vacuum (10-4 Pa) and in an air conditions with thermal cycling (-40 °C ~ 125 °C). As compared with thermal cycling in the air condition, the substantial influence of environment was found on the whisker growth. Tin whiskers grow thinner and longer in a high vacuum with thermal cycling compared to air. The details mechanism of thermal cycling whisker growth both in air and vacuum will be discussed.

2:30 PM

Investigation of Tin Whisker Growth on Patterned Surface: Chien Hao Su¹; Li-Wei Zoul¹; Hao Chen¹; Albert T. Wu¹; ¹National Central University

The reaction between Sn and Cu forms Cu6Sn5 intermetallic compound (IMC) at room temperature. The IMC provided compressive stress and induced the growth of tin whiskers on Sn coatings over Cu substrate. One of the required conditions to grow whisker is the weak surface oxide. Cracks on the oxide served as weak spots that were essential for the protrusion of whiskers to release the stresses. In this paper, we intentionally induced "weak spots" on the surface by lithography process, which was utilized to define arrayed of dots on Sn substrates. The whiskers could be found only from the patterned area. Since the number and the location of the whiskers could be predicted, the kinetics of the whisker growth could be calculated. The growth model could thus be verified or modified based on the growth rate.

2:45 PM

Oxidation Behaviors and Cosmetic Discolor of Pb-Free Solders: *Chi-Hang Tsai*¹; Yun-Min Cheng²; Jenn-Ming Song²; Shih-Yun Chen¹; ¹National Taiwan University of Science and Technology; ²National Dong Hwa University

Considering that solders may encounter oxidation problems, this study aims to investigate the thermal oxidation properties of Pb-free solders in both the liquid and solid states. With the oxidation of molten solders, a commonly-used die-attach solder, Pb-Sn, and its potential high temperature Pb-free alternatives (Bi-Ag and Zn-Sn) are investigated. The additions of Ag can significantly reduce the oxidation of Bi and thus Bi-11Ag has a



comparable performance with Pb-5Sn. As for the oxidation of solid solders, this study also deals with the oxidation behaviour and surface discolor of a commonly-used level 2 Pb-free solder, Sn-Cu-Ni. The effect of trace alloying additions (Al and P) was examined by using TGA and UV-visible spectroscopy. The results show the addition of P formed P2O5 on the solder surface. SnCuNi0.01P exhibits the greatest light reflection and thus a superior brightness. This may contribute to the effect of P to retard the formation of SnO.

3:00 PM

The Change of Melting Temperature after Soldering at Sn-10wt.%Sb and Bi-2wt.%Sn Alloys: *Minoru Ueshima*¹; ¹Senju Metal Industry

Some solder joints start to melt from less than solidus line of their solders because of the segregation of the solidification and the reaction with the electrode. The melting temperatures and microstructures of Sn-10wt.%Sb and Bi-2wt.%Sn solders jointed at the lead-frame with Ag, Cu and Ni electrodes are researched. Ag and Cu electrodes easily dissolute into Sn-10Sb alloy during the die-bonding and then each solidus line decrease from 245 to 228C and 237C, respectively. In the results, the molded joints are torn after reflow at 240C peak temperature. However, the molded joint with Ni finishing doesn't be torn after reflow because the solidus line keeps 245C after die-bonding. On the other hands, the solidus line increase to more than 250C after die-bonding at Bi-2Sn alloy.

3:15 PM

Electroless-Plated Ni Layer as a Barrier Layer for a Cu Bump/Sn/ Cu Bump Bonding Structure for the Applications of 3D Integration: *Byunghoon Lee*¹; Jongseo Park¹; Hoo-Jeong Lee¹; ¹Sungkyunkwan University

For 3D integration, searching for bonding materials with high mechanical and electrical reliabilities is a key issue. Cu bump /Sn layer/Cu bump is a widely-adopted bonding structure; nevertheless, a strong material interaction between Cu and Sn that occurs during the bonding process is potentially a serious problem for both electrical and mechanical reliabilities. In this study, we employed electroless-plated Ni as a barrier layer to suppress metallurgical interaction between Cu and Sn. We carried out material characterization using SEM and TEM on the samples bonded at different temperatures to examine the effects of inserting a bonding layer. We also examined the mechanical properties using lap-shear testing. Our analysis discloses that the Ni barrier layer effectively suppressed interdiffusion between Cu and Sn up to 250° and that at a higher temperature, however, the Ni layer succumbs to the strong interdiffusion and allowed the rapid progress of intermetallic compound formation.

3:30 PM Break

3:50 PM

Effects of Surface Finish Conditions and Loading Speeds on Shear Strengths of Sn-3.0Ag-0.5Cu BGA Solder Bump: Jae-Myeong Kim¹; Myeong-Hyeok Jeong¹; Sehoon Yoo²; Chang-Woo Lee²; Young-Bae Park¹; ¹Andong National University; ²Korea Institute of Industrial Technology

Fundamental understanding on the BGA Pb-free solder joint reliability under high speed loading condition is still needed. In order to evaluate the mechanical joint reliability of the solder ball joint, the most popular testing method is the ball shear test due to its convenient and simple experiment method. In this study, the effect of surface finish conditions and applied loading speeds on the shear strength of SAC305 BGA solder bump were systematically investigated under varying thermal aging temperature and time. The surface finishes of the electrodes of PCB were ENIG and OSP and the samples were subject to thermal aging at 150° up to 1000 hours with shear speed from 10mm/s to 1,000mm/s. The shear force increased with increasing shear speed while ductility and toughness decreased. Fundamental joint reliability with respect to thermal aging time, surface finish, and loading speed will be discussed in detail.

4:05 PM

Electromigration of SnZn and SnBi Solders: Chih-Ming Chen¹; ¹National Chung Hsing University

With the size shrinkage of the solder joints, electric current that passes through the solder joints increases in its density, and therefore electromigration becomes an unavoidable reliability issue. The SnZn and SnBi alloys are promising Pb-free solders and have been used in microelectronic packaging. Electromigration of these two Pb-free solders were investigated with current stressing at the density range of 1000~10000 A/cm^2. Effects of minor addition of third element into the solders upon their electromigration behavior were also studied.

4:20 PM

Study of EM-Induced Ni(P) Consumption of ENIG and ENEPIG Bond-Pads: C. T. Lu¹; *Cheng Yi Liu*¹; ¹National Central University

Electromigration tests on (1) Ni(P) bond-pad (ENIG) and (2) on Ni(P)/ Pd bond-pad (ENEPIG) joined with Sn solder bumps were performed with a high current density of 10^4 A/cm². We found that a serious EM-induced Ni(P) consumption and an unusual electromigration-enhanced diffusion of the interfacial Ni₃Sn₄ compound layer are observed in the Ni(P) bond-pads (ENIG) sample. Intriguingly, by introducing an additional electroless Pd layer on the Ni(P) layer, i.e., (ENEPIG), the EM-induced Ni(P) consumption was greatly reduced. In addition, the interfacial compound layer is analyzed to be the NiSn₄ phase dissolved with very limited Pd atoms. Since, no equilibrium NiSn₄ phase exists in the binary Ni-Sn phase diagram, so, we tend to believe that the formation of the (Ni,Pd)Sn₄ phase should be induced by the current stressing or the presence of dissolved Pd.

4:35 PM

Interfacial Reactions between High-Pb Solders and Ag Metallization: *Chi-pu Lin*¹; Chih-ming Chen¹; Yee-wen Yen²; ¹National Chung Hsing University; ²National Taiwan University of Science and Technology

Although the ban of Pb-containing solders in microelectronics is a global trend, high-Pb solders with weight compositions of 95Pb5Sn and 97Pb3Sn are still used in some specific applications like high-end microprocessors. Therefore, the understanding of interfacial reactions between high-Pb solders and different metallizations is important when evaluating the reliability of the high-Pb solder joints. Immersion Ag is a promising candidate of the Pb-free surface finish. In this presentation, the interfacial reactions between high-Pb solders and Ag metallization will be discussed. During the reflow, the intermetallic compound formation transforms from Ag3Sn to Ag4Sn when the composition of Sn in solder decreases. With increasing the reflow time, part of the immersion Ag layer dissolves and Pb penetrates into the gap between the Ag layer and underlying Cu substrate.

4:50 PM

Influence of Pd Concentration on the Interfacial Reaction and Mechanical Reliability of the Ni/Sn-xPd System: *Sheng-Wei Lin*¹; Yen-Chen Lin¹; Ling-Huang Hsu¹; Cheng-En Ho¹; ¹Yuan Ze University

The Pd concentration effect on the interfacial reaction of the Ni/Sn-xPd (x = 0 - 1 wt.%) system and the mechanical reliability were investigated in this study. We found that a slight variation in the Pd concentration produced a completely different reaction product(s) in spite of only a 0.1 wt.% difference. When the Pd concentration was high (more than 0.2 wt.%), a Pd-Ni-Sn layer over Ni₃Sn₄ was created. The Pd-Ni-Sn was identified to be the PdSn₄-based structure through electron backscattered diffraction (EBSD) analysis. In contrast, the Ni₃Sn₄ replaced the (Pd,Ni)Sn₄ when the Pd concentration was below 0.05 wt.%. A Pd-Ni-Sn isotherm simulated by the CALPHAD method was utilized to rationalize the above transition. Additionally, the mechanical reliability in response of the interfacial microstructure was evaluated through a high speed ball shear test. The correlation of the interfacial strength with various Pd concentrations will be established in this study.

Physical and Mechanical Metallurgy of Shape Memory Alloys for Actuator Applications: Fundamental and Engineering Modeling of Shape Memory Alloys

Sponsored by: The Minerals, Metals and Materials Society Program Organizers: S. Raj, NASA Glenn Research Center; Raj Vaidyanathan, University of Central Florida; Ibrahim Karaman, Texas A&M University; Ronald Noebe, NASA Glenn Research Center; Frederick Calkins, The Boeing Company; Shuichi Miyazaki, Institute of Materials Science, University of Tsukuba

| Tuesday PM | Room: 11B |
|---------------|-------------------------------|
| March 1, 2011 | Location: San Diego Conv. Ctr |

Session Chairs: Dimitris Lagoudas, Texas A&M University; Richard James, University of Minnesota

2:00 PM Invited

Structural Anisotropy, Orientational Flexibility and Superelasticity of a Premartensitic State: Armen Khachaturyan¹; Wei-Feng Rao¹; ¹Rutgers University

A theory and 3D modeling of a giant superelasticity in a pre-martensitic state which is a coherent system of low-symmetry nano-precipitates is developed. We took into consideration two new concepts inherent to displacively transforming phase, the structural anisotropy and orientational flexibility. Both automatically follow from a generalization of the existing theory of coherent systems by considering the transformation strain as a relaxing thermodynamic parameter. The structural anisotropy is a notion that is similar to magnetic anisotropy of ferromagnetics. It determines the crystal lattice symmetry and orientation relations of the phases. The systems with low structural anisotropy have extremely high orientation flexibility and display giant and mostly non-hysteretic strain responses. Vanishing structural anisotropy results in a new glass-like state with random orientation relations and unlimited orientational flexibility. Using 3D and 2D modeling, we formulated conditions leading to a drastic amplification of non-hysteretic strain responses that may reach orders of magnitude.

2:20 PM Invited

Basic Properties of Shape Memory Materials from First-Principles Calculations: *Peter Entel*¹; Mario Siewert¹; Antje Dannenberg¹; Markus Gruner¹; ¹University of Duisburg-Essen

The mutual influence of phase transformations, magnetism and electronic properties of magnetic shape memory materials is a basic issue of electronic structure calculations based on density functional theory (DFT). In this contribution we show that the DFT calculations can be pursued to finite temperatures which allows to derive on a first-principles basis the temperature versus composition phase diagram of the pseudo-binary Ni-Mn-(Ga, In, Sn, Sb) system. The DFT calculations allow also to make predictions of magnetostructural and magnetic field induced properties of other (new) magnetic Heusler alloys not based on manganese such as Co-Ni-(Ga-Zn) and Fe-Co-Ni-(Ga-Zn) intermetallic compounds. We will give a systematic description in how far the magnetic shape memory effect associated with magnetic anisotropy and twin mobility in tetragonal martensite depends on composition, atomic disorder and competing ferro- and antiferromagnetic interactions between the magnetic transition metal elements.

2:40 PM Invited

Modeling Martensitic Phase Transformations Using the Self-Consistent Lattice Dynamics Approach: *Ryan Elliott*¹; Venkata Guthikonda¹; ¹University of Minnesota

Few accurate models exist for martensitic phase transformations (MPTs) based on atomic composition and crystal structure. This work develops a model using a first-order self-consistent lattice dynamics approach. A renormalization of the frequencies of atomic vibration (phonons) via a set of self-consistent equations allows the model to accurately capture how atomic

vibrations affect the thermomechanical properties of the material. The model is applied to a one-dimensional bi-atomic chain. The Morse pair potential and its parameters are chosen to demonstrate the model's capabilities. The model is evaluated by generating bifurcation diagrams corresponding to thermal and mechanical loading. A first-order MPT is predicted between an entropically stabilized high symmetry phase to a low symmetry phase. It is found that the MPT can be both temperature- and stress-induced. This qualitative prediction of an MPT indicates the likelihood that the current modeling technique can be used for the computational discovery of new SMAs.

3:00 PM

A Generalized Ginzburg-Landau Model for Martensitic Transformations in Shape Memory Alloys: *Rajeev Ahluwalia*¹; Srikanth Vedantam²; Turab Lookman³; Avadh Saxena³; ¹Institute of High Performance Computing; ²Indian Institute of Technology; ³Los Alamos National Lab

The Ginzburg-Landau theory has been demonstrated to be an effective approach to describe phase transformations in shape memory materials. Recently, such models have also been used to simulate microstructure and mechanical properties. In this approach, the free energy is phenomenologically expressed as a symmetry allowed expansion in the strain components. The approach has been extensively used to study cubic to tetragonal transformations. Clearly, there is a need to extend the approach to transformations from cubic to lower symmetry phases such as orthorhombic, trigonal and monoclinic. We have developed a generalized free energy functional that can, in different parameter ranges, describe these transformations. We present simulations of microstructural evolution and mechanical response.

3:15 PM

Chemical Trends for Phase Transitions in Magnetic Shape Memory Alloys Derived from First Principles: *Tilmann Hickel*¹; Ali Al-Zubi¹; Joerg Neugebauer¹; ¹Max-Planck-Institut fuer Eisenforschung GmbH

The Heusler alloy Ni₂MnGa is a prototype system for a magnetic shape memory alloy, but its martensitic transition temperature is too low for practical applications. In order to systematically improve the performance of this class of materials, an accurate prediction of the critical temperature as function of the chemical composition is crucial. We have, therefore, developed an ab initio scheme based on density functional theory (DFT) to derive the free energies for the austenitic, the martensitic and (modulated) pre-martensitic phases of magnetic Heusler alloys. All relevant temperature effects such as quasiharmonic phonons, electronic excitations, fixed-spin magnons and chemical disorder are computed within DFT. Using this approach we successfully described the phase transition in Ni₂MnGa. We extended the concept to non-stoichiometric alloys with Ni or Mn excess, determined the resulting increase of the transition temperatures and revealed that a delicate interplay of vibrational and magnetic excitations is responsible for the observed trends.

3:30 PM Break

3:40 PM Invited

Mechanics of Shape-Memory Alloys: *Kaushik Bhattacharya*¹; ¹California Institute of Technology

This talk will describe recent advances in understanding and modeling the mechanics of shape-memory alloys. It will focus specifically on (a) multiscale modeling that seeks to understand the interplay between microstructure, polycrystalline texture and macroscopic properties and (b) a constitutive relation that implicitly accounts for the microstructure and polycrystalline texture. Illustrative examples and comparison with experiments will be provided.

4:00 PM Invited

Multivariant Modeling and Experiments of Shape Memory Alloys: *L. Catherine Brinson*¹; Aaron Stebner¹; ¹Northwestern University

As the number of shape memory alloys (SMAs) and applications continues to increase and the significance of texture evolution in shape memory behaviors becomes more evident, the need for models that simulate



the relationships between microstructural and macroscopic responses becomes more apparent. The Simplified Multivariant Model is the most recent among several generations of multivariant, micromechanical models that have been formulated and numerically implemented to address this need in both single crystal and polycrystalline SMA systems. Most recently, additional methodologies have been developed to couple these simulations with neutron diffraction data as a way to concurrently validate micro and macro scale predictions of the model, and also gain further insight into the diffraction data, such as inter-granular configurations of habit plane and correspondence variants. The model and methodologies are presented and illustrated through isothermal reorientation of NiTi martensite variants, as well as thermo-mechanical cycling.

4:20 PM

Multivariant and Rate-Dependent Calculation of Martensitic Phase Transformation: Seung Yong Yang¹; Tae-Hyun Nam²; ¹Korea University of Technology and Education; ²Gyeongsang National University

In continuum crystalline description of martensitic phase transformation, the analogy with crystal plasticity can be used. But, unlike crystal plasticity, the sum of the volume fractions of all phases should remain one. To impose this constraint in a multivariant description of martensitic transformation, a kinetic relation is used based on an Arrhenius equation. The kinetic law is capable of calculating rate-dependent behavior. We hypothesized that temperature induced self-accommodating variants form a separate phase in addition to the individual stress-induced variants. Low misfit strain energy or activation energy barrier was taken into consideration by allowing different kinetic constants for the self-accommodation group. The constitutive equations were implemented in the finite element code ABAQUS user material subroutine. Strain vs. temperature curve of NiTi shape memory alloy was calculated.

4:35 PM

Simulating Load Biased Thermal Cycling of Polycrystalline NiTi: Sivom Manchiraju¹; Darrell Gaydosh²; Ronald Noebe²; Shipeng Qiu³; Raj Vaidyanathan³; *Peter Anderson*¹; ¹The Ohio State University; ²N. A. S. A. Glenn Research Center; ³University of Central Florida,

A joint research program involving NASA, Ohio State University, University of Central Florida, and Northwestern University aims to couple experimental and computational materials science techniques across a range of length scales, to study and quantify shape memory actuator performance. An outcome is a finite element approach to simulate the thermomechanical response of polycrystalline NiTi, by coupling a crystallographic description of the B2-to-B19' transformation with crystal-based plasticity. It is informed by recent density functional theory calculations for the martensite (B19') elastic moduli, as well as experimental characterization of the texture, pseudoelastic behavior, and stress-biased thermal cycling response of solutionized polycrystalline NiTi (55wt% Ni). Key model outcomes are the ability to capture the (1) initial increase and subsequent decrease in actuator strain with increasing bias stress, and (2) evolution of martensite texture with stress-biased thermal cycling. Some significant challenges remain, including under prediction of strain ratcheting and the effect of upper cycle temperature.

4:50 PM

Modeling the Shape Memory Effect: Comparison and Validation of Two Constitutive Models: Marco Fabrizio Urbano¹; ¹SAES Getters

In order to properly exploit the functional properties of Shape Memory Alloys, a good design is necessary. Especially if complex geometries (and consequently stress-strain states) are involved, modeling could be an extremely effective tool for engineers. Although many constitutive models describing the thermomechanical behavior of Shape Memory Alloys have been developed in the last two decades, a thorough validation of their performances is still missing. In this presentation some recent works aiming at filling this gap are presented: two constitutive models are described and compared. Results predicted by the models are compared to experiments. In particular, temperature cycles at constant tension load and three point bending at constant load. Some simulations of their implementation in Ansys and Abaqus will be shown.

5:05 PM End of Session

Polycrystal Modelling with Experimental Integration: A Symposium Honoring Carlos Tome: Orientation Imaging Techniques and Related Models

Sponsored by: The Minerals, Metals and Materials Society, TMS Structural Materials Division, TMS Materials Processing and Manufacturing Division, ASM-MSCTS: Texture and Anisotropy Committee, TMS/ASM: Mechanical Behavior of Materials Committee, TMS/ASM: Computational Materials Science and Engineering Committee

Program Organizers: Ricardo Lebensohn, Los Alamos National Laboratory; Sean Agnew, University of Virginia; Mark Daymond, Queens's University

| Tuesday PM | Room: 6C |
|---------------|-------------------------------|
| March 1, 2011 | Location: San Diego Conv. Ctr |

Session Chairs: Brent Adams, Brigham Young University; Robert Wagoner, Ohio State University; David Field, Washington State University

2:00 PM Invited

A High Resolution EBSD Study of Deformation near Twins in Ti: Benjamin Britton¹; Angus Wilkinson¹; ¹University of Oxford

Twinning makes an important contribution to the deformation of many hexagonal close packed metals including Ti and its alloys. Pure Ti is particularly prone to twinning. Cross-correlation based analysis of EBSD patterns allows intra-granular lattice rotations and elastic strain variations at the 10^{-4} (rads) level to be mapped. Additionally the lattice curvature can be used to asses the density and nature of geometrically necessary dislocations present. We have investigated various compression twins in large grained grade 1 CP Ti using the hi-res EBSD method and AFM. We will be present maps of elastic strain variations, lattice rotations and GND distributions around such twins and correlate results with AFM maps of surface topography. Examples showing the interactions of twin tips with grain boundaries and at twin-twin intersections will be given.

2:25 PM Invited

High-Resolution EBSD Characterization and Analysis of Defect Structure of In-Situ Deformations of Steel: *Brent Adams*¹; Samikshya Subedi¹; Sadegh Ahmadi¹; David Fullwood¹; Robert Wagoner²; ¹Brigham Young University; ²The Ohio State University

This paper describes recent developments in high-resolution electron backscatter diffraction (HR-EBSD) characterizations and analysis of the development of defect structure during in-situ deformations of columnar steel. Cross correlations of EBSD patterns with strain-free reference patterns is used to recover the spatial fields of the elastic displacement gradient tensor. Corrections for varying pattern center (PC) are essential to minimize non-physical contributions. Application of new geometrical corrections to the cross correlations, based upon motions of the PC, are described. Insitu deformation experiments on steels in the elastic and plastic regimes are described. Comparisons of the measured elastic fields with Green's function based solutions to the equilibrium equation are shown. Novel methods for recovery of the full Nye tensor of geometrically necessary dislocations are described.

2:50 PM

Meso-Scale Treatment of Dislocation-Grain Boundary Interactions 2: Single Crystal Constitutive Model without Tacit Grain Boundary Effects: *Hojun Lim*¹; Robert Wagoner¹; Myoung-Gyu Lee²; Brent Adams³; John Hirth⁴; ¹The Ohio State University; ²Pohang University of Science and Technology; ³Brigham Young University; ⁴-

Single crystal constitutive equations based on dislocation density (SCCE-D) were developed from Orowan's strengthening equation and simple geometric relationships of the operating slip systems. The multiplication of dislocations on each slip system incorporated standard 3-parameter dislocation density evolution equations applied to each slip system independently. In contrast, the most widely used single crystal constitutive equations for texture analysis (SCCE-T) feature 4 or more adjustable parameters that are usually back-fit from a polycrystal flow curve. Tensile tests of single crystals oriented for single slip were simulated using CPFEM. Best-fit parameters were determined using either multiple or single slip stress-strain curves for copper and iron from the literature. Tensile tests of single crystals oriented to favor the remaining combinations of slip systems were then simulated. The SCCE-D method provides an improved representation of single-crystal plastic response with fewer adjustable parameters, better accuracy, and better predictivity than the SCCE-T.

3:10 PM Invited

Meso-Scale Treatment of Dislocation-Grain Boundary Interactions 3: Prediction of Dislocation Densities, Lattice Curvatures, and the Hall-Petch Effect: *Robert Wagoner*¹; Hojun Lim¹; Ji Hoon Kim²; Myoung-Gyu Lee³; Brent Adams⁴; ¹The Ohio State University; ²Korea Institute of Materials Science; ³Pohang University of Science and Technology; ⁴Brigham Young University

A practical two-scale method has been developed and implemented to predict quantitatively the Hall-Petch effect and local microstructural details such as dislocation densities and lattice curvatures. The first scale is a FE model of a polycrystal using novel single-crystal constitutive equations based on dislocation density and incorporating a back stress. The second scale redistributes mobile dislocation density consistent with the plastic strain distribution, and enforces slip transmission criteria at grain boundaries that depend on local grain and boundary properties. The following advances were demonstrated: 1) Quantitative prediction of the Hall-Petch slopes without imposing unrealistic or unobserved dislocation configurations. 2) Quantitative prediction of dislocation densities consistent with graindislocation and dislocation-dislocation interactions. 3) Computationally tractable meso-scale treatment of large numbers of dislocations, their interactions, and the relationship between their redistribution and strain.4) A simple quantitative model and method to treat grain boundaries as impediments to slip depending on local configurations.

3:35 PM Break

3:50 PM Invited

Measuring Misorientations and Grain Sizes in Severely Deformed Metals through Orientation Mapping on a Transmission Electron Microscope: Edgar Rauch¹; Muriel Veron¹; ¹SIMAP Laboratory

Severe plastic deformations are known to modify drastically the structural state of metals. However, measuring grain size or dislocation densities after large strains is not a straightforward task. Consequently, the hardening related to grain refinement is usually discussed with rather imprecise data and poor descriptions of the structural state. The present work proposes an experimental approach that gives a better insight in the structural evolution for severely deformed materials. Misorientations are measured with a dedicated TEM tool (ACOM/TEM) that will be described with some details. With this attachment, grain sizes are estimated despite the fact that they are ill-defined at very large strains. Moreover, it is demonstrated that the large dislocation densities may be reasonably approximated from the misorientations. The results are used to discuss the validity of both the Hall-Petch and Taylor/ Friedel law and to propose an alternative formulation of the flow law.

4:15 PM Invited

Quantification of Dislocation Structure Heterogeneity in Deformed Polycrystals: David Field¹; ¹Washington State University

Plastic deformation in polycrystalline materials involves a complex interaction of dislocations with defects in the lattice. A dislocation density based crystal plasticity finite element model was developed for both FCC and BCC materials. Based upon the kinematics of crystal deformation and dislocation interaction laws, and adopting information from discrete dislocation dynamics calculations, dislocation generation and annihilation are modeled. Dislocation densities evolve and are tracked as state variables in the model, leading to spatially inhomogeneous dislocation densities. These are compared against measurements obtained using electron backscatter diffraction wherein the excess component of dislocation density can be obtained. A study of the effects of different minimization schemes shows that measured densities for specific slip systems varies considerably depending upon which minimization scheme is used, but the overall densities are reasonably consistent. The experimental technique is shown on various structures and compared against modeled structures.

4:40 PM

Determining Correlations between Crystallography and Mechanical Response in a 3D Polycrystalline Material: *Alexis Lewis*¹; Siddiq Qidwai²; Andrew Geltmacher¹; ¹Naval Research Laboratory; ²SAIC

Three-dimensional reconstructions of a polycrystalline BCC microstructure were derived from serial sectioning experiments combined with electron backscatter diffraction measurements of crystallography. These reconstructed datasets were used as input for image-based finite element simulations of mechanical response at low strains. Using experimentally-measured 3D microstructure and crystallography data allowed for the direct observation of correlations between crystallography and mechanical response, most notably the relationship between the axis of applied load and the crystallographic orientation of each grain under that load. Due to the large size of the 3D dataset, representative volume elements, extracted from the microstructure based on 2-point correlations of crystallographic texture, were used in the FE simulations.

5:00 PM

Three-Dimensional Interface Curvature as a Function Crystallographic Grain Boundary Character: *David Rowenhorst*¹; Alexis Lewis¹; ¹Naval Research Lab

Grain coarsening describes the curvature driven process wherein polycrystalline systems decrease their surface energy by increasing the average grain size. In isotropic systems, the interfaces between domains are assumed to always be spherical sections where the two principle curvatures are equivalent. The results of optical serial sectioning of approximately 2100 grains in Ti-21S (a beta stabilized titanium alloy), combined with EBSD scans are used to determine the grain boundary character as a function of the five macroscopic degrees of freedom of the grain boundary as well as the local curvature of the interface. We will show that not only are there preferences for particular types of boundaries, but also that the assumption of equivalent curvatures is not valid in anisotropic systems, especially near high symmetry boundaries.

5:20 PM

On the Role of Grain Size Distribution on the Heterogeneity of Plastic Deformation: *Francis Wagner*¹; Nathalie Allain-Bonasso¹; Stephane Berbenni¹; David Field²; ¹Universite de Metz; ²Washington State University

Plastic deformation in polycrystals is well known to be a heterogeneous process due to crystallographic texture, but the role of the grain size distribution is generally neglected. Nevertheless some calculations including grain size effects have shown that it is also an important source of heterogeneity. In this paper the role of grain sizes is considered from an experimental point of view. An IF steel has been submitted to a tensile test for several deformation degrees. The grain size distribution as well as the orientation distribution have been determined from EBSD measurements before and after plastic deformation. Several quantities such as the GOS (Grain Orientation Spread), the GAM (Grain Average Misorientation) and the GND (Geometrically

5:40 PM

Microstructure Effects on Local Plasticity: Closing the Loop between Experiment and Simulation: *Michael Groeber*¹; Paul Shade²; Michael Uchic¹; ¹AFRL; ²UTC/AFRL

There is a demand for both accurate virtual representations of material microstructure and microscale experimental results to validate simulations of structures. In this work, we have attempted to close this loop by testing and investigating the same sample. A microsized tensile sample was prepared in a Dual Beam FIB microscope and tested in-situ while strain mapping the surface. The surfaces of the sample were investigated with Electron Backscatter Diffraction (EBSD) prior to, as well as after the test. Following the test, the sample was sectioned and mapped with EBSD to collect the true 3D microstructure of the entire microsample. The sample was tested to only a few percent strain in order to limit the change in microstructure. Thus, the collected microstructure can reasonably serve as the input structure to a Crystal Plasticity Finite Element Model (CPFEM). This presentation will focus on the analysis of local deformation to compare with simulations.

6:00 PM

3D EBSD Characterization of Deformed Polycrystalline Micro-Scale Tensile Samples: *Paul Shade*¹; Michael Groeber²; Michael Uchic²; Robert Wheeler³; Dennis Dimiduk²; ¹UTC / AFRL; ²Air Force Research Laboratory; ³UES / AFRL

This presentation describes the application of a dual beam focused ion beam-scanning electron microscope (DB FIB-SEM) outfitted with an electron backscatter diffraction (EBSD) system to characterize the internal microstructure and local lattice rotations within micro-scale test samples that have been deformed via in-situ SEM tensile testing. The objectives of this study are to develop an experimental methodology that can provide a high-fidelity 3D characterization of the internal grain structure of mechanical test samples that contain a limited number of grains (< 1000 grains); obtain knowledge of the external boundary conditions and measurement of the resultant stress-strain behavior of the same test samples; and, perform a 3D characterization of the internal lattice rotations that develop after a modest amount of plastic deformation. Such information is needed to assess and guide the further development of modeling and simulation methods that predict the local plastic deformation response of polycrystalline ensembles.

Processing and Properties of Powder-Based Materials: Powder Fabrication and Processing Sponsored by: The Minerals, Metals and Materials Society, TMS

Materials Processing and Manufacturing Division, TMS: Powder Materials Committee

Program Organizers: K. Morsi, San Diego State University; Ahmed El-Desouky, San Diego State University

| Tuesday PM | Room: 33A |
|---------------|-------------------------------|
| March 1, 2011 | Location: San Diego Conv. Ctr |

Session Chair: Iver Anderson, Iowa State University

2:00 PM Introductory Comments

2:05 PM

Characterization of Copper Open Cellular Structures Fabricated by Electron Beam Melting: *Diana Ramirez*¹; L Murr¹; S Li²; E Martinez¹; D Hernandez¹; J Martinez¹; F Medina³; P Frigola⁴, R Wicker³; ¹University of Texas at El Paso; ²Institute of Metal Research, Chinese Academy of Sciences; ³W.M. Keck Center for 3D Innovation; ⁴Radiabeam Technologies

Copper open cellular foams and meshes were fabricated by additive manufacturing (AM) using electron beam melting (EBM). Foam models developed from CT-scans of aluminum foams and mesh elements were

embedded in CAD models for EBM. These structures are the first directly fabricated Cu foams and meshes with low density and high porosity (densities ranging from 0.8 to 1.7 g/cm3). Corresponding stiffness or Young's modulus values measured using a resonant frequency-damping analysis technique ranged from ~1.2 to 3.7 GPa, respectively. Plotting relative stiffness (E/ Eo) versus relative density (d/do) produced a slope of ~1.6) in contrast to ~2 for aluminum and aluminum alloys using the Gibson-Ashby model for open cellular materials ((E/Eo) = (d/do)n where Eo and do are solid Cu modulus and density, respectively. Corresponding ligament hardness (H) averaged 1.6 GPa (using a Vickers indenter), corresponding to an approximate yield strength (Y) of 0.5 GPa based on assumption that Y ~ H/3.

2:25 PM

140th Annual Meeting & Exhibition

Comparative Study of Production of Boron Carbide Powder by: Resistance Furnace and Arc Furnace: *Habibollah Amini Rastabi*¹; Ayoub Karimi Dehcheshmeh¹; ¹Islamic Azad University

Boron carbide is the third hardest known material next to diamond and boron nitride. Reasonable cost of production, low density, and high chemical inertness makes boron carbide an attractive material for microelectronic, military, space and medical applications. At present work, B4C, free of impurities, was produced using reduction reaction of boron oxide by carbothermal process. Boron loss during the process, in the form of B2O2 gas; a common problem in B4C production, was minimized by adjusting the stoicheometry of feeding materials. Likewise, carbon residue was eliminated by taking appropriate composition at the starting point. The result of number of experiments showed that production of boron carbide is highly dependent on the phase change of reactant boron oxide from solid to liquid and from liquid to gaseous boron hypo-oxides. Also, the results show that the production of pure boron carbide by resistance furnace is more suitable than that by arc furnace.

2:45 PM

Prediction and Control of Nucleation Kinetics of Mono-Sized Spherical Copper Droplets: *Mehmet Islier*¹; Teiichi Ando¹; ¹Northeastern University

Production of copper balls with quality suitable for electronics packaging applications by droplet solidification depends on an ability to control the kinetics of droplet nucleation during droplet cooling. Controlling the inflight nucleation kinetics requires information on how droplets cool during their flight and a method to predict their nucleation temperatures given their cooling schedules. A recently developed droplet cooling and nucleation simulation model was used to determine and predict the in-flight nucleation kinetics of mono-size copper droplets produced by the uniform-droplet spray (UDS) process, a capillary jet breakup process, that produces mono-size metal droplets. Initial inputs needed to evaluate the values of materials specific constants in the model were obtained experimentally from the deformation morphologies of UDS droplets quenched on substrates at various heights. Continuous-cooling transformation (CCT) curves were computed for the heterogeneous nucleation on both internal and surface catalysts. Predicted CCT curves were verified by additional droplet quenching experiments.

3:05 PM

Characterization and Properties of Titanium Alloy Powder Produced by Close-Coupled Gas Atomization and of Resulting Consolidated Samples: *Andrew Heidloff*¹; Joel Rieken¹; Iver Anderson²; David Byrd²; ¹Iowa State University; ²Ames Laboratory

The capabilities of a new induction skull melting close-coupled gas atomizer utilizing a novel ceramic composite melt pouring tube has proven to be capable of producing fine, spherical Ti alloy powder with minimal impurities. Resulting powder from the atomization process was characterized using X-ray, SEM, TEM, as well as ICP-AES and LECO inert gas fusion for chemical analysis. Sieved powders were consolidated using hot isostatic pressing and post-consolidation analysis of the samples was conducted to determine the mechanical properties and to characterize the microstructure. Mechanical tests included room temperature tensile and low cycle fatigue. Work supported by Iowa State University Research Foundation, the Grow Iowa Values Fund, and Quad Cities Manufacturing Laboratory and performed at Ames Lab under contract no. DE-AC02-07CH11358.

3:25 PM

Microstructural Investigation of D2 Tool Steel during Rapid Solidification Using Impulse Atomization: Pooya Delshad Khatibi¹; Arash Ilbagi¹; Hani Henein¹; ¹University of Alberta

D2 tool steels are widely used in industry because of their good wear and abrasion properties. It is believed that excellent mechanical properties can be achieved from reduced microsegregation and good distributed carbides during the solidification process. Rapid solidification yields significant enhancement in properties through reduced microsegregation and formation of metastable phases. An understanding of the evolution of microsegregation and carbide formation during rapid solidification is necessary to control the microstructure and hence the properties of these alloys. Impulse Atomization has been used to produce D2 powders. Microstructural investigation on D2 powders shows that because of rapid solidification during Impulse Atomization, there is no carbide inside the microstructure and all the alloying elements are supersaturated inside the austenite phase. XRD results shows both small and large powders mainly contain retained austenite and small amount of ferrite phases. Further phase and microstructural investigation is going on the D2 Impulse Atomized powders.

3:45 PM Break

3:55 PM

Mechanism of Thermal Decomposition of Zinc Hydroxide Carbonate and Preparation of Complexional Ultra-Fine Zinc Oxide: Z. F. Tong¹; L. X. Lian¹; Y. L. Li¹; ¹Jiangxi University of Science and Technology

The thermal decomposition process of zinc hydroxide carbonate (Zn3CO3(OH)4•H2O) absorbed NH4+ is studied by TG,DTA,DTG. The results show mechanism model of thermal decomposition process accords with one-dimension diffusion model. The zinc hydroxide carbonate (Zn3CO3(OH)4•H2O) decomposes into complexional ultra-fine zinc oxide under the conditions of calcination temperature 350°C and 1.5h. The structure and appearance of complexional ultra-fine zinc oxide are studied by XRD and SEM, The results show the zinc oxide is particle size about 200nm and complexional and flake and hexagonal zinc oxide.Key words: zinc hydroxide carbonate; complexional ultra-fine zinc oxide; mechanism of thermal decomposition

4:15 PM

Synthesis of Silver Plating Nano-Copper Bimetallic Powders: *Wei Liu*¹; Qionghua Zhou¹; ¹Henan University of Science and Technology

The silver plating nona-copper bimetallic powders were synthesized by substitution reaction method and chemical deposition method with AgNO3 as main salt. Transmission electron microscopy (TEM) and Energy Dispersive Spectrometer (EDS) were used to characterize the as-prepared bimetallic powders. Three kinds of preparation processes (direct substitution reaction with AgNO3, substitution reaction method with [Ag(NH3)]2+ and chemical deposition method) were compared with each other. The experimental results indicate that the silver plating nano-copper bimetallic powders can be synthesized by direct substitution reaction method with relatively simple procedure. The silver content on the surface of the bimetallic powders prepared by direct substitution reaction can reach 74.78 at%. The silver content on the powders prepared with [Ag(NH3)]2+ after depositing once and twice are 35.46 at% and 70.16 at%, respectively. The bimetallic powders synthesized by chemical deposition method show a mixture structure with nano-copper and nano-silver powders rather than silver plating nano-copper structure.

4:35 PM

Effect of Pore Size on High Temperature Oxidation Behavior of Ni-Fe-Cr-Al Porous Metal: *Kee-Ahn Lee*¹; Sung-Hwan Choi¹; Song-Yi Kim¹; Jung-Yeul Yun²; Hye-Moon Lee²; Byung-Kee Kim³; ¹Andong National University; ²Korea Instituteof Machinery and Materials; ³University of Ulsan

This study investigated the effects of the pore size of Ni-22.4%Fe-22%Cr-6%Al porous metal on its high-temperature oxidation behaviors. Two types of open porous metals with pore sizes of 800 μ m and 580 μ m were used. The results of the high-temperature oxidation test showed that porous metals

compared to bulk metal exhibited far lower levels of oxidation resistance, and that the decreasing pore size led to the weakening of oxidation resistance resistance characteristics. The relationship between log Kp (oxidation rate constant) and 1/T as identified during the oxidation test was found to be linear. Activation energy values were calculated to be 198 KJ/mol and 220 KJ/mol in the 580 μ m and 800 μ m samples, respectively. This indicates its effect of compromising the overall oxidation characteristics of the porous metal. In addition, Ni-Fe-Cr-Al porous metal's high-temperature oxidation microscopic mechanism was discussed. [supported by the Fundamental R&D program for Core technology, Korea]

4:55 PM

WC Alloys Technology: Alex li1; 1Glorytek Industry(Beijing)Co., Ltd

The technology of Glorytek industry Co.,Ltd (www.alloys-welding.com)is based on a chemical process for the synthesis of WC and WC/Co powders, in which the individual W, C, and/or Co precursors are intimately mixed at the molecular level, yielding a uniquely homogeneous product with exceptional high performance. Glorytek industry has developed exceptionally hard bulk consolidated composite materials, with hardness measured up to 2300 VHN. These sintered materials exhibit unparalleled fracture toughness at this level of hardness. These materials are compression sintered in inert gas or vacuum furnaces to form highly homogeneous monoliths. The hardness of the sintered products is found to be a function of cobalt content. Typically, cutting tool applications force the minimum Co content level to be above 6%, below which the material cannot be sintered.

Properties, Processing, and Performance of Steels and Ni-Based Alloys for Advanced Steam Conditions: Alloy Design, Selection, Qualification, and Processing

Sponsored by: The Minerals, Metals and Materials Society, TMS Structural Materials Division, TMS/ASM: Corrosion and Environmental Effects Committee, TMS: High Temperature Alloys Committee

Program Organizers: Peter Tortorelli, Oak Ridge National Laboratory; Bruce Pint, Oak Ridge National Laboratory; Paul Jablonski, National Energy Technology Laboratory; Xingbo Liu, West Virginia University

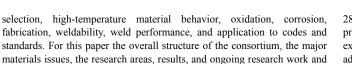
| Tuesday PM | Room: 33B |
|---------------|-------------------------------|
| March 1, 2011 | Location: San Diego Conv. Ctr |

Session Chair: Bruce Pint, Oak Ridge National Laboratory

2:00 PM Invited

U. S. Program on Advancing the Materials Technology for Advanced Ultrasupercritical Steam Boilers and Turbines: *John Shingledecker*¹; R. Viswanathan¹; R. Purgert²; P. Rawls³; ¹Electric Power Research Institute; ²Energy Industries of Ohio; ³National Energy Technology Laboratory

One method for achieving reduced emissions (including CO2) in pulverized coal-fired (PC) power plants is to increase plant efficiency by increasing steam temperatures and pressures. The current materials of construction (steels) for ultrasupercritical (USC) PC power plants limit maximum steam temperature to ~620°C (1150°F). To increase temperatures further and reduce emissions by an estimated 20% compared to a standard PC boiler, nickel-based alloys will be required. A consortium of U.S. steam boiler and turbine manufacturers, the Electric Power Research Institute (EPRI), Energy Industries of Ohio (EIO), Oak Ridge National Laboratory (ORNL) and the National Energy Technology Laboratory (NETL) supported by the U.S. Department of Energy Office of Fossil Energy and the Ohio Coal Development Office (OCDO) has been conducting a research program to develop the materials technology necessary to construct and operate an Advanced-USC (A-USC) Steam Boiler and Turbine with maximum steam conditions of 760°C (1400°F) and 35 MPa (5,000 psi). The comprehensive program, focused on nickel-based alloys, includes studies on: materials



2:30 PM Invited

needs will be presented and discussed.

Ultra-Super-Critical (USC) Power Plant Development and High Temperature Materials Research and Application in China: *Fusheng Lin*¹; Xishan Xie²; ¹Shanghai Power Equipment Research Institute; ²University of Science and Technology Beijing

The USC fossil power plants are developing rapidly since the first USC power plant had put in service on the end of 2006. Up to May 2010 there are 26 USC power plants with the steam temperature of 600° and 51 units (600-1000MW) for service in China. For further improvement of thermal efficiency and decreasing CO₂ emission China intents to develop the advanced USC power plant with the steam temperature of 700°. The key issue for USC power plant development is high temperature material. This paper will review today's high temperature materials used for 600° USC power plants in China and the high temperature materials research and development for 700° A-USC in the near future.

3:00 PM Invited

Alloy Design for Improved High-Temperature Performance: *Philip Maziasz*¹; 'Oak Ridge National Laboratory

High temperature alloys are essential for many demanding advanced energy production applications, including advanced steam conditions for coal-fired power plants. One of the most critical performance criteria for such applications is creep-rupture resistance, which critically depends on microstructural development during the early stages of service, and the stability of such structures for very long periods of time. Some principles relating alloying effects to precipitation behavior so as to create appropriate microstructures for better creep-resistance in austenitic stainless steels and ferritic steels have been developed. Some examples will be summarized, including the development of CF8C-Plus cast stainless steel. The applicability of this alloy design approach to Ni-based superalloys will also be described.Research sponsored by the U.S. Department of Energy, Office of Fossil Energy, Advanced Research Materials Program under contract DE-AC05-000R22725 with UT-Battelle, LLC.

3:30 PM Invited

The Metallurgy and Engineering of USC and A-USC Steam Turbines: Jeffrey Hawk¹; ¹U.S. Department of Energy

Steam turbines have provided electricity for well over 100 years. However, large-scale generation has only dominated energy production since 1950. Since the 1990's there has been pressure to increase the efficiency of large steam turbines, partly to improve the rate of return on initial investment, but also to decrease the amount of greenhouse gases emitted to the environment. Increasing efficiency means the temperature and/or pressure must be increased. Doing either means current materials of construction are no longer adequate in meeting the stresses generated by the moving and stationary parts. The presentation provides background information on the direction steam turbine technology has taken during the last couple of decades, addressing the way new materials have been identified and selected for use. The presentation will conclude with discussion on current strategies of alloy design for the next generation of steam turbines designed to operate at temperatures in excess of 700°C.

4:00 PM Break

4:10 PM

Ni-Base Alloys for Use as Components in Advanced-USC Steam Turbines: *Jeffrey Hawk*¹; Paul Jablonski¹; Christopher Cowen¹; ¹U.S. Department of Energy

Experience with nickel-base alloys in the NETL sponsored 760°C steam turbine program has shown that commercial, "off-the-shelf" nickel superalloys exist, and while promising, may not provide for all long-term mechanical needs associated with the steam turbine environment. One alloy, Haynes

282, has shown robust capability in terms of starting microstructure (gamma prime precipitate size and volume fraction). Another alloy, Nimonic 105, has exhibited the potential for improved creep behavior upon extended aging. In addition to the forged components in the steam turbine, cast materials for the turbine shell and valve chest also pose significant manufacturing challenges, primarily in terms of casting size and environment. This presentation will summarize the progress to date in identifying the most promising alloys, providing information on mechanical behavior and assessing their potential for use in A-USC steam turbines.

4:30 PM

140th Annual Meeting & Exhibition

Castability of Traditionally Wrought Ni-Based Superalloys for USC Steam Turbines: *Paul Jablonski*¹; Christopher Cowen¹; Jeffrey Hawk¹; Neal Evans²; Philip Maziasz²; ¹US Department of Energy; ²ORNL

The high temperature components within conventional coal fired power plants are manufactured from ferritic/martensitic steels. In order to reduce greenhouse gas emissions the efficiency of pulverized coal steam power plants must be increased. The proposed steam temperature in the Advanced Ultra Supercritical (A-USC) power plant is high enough (760°C) that ferritic/ martensitic steels will not work due to temperature limitations of this class of materials; thus Ni-based superalloys are being considered. The full size castings are quite substantial: ~4in thick, several feet in diameter and weigh 5-10,000lb each half. Experimental castings were quite a bit smaller, but section size was retained and cooling rate controlled in order to produce relevant microstructures. A multi-step homogenization heat treatment was developed in order to better deploy the alloy constituents. The castability of two traditionally wrought Ni-based superalloys to which minor alloy adjustments have been made in order to improve foundry performance is further explored.

4:50 PM

Castability of HAYNES 282 Alloy: *Henry White*¹; Zenon Pirowski²; Robert Purgert³; ¹Haynes International; ²Foundry Research Institute; ³Energy Industries of Ohio

Excellent high temperature mechanical properties, weldability, and fabricability makes HAYNES 282 alloy an attractive material for high temperature/ high pressure boiler and turbine components in Advanced Ultrasupercritical Power Plants. Several programs are in place in the United States and Overseas to gather the necessary data in order to utilize the material in plant construction. In this presentation we report on casting trials for the turbine program which was funded by the Energy Industries of Ohio and performed at Foundry Research Institute in Poland. Optical light and scanning electron microscopy were used to evaluate the structure and processing of the as cast material. A comparison between cast and wrought properties will be provided.

5:10 PM

Simplified Production of Ni-Based Oxide Dispersion Strengthened (ODS) Alloys via Gas Atomized Precursor Powder Approach: John Meyer¹; Iver Anderson²; Joel Rieken¹; David Byrd²; ¹Iowa State University; ²Ames Laboratory - US DOE

Oxide dispersion strengthened (ODS) Ni-base superalloys have been considered promising candidate materials to fulfill the corrosion, erosion, oxidation and creep challenges imposed by proposed power plant environments. Current processing of Ni-based ODS materials is very time, energy and cost intensive as well as susceptible to contamination. Gas atomization reaction synthesis (GARS) with a mixed (Ar/O₂) atomization gas is being developed as a simplified route for generation of ODS precursor powders on a small scale. Already, hot consolidation conditions that encourage the necessary oxide exchange reactions have been verified for Fe-based ODS alloy billets and a preliminary kinetic study determined Ni-base, Ni-Cr-Y-(Hf or Ti) containing, alloys viable for this production method. Results of experimental trials will be reported in terms of powder characterization and consolidation results. Supported by Carpenter Technology and USDOE-FE-ARM Program through Ames Laboratory contract no. DE-AC02-07CH11358.

Recent Developments in the Processing, Characterization, Properties and Performance of Metal Matrix Composites: Processing, Microstructure and Mechanical Properties II

Sponsored by: The Minerals, Metals and Materials Society Program Organizers: Martin Pech-Canul, Centro de Investigacion y de Estudios Avanzados del Instituto Politecnico Nacional; Zariff Chaudhury, Arkansas State University; Golam Newaz, Wayne State University

| Tuesday PM | Room: 6A |
|---------------|-------------------------------|
| March 1, 2011 | Location: San Diego Conv. Ctr |

Session Chair: Martin Pech-Canul, Centro de Investigacion y de Estudios Avanzados del Instituto Politecnico Nacional

2:00 PM

Deformation and Cavitation in Non-Contact Creep Studies for a Nb-Based Superalloy: *Robert Hyers*¹; Xiao Ye¹; Jan Rogers²; Laurent Cretegny³; ¹University of Massachusetts; ²NASA/MSFC; ³GE Global Research

A non-contact method for measuring creep at extremely high temperatures has been developed. Samples are high-precision machined spheres, levitated in the NASA MSFC Electrostatic Levitation Facility and heated with a laser. An induction motor rotates samples up to 30,000 revolutions per second. The rapid rotation loads the sample through centripetal acceleration, producing a shear stress of about 60 MPa at the center, causing the sample to deform. Deformation of the sample is captured on high-speed video and analyzed. This method has been applied to new materials, including a niobium-based superalloy, which is a metal and silicide composite (MASC). Microstructural analysis of crept samples provides insight into creep mechanisms. An overview of the method and results from these studies will be presented.

2:20 PM

Effect of MgAl2O4 on the Superficial Hardness of Hybrid-Multimodal Al/SiC Composites Processed by Reactive Infiltration: *Miguel Montoya-Davila*¹; Martin Pech-Canul²; Maximo Pech-Canul²; Rodrigo Escalera-Lozano³; ¹Universidad Autónoma de Zacatecas; ²Centro de Investigación y de Estudios Avanzados del Instituto Politécnico Nacional; ³Universidad del Istmo

The effect of MgAl2O4 formed at the reinforcement/matrix interface, on the superficial hardness of hybrid Al/SiC composites processed by reactive infiltration was investigated. Composites were prepared from porous preforms of a-SiC and silica-coated a-SiC powders of 10, 86, and 146 µm. The preforms, with particle size distribution from monomodal to trimodal, contained 0.6 volume fraction of SiC. The infiltration tests with the alloy Al-13.3Mg-1.8Si (wt. %) were carried out in Ar->N2 atmosphere at 1100°C for 60 min. The composites were characterized by X-ray diffraction (XRD) and scanning electron microscopy (SEM). In addition to density and residual porosity, superficial hardness measurements were performed. Results show that with spinel at the interfaces, residual porosity decreases and density and superficial hardness are slightly improved. This is attributed to the increase in the metal/ceramic interfacial joints by formation of the spinel phase and to an enhanced matrix/reinforcement load transmission.

2:40 PM

Corrosion and Wear Behaviour of Aluminum Alloy 6061-Fly Ash Composites: *Ajit Bhandakkar*¹; B. Balaji¹; R. C. Prasad¹; Shankar Sastry¹; ¹Indian Institute of Technology

The environmental degradation of aluminium metal matrix composites have been a subject of research for the damage tolerant design requirement in aerospace and automobile components. In the present investigation AA6061 aluminium alloy as matrix material and up to 10 wt% of low cost fly ash particulate composite were fabricated using liquid metallurgy stir casting route. Potentiodynamic and cyclic polarization studies were carried out in 3.5% NaCl solution on AA6061 and AA6061-fly ash composites to study their corrosion behavior. Polarization results in 3.5% NaCl solution indicates that the composites are more susceptible to corrosion than the base alloy. However, the base alloy and composite have same pitting and repassivation potential. The wear rate, frictional force and the frictional coefficient of composite was found to decrease with the increase in the reinforcement from 5 to 10 wt%. The environmentally degraded and worn out samples of base alloy and composites were analyzed using optical and scanning electron microscopes.

3:00 PM

Interface Evolution in Tungsten Wire Reinforced Stainless Steel Composites: Pawan Kumar¹; Milo Kral¹; ¹University of Canterbury

There is potential for improving creep properties of high temperature steels by tungsten wire reinforcement. Fiber/matrix interfaces have a significant influence on the properties of metal matrix composites, especially when they are used for high temperature applications, for example due to differences in thermal expansion coefficients. The present study investigated interactions between tungsten wires in two cast stainless steel matrices. Intermetallic phases develop at the wire-matrix interface during solidification. When the composite is aged at high temperatures, these phases further develop as a function of temperature, time and matrix composition. A combination of scanning electron microscopy, energy dispersive spectroscopy and electron backscatter diffraction was used to identify the constituents present at the interface, their chemistry and interface growth kinetics.

3:20 PM Break

3:40 PM

Effects of Annealing on the Growth Behavior of Intermetallic Compounds on the Interface of Copper/Aluminum Clad Metal Sheets: *Li Xiaobing*¹; Zu Guoyin¹; Deng Qiang²; ¹Northeastern University; ²Pangang Group Company LTD

The growth behavior and composition of intermetallic compound (IMC) on the interface of copper/aluminum clad sheets fabricated by the asymmetrical cold rolling on the different annealing process were investigated by means of OM, SEM, EDS and XRD techniques. The effect of temperature on the morphology and distribution of IMC is obvious at elevated temperature from 200°C to 500°C. The IMC begin to appear on the local area at 300°C and the thickness of the IMC layer increases rapidly with the rise of temperature. The growth rate of the IMC layer is slow for the annealing time from 20 min to 180 min. The composition of inter-layer varies into complicated with the rise of temperature. According to the results, the optimal annealing process can be chosen at 400°C for 20 min.

4:00 PM

Contribution of Different Strengthening Mechanisms in Particulate-Metal Matrix Nanocomposites: Z. Razavi Hesabi¹; J. Gracio²; S. Ahzi³; *Hamid Garmestani*³; ¹Georgia Institute of Technology - and - University of Aveiro; ²University of Aveiro; ³Georgia Institute of Technology

The relative contribution of different strengthening mechanisms in particulate metal matrix composites, namely, load-bearing, grain boundary strengthening, Orowan and enhanced dislocation density strengthening due to thermal expansion mismatch between ceramic particles and metal matrix, has been evaluated for a wide range of particle sizes varying from micrometer to nanometer. On the basis of the dislocation theory, a critical particle size (dc) was determined below which thermal expansion mismatch strengthening is absent in metal matrix nanocomposites (MMNCs). Nanoparticles located at grain boundaries may not play any role in strengthening by Orowan mechanism, however, they significantly affect grain size leading to increase of relative contribution of grain boundary strengthening. The data analysis shows an increase in the slope of Hall-Petch equation (K value) when nanoparticles are located at grain boundaries. In this work, we show that different strengthening mechanisms should be weighted as a function of microstructural features dependent on the volume fraction, size, and strongly distribution and location of nanoparticles.



4:20 PM

Manufacturing of an Aluminum Composite Structure Using a New Method and Its Comparison with Two Different Conventional Methods: *Atefeh Nabavi*¹; J. Vahdati Khaki¹; ¹Ferdowsi University of Mashhad

In this study, a novel method for manufacturing of metal foam sandwich panels via self-propagating high temperature synthesis (SHS) has been introduced and investigated. In this method, a powder mixture of metallic aluminum and copper oxide was placed in core-sheet interface and then sandwich panel was heated under static pressure. During heating, SHS reaction (3CuO+2Al=Al2O3+3Cu, H<0) occurred in the sheet-core interface and the generated heat from this exothermic reaction caused sheets to join the core by melting the interface and nearby. By plotting the hardness values of the panels' sheets across distance, it was found that the generated heat of the exothermic reaction caused a local melting of the panel sheets and the core. In addition, in order to evaluate the shear strength of the interface, the shear test was applied to manufactured sandwich panels and its results were compared with sandwich panels which were produced by two different conventional methods; diffusion and adhesive bonding processes. Furthermore, by the aid of energy dispersive spectrometer (EDS) and x-ray diffraction (XRD) analyses, the formation of copper in the core-sheet interface and its diffusion into the sheets and the core were investigated. The results showed that metal foam sandwich panels produced by using SHS method have higher joint strength than those which were produced by diffusion and adhesive bonding processes, and the maximum shear strength of the interface was achieved in shorter heating time. Significantly, this innovating method for manufacturing metal foam sandwich panels can be applied as a proper and alternative method.

4:40 PM

Joining of Advanced Aluminum-Graphite Composite: *Wayne Hung*¹; Manasa Velamati¹; Mauricio Garza²; Edgar Aguilar²; Mike Powers³; ¹Texas A&M University; ²COMIMSA; ³Agilent Technologies

Advanced aluminum graphite (Al-Gr) composites have unique thermal properties due to opposite coefficients of thermal expansion of aluminum and graphite. The thermal and mechanical properties of such composites are anisotropic due to directional properties of graphite fibers and their designed orientation. A joint of components with different fiber orientations would theoretically produce an isotropic material for thermal management purpose. This paper presents research results for welding and brazing of Al-Gr composites using different joining techniques. A laser beam melts the matrix and delaminates graphite fibers. The molten aluminum reacts with graphite to form aluminum carbide Al4C3. The joint strength is compromised when laser welding at optimal conditions to minimize the carbide formation. Brazing is preferred since the low melting temperature of a filler material suppresses the formation of Al4C3 while minimizing shrinkage cavities in the joint. Exceptional joint strength is obtained when resistance brazing Al-Gr composites with Al-Zn filler.

Refractory Metals 2011: Refractory Metal-Based Alloys *Sponsored by:* The Minerals, Metals and Materials Society, TMS Structural Materials Division, TMS: Refractory Metals Committee *Program Organizers:* Omer Dogan, DOE National Energy Technology Laboratory; Jim Ciulik, University of Texas, Austin

| Tuesday PM | |
|---------------|--|
| March 1, 2011 | |

Room: 19 Location: San Diego Conv. Ctr

Session Chairs: Omer Dogan, National Energy Technology Laboratory; Evan Ohriner, Oak Ridge National Laboratory

2:00 PM Invited

Potential Next Generation Airfoil Alloys for Advanced Land-Base Gas Turbines: *Jeffrey Hawk*¹; ¹U. S. Department of Energy

Advanced, super high efficiency gas turbine systems will necessarily need to operate at conditions that correspond to blade metal temperatures in excess of the melting temperature of current state-of-the-art Ni-base superalloys (i.e., hydrogen or oxy-combustion firing conditions). Consequently, any and all high melting temperature alloys systems must be investigated to determine which might be suitable for manufacture and testing. This presentation outlines the current NETL path forward in developing these substrate materials. A short introduction to NETL's materials development program will be given, followed by a discussion of several possible systems of interest (e.g., Nb-based refractory metal silicides, Nb-based alloys, ceramic matrix composites). The merits of each system, as well as, the research required for development will be described. The path forward is discussed next with emphasis on reducing the development time by utilizing computational materials modeling to pre-screen potential materials before attempting to produce those materials in the laboratory.

2:20 PM

Strengthening in High Entropy Alloys: *Garth Wilks*¹; Oleg Senkov¹; Daniel Miracle¹; ¹Air Force Research Laboratory

High Entropy Alloys (HEAs) represent a novel shift in strategy for alloy development. In conventional alloys, complex formulations are usually avoided in order to prevent the formation of intermetallic compounds that degrade material properties, whereas HEAs capitalize on the high entropy of a cocktail of constituents to frustrate formation of the same. Often, this strategy results in an alloy with a single phase consisting of a simple crystal structure. While strength in these materials has been suggested to operate under the agency of a solid-solution like strengthening mechanism, a critical analysis of available HEA data in the literature will be presented which broadly discusses observed trends in properties (e.g. lattice parameter and yield strength) as a function of constitution and highlights experimental observations from the authors' studies of refractory-based HEAs.

2:40 PM Invited

Processing Methods for Iridium and Iridium Alloys: *Evan Ohriner*¹; ¹Oak Ridge National Laboratory

Iridium and iridium alloys have a combination of properties that recommend them for a variety of applications. Their high melting temperature, resistance to oxidation, and strength at elevated temperature have led to their use in crucibles, spark plugs, nuclear fuel containers, and coatings for rocket thrusters. However, these same properties, combined with potential sensitivity of material properties to impurities and microstructure, result in a material that is often difficult to fabricate. The variety of methods used to fabricate iridium and iridium alloys are reviewed, including both traditional and novel methods. Metal purification, melting, forming and joining are traditional methods that have continued to develop. Powder metal processing and iridium coating technology are now also available as fabrication methods. This research was sponsored by the Office of Space and Defense Power Systems, U. S. Department of Energy, under Contract DE-AC05-000R22725 with UT-Battelle, LLC.

3:00 PM

Surface Processing of an Iridium Alloy for Control of Emissivity: Evan Ohriner¹; G. B. Ulrich¹; R. G. Miller¹; W. Zhang¹; ¹Oak Ridge National Laboratory

The effects of surface processing on the microstructure and properties of DOP-26 iridium alloy (Ir-0.3% W-0.006% Th-0.005% Al) are investigated. Surface processing is used to control emissivity of components operating at elevated temperature. The surface treatments include grit blasting with tungsten carbide media and pulse laser heating. The effects of processing parameters on surface morphology, grain structure, and emissivity are evaluated. The results are compared to those from numerical modeling of surface processing and material grain growth behavior. Recrystallization and grain growth is evaluated for both as-treated surfaces and following post-treatment annealing. This research was sponsored by the Office of Space and Defense Power Systems, U. S. Department of Energy, under Contract DE-AC05-000R22725 with UT-Battelle, LLC.

3:20 PM Break

3:40 PM

Improving Chromium Ductility: *Hailey Murdock*¹; Jamie Kruzic²; Omer Dogan¹; ¹National Energy Technology Laboratory; ²Oregon State University

The next generation of high temperature structural alloys for gas-turbines must exhibit exceptional resistance to fracture, creep, oxidation and fatigue at high temperatures. Chromium is being considered due to its high melting point (>1800°C), relatively low density (~7.2 g/cc), high temperature strength, and oxidation resistance. Limiting chromium is its high ductile-to-brittle transition temperature (DBTT). First principles calculations revealed elements, when alloyed with chromium, which have potential to reduce the ductile-to-brittle transition temperature. Experiments investigating room and elevated temperature deformation behavior of Cr-V alloys are presented. Cr-V samples (0 – 75% V) were prepared from powders, hot isostatically pressed, annealed at 1300°C for 120 hours, and extruded at 130 MPa and 1250°C. Extrusion achieved better homogeneity of the alloys as confirmed by electron microprobe data. Results of room and elevated temperature hardness tests, three-point bend tests, tensile tests and the effect of vanadium on the ductile-to-brittle transition temperature are described.

4:00 PM

High-Temperature Oxidation Behaviour of Co-Re-Cr-Based Alloys: Bronislava Gorr¹; Steffen Burk¹; Hans-Jürgen Christ¹; ¹University Siegen

Co-Re-Cr-based model alloys have been developed for high-temperature applications beyond 1200°C. The purpose of the present investigation is to gain an insight into the oxidation mechanisms of the model Co-Re-Cr alloys and to find ways to improve oxidation resistance of this class of materials. The first generation of this class of alloys showed a rather poor oxidation resistance during exposure to laboratory air. As a consequence of the lacking protectiveness of the oxide layer, the vaporization of rhenium oxide takes place during oxidation. It has been found that Si stabilizes the Cr2O3 scale, enhancing the oxidation resistance significantly. Other concepts to improve the oxidation resistance of this class of materials are discussed, such as the formation of a borosilicate layer or protective Al2O3 scale on the substrate surface.

4:20 PM

Computational Study of Microstructure-Property Relationships in High Temperature Materials for Fossil Energy Applications: An Integrated Phase Field and Numerical Viscoplasticity Approach: Kaisheng Wu¹; Omer Dogan¹; ¹National Energy Technology Laboratory

An integrated computational approach has been developed to investigate the correlations between complex microstructures and mechanical properties. In this approach, a phase field model was utilized to simulate the evolution of the complex microstructures in response to a variety of processing conditions such as different heat treatment schedules. Microstructure features including grain boundary segregation, grain growth, and second phase precipitations, etc., were taken into account in multi-component and multiphase systems. The results were incorporated into a numerical viscoplasticity model which was modified based on Fast Fourier Transform (FFT) algorithm to simulate the overall mechanical and microstructural response of the materials subjected to plastic deformation. Several examples of applying the developed model to high temperature materials, including refractory metals, for fossil energy applications will be discussed.

4:40 PM

Characterization of Osmium-Ruthenium Thin Films for Cathode Coatings: *Phillip Swartzentruber*¹; T. John Balk¹; Scott Roberts²; ¹University of Kentucky; ²Semicon Associates

Osmium-Ruthenium (OsRu) alloy thin film coatings were characterized to understand the effects of film structure on thermionic emission from dispenser cathodes. Electron microscopy and x-ray diffraction of coated dispenser cathodes were used to characterize the various film structures, and life testing was conducted to gauge the improvement in cathode emission due to each film structure. In collaboration with industrial partner Semicon Associates, three novel film structures were studied in addition to the standard

Semicon film. Different film architectures were created, with varying levels of substrate bias during film deposition. The films were simultaneously magnetron sputtered on porous tungsten pellets for characterization and on cathode assemblies for life testing. The cathode assemblies were life tested for 1000 hours. Cathode performance will be discussed in light of the microstructural features of each film.

Shape Casting IV: Light Metals Division Symposium in Honor of Prof. John T. Berry: Solidification

Sponsored by: The Minerals, Metals and Materials Society, TMS Light Metals Division, TMS: Aluminum Processing Committee, TMS: Solidification Committee

Program Organizers: Murat Tiryakioglu, University of North Florida; Paul Crepeau, General Motors Corporation; John Campbell, University of Birmingham

| Tuesday PM | Room: 15B |
|---------------|-------------------------------|
| March 1, 2011 | Location: San Diego Conv. Ctr |

Session Chairs: William Griffiths, Univ of Birmingham; Peter Schumacher, Univ of Leoben

2:00 PM Introductory Comments

2:10 PM

Review of Defect Behavior in Ni-Based Superalloys: *John Campbell*¹; ¹University of Birmingham

The Ni-base superalloys, normally melted and cast in vacuum, entrain their surface oxide film during turbulent pouring of the melt, which unfortunately at this time, is universally practiced for investment castings of these materials. The entrained film automatically becomes a bifilm crack, so that cast alloys have a large population of cracks that controls their failure behavior. The problems of the growth of single crystals, and the welding of polycrystalline alloys are reviewed to illustrate the central role of bifilms in the cracking of turbine blades, the heat affected zones of welds and the reliability of properties. It has been demonstrated that improved gravity pouring systems can significantly reduce these problems, but only countergravity filling of molds is expected to result in defect-free castings.

2:35 PM

Premium Quality Super Duplex Stainless Steel Castings without Secondary Refining: Bob Puhakka¹; ¹Alloy Casting Industries

The ASTM A890/ A995 super duplex stainless steels are a popular family of high alloy cast steels used extensively in the power generation and energy sectors. The manufacturing steps for these alloys have, up to now, required the use of costly secondary refining processes such as Argon Oxygen Decarburization (AOD). This paper will describe and validate a set of process parameters that obviate the need for secondary refining. Initial results indicate that the principle embrittling features, carbides and sigma phases, are not found, confirming the proposal that these phases form on bifilms entrained by pouring turbulence. Other significant benefits from the absence of bifilms appear to include the elimination of cracking and leakage defects.

3:00 PM

Direct X-Ray Observation of High Temperature Deformation in Aluminum Alloy Composites: *Richard Hamilton*¹; Andre Phillion²; Alex Leung¹; Thomas Connolley³; Peter Lee¹; ¹Imperial College London; ²University of British Columbia; ³Diamond Light Source

The development of a novel tension/compression rig capable of loading samples at high temperature during x-ray observation has enabled in-situ imaging of semi-solid deformation using both laboratory and synchrotron sources. This study focuses on phenomena of interest to the aluminum alloy processing industry, where defects formed in the mushy zone during processing can result in significant costs. Experiments were devised to apply



a measured, controlled load to the specimen to enable direct observation of the formation and deformation of the microstructure and flow of interdendritic fluid. The effect of composite additions, along with cooling rate and strain rate on the mechanisms of failure, initiation, growth, and liquid healing were studied whilst monitoring the load. The localization of strain followed by void formation and coalescence was observed. Finally, post failure x-ray tomography allows 3D characterization of the final fracture helping to explain the failure mechanism.

3:25 PM

In-Mold Thermal Analysis of Ductile Cast Iron: Morten Onsoien¹; ¹SINTEF

The objective of the present work is to study characteristic solidification data of three experimental ductile irons produced using a flow-through inmould melt treatment technique, by means of in-mould thermal analysis. All produced irons were, in addition, subjected to chemical analysis and quantitative metallography, as well as an evaluation of shrinkage porosity and carbide forming propensity. Applied melt treatment alloys were based on FeSiMg with small contents of cerium, lanthanum or misch-metal. Based on the obtained results, it was concluded that in-mould thermal analysis provides an effective way of monitoring the graphite nucleation throughout the solidification. Furthermore, the selected melt treatment resulted in ductile irons having very high nodule counts, up to 1162 nodules mm-2, very low shrinkage porosity and very low carbide forming propensity.

3:50 PM Break

4:10 PM

Modeling of Hot Tearing and Its Validations in Metal Castings: *Jianzheng Guo*¹; J. Z. Zhu¹; Sam Scott²; ¹ESI US R&D, Inc.; ²ESI NA

Hot tearing is one of the most serious defects for a metal casting. The nucleation and propagation of the hot tearing can result in permanent defects in the casting, which may cause the final cast product to be unusable. It is believed that the imposed strains and stresses on the solid framework in the mushy zone by the solidification shrinkage and thermal contraction create the conditions for hot tearing. It has been very well documented that the composition of the alloy and the mechanical properties of the metals in the semisolid state play critical roles in the formation of hot tears. To predict the susceptibility of hot tearing in a casting, a hot tearing indictor is proposed which is based on the Gurson's constitutive model and uses the thermophysical and thermomechanical properties obtained from the thermodynamic calculation in the final stage of the solidification. The numerical implementation of the hot tearing indicator is validated by experiments.

4:35 PM

Effect of Alloying Elements (Magnesium and Copper) On Hot Cracking Susceptibility of AlSi7MgCu-Alloys: Salar Bozorgi¹; *Katharina Haberl*¹; Christian Kneissl²; Thomas Pabel²; Peter Schumacher¹; ¹University of Leoben; ²Austrian Foundry Research Institute

Hot cracking during solidification can be a serious problem in aluminium casting alloys under certain conditions. This feature is well known, but still insufficiently investigated in shape casting. This study gives a brief overview on the factors influencing hot cracking during shape casting. Five different AlSi7MgCu-alloys with varying Mg and Cu contents were examined. Theoretical models including the cracking susceptibility coefficient (CSC) from Clyne and Davies have been considered. Thermodynamic calculations of the behaviour of the fraction solid during solidification have been compared to an experimental based hot cracking indexing (HCI) method. Scanning electron microscopy (SEM) was used to compare existing microstructure and precipitated thermodynamic phases. Furthermore, SEM was used to investigate crack surfaces initiated by a dog bone shaped mold during casting. A good correlation between theoretical models and experimental hot cracking index method was observed.

5:00 PM

Hydrogen and Cooling Rate Effects on Microporosity Formation in the Production of Defect-Controlled Fatigue Specimens: *Rosario Squatrito*¹; Ivan Todaro¹; Lorella Ceschini¹; Luca Tomesani¹; ¹University of Bologna

In experiments aimed at the production of fatigue specimens, the increased number of nearly identical specimens needed for each processing condition, together with the high sensitivity to pore size, call for very strict requirements of both the casting tool and the processing conditions. An experiment for producing aluminium alloy fatigue specimen by gravity casting with controlled microstructure and defects is here presented. The main requirements to be obtained on a set of specimens (extracted from a single casting block) were to have the same microstructure and gas porosity content. The main process parameters were the hydrogen level of the melt, the addition of oxides for improving the number of pore nucleation sites and the cooling rate within the casting mould. The distribution of the relevant properties (SDAS, %area of porosity) was measured throughout the casting plates in order to validate the design criteria of the both experiment and the mould

5:25 PM

Effects of Gravity on the Columnar to Equiaxed Transition in Directional Solidification: *Wajira Mirihanage*¹; David Browne¹; ¹University College Dublin

In industrial casting processes, microstructure plays a major role in determining the properties of the final cast product. Columnar to equiaxed transition (CET) is a frequent result of the evolving grain structure during alloy solidification. In this contribution, we analyze CET in directional solidification via numerical simulations. The numerical model employs front tracking to track columnar growth and a volume average approach to track the evolution of the equiaxed zone. The effects of gravity, thermal natural convection and dendrite transport were integrated into the model. Simulations of vertical directional solidification of an Al-7%wt.Si alloy both in and opposite the direction of gravity were conducted for different cooling conditions. Here, we present a preliminary analysis of these numerical simulations and a comparison of the predictions with previously published theoretical and experimental work.

Size Effects in Mechanical Behavior: Capturing the Size Effect through Modeling and Simulation

Sponsored by: The Minerals, Metals and Materials Society, Not Applicable, TMS: Nanomechanical Materials Behavior Committee *Program Organizers:* Erica Lilleodden, GKSS Research Center; Amit Misra, Los Alamos National Laboratory; Thomas Buchheit, Sandia National Laboratories; Andrew Minor, UC Berkeley & LBL

| Tuesday PM | Room: 2 |
|---------------|-------------------------------|
| March 1, 2011 | Location: San Diego Conv. Ctr |

Session Chairs: Thomas Buchheit, Sandia National Laboratories; Srinivasan Srivilliputhur, University of North Texas

2:00 PM

Gradient Theory and Size Effects: *Elias Aifantis*¹; ¹Aristotle University of Thessaloniki

Various forms of gradient theory are used to interpret size effects at micron and nano scales. They include size-dependent material moduli, sizedependent strength and fracture criteria, as well as size-dependent stressstrain curves.

2:20 PM

Deformation of Polycrystalline Magnesium Thin Film Size Effects: *Mark Horstemeyer*¹; Amitava Moitra¹; Kiran Solanki¹; ¹Mississippi State University

The inelastic behavior of columnar nanocrystalline magnesium has been studied using molecular dynamics simulation. Polycrystalline materials

are analyzed using Voronoi tessellation in which the randomness of the microstructure is generated using a Delaunay network from which a random distribution of grains is generated. Different specimen sizes and grain sizes were examined under different applied stress states (tension, compression, and shear). We have found that the grain reorientation occurs within the elastic regime to release the stored energy by local plastic deformation in grain boundary (GB) regions. The effect of thermal fluctuations in dislocation formation and nucleation leading to the yielding mechanism has been observed and analyzed. Evolution of twin and dislocation densities are also been estimated. A size scale effect related to the volume averaged yield stress in the specimen was evidenced.

2:40 PM

Controlling the Strength of Nanocrystalline Metals and Alloys: On the Importance of the Grain Boundary Relaxation State: Jonathan Schäfer¹; Alexander Stukowski¹; *Karsten Albe*¹; ¹TU Darmstadt

Plastic deformation in various nanocrystalline fcc metals and their alloys is studied by means of atomic scale computer simulations. The distribution of solutes is equilibrated using a hybrid Monte-Carlo/Molecular Dynamics scheme before samples are deformed under uniaxial load. The relaxation state of the grain boundary is measured by means of the atomic free volume and the evolution of line defects within the grains is monitored using a novel dislocation extraction algorithm. By comparing chemically and structurally relaxed samples we find that the relaxation state of the GBs is controlling the maximum strength of all studied material systems and for all grain sizes. The (chemical) equilibration is proven to raise the barrier for GB mediated processes. Also in the case of grain sizes, where the major carrier of plastic deformation is dislocation slip, the relaxation state of the GB is shown to have a significant effect.

3:00 PM

A Continuum Theory of Dislocation Dynamics - Microstructure Evolution, Size Effects and Comparison With DDD: Stefan Sandfeld¹; Thomas Hochrainer²; Michael Zaiser³; Peter Gumbsch¹; ¹Karlsruhe Institute of Technology; ²Florida State University; ³The University of Edinburgh

Progressive miniaturization of components further increases the demand for physically-based continuum theories of plasticity, which can predict size-dependent behaviour by accounting for length scales associated with the dislocation microstructure. An important recent development has been the formulation of a Continuum-Dislocation-Dynamics theory (CDD) which provides a kinematically consistent continuum description of the dynamics of systems of curved dislocations. This theory overcomes the limitations of classical continuum methods while it is not constricted by the number of interacting line segments. We outline the theoretical foundations of CDD and demonstrate the applicability by presenting several model systems, among them bending and shearing of a thin single crystalline film, torsion of a wire, and shearing of a composite material. The microstructure evolution along with size-effects will be compared to results from DDD-simulations and classical plasticity models.

3:20 PM

Effect of Precipitate Morphology on Chemical Mixing during Severe Plastic Deformation: *Nhon Vo*¹; Robert Averback¹; Pascal Bellon¹; Yinon Ashkenazy¹; ¹University of Illinois Urbana Champaign

The effect of precipitate morphology on atomic mixing during severe plastic deformation (SPD) was investigated using molecular dynamics (MD) computer simulations. Different initial precipitate morphologies in fcc A75B25 alloys with heats of mixing ranging from 0 to 21 kJ/mol were cyclically deformed to strains up to e = 200. For highly immiscible alloys (~16 kJ/mol), the precipitates always acquired a platelet structure during shear, independent of their initial microstructures. We attribute this tendency to dislocation localization on the interface and enhanced local atomic rearrangements. We also examined SPD in Cu-Nb for which bcc precipitates strongly on the specific interface, with Kurdjumov-Sachs (KS) interfaces behaving very differently than non-KS interfaces. The role of temperature in the mixing mechanism is also discussed.

3:40 PM Break

4:00 PM Invited

Deformation of Nanoscale Single Crystal Gold by Atomistic Simulation: Shivraj Karewar¹; Niraj Gupta¹; Alex Stukowski²; Michael Baskes³; *Srinivasan Srivilliputhur*¹; ¹University of North Texas; ²Technical University of Darmstadt; ³Los Alamos National Laboratory

We compare the deformation behaviour of gold single crystal nanoparticles with $6 \sim 30$ nm diameters with that of gold spherical shells of varying inner to outer diameter ratios. Gold nanoparticles were modelled with an EAM potential and the indenter was described by repulsive potential. Yield strength dependence on sample size, geometry, and temperature was studied in these nanoparticles. Yield strength increases with increase in size from 6 nm to 20 nm and decreases after that until 30 nm. An increase in temperature lowers the yield strength in the nanoparticles, and the effect is more pronounced for larger radii. The deformation mechanism is aided by the continuous displacement burst accompanying dislocation escape from the nanoparticles. Based on this, a dislocation starvation mechanism has been discussed. Extended dislocations were found to be the prominent defect type. Spherical shell calculations are under way.

4:30 PM

Two-Dimensional Discrete Dislocation Plasticity Incorporating Anisotropic Elasticity: Siamak Shishvan¹; *Erik Van der Giessen*²; ¹University of Tabriz; ²University of Groningen

The modeling of discrete dislocation plasticity (DDP) has become a powerful tool to study the size-dependent behavior of materials and (sub) micron-size devices. By construction, plastic deformation in DDP is anisotropic, but almost all current implementations treat dislocations as line singularities in an isotropic elastic crystal. This unbalance in anisotropy originates from the fact that the three dimensional anisotropic elastic fields of a dislocation are extremely complex. Here we present a DDP method for two-dimensional problems, which relies on the fact that plane-strain plastic deformation of cubic crystals is possible in specific orientations when described in terms of edge dislocations on three effective slip systems. The long-range fields of such dislocations are known and recapitulated. To handle polycrystalline problems, we follow O'Day and Curtin in treating each grain as a separate plastic domain, and adopt superposition to determine the overall response taking into account the boundary conditions.

4:50 PM

Frank Read Sources in the Continuum Theory of Dislocations: Thomas Hochrainer¹; *Stefan Sandfeld*²; Jochen Senger²; Peter Gumbsch²; ¹The Florida State University; ²Karlsruher Institut fuer Technologie

Several small scale experiments revealed that size effects in plasticity are not always tied to strain gradients, but may also appear in largely homogeneous deformations, e.g. as in micro-compression tests. We recently introduced the continuum theory of dislocations which features natural boundary conditions, dislocation fluxes and source limitation. In the current paper we present the treatment of Frank-Read sources in this framework. We note that this approach properly accounts for the plastic slip introduced while forming a new loop from a source. Discrete dislocation dynamics simulations are used to deduce laws for the triggering of existing sources and for the creation of new sources from dislocation reactions. Small numerical examples illustrate the resulting microstructure evolution which is compared with DDD results.

5:10 PM

A Discrete Dislocation Analysis of Size Effects on Void Growth in Single Crystals: *Shyam Keralavarma*¹; Javier Segurado²; Javier LLorca²; Ahmed Benzerga¹; ¹Texas A&M University; ²Polytechnic University of Madrid

The growth of sub-micron sized voids in single crystals is analyzed using discrete dislocation dynamics. A two dimensional plane strain analysis of self-similar square crystals containing circular voids in the center and subjected to uniaxial and biaxial deformation is performed. Edge dislocations, modeled as discrete points in two dimensions, move along well-defined slip systems and interact through their long range elastic



fields. Physics-based constitutive rules are implemented to model their short range interactions including junction formation and dynamic evolution of the source and obstacle population, allowing for an adequate representation of strain hardening. Two types of boundary conditions for dislocation slip are analyzed: (i) free boundaries simulating deformation of free-standing crystals and (ii) slip blocking at the boundaries to simulate the deformation of a grain in a polycrystal. We discuss possible micro-mechanisms for the observed size effects in the stress-strain response and the void growth rates.

5:30 PM Invited

Dislocation Core Spreading in Gum Metals: *Daryl Chrzan*¹; Matthew Sherburne¹; Yuranan Hanlumyuang¹; Tianshu Li²; John Morris¹; ¹University of California Berkeley; ²University of California Davis

The structure of dislocation cores in elastically anisotropic (nominally) BCC alloys is considered. A definition of the dislocation core radius based on linear elasticity theory and the the ideal strength of a material is introduced. For screw dislocations in BCC crystals, the core radius so obtained scales inversely with $(C_{11}-C_{12})^{-1/2}$. The design criteria for the Ti-Nb alloys known as Gum Metals was aimed at driving $(C_{11}-C_{12})$ towards zero. This has the immediate consequence that dislocation core radii in Gum Metals are driven towards infinity. The implications of the diverging dislocation core radii are explored using atomic scale calculations of dislocation core structures in Ti-V approximants to Gum Metal. The atomic scale structures predicted to arise from core overlap in TiV alloys are reminiscent of the nanodisturbances observed in Gum Metals. This research is supported by the National Science Foundation and Toyota Research and Development.

Surfaces and Heterostructures at Nano- or Micro-Scale and Their Characterization, Properties, and Applications: Magnetic Heterostructures II - and -Energy and Catalysis Technologies I

Sponsored by: TMS Electronic, Magnetic, and Photonic Materials Division, TMS Materials Processing and Manufacturing Division, TMS: Nanomaterials Committee, TMS: Surface Engineering Committee

Program Organizers: Nitin Chopra, The University of Alabama; Ramana Reddy, The University of Alabama; Jiyoung Kim, Univ of Texas; Arvind Agarwal, Florida International Univ; Sandip Harimkar, Oklahoma State University

| Tuesday PM | Room: 31B |
|---------------|-------------------------------|
| March 1, 2011 | Location: San Diego Conv. Ctr |

Session Chairs: Nitin Chopra, The University of Alabama; Ramana Reddy, The University of Alabama

2:00 PM Invited

Green Magnetic Energy: Mn(Bi,Al) Nanomagnets: *Yang-Ki Hong*¹; ¹University of Alabama

The figure of merit for permanent magnet is the maximum energy product (BH)max in the units of MGOe. Sintered Nd2Fe14B and SmCo magnets show high 64 and 28 MGOe of theoretical (BH)max, respectively. However, low operation temperature of NdFeB, which may lead to loss of machine power, and availability of rare-earth and transition elements are potential barriers to EV motor and other applications. Thus, aiming at developing high temperature magnets without rare-earth and transition elements, we have theoretically calculated the (BH)max for MnBi and t-phase MnAl alloys using density functional theory and modified Skomski's equation. Our calculations predict 20 MGOe (3.66 μ B/f.u.; Hk = 53 kOe) and 12.5 MGOe for MnBi and MnAl alloys, respectively. Accordingly, it is envisioned that core-shell MnBi-soft metal and MnAl-soft metal micro/nanoparticles will exhibit large remanent magnetization, thereby increasing the (BH)max to 51 MGOe and 53 MGOe for MnAl and MnBi core-shell nanoparticles, respectively.

2:30 PM

HR-STEM Imaging and EELS Characterizing of Nano-Scale Defects in Sputter Deposited Thin Films of Double-Perovskite Sr2FeMoO6 (SFMO): *Robert Williams*¹; Jeremy Lucy¹; Rebecca Riccardo¹; Patrick Woodward¹; Fengyuan Yang¹; Hamish Fraser¹; Adam Hauser¹; Manisha Dixit¹; ¹The Ohio State University

Oxides are promising candidates in the emerging field of spintronics. Some oxide systems of interest include single perovskites such as SrTiO3 (STO) and double perovskites such as Sr2FeMoO6 (SFMO). The magnetic properties of these systems have been found to depend on the amount of disorder present as well as defects. The major challenge during processing is the obtaining of the necessary long-range order while preventing defect formation due to processing parameters. This requires structural and chemical characterization ranging from identification of defects and morphology as well as correlating microstructure-property relationships. For this work thin films of SFMO have been sputter deposited on STO with varying parameters and HAADF-STEM imaging and EELS analyses have been conducted using an aberration-corrected FEI Titan[™]80-300 STEM to provide microstructural and chemical information. HAADF_STEM images of SFMO ordering are presented as well as characterization of interfacial defects. NSF Materials Research Science and Engineering Center (DMR-0820414).

2:45 PM Break

2:55 PM Introductory Comments for Energy and Catalysis Technologies

3:00 PM Invited

High Efficiency Photolytic Nanostructures for Hydrogen Production: Kaan Kalkan¹; ¹Oklahoma State University

Conversion of sunlight to chemical fuels by artificial photosynthesis has been a long-sought goal. In particular, significant research activity was stimulated towards photolytic cells producing hydrogen in 1972, when Fujishima and Honda demonstrated water could be split into hydrogen and oxygen under sunlight (photolysis) using a light-absorbing semiconductor electrode. Since then, however, the development of efficient photolytic devices has been hindered by the challenge of meeting the following requirements all in one device: i) efficient channeling of photogenerated electrons and holes to redox reactions at the interfaces; ii) efficient absorption of sunlight; and iii) avoidance of photo-oxidation of the semiconductor electrode. The present work demonstrates a hydrogen generating photolytic device, which consists of a low band gap oxide semiconductor nanowire decorated with metal nanoparticles. The multifunctional (i.e., electronic, photonic, and plasmonic) nanowire-nanoparticle conjugates are synthesized via sol-gel and reduction chemistries, respectively. A quantum efficiency of 0.8 is measured for the photolysis.

3:30 PM Invited

Visible Light Photoreduction of CO2 Using Heterostructures of Nanocrystalline TiO2 and Semiconductor Quantum Dots: Christopher Matranga¹; Congjun Wang¹; Robert Thompson¹; John Baltrus¹; ¹US DOE - NETL

The design of photocatalysts for converting CO2 into value-added chemicals and fuels is a critical area of research supporting our nation's development of new CO2 management technologies. Historically, titanium oxide photocatalysts have been investigated for this application, however, the large band gap of this material limits it to the UV region of the solar spectrum and rapid charge carrier recombination can reduce this material's catalytic efficiency. We report on the use of heterostructures of semiconductor quantum dots (QDs), such as CdSe, with nanocrystalline TiO2 for the photocatalytic reduction of CO2. These heterostructures simultaneously improve the visible light activity of this catalyst system and spatial separate the photogenerated charge carriers, thereby reducing recombination. Our results show that these heterostructures are capable of photoreducing CO2 using only visible light ($\lambda > 420$ nm) to produce CH4 , CH3OH, and trace amounts of CO and H2.

4:00 PM Invited

Controlling Defect Density in Polymer-Fullerene Bulk Heterojunction Solar Cells by Optimizing Growth Conditions: Kanwar Nalwa¹; Rakesh Mahadevapuram¹; Yuqing Chen¹; Santosh Pandey¹; *Sumit Chaudhary*¹; ¹Iowa State University

Although promising, the performance of polymer:fullerene bulkheterojunction solar cells is still limited by several factors including recombination at interfacial states. Hence, it is important to study and quantify the factors that govern the density of defects states (DODS). To understand the effect of growth rate on the DODS of poly(3-hexyl thiophene (P3HT) based solar cells, three types of P3HT:fullerene cells (A, B, and C) were fabricated with growth rate (solvent drying time upon spin coating) of ~ 40 , 7 and 1 minutes, respectively. Capacitance and sub-band gap characterizations showed that slowest growth of device A led to reduction of DODS by an order of magnitude as compared to fastest grown device C. The slow growth assists the formation of self-organized ordered structure in the P3HT/fullerene blend system diminishing morphological defects. These observations were also confirmed by analysis of dark current-voltage curves.

4:30 PM

Photovoltaics Using Doped and Undoped Amorphous Silicon Heterojunctions with Conjugated Polymers: Rakesh Mahadevapuram¹; Kanwar Nalwa¹; Vikram Dalal¹; *Sumit Chaudhary*¹; ¹Iowa State University

Polymer based photovoltaic (PV) technology is an exciting solar-electric conversion paradigm due to high extinction coefficient of polymers and lowcost manufacturability. Amorphous Silicon (a-Si:H) based solar technology is another emerging thin-film technology that promises to alleviate the cost issues of traditional crystalline Si based PVs. It is natural to think that marriage of a-Si:H and organics may open new avenues in PV device architecture. However, recent research efforts in this area are few and there is a need for in-depth analysis of Si-organic interfaces. In this direction, we fabricated polymer PVs in a bilayered configuration with a-Si:H, both doped and undoped. We observed that intrinsic a-Si:H based cells produced highest photocurrent; n-type a-Si:H based device shows highest fill factors implying efficient electron collection, whereas the p-type a-Si:H based device shows worst performance due to energy level mismatch. Detailed understanding of the Si/organic interfaces and future prospects will be presented.

4:45 PM Invited

Characterization and Modeling of 3D Photovoltaics: Jonathan Guyer¹; Daniel Josell¹; ¹NIST

First generation (thick layers of crystalline silicon) and second generation (thin films of CdTe, CIGS, etc.) PV devices are both well established, with well defined techniques for fabrication and characterization. Third generation PV encompasses a wide diversity of materials and nanostructures and commercially viable technologies, and means of fabrication are yet to be determined. Many of the proposed structures have considerable microstructural variability that complicate interpretation of macroscopic device measures. We are developing idealized, three-dimensionally patterned templates that can serve as test structures to enable measurement of critical device and materials properties. Initial heterostructures are based around electrodeposited CdTe. To guide and interpret the experimental measurements we are developing open source models of carrier and light transport within arbitrary 2D and 3D device geometries. This talk will compare experimental measurements with simulation results and discuss how the model is used to guide new device geometries.

5:15 PM Invited

Engineering Carbon Nanomaterials for Energy Application: *Wonbong Choi*¹; ¹Florida International University

This talk will focus on engineering of carbon nanomaterials, carbon nanotubes (CNTs), and graphene for various applications in future energy. Particularly, the interfaces of CNT-CNT, CNT-substrate, graphene-substrate and graphene-CNT will be used to highlight the challenges towards energy applications. Our recent results of electrical functionality in carbon nannomaterials will be presented. Some of these results offer excellent opportunity to have high efficiency devices and systems, high efficiency Li-ion battery based on interfacial controlled CNTs and flexible solar electrode based on large graphene structure. Our efforts on the strategies of manipulation of carbon nanomaterials interface and its characterization at nanoscale will be reviewed and critical issues will be discussed.

Thermally Activated Processes in Plastic Deformation: Deformation Mechanisms and Polycrystal Plasticity

Sponsored by: The Minerals, Metals and Materials Society, TMS Materials Processing and Manufacturing Division, TMS/ASM: Computational Materials Science and Engineering Committee *Program Organizer:* Christopher Woodward, Air Force Research Laboratory

| Tuesday PM | F |
|---------------|---|
| March 1, 2011 | L |

Room: 1B Location: San Diego Conv. Ctr

Session Chairs: Dennis Dimiduk, Air Force Research Laboratory; Yoon-Suk Choi, UES Inc

2:00 PM Invited

High Energy X-Ray Diffraction Methods for Dynamic Characterization of Non-Linear Material Behaviors: *Matthew Miller*¹; ¹Cornell University

The current generation of engineering material behavior models has created an incredible challenge for the experimental characterization community. Traditional experiments are pre-deformation and post-mortem snapshots of microstructure coupled with macroscopic stress-strain behaviors. New high energy synchrotron x-ray diffraction tools, capable of structural and mechanical characterization on the grain and subgrain size scale, are currently coming online. This talk presents an overview of the current generation of experiments beginning with a general diffraction primer followed by specific descriptions of the classes of experiments that are currently available and soon coming online for quantifying microstructure and mechanical response at the size scale of the grain and below. The talk emphasizes the potential that exists for combined experiment/simulation methodologies. The establishment of a community around the diffraction experiment that would encourage and enable the mechanics community to move upstream, closer to the actual scattering event, is proposed.

2:30 PM Invited

Physics Based Single Crystal Deformation Material Modeling for Aerospace Applications: *Alexander Staroselsky*¹; Brice Cassenti²; ¹Pratt & Whitney; ²University of Connecticut

In this presentation we discuss modeling of high temperature creep, plasticity, and fatigue using physics based crystal-plasticity methods. The work is focused on prediction of elastic-visco-plastic response of Ni-based superalloys using finite element methods. Damage accumulation causes tertiary creep and shear localization around local concentrators, which is essential for airfoil life prediction. We analyze the relative importance of each of the damage modes at different temperatures and stress levels. A computational transient thermal analysis of a turbine airfoil provides the illustration of the TMF/LCF life prediction for different engine operating conditions such as rotor speed, compressor discharge pressure, turbine inlet temperature and pressure at different mission points such as take-off, climb, end-climb, cruise and descent. We close the presentation by reviewing the current status of physics based FE modeling from the perspective of aerospace industry and discuss the current challenges in validation and modeling development.

3:00 PM Invited

Modeling the Orientation Dependence and Nonlinearity in the Creep of Single Crystal Superalloys Using a Semi-Mechanistic Approach: Y. Sun¹; ¹Rolls Royce

This paper will demonstrate the role of creep and rupture of single crystal superalloys in life models for gas turbine engine airfoils and the use of a



semi-mechanistic approach for modeling the orientation dependence and nonlinearity of creep. In a turbine engine deformation by creep is responsible, not just for failure by rupture, but also for the forces that drive fatigue crack initiation and propagation at stress risers. In the semi-mechanistic approach creep is modeled using strain-hardening and strain-rate sensitivity. The approach gives a single, explicit solution for the creep strain that covers the primary "steady-state" and tertiary stages of creep. Orientation dependence is addressed through the anisotropy in the work hardening rate and slip multiplicity. The model is applied to CMSX-4 single crystals and is shown to provide good representation of the orientation dependence of creep and rupture in this material as well as single crystal superalloys in general.

3:30 PM

Local Strain Accommodation in Polycrystalline Ni-Base Superalloys: *Jennifer Walley*¹; Robert Wheeler²; Michael Uchic³; Michael Mills¹; ¹The Ohio State University; ²UES; ³Air Force Research Laboratory

A new in-situ experimental methodology was used to characterize local strain heterogeneities in nickel-based superalloys that have relatively fine grain size (Dave<50µm). Initial work was performed on Rene 104 that was heat treated to produce two sets of samples with similar grain size distributions, but different γ ' distributions and grain boundary morphologies. One sample set has planar boundaries and a bimodal γ ' distribution, the other has serrated boundaries and a trimodal γ ' distribution. Quasi-isostatic tensile tests were performed at elevated temperatures in a scanning electron microscope, with images acquired at regular strain intervals. Samples were processed prior to testing using electron beam lithography techniques to produce a suitable speckle pattern to facilitate local strain analysis by digital image correlation techniques using Correlated Solutions VIC-2D software. The initial data indicates that interesting strain heterogeneities develop and correlate with grain size, orientations, and boundary relationships between the tensile axis and other boundaries.

3:50 PM

Comparison of Deformation Mechanisms for Constant Strain Rate and Creep Testing of a Ni-Based Superalloy: *Hallee Deutchman*¹; Patrick Phillips¹; Michael Mills¹; ¹The Ohio State University

The effect of strain rate on deformation mechanisms was investigated under creep and constant strain rate conditions on an advanced polycrystalline Nibased disk superalloy. A detailed microstructure characterization aimed at measuring the gamma-prime precipitate size, morphology, distribution, as well as grain size and degree of grain boundary serration, was performed prior to mechanical testing experiments so that the effects of microstructure can be correlated with the deformation response. Constant load creep tests and constant strain rate tests were performed at the same temperature so that the influence of strain rate on deformation substructure can be assessed. Following mechanical testing, a thorough TEM characterization study was done to determine the operative deformation mechanisms. Significant differences have been observed with dislocation-mediated mechanisms at higher strain rates and microtwinning and faulting of precipitates at low strain rates. Funding for this work has been provided by AFOSR through the Metals Affordability Initiative (MAI) program.

4:10 PM Break

4:25 PM Invited

Challenges in the Micromechanical Modelling of Hot Deformation: *David Dye*¹; Nicholas Jones¹; ¹Imperial College

Micromechanical models, both self-consistent homogenization schemes (see the Tome symposium at this meeting) and spatially-explicit crystal plasticity FE, have developed rapidly over recent years. The methods are briefly introduced and some popular underlying single crystal flow rules examined, along with their application to room temperature deformation. Hot deformation presents additional challenges, as the microstructure evolves under the influence of defects such as dislocation networks. This evolving microstructure often dominates the flow behaviour. Examples include recrystallisation, the break-up of precipitates, hard body rotation and phase evolution. Of particular interest is the rapidly evolving ability to examine these processes in situ using diffraction techniques and microscopy, with time resolutions of ~1ms now becoming achievable. Thus, it is now possible to imagine developing micromechanics models that go beyond empirical flow rules. Examples from nickel superalloys, from beta, alpha-beta and near-alpha Ti alloys, from TWIP steels and from Zry-4 will be examined.

4:55 PM

Thermal Aging of IN718Plus Superalloy and Relaxation of Laser Shock Peened Residual Stresses: *Vibhor Chaswal*¹; S. Mannava¹; Dong Qian¹; Vijay Vasudevan¹; Kristina Langer²; ¹University of Cincinnati; ²Air Force Research Laboratory

Thermal aging is conducted on as-received IN718Plus aeroengine superalloy at 923K, 973K, 1023K, 1073K up to 1000h under ambient conditions to replicate in service exposure and on laser shock peened (LSP) coupons at 973K to investigate operative stress relaxation mechanisms. Microstructural evolution of gamma prime precipitates and eta-Ni3Ti is investigated using transmission electron microscopy and convergent beam electron diffraction. Based on quantitative measurements and image analysis, gamma prime coarsening is found to follow LSW kinetics with average activation energy of 318 kJ/mol. At smaller precipitate sizes, higher activation energy is observed and a procedure for goodness of data is arrived at employing Johnson Mehl Avarami formulation. At longer aging, gamma prime transforms to hexagonal eta-Ni3Ti involving a faulting mechanism. Up to 50% thermal relaxation of residual stresses was measured between LSP treated and LSP+Aged samples using both conventional and synchrotron x-ray diffraction techniques. Results are correlated with dislocation substructure and dislocation-precipitate interactions involved.

5:15 PM

Localized Deformation during Macroscopically Uniform Plastic Flow of a Dynamically Strain Aging Alloy: *R. Storer*¹; M. Lebyodkin²; P. Kurath¹; A. Beaudoin¹; C. Fressengeas²; ¹University of Illinois at Urbana Champaign; ²Universite Paul Verlain-Metz/CNRS

Dynamic strain aging presents a competition between the interaction of solute atoms with dislocations and plastic strain rate, through the thermal breakaway of dislocations from obstacles. The Portevin - Le Chatelier (PLC) effect presents evidence of the collective dislocation activity in the presence of dynamic strain aging: continuously propagating and hopping bands are vivid examples of plastic bursts at sample length scale, with allied serrations in the stress-time curve. Closer study, through digital image correlation and analysis of (small) transients in the stress response, suggests that dislocation-solute interaction extends to regimes of "uniform" plastic response. The present effort provides an experimental study of an Al-Mg alloy, with spatio-temporal resolution sufficient to reveal patterns of localized deformation with stress transients much less than those typically associated with the PLC effect.

5:35 PM

Comparative Hot-Work Constitutive Analyses of Carbon/HSLA and Stainless Steels with Linkage to Microstructural Evolution: *Hugh McQueen*¹; Yong Li¹; I. Rieiro²; M. Carsí³; O. Ruano³; ¹Concordia University; ²Universidad de Castilla-La Mancha; ³Centro Nacional de Investigaciones Metalúrgicas

Constitutive analysis (Garofalo's sinh equation) for torsion test peak stresses of 0.29C, 0.15V steel over 850-1200°C, 0.6-30/s was conducted by an integrated automatic program (RCR) without pre-specifying any empirical constants. Here the tuning data has been analyzed using the traditional practice of selecting stress multiplier (SM) values previously employed for C/HSLA steels; this allows plotting data on common graphs to compare changes including Q due to composition. Although the activation energies Q vary very little, the RCR method predicted the stresses beyond the tuning set extremes. The similarities confirm that the RCR results can be linked to the previously derived flow curve models and to the related microstructural evolution determined optically and substructures (SEM-EBS, TEM of austenitic stainless steels). In turn the structures can be related to magnetically measured rates of transformation to ferrite and to bainite.

5:55 PM

A Crystalline Law for Thermally Activated Plastic Deformation: Ghiath $Monnet^1$; $\ ^1\text{EDF}$

Based on Dislocation Dynamics (DD) simulations in iron at low temperature, we propose constitutive equations providing the strain rate intensity on a given slip system as a function of the shear stress, temperature, obstacle density and strength. The model differs from the Kocks-Mecking formalism in the sense that strengthening is not always conditioned by applied work against the dislocation line tension. In this model the kingpair kinetics is integrated into the flow rule. DD simulations show that the difference in mobility between dislocations, leading to a significant decrease in the interaction strength. Depending on the obstacle nature and concentration, two strengthening components may prevail: one is due to the decrease of the average length of screw dislocations, are curved under the effect of the applied stress.

NOTES

0.00 0.25